Citation: Downing Spencer, J.E. (1990). A study of organotitanium coupling agents for adhesion promotion and of chemical reactions on alumina surfaces by inelastic electron tunnelling spectroscopy. (Unpublished Doctoral thesis, City, University of London)

A STUDY OF ORGANOTITANIUM COUPLING AGENTS FOR ADHESION PROMOTION AND OF CHEMICAL REACTIONS ON ALUMINA SURFACES BY INELASTIC ELECTRON TUNNELLING SPECTROSCOPY

BY

JONATHAN EDMUND DOWNING SPENCER

A THESIS SUBMITTED FOR THE DEGREE OF
DOCTOR OF PHILOSOPHY

AT

THE DEPARTMENT OF CHEMISTRY
CITY UNIVERSITY
LONDON

MAY 1990

LIST OF CONTENTS

LIST OF CONTENTS (cont.)

LIST OF CONTENTS (cont.)

LIST OF CONTENTS (cont.)

LIST OF CONTENTS (cont.)

LIST OF CONTENTS (cont.)

LIST OF CONTENTS (cont.)

LIST OF CONTENTS (cont.)

LIST OF FIGURES

LIST OF FIGURES (cont.)

LIST OF FIGURES (cont.)

LIST OF APPENDIX FIGURES

LIST OF APPENDIX FIGURES (cont.)

LIST OF TABLES

LIST OF TABLES (cont.)

LIST OF APPENDIX TABLES

ACKNOWLEDGEMENTS

I would like to extend my sincere appreciation and gratitude to my supervisors; Mr. Brian Field, for his guidance, motivation and patience, and Mr. Keith Allen for his guidance and for the financial support of this work by the Adhesion Science Group at the City University.

I would also like to thank the technicians and staff of the Chemistry Department at the City University for their help and advice.

For P.D.S., M.D.S. and M.K.W.

ABSTRACT

Chemical reactions taking place on an alumina surface have been investigated by incorporating this surface within an Al-AlO$_x$-Pb tunnelling junction and scanning the inelastic electron tunnelling spectrum.

This approach has been employed to study reactions involved in substrate-coating situations, of particular relevance to adhesive bonding. It has been shown that the glass-fibre circuit board (PCB) substrates used in this study may be reused after suitable cleaning. A "dry atmosphere" bag has been incorporated into the procedure to facilitate the doping and subsequent study of air-sensitive materials.

Three organotitanium compounds; titanium acetylacetonate (TAA), triethanolamine titanate (TEAT) and octylene glycol titanate (OGT), which are used commercially as primers or adhesion promoters for surface coatings have been investigated. Mechanisms of their solution hydrolysis and of their interaction with the alumina surface are proposed. The interaction of these primed alumina surfaces with simulated organic coating bases has also been studied. Hence a mechanism for the interaction of a coating promoter with both a metal oxide surface and with the surface coating itself has been evaluated.

In addition, since atmospheric surface contamination will undoubtedly affect any subsequent process, the surface reactions of simple gaseous molecules on alumina have been investigated. These have incidentally thrown light onto the mineralogical theory of the origin of life. The first experimental support for Bernal and Cairns-Smith's mineralogical theory for the origin of life has been established by demonstrating that an alumina surface incorporated in a tunnel junction has the catalytic ability to synthesize amino acids from ammonia, water and carbon dioxide, and sugars from wet carbon monoxide or formaldehyde. These reactants were likely components of the earth's prebiotic atmosphere. The role of such an inorganic template in the surface catalyzed theory of the origin of life is considered.

"MOST REALITY IS INDIFFERENT TO OUR DESCRIPTION OF IT."

Richard Rorty in "Contingency, Irony and Solidarity", Published by Cambridge University Press (1989).

PART I BACKGROUND AND REVIEW OF PREVIOUS WORK

CHAPTER ONE - AN INTRODUCTION TO IETS AND THE THEORY INVOLVED.

1.1 INTRODUCTION TO IETS.

Inelastic Electron Tunnelling Spectroscopy (IETS) provides information concerning the vibrational and excitational modes present in molecular species adsorbed onto an electrically insulating substrate.

The objective of this introduction is not to cover the entire IETS literature to date; rather it is hoped that it may stimulate an interest in IETS amongst researchers by outlining some of the systems already studied using IETS and to provide sufficient background information to enable the reader to understand the process of tunnelling electrons and the methods of spectral production.

1.1.1 What is IETS ?

The concept of tunnelling electrons is described in quantum mechanical terms later in Section 1.2 [Schrödinger, 1926]. Electron tunnelling between metals separated by a thin insulating barrier, has been widely studied by physicists during the last twenty nine years, the solid state properties of the tunnelling media being of main interest. Giaever first experimentally demonstrated tunnelling electrons in 1961 and was later awarded the Nobel prize for his work in this field [Giaever, 1974]. However, it was not until 1966 that Jaklevic and Lambe illustrated that species doped within the metal-insulator-metal (M-I-M) junction absorbed energy from tunnelling electrons [Jacklevic and Lambe, 1966]. The transmission of energy from electron to dopant was detected using a second derivative technique to ascertain the small changes that occurred in the electrical properties of the M-I-M junction. These changes were shown to occur at characteristic voltages which Jaklevic and Lambe were able to relate to vibrational states of the dopant molecule. The term "inelastic" is used to describe tunnelling process where the electron gives up energy to the dopant species. This differentiates the process from the principal, electrical current transmission across the barrier which is without energy loss and so described as "elastic" tunnelling. It was from this observation that the technique of Inelastic Electron Tunnelling Spectroscopy (IETS) has evolved.

1.1.2 Why Chemists Should Know About IETS ?

Whilst most workers in this field are more interested in the physical aspects of this technique, particularly in studying band gaps in semiconductor materials, the potential for chemists is great. The molecular interaction of the adsorbate with a surface can be studied and hence such areas as corrosion, heterogeneous catalysis and adhesion may benefit from IETS studies. The spectral range covered by IETS is also significant. Most studies in IETS concentrate on the vibrational spectra of adsorbed molecules. This occurs at bias voltages applied across the tunnel junction of between 0 and 500 mV (since the equivalent electron energy will be 1meV per 1mV of applied potential, and as 1 meV $\equiv$ 8.065 cm^{-1}, this is equivalent to an energy range of 0 to 4000 cm^{-1}). However, there is no theoretical reason why higher energy spectra, e.g. electronic, should not be studied. The main obstacle to studying higher energies is the dielectric strength of the insulator. The higher bias voltages required to study electronic transitions can result in insulator dielectric breakdown. In the case of the standard $Al\text{-}AlO_x\text{-}Pb$ junction, most widely used and used in this study, breakdown has been shown to occur at about 2.2 volts. Even so, low lying electronic transitions have been observed [Léger et al., 1972] [DeCheveigne et al., 1977] [DeCheveigne et al., 1975] [Adane et al., 1975] and are discussed in Section 2.5. Léger observed electronic transitions in several large molecules such as metal phthalocyanines, tetracene and ß-carotene [Léger et al., 1972]. One further problem, in the observation of higher energy transitions, is the reduced sensitivity of the second differential detection technique arising from the greatly increased conduction at the higher bias voltages. The following excitations have been observed using IETS :

Type of Excitation	Excitation Potential
Phonons in metal electrodes at the metal insulator interface [Adler, 1969].	Up to 50 mV
Molecular or lattice vibrations of the insulating barrier [Jaklevic and Lambe, 1970].	50 - 120 mV
Vibrations of molecules contained within the insulator region.	120 - 500 mV
Electronic transitions (see Section 2.5).	> 1V

The most useful attribute of IETS for chemists is the high sensitivity of the technique. Even a basic IET spectrometer, without signal enhancement, is capable of studying surface coverage of less than a monolayer.

1.1.3 A Comparison of IETS with Other Surface Spectroscopies.

In this comparison IETS has been compared with other better known surface vibrational spectroscopies. Other surface techniques such as ESCA and XPS yield information about the chemical elements present on the surface rather than the bonding and surface interactions involved.

The major advantages that IETS has over other surface spectroscopies, such as infrared and Raman, are:

i. IETS has the ability to observe both Raman and infrared active vibrational modes. Optically forbidden vibrational modes are also able to be observed using IETS (see Section 2.7.1).

ii. IETS has far greater sensitivity than any of the other surface spectroscopies [Langan and Hansma, 1975].

Only in the last few years have surface infrared techniques been able to approach the level of sensitivity set by IETS and then only by using sophisticated data handling techniques. With IETS, high sensitivity is obtained with minimal data handling and very simple signal averaging. Hence, there is still considerable potential for further improvement of the sensitivity of IETS.

Finally, IETS can often afford information about dopant-surface interactions which other surface infrared and Raman techniques cannot always achieve.

A near comprehensive review of other modern surface spectroscopic techniques has recently been produced [Woodruff and Delchar, 1986]. In fact the only surface technique it fails to consider is IETS. This illustrates the lack of appreciation of IETS as a surface spectroscopy by the more conservative surface spectroscopists.

Other recent reviews of the theoretical aspects and practical applications of IETS in chemistry have been carried out by Lewis et al. [1988] and Brown [1988].

1.2 AN INTRODUCTION TO THE THEORY OF ELECTRON TUNNELLING.

In 1926, Schrödinger first accounted for the behaviour of tunnelling electrons [Schrödinger, 1926]. He explained their wave properties and how they are able to pass though a classically forbidden area, such as a thin insulator, within a tunnel junction. This is achieved in quantum mechanical terms by considering the stationary state solution to Schrödinger's wave equation. This solution accounts for what happens when a sub-atomic species encounters a potential barrier. However it does not completely cover the situation when considering a particle in motion and will not give any information about it's position with respect to time.

Schrödinger's wave equation for one dimension, x, is given by:-

$$\left[\frac{-h^2}{2m} \frac{d^2}{dx^2} + V(x) \right] \psi(x) = E \psi(x)$$

where m = mass of the particle
h = Planck's constant / 2π
$V(x)$ = Potential Field
and $E(x)$ = Electron Energy

When considering a free electron (e^-) in the absence of any potential field, $V(x)$, the equation becomes:-

$$\frac{-h^2}{2m} \frac{d^2}{dx^2} \psi(x) = E \psi(x)$$

which can be written as:-

$$\boxed{\frac{d^2}{dx^2} \psi(x) + k^2 \psi(x) = 0 \quad \ldots (1)}$$

where $k^2 = 2mE/h^2$

The general solution to equation (1) is:-

$$\psi(x) = Ae^{ikx} + Be^{-ikx}$$

Figure 1.1 illustrates the position when an electron encounters a potential barrier at x=0. From the above equation, electrons moving in the +x direction (from right to left) will be described by the term e^{ikx} and electrons moving in the -x direction will be described by e^{-ikx}. The electron is considered to be travelling from the -x direction (from left to right). There are two electron movement scenarios that need consideration. These are by both the classical and quantum mechanical approaches.

(i) The electron energy is greater than the height of the potential step.

(ii) The electron energy is less than the height of the potential step.

In (i), using a classical approach, the electron can pass into region II as $1/2mv^2 > V_o$. The reduction in velocity of the electron is given by the conservation of momentum.

$$1/2mv_I^2 = 1/2mv_{II}^2 + V_o$$

In (ii), with $1/2mv^2 < V_o$, the electron would not pass into region II and would be reflected at x=0. The electron would not be allowed in region II as this would result in it possessing negative energy which is classically forbidden.

Applying a quantum mechanical approach, in case (i) the electron is described by Equation (1) and thus the solution is as before:-

$$\psi(x) = Ae^{ikx} + Be^{-ikx}$$

In region II, Schrödinger's equation becomes:-

$$\frac{-h^2}{2m}\frac{d^2}{dx^2}\psi_2 + V_o\psi_2 = E\psi_2$$

on rearranging

$$\boxed{\frac{d^2}{dx^2}\psi_2 + k'^2\psi_2 = 0 \quad \ldots (2)}$$

where $k'^2 = 2m(E-V_o)/h^2$

and E = electron energy

In region II the electrons are travelling in the +x direction and hence the solution to equation (2) is:-

$$\psi_2(x) = Ce^{ik'x}$$

Figure 1.1. The Potential Step.

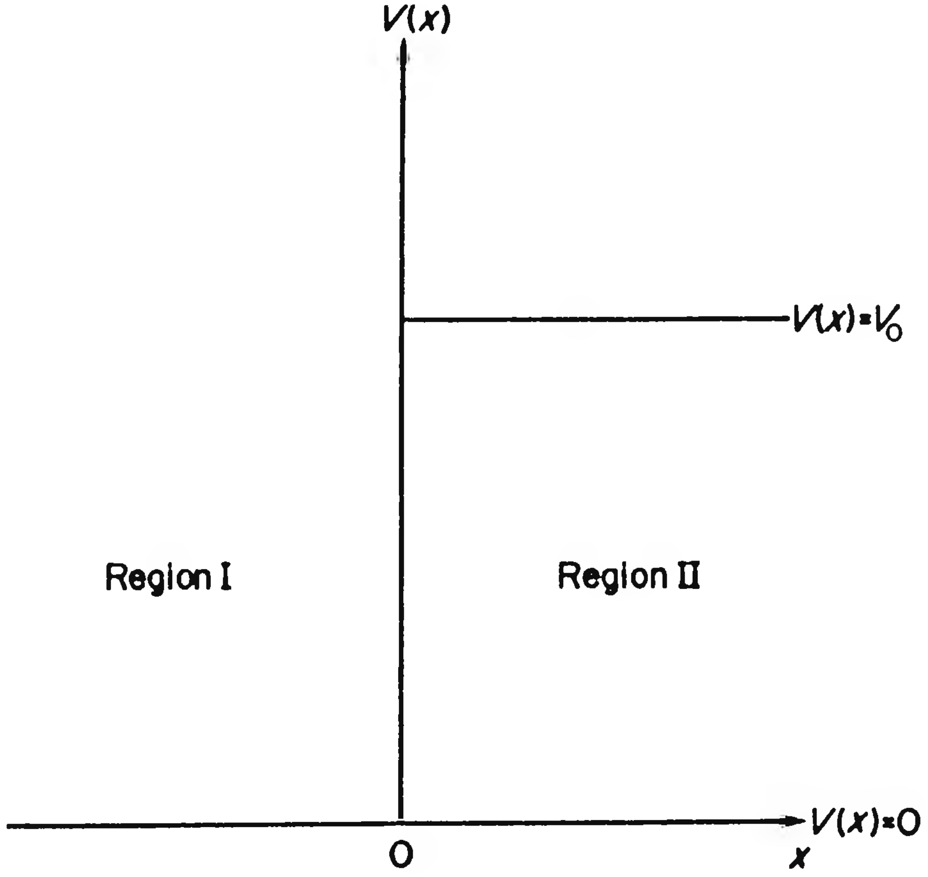

Normally, in the classical case, all electrons with incident energy greater than V_o would be expected to pass into region II. However, it is shown that B is finite, indicating that electrons are moving in the -x direction. This suggests that some electrons are reflected in x=0 even though their energy is initially greater than the step height.

In case (ii), the Schrödinger equation in region I is as it was before with the same solution as before i.e.:-

$$\frac{d^2}{dx^2} \psi_2 + k^2 \psi_1 = 0$$

In region II the Schrödinger equation becomes:-

$$\frac{h^2}{2m} \frac{d^2}{dx^2} \psi_2 + V_o \psi_2 = E \psi_2$$

$$\text{or} \quad \frac{d^2}{dx^2} \psi_2 + k''^2 \psi_2 = 0$$

where $k''^2 = 2m(E-V_o)/h^2$

and E = electron energy

So the solution again is a linear combination of $e^{ik''x}$ and $e^{-ik''x}$. In this case the increasing exponential must be disregarded as the amplitude of the wave must decrease in region II due to the loss of energy. Therefore, the solution must be:-

$$\psi_2(x) = Ce^{-ik''x}$$

We know that $\psi_2(x)$ is not zero and therefore there must be a finite probability of finding an electron in region II. The probability decreases with the increase in x.

To appreciate the tunnelling process it is necessary to consider a potential barrier rather than a potential step such as in Figure 1.2. For regions I and III $V(x) = 0$ For region II $V(x) = V_o$ and $0 < x < L$. Quantum mechanics shows that the wave function for the electron is not 0 but it will decrease with an increase in x. So if the barrier is thin, so that L is small, the reduced amplitude wave function still occurs in region III. In a tunnelling spectrum, the electron which is operating normally with a potential of 0 to 500 mV, the peak position is directly related to the energy of the vibrational mode of the dopant molecules and is explained by considering the situation when a voltage is applied across a tunnel junction of metal-insulator-metal composition. When a voltage is applied to two dissimilar metals separated by an insulating barrier the intrinsic Fermi levels of the metals will differ in energy by several electron volts, as shown in Figure 1.3. Elastic electron tunnelling can occur giving a current which shows an approximately linear relationship to the voltage applied. However, if an additional conduction path such as inelastic electron tunnelling exists a discontinuity will appear in the gradient of the current/voltage plot, as shown in Figure 1.4a. For inelastic electron tunnelling to occur $eV \geq h\nu$, where ν is a vibrational frequency of the dopant molecule and V is the barrier potential. The discontinuity in the current/voltage curve gradient will therefore occur when $eV = h\nu$. As the voltage increases the difference in the two metals' Fermi levels increases and more vibrational modes are accessible and a series of discontinuities seen. Identification of the discontinuities is facilitated by use of the second derivative of the current/voltage curve, i.e. d^2I/dV^2 as shown in Figure 1.4c.

The effect of the bias polarity on vibrational mode energy has been studied using IETS [Reynolds et al., 1987]. It was shown that for certain vibrational modes (primarily the O-H stretching mode in an undoped junction) the peak position was affected by the change in the electric field caused by changing the polarity of the bias of the tunnel junction (typically $2mV \cong 16cm^{-1}$).

Figure 1.2. The Potential Barrier.

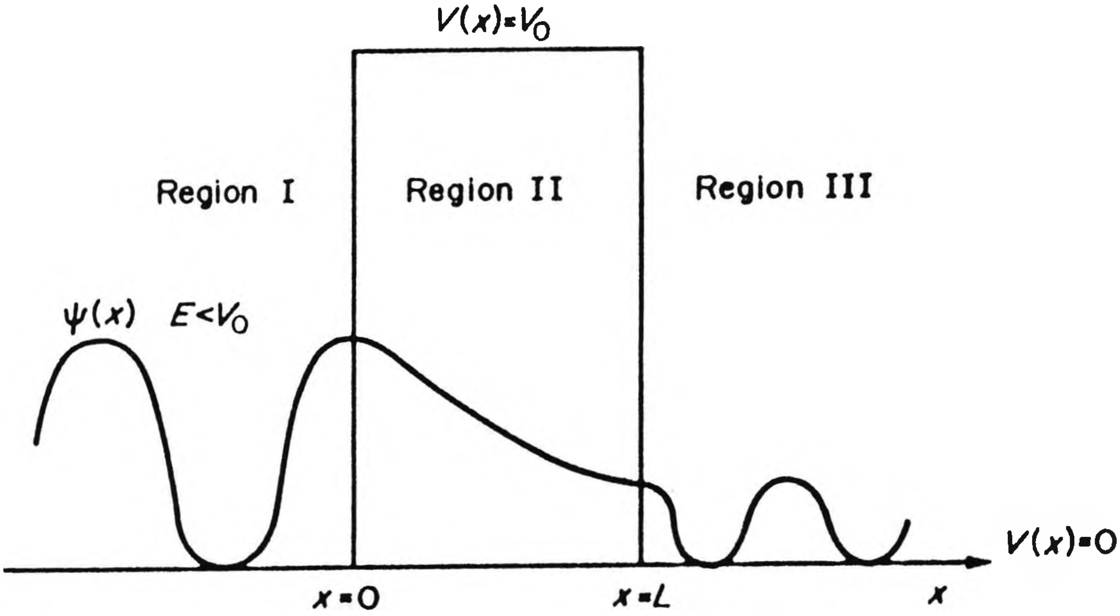

Figure 1.3. Schematic Diagram of the Fermi Levels in Tunnelling Between Normal Metals.

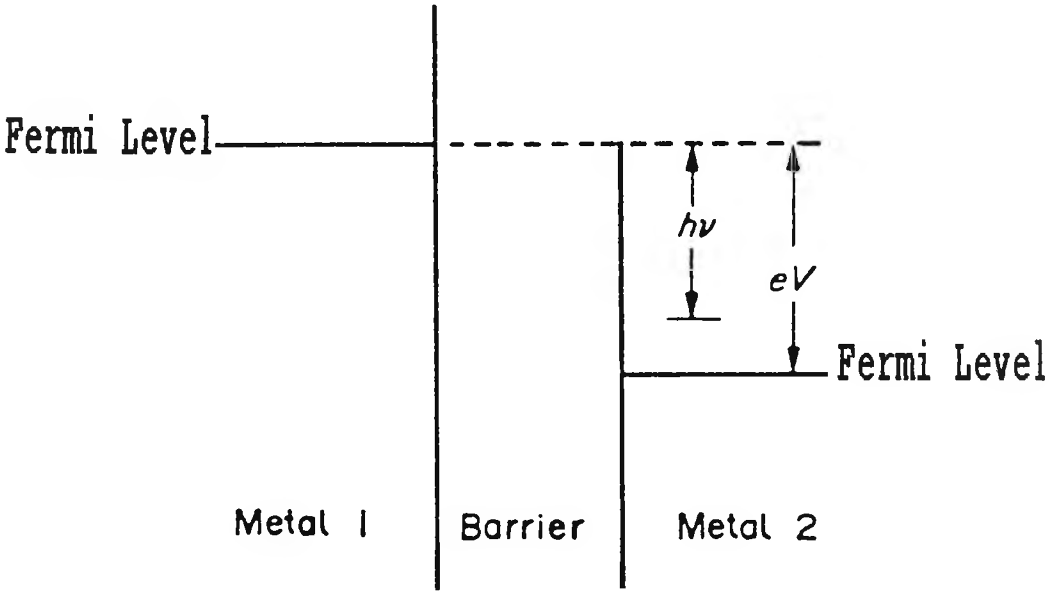

Figure 1.4. The Current / Voltage Curve and its Derivatives.

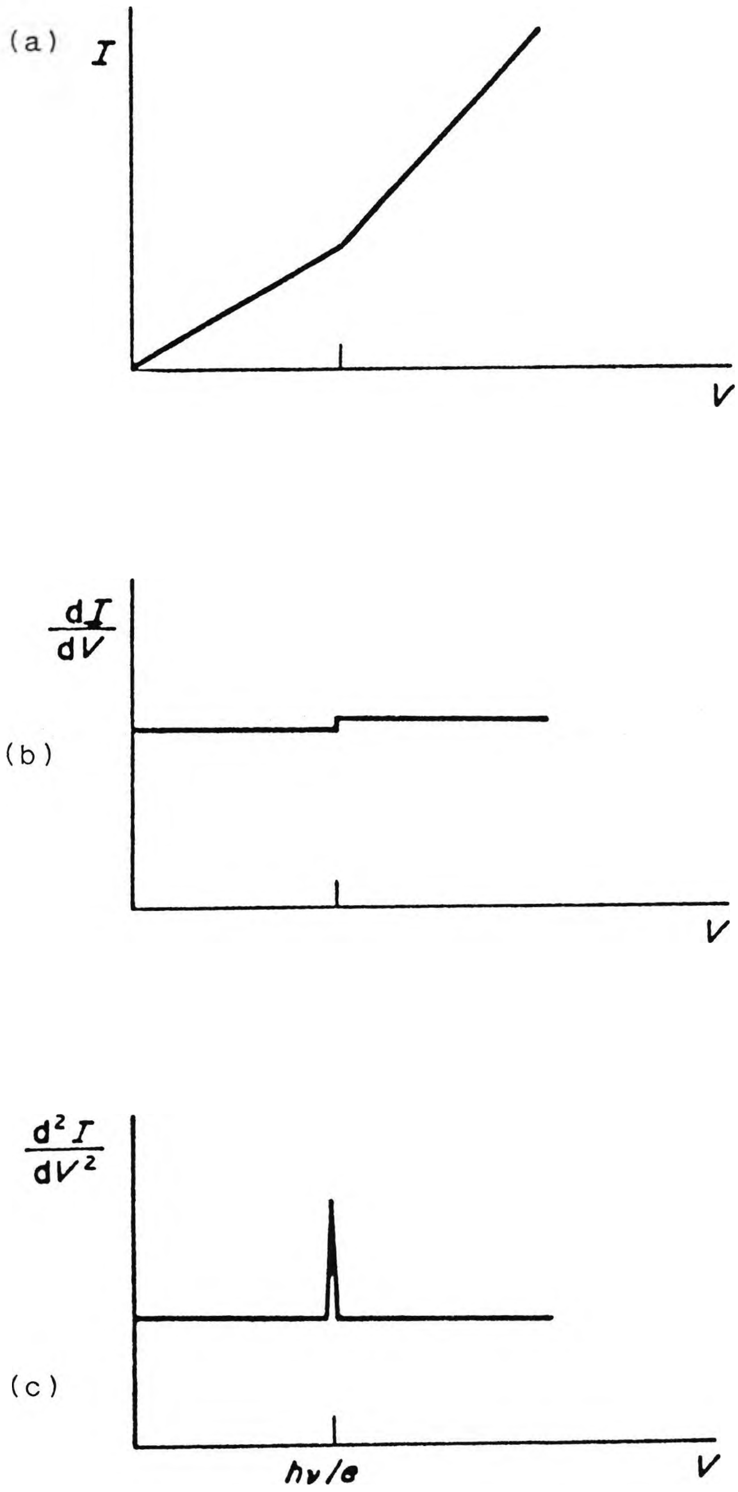

1.3 PEAK INTENSITY AND BROADENING EFFECTS.

There are three intrinsic parameters which affect the intensity and width of a peak in an IET spectrum in addition to the natural peak width. These are discussed in turn below.

1.3.1 A.C Modulation Voltage Broadening.

The applied A.C. modulation voltage used in the second derivative detection system results in the broadening of the observed peaks. The higher the A.C. modulation voltage the broader the peak.

The effect of modulation broadening was first discussed by Klein et al. and was developed in work done by Léger [Klein et al., 1973] [Léger, 1981]. The current through the junction as a function of time can be described as follows:-

$$\boxed{I = f(eV_o + eV_w.\cos 2wt) \qquad \ldots (3)}$$

where $f(V_o)$ is the junction characteristic at voltage V_o. V_w is the modulation amplitude at frequency w.

Let $f''(eV)$ be the theoretical second derivative and $F''(eV)$ be the experimentally derived function. To determine the second differential, d^2I/dV^2, this value at this frequency can be described as:-

$$I_{2w} = \frac{2}{\tau} \int f(eV_o + eV_w.\mathrm{coswt})\ \mathrm{cos2wt.dt}$$

Two partial integrations give the equation :-

$$\boxed{I_{2w} \quad \alpha \quad \int_{-eV_w}^{eV_w} F''(eV_o + E)[(eV_w)^2 - E^2]^{3/2}\ dE \qquad \ldots\ (4)}$$

where $E = eV_w\mathrm{coswt}$

A plot of Equation 4 is given in Figure 1.5. It shows a peak shape for a vibrational mode of negligible natural width in the absence of any other broadening effect (see later in this Section). ΔV, the root mean square of the applied modulation voltage, is used as this is the conventional experimental value measured. The electronic circuitry is designed so that the spectrometer operates at the lowest modulation voltage possible. However there is a limit to this in that at very low modulation voltages, less than 0.5 mV, the second differential signal is so small that the response is seriously reduced. So to obtain any spectral signal the scan time would have to be increased by an enormous amount. The second differential response varies approximately with the square of the modulation voltage.

Figure 1.5. Peak Shape due to A.C. Modulation Voltage Broadening.

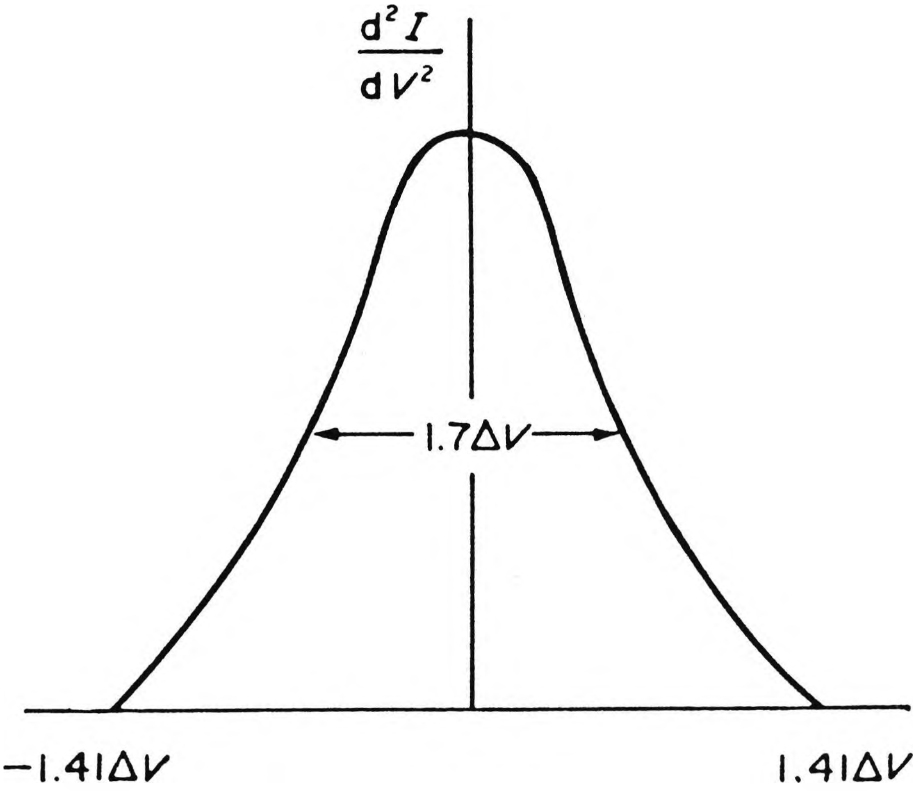

1.3.2 Thermal Broadening.

The effect of thermal broadening, first discussed by Lambe and Jaklevic, results from thermal smearing of the Fermi levels above absolute zero temperature (0K) [Lambe and Jaklevic, 1968]. This temperature effect allows tunnelling to occur above and below the actual bias voltage required to observe a particular vibrational mode. Their treatment is outlined below.

Consider a peak of negligible width of energy $h\nu$. The inelastic electron tunnelling current can be expressed as follows:-

$$\boxed{I_i = C \int_{-\infty}^{+\infty} dE f(E)[1 - f(E + eV - h\nu)] \quad \ldots (5)}$$

where I_i = inelastic electron tunnelling current

h = Planck's constant

$f(E)$ = Fermi function

E = total electron energy

ν = vibration frequency

C = parameter which includes tunnelling effects independent of the electron energy and electron - molecule coupling interactions.

Equation (5) is a mathematical expression for the electrons which have enough energy to tunnel from a filled state in one electrode to an empty state in the other electrode. Evaluating the integral gives:

$$I_i = C \int_{-\infty}^{+\infty} dE \left[\frac{1}{1 + \exp(E/kT)} \right] \times \left[1 - \frac{1}{1 + \exp\{(E + eV - h\nu)/kT\}} \right]$$

where V = applied voltage

T = temperature (K)

k = Boltzman's constant

Differentiating twice gives:

$$\boxed{\frac{d^2 I_i}{dV^2} = C \frac{e^2}{kT} \frac{e^x (x - 2) e^x + (x + 2)}{(e^x - 1)^3} \quad \ldots (6)}$$

where $x = (eV - h\nu)/kT$

Although d^2V/dI^2 is the derivative evaluated by experiment, and not d^2I/dV^2, which has been calculated, the two can be related as follows:

$$\frac{d^2 V}{dI_i^2} = - \left[\frac{dV}{dI} \right]^3 \frac{d^2 I_i}{dV^2}$$

dV/dI effectively being constant. Hence from equation (6) it is possible to predict peak width arising from thermal broadening. This is illustrated in Figure 1.6. Experimental work by Jennings and Merrill has confirmed the temperature dependence of peak widths as predicted by Lambe and Jaklevic [Jennings and Merrill, 1972]. Typical peak widths are 150 meV (1210 cm^{-1}) at room temperature, 36 meV (290 cm^{-1}) at liquid nitrogen temperature (77K) and 2meV (16cm^{-1}) at liquid helium temperature (4.2K). Therefore, for good resolution to be possible the spectra need to be produced from junctions at 4.2K or less.

1.3.3 Superconductivity Effects.

A consequence of the low temperature required for good spectral resolution is that one or more of the electrodes in a tunnelling junction may be superconducting. The presence of a superconductor is distinctly beneficial to the resolution of spectra obtained by IETS. The improvement in peak resolution arises from the resulting energy gap of 2Δ centred on the Fermi level in the superconducting metal state. The reduction in the number of electrons that can be thermally excited across the superconducting gap significantly restricts the smearing of the Fermi level that occurs when a metal is in its normal state. Gaiever et al. reported an increase in resolution by a factor of five by using superconducting instead of normal, non-superconducting electrodes [Giaever et al., 1962].

Figure 1.6. Peak Shape Due to Thermal Broadening.

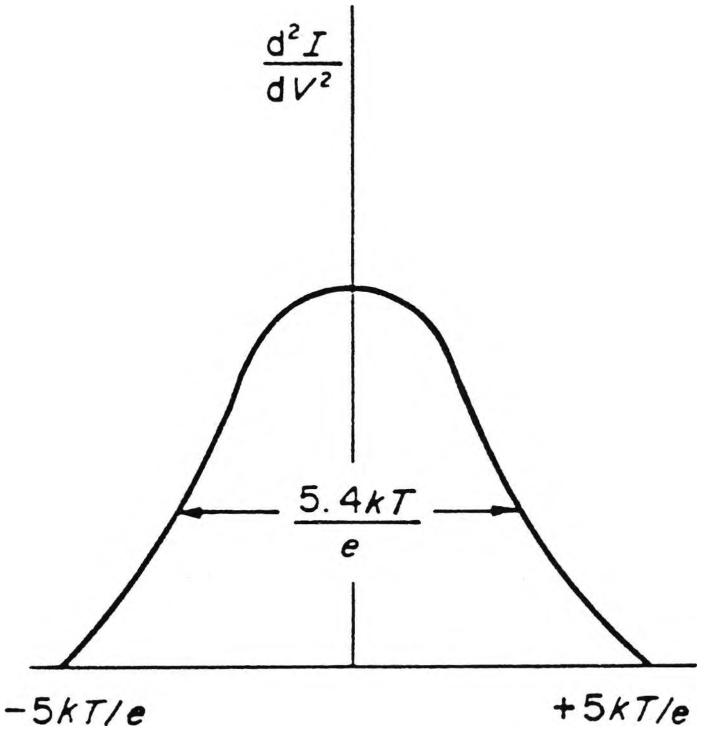

1.3.4 Sensitivity.

The most significant advantage of IETS is the sensitivity of the technique. Electrons couple more strongly to molecular vibrations than do photons. Hence it has greater sensitivity than infrared and Raman spectroscopies. There is much evidence to suggest that the doped species in tunnelling junctions may consist of a monolayer or less [Langan and Hansma, 1975]. This work also included studies on quantitative measurement of adsorbate species by IETS, but while results are promising, further work is required. Difficulties arise due to problems in interpreting and predicting peak intensities, as discussed by Scalapino and Marcus [Scalapino and Marcus, 1967], Lambe and Jaklevic [Lambe and Jaklevic, 1968] as well as Cunningham and Weinberg [Cunningham and Weinberg, 1979]. This topic is further complicated by the selection rule employed in IETS as outlined in the next Section. The study of spectral peak intensities has been discussed previously in far greater detail [Naylor, 1982] [Lewis, 1985].

1.3.5 The Selection Rule.

Present experiments indicate that the only selection rule which seems to be applicable to inelastic electron tunnelling spectroscopy is a molecular orientational one.

If a particular bond is parallel to the surface the tunnelling electron seems to interact very weakly or not at all with the bond and the vibration mode remains unobserved. If a bond tends to be perpendicular to the surface, maximum interaction has been shown to take place between the tunnelling electron and so the vibration is observed (see Figure 1.7). Shott and Field have confirmed this selection rule by considering the spectrum of N^3-benzoyl-3',5'-diacetyl-2'-bromo-2'-deoxyuridine [Shott and Field, 1980]. Rings 1 and 2, as shown in Figure 1.8, are perpendicular to one another and hence this compound is useful in determining the operation of the orientational selection rule. The spectrum was obtained using a solution of the compound in benzene. The carbonyl groups of ring 2 and the C-N bands and skeletal vibrations of the ring were found to be absent in the spectrum produced. Vibrations associated with ring 1, especially that of the cyclic ether, are all observed. This leads to the conclusion that the molecule is adsorbed onto the surface of the alumina with the ring 2 parallel to the surface and ring 1 perpendicular to the surface. Hence by considering the vibrational modes seen in an IET spectrum it is possible to determine the orientation of the molecule on the surface.

Both infrared and Raman active vibration modes are seen in IETS as has been shown by Bogatina et al and Simonsen et al. Bogatina examined the spectrum of benzene in a Pb-PbO_x-Pb junction [Bogatina et al., 1974]. Benzene has sufficient symmetry that there are separate Raman and infrared active modes. In molecules of insufficient symmetry both the dipole moment and the polarisability oscillate during the vibration leaving no vibrational modes totally independent of either Raman or infrared modes. Both Raman and infrared modes were observed with no evidence to indicate a difference in intensity between the two. Simonsen et al. studied anthracene, producing a spectrum with both Raman and infrared modes observed [Simonsen et al., 1974]. In both the benzene and the anthracene spectra some expected vibrational modes were not observed. This has been attributed to the geometrical selection rule.

Figure 1.7. The Orientation Selection Rule of IETS.

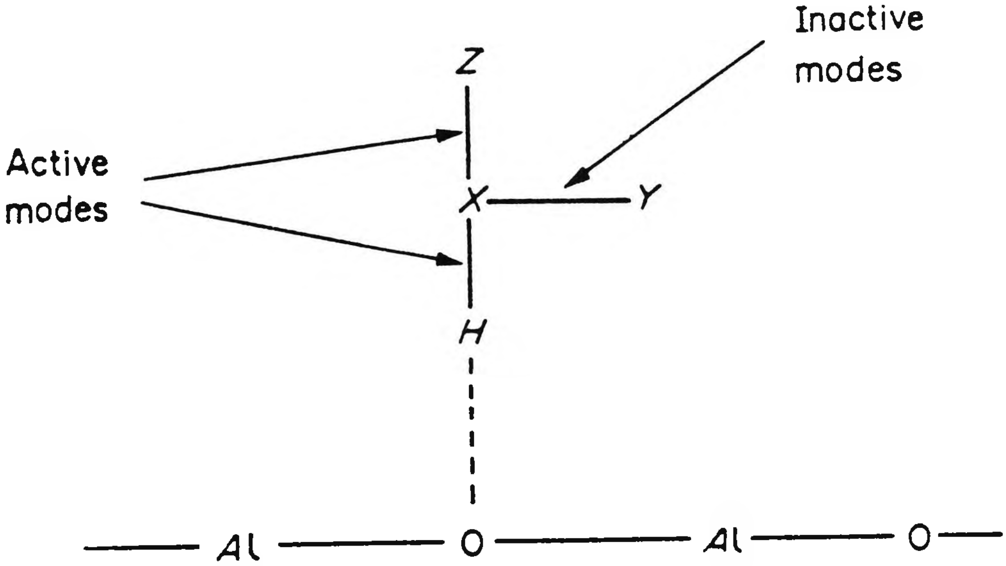

Figure 1.8. The Structure of N^3-benzoyl- 3',5'-diacetyl-2'-bromo-2'-deoxyuridine.

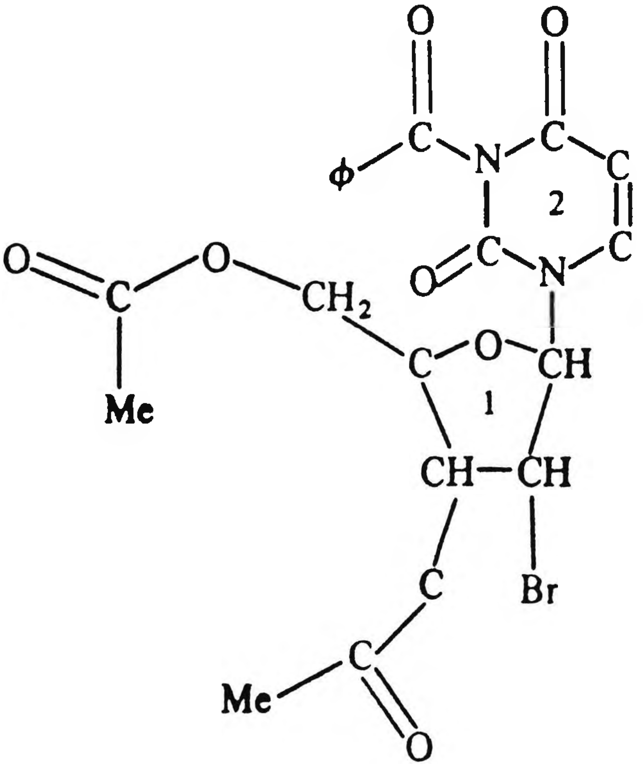

CHAPTER TWO - THE CHEMICAL APPLICATIONS OF IETS.

2.1 INTRODUCTION.

The present chemical applications of IETS may be placed into six broad classes. These applications are illustrative, rather than comprehensive because the objective of this chapter is to indicate the present uses of IETS for chemists:

1) Surface induced reactions.
2) Adhesion and corrosion studies.
3) Molecular orientation studies on surfaces.
4) Electronic transition studies.
5) Systems of biological interest.
6) Inorganic studies.

2.2 SURFACE INDUCED REACTIONS.

This is possibly the most interesting of the chemical applications of IETS. Due to the relative sensitivity, wide spectral range and good resolution of the technique, it is possible to monitor not only the production of surface induced reaction products but also, in certain instances, the reaction intermediates.

2.2.1 Surface Adsorption and Reaction.

Formic Acid

By studying the adsorption of small molecules on the alumina surface, simple surface reactions can be observed. Larger molecules could block some potential reaction sites and may inhibit surface reactions. Formic acid has been shown to react with the alumina surface to produce the formate ion $HCOO^-$ [Klein et al., 1973]. Figure 2.1 shows the tunnelling spectrum of formic acid. The absence of C=O and C-OH stretching modes, as well as the presence of COO^- vibration modes, is indicative of the formation of the anion. This behaviour is often observed with different types of carboxylic acid as the COO^- anion is very stable on the oxide surface of the tunnel junction.

The reaction between CO_2 and H_2O has been studied and shown to produce "formic acid like" species on the tunnel junction surface [Field et al., 1985]. Similarly NH_3 and CO_2 with water have been shown to produce simple amino acids. CO and water co-adsorbed on alumina produce spectra similar to carbohydrates [Field and Spencer, 1989].

The Effect of Pretreatment of the Alumina Substrate

The effect of pre-adsorption of HCl onto the alumina of a tunnel junction and the subsequent surface reactions have been studied. In particular the adsorption of carboxylic acids, ethanol and pyridine onto the HCl treated insulator oxide surface have been investigated [DeCheveigne et al., 1985]. These studies tend to suggest that :-

a) Complete dissociative adsorption of HCl occurs on the surface.
b) Inhibition of the adsorption of carboxylic acids and alcohols occurs.
c) The adsorption of pyridine seems not to be affected.

Mechanisms for these effects have been put forward [DeCheveigne et al., 1985].

Figure 2.1. Tunnelling Spectrum of Formic Acid [Klein et al., 1973].

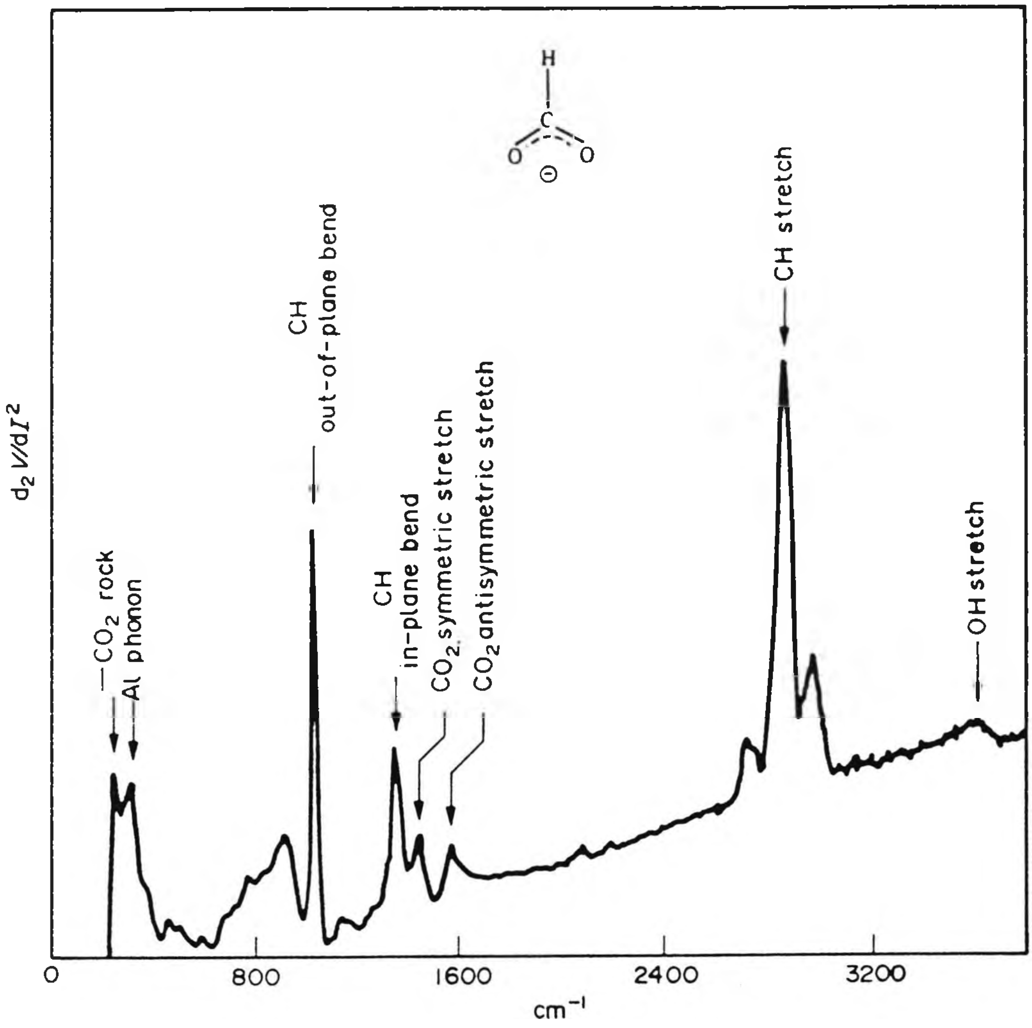

Surface Reactions Involving Reduction

The adsorption and subsequent surface reactions of p-nitrobenzoic acid and of p-nitrophenol on the alumina substrate have been studied [Monjushiro et al., 1985]. It has been shown that p-nitrobenzoic acid adsorbs by the formation of a carboxylate anion, as in formic acid, and p-nitrophenol produces a phenate anion on the surface. It is suggested that, through reaction with the hydroxylated alumina surface, adsorbed nitro-substituted molecules undergo reduction. This mechanism has been indicated by the introduction of D_2O to produce Al-OD surface species and observing the deuterium exchange to the adsorbed molecule. This has been confirmed by the study of p-aminobenzoic acid itself. Reactions similar to the above are considered in Section 6.3.2.

2.2.2 Polymerization.

Studies have shown that $Zr(BH_4)_4$ may be used as a "supported homogeneous" catalyst for the polymerisation of alkenes and alkynes [Evans and Weinberg, 1980] and, more recently, unsaturated cyclic hydrocarbons [Forester, 1987] on the alumina of the tunnel junction; although this process is less rapid than using a Natta type of catalyst. IETS has been applied to observe the vibrational modes of acetylene, ethylene and propylene under these conditions.

Acetylene was found to produce long polymer complexes, with no observable effect on the existing ligands on the Zr, from a small number of active sites. Ethylene and propylene showed the formation of polymeric surface species with similar types of $-CH_3$ and $-CH_2-$ groups.

By varying junction conditions, such as :

a) degree of hydroxylation of the oxide

b) varying the oxide studied (only AlOx studied so far)

c) using different supported catalysts

it should be possible to study in detail the increased efficiency of these systems.

2.2.3 Metal Supported Catalysis.

The uses of metal supported catalysts in industrial processes are numerous. IETS has already been shown to be of great importance in the identification of surface reaction products and some intermediates. Many supported metals have been studied,including Fe, Co, Ni, Ru, Rh, Pd, Ag and Pt on magnesia and on alumina. The method used to produce such catalysts consists of evaporating pure metal, by an electrically heated tungsten filament, onto the insulating barrier to create metal clusters. An alternative method is the thermal decomposition of a suitable organometallic compound pre-adsorbed onto the tunnelling barrier. A recent study of the use of IETS as a vibrational probe for the chemisorption of homogeneous metal cluster catalysts onto alumina and magnesia has been carried out [DeThomas, 1987]. Using simple adsorbate molecules, such as CO, the chemisorption characteristics have been studied by observation of the tunnelling spectrum and the modes of chemisorption determined [Hansma et al., 1976] [Jaklevic et al., 1986]. These studies may be directly compared with similar systems analyzed by infrared and Raman spectroscopy. The peak assignments may be checked by use of different isotopes in the adsorbate molecule. An extension of these studies is the formation of hydrocarbons by heating chemisorbed CO on Rhodium in an atmosphere of H_2 and analysing the products [Kroeker et al., 1980].

2.2.4 Intermediates.

As well as the observation of an ethylidene intermediate in the hydrogenation of CO on Rhodium [Templeton, 1984], other reaction intermediates that are stabilised by the oxide surface have been observed [Kroeker et al., 1980].

2.3 ADHESION AND CORROSION STUDIES.

Aluminium is the one of the most widely studied substrates for adhesive bonding due to its extensive use in the aerospace industry. This is fortunately convenient as alumina is the most common surface oxide studied in IETS tunnel junctions. It therefore seems that IETS is "tailor - made" for the study of adhesion to aluminium by observing reactions taking place on the metal oxide surface. A related study to that of adhesion is the investigation of the surface adsorption of polymers.

Another industrially important, surface initiated effect, is metallic corrosion. Some preliminary IETS studies in this area have already been carried out and are outlined below.

2.3.1 Adhesion Studies.

Many adhesive systems have received a preliminary study and the potential applications of IETS in the field of adhesion have been demonstrated [White et al., 1978]. However, apart from a small amount of work on other adhesive species [Reynolds et al., 1982], the most important studies have been on the interaction of epoxide adhesives with alumina [Comyn et al., 1981]. In addition to the effective interaction of the epoxides with the alumina, other constituents of adhesives, such as hardeners, have been studied [Comyn, 1984]. Several methods of interaction have been put forward and the inherent reactions that occur within the adhesive joint between the constituent parts have been elucidated by the use of IETS. Environmental effects, such as the weathering of adhesive bonds by exposure to high temperature and moisture environments, have also been studied. An example is the aging of diaminodiphenylsulphone (DPS) which is used in the industrial adhesive Hercules 3501 [White et al., 1978]. IETS has be used to produce evidence on the occurrence of corrosion and adhesive failure and the effect of water on the adhesive/surface interface [White et al., 1981]. The failure of Novolac phenol-formaldehyde resin joints by the effect of exposure to water vapour has been described using IETS [Brown et al., 1987].

The adsorption of a simulated epoxy resin fragment onto alumina has been studied using IETS and by low temperature matrix isolation infrared spectroscopy [Brown et al., 1985].

2.3.2 Polymers.

A related study to that of adhesion is the investigation of reactions involving polymers. These may contain similar functional groups to those in adhesives. Polyvinylacrylate (PVA) and polymethylmethacrylate (PMMA) have been incorporated into tunnel junctions for such studies [Comyn et al., 1986] [Mallik et al., 1985]. PVA has been shown to undergo hydrolysis on the alumina surface, producing PVOH (polyvinylalcohol) and acetic acid, which are subsequently adsorbed. PMMA shows a similar cleavage of the ester group producing carboxylate vibrational modes. The carboxylic acid is adsorbed, in the usual way (see Section 2.2.1), and the alcohol desorbed.

Other polymers, such as polyacetonitrile produced by the glow discharge of acetonitrile, have been studied using IETS [Comyn et al., 1986]. Low concentrations of the polymer (less than a monolayer) are easily detected by this very sensitive analytical technique. It has been shown that acetonitrile, polymerized by glow discharge and adsorbed onto the surface within the tunnel junction, has a very similar structure to that of bulk polyacetonitrile [Kaul and Kamfrath, 1986].

The effect on the structure of a highly conjugated organic monomer and its polymer, such as 4BCMU and poly-4BCMU, after adsorption onto an alumina surface has been studied [Burzinski et al., 1987]. It was found that rigid forms of poly-4BCMU were adsorbed onto the alumina surface producing a more flexible coil polymer form due to the destruction of the H-bonding network.

2.3.3 Corrosion Studies.

Corrosion of aluminium alloys by organic liquids is a significant industrial problem. Chlorinated solvents are used for metal cleaning and vapour degreasing which on a large scale encourages corrosion of the aluminium surfaces. IETS is ideal for studying these systems as the technique can identify reaction products and intermediates in very small concentrations and therefore aid in the study of corrosion inhibitors.

The corrosion of aluminium has been studied, and we will consider the attack of CCl_4 only as an illustration. Stern and Uhlig proposed that the reaction occurring during the corrosion of aluminium by CCl_4 was as follows [Stern and Uhlig, 1953]:-

$$2Al + 6CCl_4 \Longrightarrow 3C_2Cl_6 + 2AlCl_3$$

The process is thought to be initiated by a free radical reaction such as :-

$$CCl_4 \Longrightarrow \cdot CCl_3 + \cdot Cl$$

allowing for the production of the $CCl_3^+[AlCl_4]^-$ complex. Alternative mechanisms have been suggested, however Archer and Harter confirmed the presence of the $\cdot CCl_3$ radical [Archer and Harter, 1978]. This was shown by producing a carbon tetrachloride doped tunnel junction by the spin doped method (see Section 5.7.2). It was found to contain vibrational modes associated with CCl_4, CCl_3, C_2Cl_6, AlCl, $AlCl_2$, $AlCl_3$ and the complex $CCl_3^+[AlCl_4]^-$ [Ellialtioglu et al., 1980] and therefore provided evidence for the reaction mechanism proposed above. The corrosion of alumina by chloroform is also considered in Section 6.3.1.

Formamide is known to be a corrosion inhibitor for the systems described above. IETS has provided information on the mode of this corrosion inhibition [Ellialtioglu et al., 1981]. The spectrum produced from an Al-AlO_x-Pb junction doped with CCl_4 containing formamide indicated that the formamide molecules were preferentially adsorbed onto the alumina (shown by the absence of C-Cl vibrational modes) but the adsorbed species was not the same as the non-adsorbed molecules. Hence, a model of the interaction could be produced.

Such studies into corrosion inhibition have been followed by investigations of more inhibitors with functional groups similar to those already studied [Ellialtioglu, 1984] [White et al., 1981].

2.4 MOLECULAR ORIENTATION STUDIES.

The study of specific orientations of molecules on the alumina surface of a tunnel junction require the acceptance of the selection rule outlined previously in Section 1.3.5. Without the orientational selection rule restricting the observation of vibrational modes, it would be impossible to indicate the alignment of adsorbed molecules on the insulating surface. By accepting that vibrational modes of bonds parallel to the surface will not normally be observed in the IET spectrum and by analysing for the presence or absence of vibrational modes of molecules, their surface orientation may be inferred.

Although no detailed theoretical justification has been produced for the orientational selection rule (which appears to be inherent in IETS) several studies have satisfactorily shown the selection rule to apply and therefore IETS may be used in surface orientation studies.

2.4.1 Adsorbed Acid Species.

As outlined in section 2.1.1 the interaction of carboxylic acids adsorbed onto the alumina surface of a tunnel junction tends to be through the transfer of a hydrogen atom to the surface and the subsequent ionic attraction of the resultant carboxylate anion. This has been shown to occur in the case of the benzene dicarboxylic acids. Lewis and Field [1985] have shown that when the three isomers of phthalic acid (phthalic, isophthalic and terephthalic) are introduced as 1% w/v solutions in ethanol onto the alumina, the aromatic ring vibrational modes are observed. This suggests that the planar rings are standing on the carboxylate anion, perpendicular to the surface. The C=O and C-OH vibrational modes of the unreacted carboxylic acid group are absent and therefore it must be parallel to the surface. An intermolecular H-bonding system is suggested for two adjacent adsorbed molecules of phthalic and isophthalic acid and for adjacent molecules of adsorbed terephthalic acid. The H-bonding systems have been inferred from the resultant shifts in the ring and COOH deformation modes. More concentrated ethanolic solutions of the phthalic acid isomers have also been studied [Higo et al., 1985] and various orientations of the surface adsorbed molecules suggested. Hall and Hansma [1978] have shown that sulphonic acids are adsorbed onto the alumina surface in a similar fashion to carboxylic acids. Sulphonate anions are produced, in a similar fashion to carboxylate anions, on the surface.

At present a general theory to explain and predict the relative intensities of peaks within an IET spectrum has not been developed. Once produced, such a theory would be able to determine the exact orientation of complex molecules on insulator surfaces from their experimentally measured tunnelling spectra intensities.

2.5 ELECTRONIC TRANSITION STUDIES.

In addition to the study of the vibrational modes of adsorbates in tunnelling junctions certain species exhibit electronic transitions. The main problem in researching these effects however is that tunnel junctions tend to dielectric breakdown at the biases required to monitor these transitions. This problem may be circumvented by considering either:-

(i) Dyes - which have electronic transitions in the visible range of the spectrum (These tend to be large organic molecules).

(ii) Rare earth oxides - which have low energy electronic transitions.

(iii) The use of high dielectric strength oxides within the tunnel junction - Niobium oxide is a theoretical possibility but no experimental work on these systems has been carried out.

2.5.1 Dyes.

Many different types of dyes have been studied, the largest of these group being the metal phthalocyanines [Luth et al., 1978]. These show that both the optically allowed singlet-singlet transitions and the optically forbidden singlet-triplet transitions may be seen in the IET spectra with similar intensities. It is apparent that the optical selection rules, based on spin conservation, do not apply to IETS. However, the optically forbidden transitions observed by IETS tend to be broad and the optically allowed transitions weaker in the IET spectra than their optical counterparts. The width of the peaks produced may be accounted for by the strong interactions of the molecules with a disordered environment. But the intensities are comparable with optical spectra of thin molecular films. The relative weakness of singlet-singlet transitions would be expected to occur as the tunnelling electron loses more energy in excitation stimulation. The electron may be said to encounter a much higher potential barrier than one that loses less energy. The high electron energy loss in generating electronic spectra results in a much smaller tunnelling probability [Léger et al., 1972].

2.5.2 Rare Earth Oxides.

Tunnel junctions of the type $Ho/Ho_2O_3/Pb$ and $Er/Er_2O_3/Pb$ have been made [Adane et al., 1975] and the optically forbidden transitions of $^5I_8$ - $^5I_7$ in the Ho^{3+} ion and $^4I_{15/2}$ - $^4I_{13/2}$ in the Er^{3+} ion were observed. Any optically allowed electronic transitions would be too energetic to be seen by IETS. Dielectric break down of the insulating barrier would occur before achieving a sufficiently high electron energy (i.e. greater than 5eV).

These examples show the possible uses of IETS in the study of electronic transitions. However, the peak broadening due to the ill-defined molecular environment within the junction and the inherent limit due to the dielectric breakdown of aluminium oxide tunnelling junctions (ca. 2 V) limits the practical applications of the technique with present insulating barriers.

2.6 SYSTEMS OF BIOCHEMICAL INTEREST.

IETS has been of significant use in the analysis of biochemical molecules. These have varied from the simplest "building block" amino acids and nucleotides to complex nucleic acids and proteins. The spectra produced compare well with the equivalent infrared and Raman spectra, and thus systematic interpretations of the vibrational modes of adsorbed molecules are possible. This section will outline the different groups of biological molecules that have been adsorbed on a Al-AlOx-Pb tunnel junction with illustrative examples.

2.6.1 Amino Acids.

The study of simple amino acids introduced the application of IETS to biological systems. Figure 2.2 shows the spectrum of glycine adsorbed from an aqueous solution [Simonsen et al., 1974]. In such a solution the molecule exists almost totally as a dipolar ion, and strong signals for the $-CO_2^-$ and $-NH_3^+$ ions are observed. The carboxylate ion therefore interacts with the alumina surface in the usual manner (see Section 2.2.1). Figure 2.2 is consistent with the equivalent infrared and Raman spectra of glycine. In the case of amino acids containing aromatic rings,such as L-phenylalanine [Wolfram (Editor), 1978] the ring modes are easily seen and therefore their surface orientation may be suggested. Further IETS studies of polypeptides, containing two to five amino acid segments, have been carried out [Clark and Coleman, 1980]. The resulting spectra show shifts in the vibrational signals from those of the simple amino acid; and the modes of the ring structures tend to dominate the spectra of such polypeptides. However, overlapping modes from various constituent parts of the molecules are unresolved and form broad envelopes. IETS easily distinguishes between different amino acids by the observation of specific peaks in the spectra: for example, the S-H stretching mode in cysteine near 2600 cm^{-1} [Simonsen and Coleman, 1973a and 1973b].

The synthesis of amino acid like species has been proposed as the result of the surface reaction of NH_3, CO_2 and H_2O [Field and Spencer, 1989].

The extension of IETS to more complex biological molecules has not been systematically explored, however some complex molecules have been studied, e.g. Haemoglobin [Simonsen and Coleman, 1974] and DNA [Hansma and Coleman, 1974].

Figure 2.2. Tunnelling Spectrum of Aqueous Glycine [Simonsen et al., 1974].

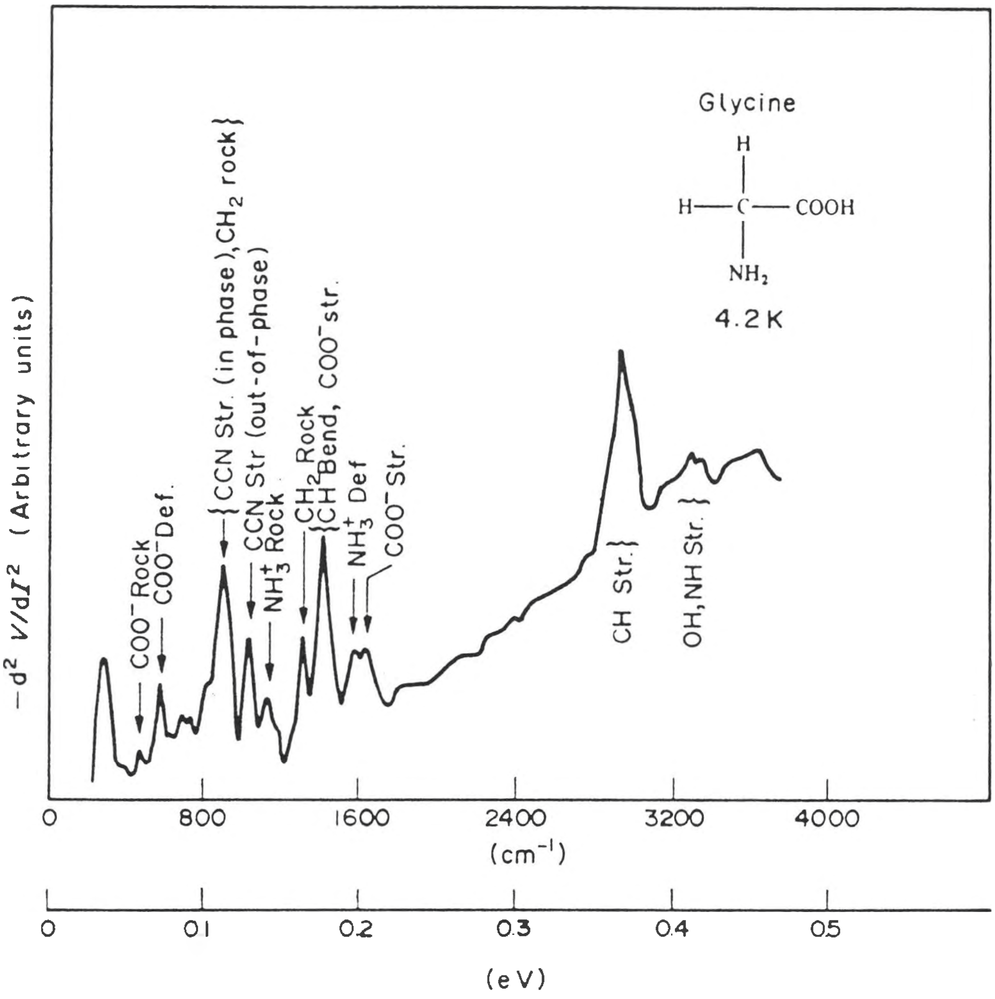

2.6.2 Pyrimidine and Purine Bases.

IET spectra have been produced for the pyrimidine and purine bases [Simonsen and Coleman, 1974] [Clark and Coleman, 1980]. It was found that the spectra of the bases were easily recognizable and are consistent with the equivalent infrared and Raman spectra. However shifts in the vibrational frequencies were seen and were thought to be caused by H-bonding in the surface interaction. The mode of attachment of the bases to the oxide surface was thought to be through interaction with the nitrogen atom in the base ring as the ring modes were shown to be dominant and therefore perpendicular to the surface.

2.6.3 Nucleotides and Nucleosides.

The extension of the studies outlined above to nucleotides and nucleosides is logical [Simonsen and Coleman, 1974] [Clark and Coleman, 1980]. Again the dominant vibrational modes in nucleotides were shown to be those of the base rings. The introduction of a sugar - phosphate group produced both vibrational modes from the additional groups and shifts of the base modes. This is consistent with the shifts observed in the equivalent infrared and Raman spectra. At pH 7, phosphomonoesters ($-PO_3^{2-}$) have been observed in the spectra of both nucleosides and nucleotides [Clark and Coleman, 1976].

Above pH 7, the $-PO_3^{2-}$ species are absent and may have reacted with the Al present on the surface. Well resolved spectra of polynucleotides have also been observed [Clark and Coleman, 1980].

The surface adsorption and orientation effects of nucleotides [Hansma (Editor) - Chapter 7, 1982] as well as the UV radiation damage on nucleotides [Clark and Coleman, 1980] have been documented.

Hansma and Coleman have produced IET spectra of nucleic acids [Hansma and Coleman, 1974]. Although the complexity of these systems is large and the resolution of these spectra a controlling factor, they showed that IETS could be used for identification purposes. More recently, improved spectral resolution has shown that comparative work on nucleic acids with infrared and Raman spectroscopies is possible.

The above examples show that although much information has been produced from the IETS of biological systems, a great deal of systematic work is still required so that the technique may realise its full potential in this field.

2.7 INORGANIC STUDIES.

Many inorganic systems have been studied using IETS. By viewing an inorganic species in a tunnel junction the technique may be considered as a molecular spectroscopy capable of studying transient species similar to that in matrix isolation spectroscopic techniques. However, by considering the species within the junction, the study of its adsorption onto the oxide may be considered as a surface spectroscopic technique (surface catalysis is considered primarily in Section 2.2). Therefore a large number of interactive and molecular properties of inorganic species may be studied.

2.7.1 Photon Forbidden Vibrational Transitions.

IETS has been shown to be able to detect both infrared and Raman active vibrational modes of a molecule adsorbed on the insulator of a tunnel junction. However, more recently, IETS has been used to observe certain vibrational modes in transition metal complexes, such as $K_4M(CN)_6$ (where M = Fe, Ru or Os) that are neither infrared nor Raman active [Williams, 1984]. In the above case two peaks in the 300 - 799 cm^{-1} range, corresponding to the t_{2g} and t_{2u} vibrational modes of the complex, have been observed. These studies have been used in the new assignment of the Raman spectra of $K_4Os(CN)_6$. The assignments of the M-C-N vibrational modes and others have been confirmed using isotopic labelling and shift measurement [Hipps and Mazur, 1980].

2.7.2 Structural Assignment of Adsorbed Metal Complexes.

IETS has been used in the structural assignment of hydridotriosmium decacarbonyl adsorbed onto the alumina surface of a tunnel junction (Figure 2.3) [Hillard and Gold, 1985]. The effect of the hydroxylation of the surface was considered and gave rise to three different situations :-

1) On a fully hydroxylated surface $Os_3(CO)_{12}$ was present.
2) On a partially hydroxylated surface hydridotriosmium clusters were formed. This was shown by the production of a Os-H-Os vibrational band in the spectrum.
3) If the junction was heated in air to 250°C an unknown species was produced which was characterised by an intense C-H vibrational band.

In the situation where the hydridotriosmium complex was produced the structure was assigned by use of the crystal structure and the orientation selection rules.

Figure 2.3. Suggested Structure of Hydridotriosmium Decacarbonyl on the Alumina Surface (Carbonyl Groups Omitted for Clarity).

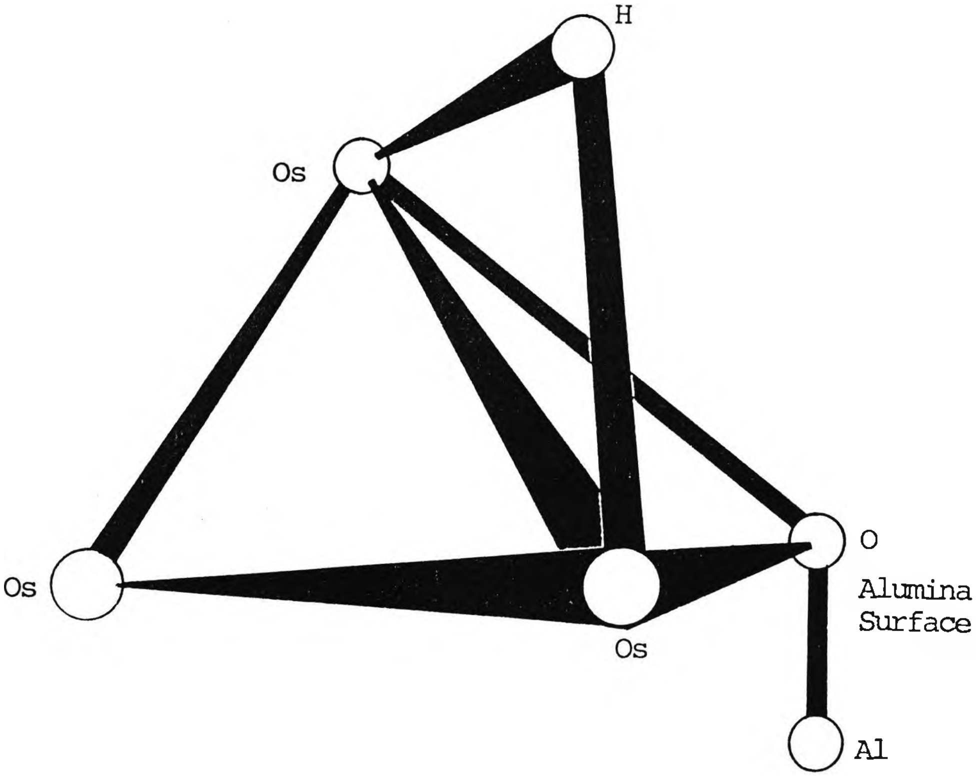

Hipps and Mazur adsorbed Ni and Co glycinate complexes onto the alumina surface [Hipps and Mazur, 1981] in an attempt to discover the method of coordination employed by the complex to the surface. Unfortunately, it was not possible, from the IET spectra in conjunction with infrared studies, to determine whether a mono- or diglycinate complexes were present in the adsorbate.

2.7.3 Reduction of Metals Within Complexes.

The effect of the hydrated magnesia and alumina insulating substrates on metals within complexes adsorbed onto the surface has been studied. For example, $Fe(CN)_6^{3-}$ has been shown to exhibit no Fe^{3+} characteristics whilst adsorbed on the alumina surface [Hipps and Mazur, 1980]. Fe^{3+} species have been shown to exist by the addition of HCl and NaOH. However with a gold top electrode other surface reactions have been shown to arise. These reactions may be avoided by cooling the junction whilst depositing the top electrode.

In the case of $Mo_2(CN)_8$, reduction of the metal within the complex has been shown to occur on the alumina surface [Williams, 1984].

Other systems involving inorganic entities have been studied, such as the method of adsorption of (n-butyl) tin chloride and mercury-1-nitrate [Field - unpublished]. This illustrates the utility of IETS in studying metal to ligand and metal to metal vibrations.

It is impracticable to detail here all the potential uses of IETS in the study of inorganic species as the diversity of application is so large. Such characteristics as electronic transitions in inorganic complexes and the uses of inorganic complexes, such as $Zr(BH_4)_4$, and metals in the field of catalysis have been outlined in Sections 2.7.1 and 2.2.3.

2.8 CONCLUSIONS.

Considering that inelastic electron tunnelling spectroscopy has been studied for twenty-four years and that significant instrumental advances in the production of high resolution spectra have taken place during this period; it is somewhat surprising that the technique is still largely unfamiliar to the majority of chemists.

As has been shown in this chapter, preliminary studies in the application of IETS to many fields of study have been carried out. It would therefore be expected that considerable research effort would be extended into these studies in the near future. By doing so, the full potential of IETS as an surface spectroscopic technique will be achieved.

CHAPTER THREE - COUPLING AGENTS FOR ADHESION PROMOTION

3.1 INTRODUCTION.

Coupling agents, also known as adhesion promoters and surface primers, enable and "promote" the bonding of non-compatible substances or surfaces to a substrate and additionally increase to a very marked degree the durability of adhesive joints in adverse conditions. This could be either to aid the production of an adhesive joint between substrates such as metals, ceramics, wood or glass, or to enable the adhesion of organic surface coatings to the above substrates. Many coatings show a loss of adhesion under conditions of high humidity and under water immersion. The improvement of these adhesion processes leads to a reduction in other effects such as corrosion or adhesive joint failure.

Many surface preparation techniques are used to maximize adhesive processes. These range from the removal of surface contamination by vapour or solvent degreasing and grit blasting to change the surface profile, to chemical treatment of the surface, such as anodization, phosphating of steel and conversion coating aluminium substrates. Although these more conventional practices are very widely used by industrialists an effective tool of increasing importance is the use of adhesion promoters.

Adhesion promoters are used to form primary bonds to either the substrate or to the surface coating / adhesive, or both, with the aim to improve the initial "wet" adhesion process by increasing the surface interaction of the substrates. In addition to the improvement in adhesion, some coupling agents modify bulk properties. For example, some have been shown to improve polymer composite performance by changing the viscosity of filled polymer systems.

It is surprising however, considering the large amount of interest in adhesion promoters generated by the reinforced plastics and adhesives industries, that the apparent interest is not reflected by the amount of published literature on the subject. This may be explained by the problem of commercial secrecy as manufacturers are unwilling to share propriety knowledge with competitors in a highly competitive industry.

The first real coupling agents, manufactured in the mid- 1950s, were the amino-functional silanes. These were used to improve the interfacial adhesion of phenolic resin based composites especially when exposed to water. These coupling agents were the forerunners of the huge series of silane adhesion promoters used in polyester resin based composites. The most important of these were the vinyl silanes. Shortly afterwards, chromium complexes were developed for use on glass substrates and methacrylate functional silanes were produced for use in the rapidly growing field of glass fibre reinforced polyester composites. In the mid-1960s the extent of the detrimental effect of water on adhesives and surface coatings was realized [Falconer et al., 1964] and the potential use of silane coupling agents noted. During the 1960s and early 1970s a considerable amount of theoretical and experimental effort was expended on silane chemistry [Erickson and Plueddemann, 1974]. A more detailed study of silanes as adhesion promoters is carried out in Section 3.2.

In the late 1960s and early 1970s the next series of coupling agents to be developed were the titanates. As well as performing well as adhesion promoters for adhesives and surface coatings they were found to possess other beneficial properties for use with composites. These coupling agents are considered in further detail in Section 3.3.

More recently, zirconates and zircoaluminates have been attracting attention and are now being found to be of use in surface coatings.

A generalized mode of action has been proposed for the reaction of an alkyl adhesion promoter or coupling agent with a surface [Monte and Sugerman, 1984]. Coupling Agents tend to be hydrolysable to a greater or lesser extent which seems to make the reaction below probable.

$$(R\text{-}X\text{-}O)_3\mathbf{A}\text{-}OR^1 \quad + \; M\text{-}OH \quad \Longrightarrow \quad (R\text{-}X\text{-}O)_3\mathbf{A}\text{-}OM \quad + \; R^1\text{-}OH$$

A, generally represents Si (silanes), Ti (titanates) or Zr (zirconates). $-OR^1$, is normally an easily hydrolysable group which reacts with the hydroxyl group on the inorganic substrate M (metal, glass etc.). The side group -R allows the adhesion promoter to be compatible with the polymer phase. The variation of X may allow the adhesion promoter to have an increased composite performance.

The above reaction may not be the initial reaction involved in adhesion promotion as hydrolysis of the coupling agent may occur before any surface reaction can take place. This normally occurs with silanes (see Section 3.2.1).

Several extensive reviews have been published concerned with the roles and uses of adhesion promoters. The most useful of these are the review by Cassidy and Yager, which deals with this subject from its birth to 1970 approximately [Cassidy and Yager, 1971], and the review by Walker which considers the theory and use of adhesion promoters from 1970 to the present [Walker, 1987]. This Chapter will deal with only a small number of the total uses of adhesion promoters in this study, a more exhaustive bibliography may be produced from these reviews.

3.2 SILANE COUPLING AGENTS.

Silanes have the general structure $R-Si(OR^1)_3$, where R is an organo-functional group, for example amino or vinyl, and OR^1 may be a halide, alkoxide or acyloxy group, capable of undergoing hydrolysis. Silanes have been used extensively in composite technology [Plueddemann, 1982] and surface coatings. A measure of their importance is the large number that have been used for specific cases in the field of adhesion promotion. A list of some of the more well used silanes is given by Walker [Walker, 1987].

As silane molecules are bifunctional, they allow a bridge to form between the metal or inorganic substrate, by interaction with the silanol group, and a polymeric binder, polymer or adhesive by reaction with the organo-functional group. The most important coupling reactions of silanes may be described as below:

(1) **HYDROLYSIS**

$$R-SiX_3 + 3H_2O \Longrightarrow R-Si(OH)_3 + 3HX$$

(2) **HYDROGEN BONDING** to the surface

(3) **CONDENSATION** with the surface

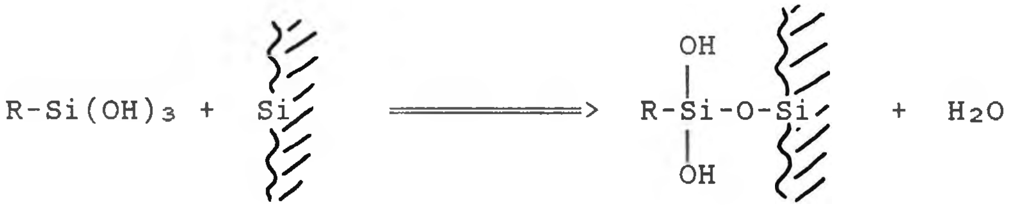

$$R\text{-}Si(OH)_3 + Si \Longrightarrow R\text{-}\overset{OH}{\underset{OH}{Si}}\text{-}O\text{-}Si + H_2O$$

(4) **POLYMERISATION**

$$R\text{-}Si(OH)_3 + R\text{-}Si(OH)_3 \Longrightarrow R\text{-}\overset{OH}{\underset{OH}{Si}}\text{-}O\text{-}\overset{OH}{\underset{OH}{Si}}\text{-}R + H_2O$$

3.2.1 Silane Adhesion Promotion Mechanism

Several theories for the mechanism of the adhesion promotion afforded by silanes have been proposed. An excellent review of these is available [Rosen, 1978]. A brief description of the more important theories follows.

(a) Chemical Bond Theory.

This theory suggests that trialkoxysilanes bond to the surface through surface-OH groups to produce interfacial covalent bonds. The major problem with this theory tends to be that it does not explain the observed increase in "wet" bond strength (the strength of the bond prior to drying) when most metallosiloxane bonds (-Si-O-M-) are susceptible to hydrolysis.

(b) Deformable Layer Theory.

This theory proposes a plastic interface in the polymer/metal zone so that stresses between the polymer and the metal may be relieved.

(c) Surface Wettability Theory.

The theory suggests that improved wetting of filler particles in an adhesive or composite produces increased physical adsorption and therefore improved adhesion. It is difficult to see how physical adsorption increases bond strength when the polymer is in competition with water and other weakly bonded layers.

(d) Restrained Layer Theory.

This theory is similar to the chemical bond theory but also proposes that an interfacial region is produced between say a metal and a polymer with a modulus of intermediate value between that of the metal and the polymer. This would allow a transfer of stress from the metal to the polymer and therefore improve bond strength.

(e) Reversible Hydrolytic Bond Theory.

This combination theory suggests that a chemical reaction takes place between the polymer and the substrate with a restrained layer of intermediate modulus being also produced. This would allow stress relaxation by the reversible breaking of stressed bonds without a loss of adhesion. It also suggests that although SiO-Metal bonds may be broken by the intrusion of water they may also reform with a recovery of adhesion. This theory cannot deal with the mechanism of adhesion promotion by some silanes which are known not to react with the polymer but to produce increased bond strength by physical entanglement of the organo-functional groups instead.

From the theories above, several basic requirements of the silane adhesion promoter are demanded. Reaction should take place between the organo-functional group of the silane and the polymeric matrix of the coating or adhesive. There must also be some mechanism to allow the silane to concentrate at the metal or ceramic surface. The later requirement is most important when the silane adhesion promoter is incorporated into a coating or adhesive as an additive. Plueddemann has suggested that the effectiveness of an adhesion promoter as a primer for coatings may depend as much on the physical properties of the substrate to be coated as on the chemistry of the coupling agent [Plueddemann, 1981]. If this is accepted it is important that each "end-use" should be optimised in terms of:

(i) Selection of the coupling agent
(ii) Method of application
(iii) pH of applicant solution
(iv) Cure conditions

before the application of the coating. If this procedure is not carried out it is not inconceivable that the final adhesion may be of lower strength than between that of the coating or adhesive with a non-treated surface.

3.2.2 The Structure of Silanes Films on Metals and Glass.

Bascom employed a variety of techniques in a study of silane films deposited onto metal and glass substrates. In examining chloro-, vinyl- and amino- functional silanes he concluded that the films were deposited as polysiloxanes [Bascom, 1972]. He found that a percentage of the deposited films could be easily removed by organic solvents or water. He found that the remaining material was an open polymeric structure as it was easily penetrated by wetting liquids in contact angle measurements. It was also discovered that films deposited from non-polar solvents were relatively thick (>1000 Å) and resistant to desorption, whereas those deposited from polar solvents were less than 100 Å thick and easily disrupted by polar solvents.

It was concluded that silane films can contain different strata. These may consist of a substrate-silane interface with covalent bonding, a relatively cross-linked intermediate layer close to the substrate surface and a layer of relatively non-cross-linked material. In the production of silane films on metals and glasses discrete "islands" and agglomerates are normally produced. Over the years there has been little direct evidence for the production of direct covalent bonds between the silane and the substrate. One of the few is that by Gettings and Kinloch who observed the SIMS spectrum of a steel surface treated with an aqueous solution of 3-glycidoxypropyltrimethoxysilane [Gettings and Kinloch, 1977]. An ion of mass 100 was detected and assigned to $FeSiO^+$. The authors claimed that "this is strong evidence for the formation of a chemical bond, probably -Fe-O-Si-, between the metal oxide and the polysiloxane primer".

Boerio and Williams have studied the structure of films formed by the adsorption of 3-aminopropyltriethoxysilane (3-APS) onto iron substrates using reflection-adsorption infrared spectroscopy (RAIRS) [Boerio and Williams, 1981].

Allen and Stevens employed specular reflectance infra-red spectroscopy to elucidate the structure of thin films of 3-glycidoxypropyltrimethoxysilane on aluminium substrates [Allen and Stevens, 1982]. This study investigated the effect of coating thickness on the extent of silane hydrolysis in the coating.

Studies using FTIR and ESCA spectroscopic techniques suggest that some organosilanes, e.g. 3-APS, undergo hydrolysis and polymerization on several surfaces to form somewhat cross-linked polysiloxanes [Sung et al., 1980 and 1981], as shown in the reaction mechanism below.

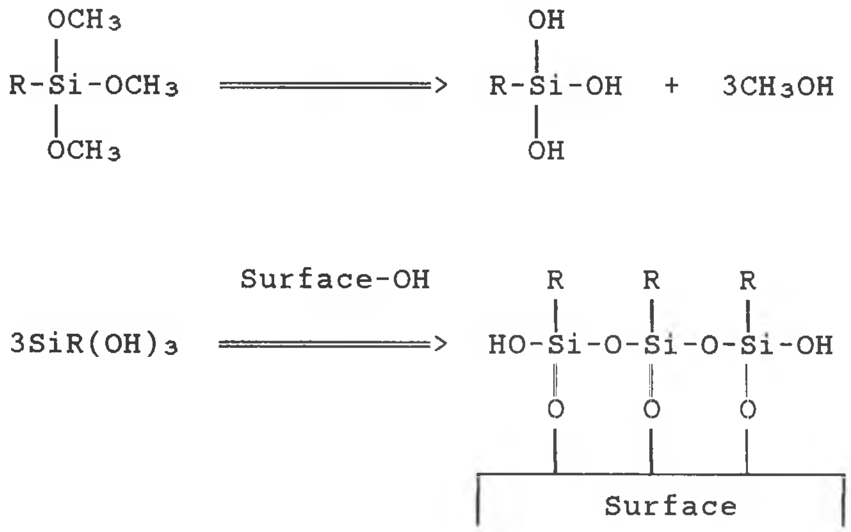

$$\text{R-}\overset{\overset{\displaystyle OCH_3}{|}}{\underset{\underset{\displaystyle OCH_3}{|}}{Si}}\text{-}OCH_3 \Longrightarrow \text{R-}\overset{\overset{\displaystyle OH}{|}}{\underset{\underset{\displaystyle OH}{|}}{Si}}\text{-}OH + 3CH_3OH$$

$$3SiR(OH)_3 \xRightarrow{\text{Surface-OH}} \text{HO-}\overset{\overset{\displaystyle R}{|}}{\underset{\underset{\displaystyle O}{\|}}{Si}}\text{-O-}\overset{\overset{\displaystyle R}{|}}{\underset{\underset{\displaystyle O}{\|}}{Si}}\text{-O-}\overset{\overset{\displaystyle R}{|}}{\underset{\underset{\displaystyle O}{|}}{Si}}\text{-OH}$$

Silanes have been shown to cross-polymerize as above on many different substrates, such as sapphire [Sung et al., 1980] [Sung et al., 1983], glass fibre [Sung et al., 1983], alumina [Werrett et al., 1986] and mica [Favis et al., 1984].

The study of silane adhesion promoters by means of inelastic electron tunnelling spectroscopy is covered in greater detail in Chapter 4.

3.2.3 Methods of Using Silanes as Adhesion Promoters

There are three main methods of applying silanes as adhesion promoters - as solutions in organic solvents, as formulated primers and incorporated into a single-pack self-bonding concept. Thus they may be used both as pre-treatments and as additives to adhesives and coatings.

The mode of operation and application of these different silane adhesion promoters is outlined in the review by Walker [1987]. A comprehensive review of the methods of using silane coupling agents with epoxide and polyurethane paints as well as other coatings is also covered in this publication. Other specific uses of silane adhesion promoters are outlined by Plueddemann [1982] and by Rosen [1978].

3.3 TITANATE COUPLING AGENTS.

Organic titanate adhesion promoters have only become widely used industrially since the early 1970s. They seem to be used primarily as coupling agents in filled systems, to promote bulk effects in composites. As suggested with the silanes, but more so in the case of titanates, the lack of published data may be put down to the problems of corporate secrecy.

3.3.1 Titanate Adhesion Promoter Nomenclature.

A comprehensive range of titanate coupling agents is marketed by Kenrich Petrochemicals Inc. under the name Ken-React^{R} and, as used in the study detailed in Chapter 6, from Dynamit Nobel. These are available in an ever increasing variety of chemical types known as monoalkoxy, chelate, coordinate, quat, neoalkoxy and cycloheteroatom titanates. It is therefore not surprising that the vast majority of the scientific data available on titanate adhesion promoters has been published by Monte and Sugerman at Kenrich. Examples of these titanates are shown in Table 3.1. Titanates are effectively the organic derivatives of orthotitanic acid ($Ti(OR)_4$). The most important chemical groups of titanate adhesion promoters are those of the monoalkoxy and chelate varieties.

In the case of titanium chelate complexes the central titanium atom as well as having "normal" covalent bonds to its ligands may also coordinate to those ligands containing certain functional groups (such as hydroxyl, carboxyl, keto, amino or other groups) if the molecular ratios are correct.

Table 3.1. Typical Titanate Adhesion Promoters Commercially Available [Walker, 1987].

Chemical description	*Structure*	*Type*
Isopropyl tri(*N*-ethylaminoethylamino)-titanate	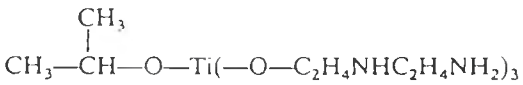 $CH_3-\overset{CH_3}{\overset{\vert}{C}}H-O-Ti(-O-C_2H_4NHC_2H_4NH_2)_3$	Monoalkoxy
Isopropyl tri-isostearoyl titanate	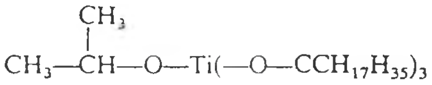 $CH_3-\overset{CH_3}{\overset{\vert}{C}}H-O-Ti(-O-CCH_{17}H_{35})_3$	Monoalkoxy
Titanium di(dioctylpyrophosphate)oxy-acetate	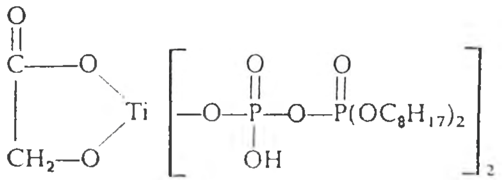	Monoalkoxy
Tetra-isopropyl di(dioctylphosphito)-titanate	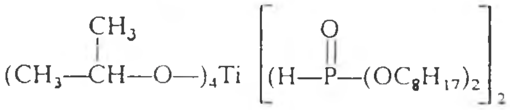 $(CH_3-\overset{CH_3}{\overset{\vert}{C}}H-O-)_4Ti\left[(H-\overset{O}{\overset{\Vert}{P}}-(OC_8H_{17})_2\right]_2$	Coordinate
Neoalkoxy tri(*p*-*N*-(β-aminoethyl)amino-phenyl)titanate	$RO-Ti\ (OC_6H_4NHC_2H_4NH_2)_3$	Neoalkoxy

3.3.2 Reactions of Titanate Adhesion Promoters.

The claim has been made that the typical titanate coupling agent provides six functions [Anon, 1985], however only three of these may be considered to be relevant to their use as adhesion promoters. These may be summarized as follows :-

(i) Reaction of the alkoxy group of the titanate with "free" protons at the inorganic substrate surface to form an organic monomolecular layer on the surface of the substrate.

(ii) Transesterification, resulting in the cross linking with carboxyl and hydroxyl groups in the polymer substrate.

(iii) To a lesser extent, van der Waals entanglement between the polymer chains and the long carbon chains of the titanate.

Titanate coupling agents are unique in that their reaction with the free protons on the substrate results in a monomolecular layer on the inorganic surface whether it be particulate filler or metallic substrate.

The reaction is thought to proceed as follows [Anon, 1985] :-

$$R^1OTi(OR)_3 \quad + \quad MOH^* \quad \Longrightarrow \quad MOTi(OR)_3 \quad + \quad R^1OH^*$$

where H* is the "free" proton on the inorganic substrate surface.

In this section only the more important reactions of monoalkoxy and chelate titanates will be discussed. A more detailed and extensive review of the mechanism of titanate coupling is available [Monte and Sugerman, 1982].

(A) Alkoxy Titanates

A most important reaction of alkoxy titanates (also known as monoalkoxy titanates) is the hydrolysis to titanium oxide hydrates finally [Anon, 1980].

1) $Ti(OR)_4 + H_2O \Longrightarrow Ti(OR)_3OH + ROH$

2) $2Ti(OR)_3OH \Longrightarrow (OR)_3Ti\text{-}O\text{-}Ti(OR)_3 + H_2O$

3) $2(OR)_3Ti\text{-}O\text{-}Ti(OR)_3 + H_2O \Longrightarrow RO[\text{-}Ti(OR)_2\text{-}O\text{-}]_4R + 2ROH$

4) $RO[\text{-}Ti(OR)_2\text{-}O\text{-}]_xR + H_2O \Longrightarrow HO\text{-}[\text{-}Ti(OH)_2\text{-}O\text{-}]_xH + ROH$

5) $HO[\text{-}Ti(OH)_2\text{-}O\text{-}]_xH \Longrightarrow X\ TiO_2.H_2O$ (Titanium oxide Hydrates)

These reactions can be regulated by the choice of alkoxide ligand used. The rate of hydrolysis can also be reduced by making the alkoxy titanate up in a solution of its parent alcohol. Reactions 1 to 3 may even be induced by the moisture present in the normal atmosphere to produce the condensed polymeric alkoxy titanates which are usually less reactive than the monomeric species. These polymeric alkoxy titanates can be produced on substrate surfaces in a similar manner to that of the silanes illustrated in Section 3.2.2 [Favis et al., 1984]. The extent of this polymerization is dependent on such variables as:

(i) Moisture present.
(ii) Type of surface onto which the titanate monomer is adsorbed.
(iii) Type of organic ligand present in titanate.

A comparison of the effectiveness of a specific monoalkoxy titanate with a silane adhesion promoter has been carried out [Sung et al, 1983]. In this study, the adhesion of an aluminium-polythene adhesive joint is considered using FTIR and ESCA techniques. The mechanism of reaction of the silane is discussed in Section 3.2.2. Extensive hydrolysis and polymerisation was observed for the silane (3-APS) whereas no such evidence was seen for reaction of the titanate, isopropyltriisosteroyl titanate (KR-TTS), with the surface. This accounted for the fact that the effect of the silane was much greater as an adhesion promoter than that of the titanate. A comparison of the reaction mechanisms for monoalkoxy titanates and trialkoxy silanes with the surface of an inorganic filler is illustrated by Monte and Sugerman [1982]. Whereas the titanate is thought to react with the proton of an hydroxyl group on the surface, the silane requires hydroxyl functionality (hydrolysis of the silane is the first step to surface reaction).

Although the titanate in the above study was found to be a less effective adhesion promoter than a corresponding silane, titanate coupling agents have been found to be of considerable importance in some more specialized fields of study, such as printing ink manufacture. These will be dealt with later in this Chapter.

In addition to direct hydrolysis alkoxy titanates can also react with hydroxyl groups present in polymers, as follows, to produce a crosslinking effect.

$$\mathrm{Ti(OR)_4} + \text{HO-Polymer} \Longrightarrow \mathrm{(RO)_3Ti}\text{-O-Polymer} + \mathrm{ROH}$$

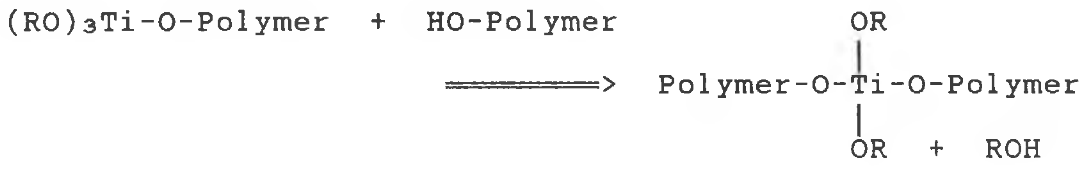

$$\mathrm{(RO)_3Ti}\text{-O-Polymer} + \text{HO-Polymer} \Longrightarrow \text{Polymer-O-}\overset{\mathrm{OR}}{\underset{\mathrm{OR}}{\mathrm{Ti}}}\text{-O-Polymer} + \mathrm{ROH}$$

This ability is of great importance in the use of titanate in printing ink formulation (see Section 3.3.4).

The extent of crosslinking is dependent on the structure of the polymer (nature and position of hydroxyl groups, other functional groups and molecular weight) as well as the nature of the titanate.

(B) Titanium Chelate Complexes as Adhesion Promoters

In titanium chelate complexes one or more of the normal covalent bonds of an alkoxy titanate are replaced by a coordinate bond from a functional group within the ligand already covalently bonded to the central Ti atom. These species sometimes are also known as titanium acid esters.

For example:

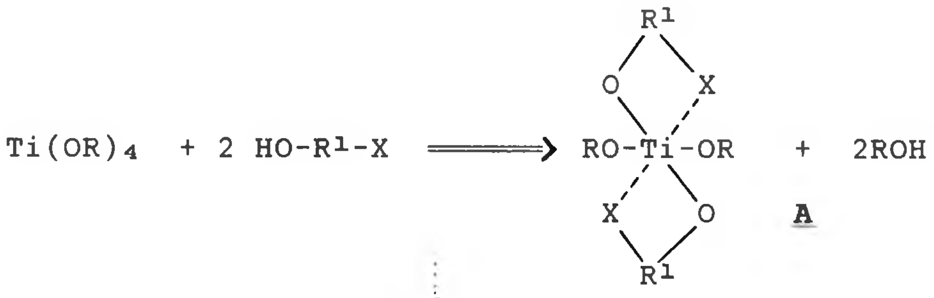

When -R^1-X =
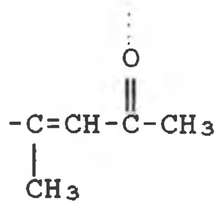
$$-\overset{\displaystyle CH_3}{\underset{}{C}}{=}CH-\overset{\displaystyle O}{\overset{\|}{C}}-CH_3 \quad \text{with } CH_3 \text{ below the first C}$$

then **A** = Titanium Acetylacetonate (TAA).

Titanium chelate complexes are protected from hydrolysis by the nature of their structure. The reactivity of the remaining alkoxy groups is greatly inhibited and therefore titanium chelate solutions may be stable for periods of up to several months. The effect of the chelate group is also to inhibit the reaction of the other -OR groups with functional groups present in polymers. In the case of titanium acetylacetonate the polymerization will only proceed as far as linear crosslinking at room temperature. Only if heat is applied can the chelate group be split off as well.

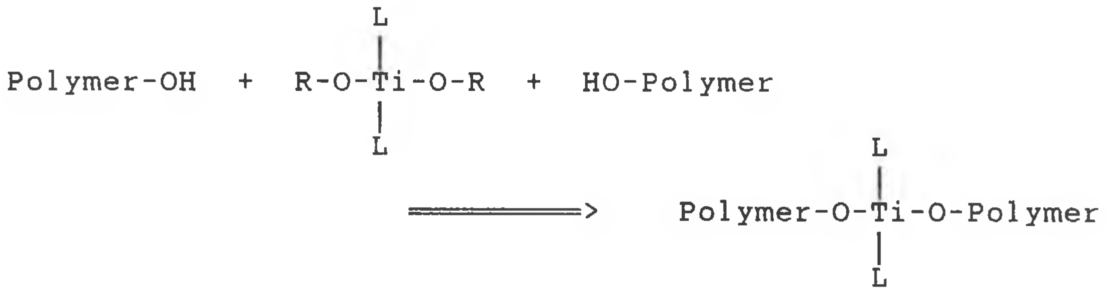

$$\text{Polymer-OH} + \text{R-O-}\overset{\text{L}}{\underset{\text{L}}{\text{Ti}}}\text{-O-R} + \text{HO-Polymer} \Longrightarrow \text{Polymer-O-}\overset{\text{L}}{\underset{\text{L}}{\text{Ti}}}\text{-O-Polymer}$$

3.3.3 Applications of Titanate Adhesion Promoters.

As with silanes, titanate adhesion promoters may be used as pretreatment primers and as additives to coatings or adhesives.

When used as a primer, in either water or organic solvent solution, the technical literature stresses that it is important that only a low concentration of titanate is used, typically between 0.2 to 1% by mass. Also it is important to remove any excess titanate from the surface by washing with the solvent (or water) used in the preparation of the solution used to deposit the film.

When used as an additive, titanates must be dispersed directly into the polymer solution using high shear mechanical mixing and total dispersion is essential for effective adhesion promotion.

Several reviews are available that detail the specific uses of organic titanates [Sung et al., 1983] [Monte and Sugerman, 1983a, 1983b and 1983c]. These are primarily concerned with alkoxy titanates. Titanium chelate complexes are used mostly as primers and binders for printing inks. This application is dealt with specifically later in this Chapter.

The most important areas for application of alkoxy titanates are:-

(1) Promotion of adhesion between polymers, composites and metals.

(2) Promoted dispersion of inorganic solids within organic phases.

The reviews sited above contain comprehensive accounts of the industrial applications of alkoxy titanates, and therefore only selected applications will be described here as illustration.

All the trade literature [Anon, 1985] [Anon, 1980] [Cleveland Society for Coatings Technology, 1979] stresses that the correct dosage of titanate adhesion promoter must be used. Excessive quantities of coupling agent are thought to be the most significant factor in adhesion failure. The amount required to produce a monomolecular layer on the substrate surface is dependent on such factors as the nature, particle size and shape of the filler and the substrate geometry. Excess titanate results in an amount of unreacted titanate on the surface and in the loss of adhesion of the adhesive or coating. Several rules of thumb have been produced to ensure that the correct titanate dosage is applied [Walker, 1987].

(A) Adhesion Promotion Using Titanates.

In general, titanates with more polar organic moieties, such as isopropyltri(N-ethylaminoethylamino) titanates, are recommended for adhesion promotion to polar substrates such as metals, ceramics, acrylics and engineering thermoplastics. Titanates with relatively more non-polar organic ligands, such as aliphatic carboxyl titanates will adhere better to more non-polar substrates such as polyolefins, chlorinated and fluorinated polymers and silicones.

An industrially used titanate, KR 158FS, has been used to illustrate the coupling affinity of titanates for metal substrates [Sung et al., 1983]. A copper substrate was immersed into a 0.5% solution of KR 158FS in isopropyl alcohol (IPA). On subsequent washing with IPA and using ESCA it was found that the KR 158 FS had adhered to the copper by the dissociation of the dialkyl phosphite ligands. The experiment also showed that the titanate had formed a 80% monolayer coverage on the copper surface. This indicated that such a coupling agent would afford good adhesion promotion between an adhesive and the copper. The experiment indicated that the increased hydrophobicity of the coated surface could lead to the corrosion inhibition of the copper surface.

Alkoxy titanium- and zirconium- tricarboxylates (laurates and stearates) have been studied with a view to evaluating their potential as coupling agents for epoxy adhesives on silica and alumina [Calvert et al., 1983].

Other examples of adhesion promotion are illustrated later in this report.

(B) Dispersion Promotion Using Titanates.

It has conclusively been shown that the dispersion of an inorganic filler (e.g. filler, reinforcer etc.) can be enhanced in the presence of an organic titanate [Monte and Sugerman, 1983c]. This occurs because the titanate produces a monolayer on the surface of the inorganic species, eliminating the water of hydration present and therefore the phases are made compatible. The ability to disperse inorganic material in media of different polarity has been shown to be of great use in the catalysis of polyesterification reactions and the polymerization of urethane. This is due to the increased dispersion of the reactants involved in these reactions (See Figure 3.1). In improving the dispersion of particulates in a paint medium, titanates have also been able to reduce the critical pigment volume concentration (CPVC). Some reduction in viscosity may be seen, allowing easier handling of the paint or allowing higher filler content at the same viscosity. This will also produce a higher moisture scavenger protection for the primer. Specific cases of titanate use in this way have been reviewed [Walker, 1987].

IBM found that disks coated with an iron oxide-epoxy-phenolic mixture containing a pyrophosphato titanate gave improved performance over any other commercial disks. This was due, not only to the improved dispersion and chemical bonding of the iron oxide within the coating, but also to the catalysis of resin reactions which provided strength to the disk without needing to add a particulate reinforcer such as aluminium. Similar reactions are known to take place in inks (polymerization of the ink base) to produce increased ruckle stability, see Section 3.3.4.

Figure 3.1. <u>Titanates as Dispersion Promoters</u>

[Monte and Sugerman, 1982].

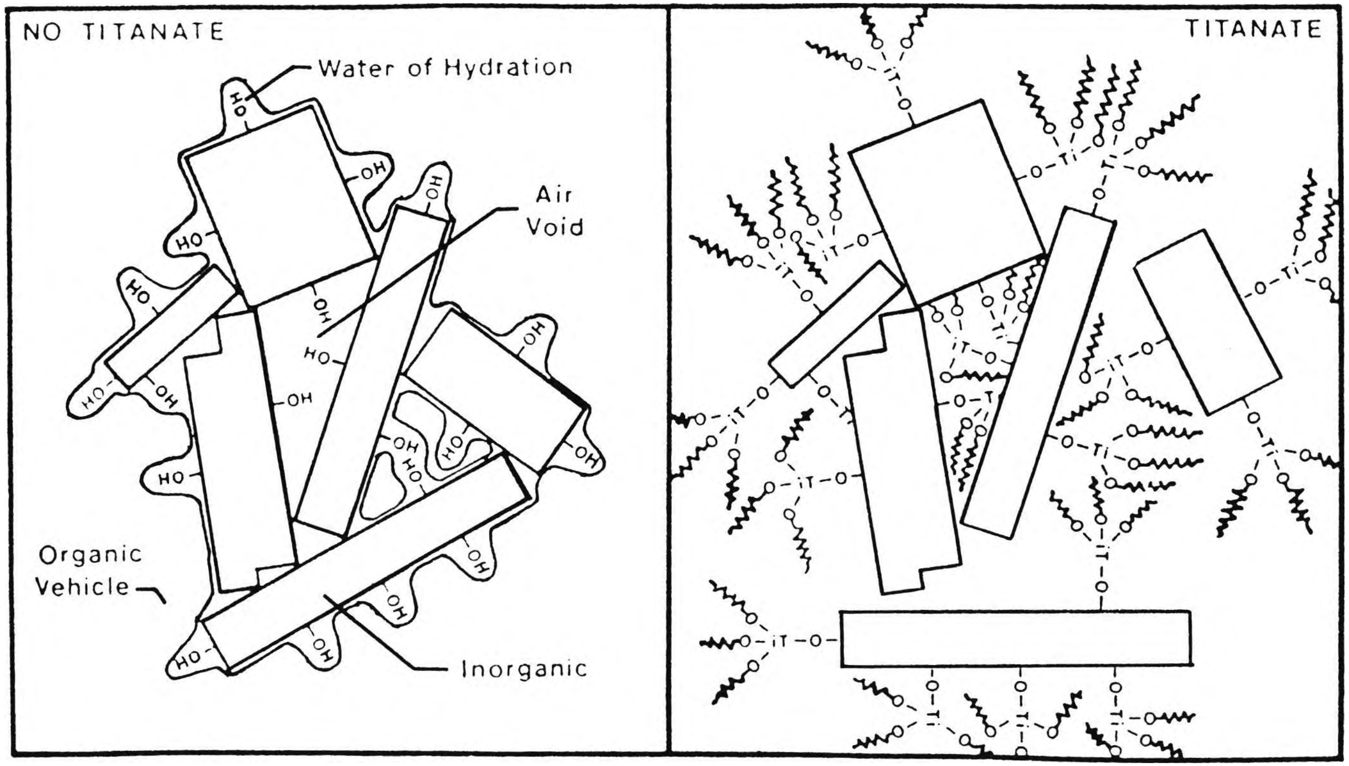

Other applications of titanates have also been realized in their affect on physical properties of composites. [Sung et al., 1983]. For example, the use of organic titanates has been shown to improve the adhesion between the filler and the cellular matrix in polyurethane foams and also affect their compressibility. It has also been shown that the addition of organic titanates to varnish composites could vary their electrical conductivity (for use as electromagnetic and radio frequency shielding applications) and viscosity [Sung et al., 1983]. As well as the useful applications cited above, organic titanates have been shown to be of great use in the printing ink industry.

3.3.4 The Use of Titanates in the Printing Ink Industry.

The reactions of titanates enable them to impart special properties to binders (also known as bases) used in printing ink manufacture, such as nitrocellulose [Anon, 1980] and cellulose acetate propionate [Walker, 1986]. Titanates have been found to especially improve the binder's adhesive properties and its stability to heat and solvents. Titanates have also been shown to improve the anti-settling properties of heavily loaded pigment-based inks and other heavily loaded systems.

As with the silane adhesion promoters, there are two ways of applying the titanate coupling agents to printing inks:-

(a) Pre-treatment of the substrate surface.

(b) Addition to the bulk printing ink, as an additive.

(a) Surface Pre-treatment

For some time it was noticed that the application of lacquers and inks to certain surfaces, such as polyolefins, polyesters and aluminium, was difficult to achieve. In 1962 [Anon, 1962] it was discovered that the pre-treatment of such "difficult" substrates with alkoxy titanate solutions produced enhanced adhesion between the lacquer or ink and the surface. The effect of the applied titanates was essentially to produce a very thin, continuous film of titanium dioxide hydrate (reaction scheme shown in Section 3.3.2). This film not only adheres well to the substrate but also produces a better adhering surface for the ink or lacquer to bind to. The method for the application of surface pre-treatment titanate solutions was by rolling the 1-5% solution onto the substrate and by heating the coated substrate in humid air (60%), so that the solvent was removed. The moisture in the air initiates the hydrolysis and the adhesion promoting coating was formed. The choice of solvent and starting titanate was dependent upon which solvent easily wets the substrate. Both aqueous and non-aqueous solvents were used. This pre-treatment has been shown to be very effective in the adhesion promotion seen between nitrocellulose lacquers and polypropylene substrates, both using alkoxy and chelate type titanates [Anon, 1980].

(b) Addition of Titanates to Printing Inks :-

In many cases the pre-treatment method of adhesion promotion, outlined above, is impractical industrially for technical and cost reasons. In which case, improved adhesion to "difficult" substrates can be obtained by the incorporation of the titanate within the lacquer or ink. For this method to be effective two conditions must be satisfied.

a. Reactivity of the titanate with the printing ink binder or other constituents must be reduced so that there is no detrimental affects on the storage stability or the viscosity of the ink.
b. The titanate must maintain a high interfacial activity (surface affinity) within the ink, to be able to promote adhesion when required.

For these conditions to be satisfied, titanium chelates have been found to be of most use. Alkoxy titanates are too reactive, even at very low concentrations and produce a yellowing of nitrocellulose and a gelling of nitrocellulose solutions [Anon, 1980]. Due to their reduced reactivity, chelate complexes are less likely to gel the binder solution and therefore have shelf-lives in terms of months, but they are still active at the substrate-ink interface.

Some other improvements have been achieved by using titanates in printing inks. As a result of the reaction of the binder with the titanate, the binder after the drying stage (curing), shows greater stability to water and heat. The crosslinking reactions, explained in Section 3.3.2 are therefore very useful. Practically, this again highlights the advantage of using titanate chelate complexes over alkoxy titanates as the later are often unstable to the ink binder before the drying stage. The crosslinking reactions are outlined below [Anon, 1980]:-

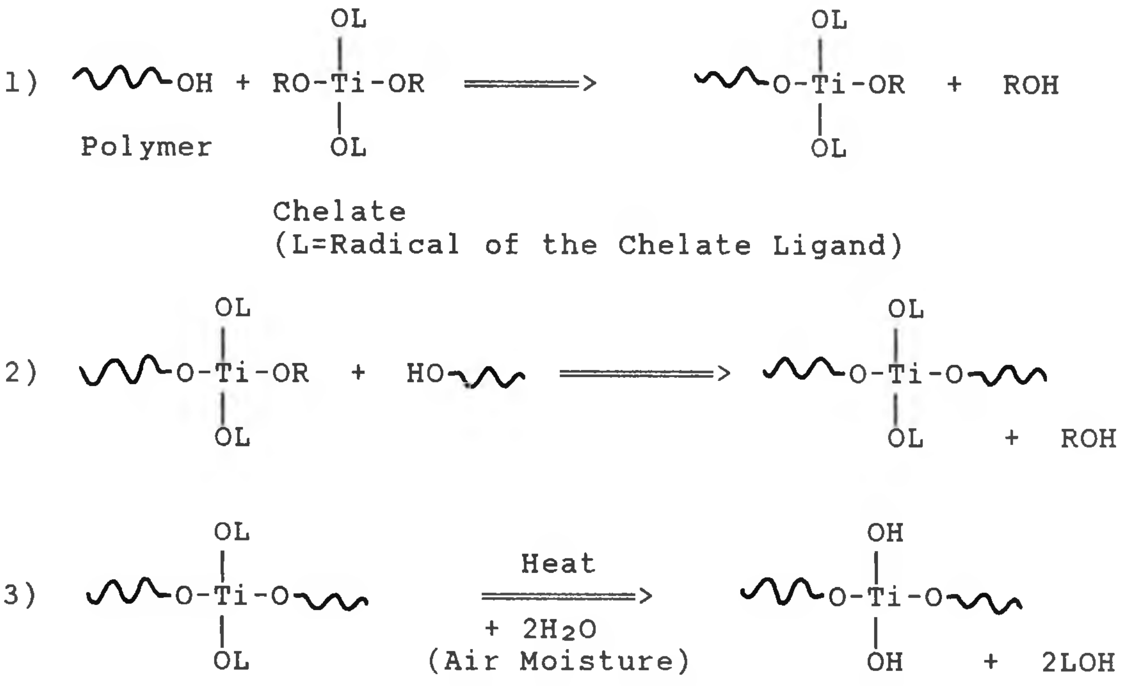

4)

OR FROM 3)

5)

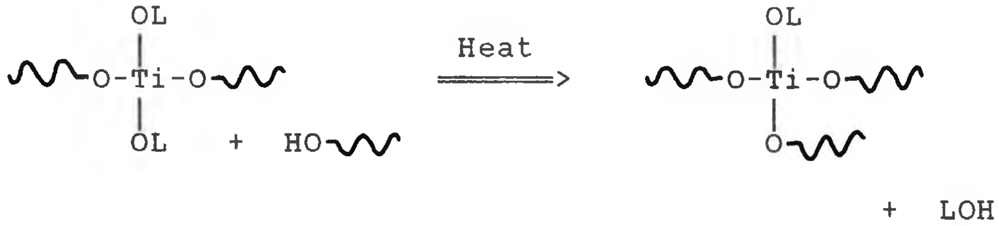

Titanium chelate complexes, and especially titanium acetylacetonate, have been shown to improve the solvent stability of nitrocellulose based inks and therefore improve their shelf-life [Anon, 1980]. TAA has also been shown to be a superb adhesion promoter in cellulose acetate propionate based inks on polyolefinic substrates.

As described in Section 3.3.3, titanates are known to have a positive effect on the dispersion of inorganic particulate material within a non-compatible solvent. This effect has been shown to be beneficial in the dispersion and wetting of pigments and other additives within printing ink solutions [Anon, 1985].

Prior to the use of titanates in printing ink and lacquer solutions it is always necessary to check that detrimental reactions between the titanate and any other ingredient of the mixture do not occur.

Silanes have been shown to be extremely good coupling agents in some applications (see Section 3.2), however they have not tended as yet to be used as adhesion promoters within printing inks. This may just be due to the fact that titanates, and especially titanium chelate complexes, have been found to have the correct reactivity in such systems.

3.4 OTHER ADHESION PROMOTERS.

3.4.1 Zirconium Adhesion Promoters.

The use of zirconium adhesion promoters dates back to the early 1970s. Zirconates offer two major advantages in use; in general they do not produce coloured products in contact with phenols and they do not behave as activators in peroxide free-radical curing systems. Zirconates can usually exist as water and organic solvent soluble forms; however the aqueous chemistry is dominated by the hydrolysis of the coupling agents to produce polymeric species. A recent review of zirconate applications is available [Walker, 1987].

A zirconate coupling agent that has been used to promote the adhesion of printing inks to"difficult" substrates such as polyolefins is zirconium propionate [Moles, 1983 and 1985]. It has been used in both cellulose acetate propionate and nitrocellulose based inks. Although the mode of action of zirconium propionate is not known with certainty a mechanism for adhesion promotion has been proposed (see Figure 3.2). The corona discharge of polyolefinic substrates produces functional groups such as carboxyl, hydroxyl and carbonyl, which can interact with the adhesion promoter. Due to its easily hydrolysable nature zirconium propionate is unsuitable for use in aqueous based inks, but with other bases it produces good adhesion promotion and ruckle resistance.

As with silane and titanate coupling agents, the suitability of a particular zirconium compound in a specific application must be considered in detail to obtain the optimum properties. The effect on other technical requirements such as viscosity, self-life etc., must also be determined.

3.4.2 Other Adhesion Promoters.

A very wide range of inorganic, organometallic and organic compounds have been used as coupling agents, usually for specific adhesives and coatings applied to selected substrates. A comprehensive review of these compounds has been provided [Cassidy and Yager, 1972]. A list of the more usual of these follows.

Figure 3.2. <u>Proposed Mechanism for Zirconium Propionate</u> [Moles, 1983].

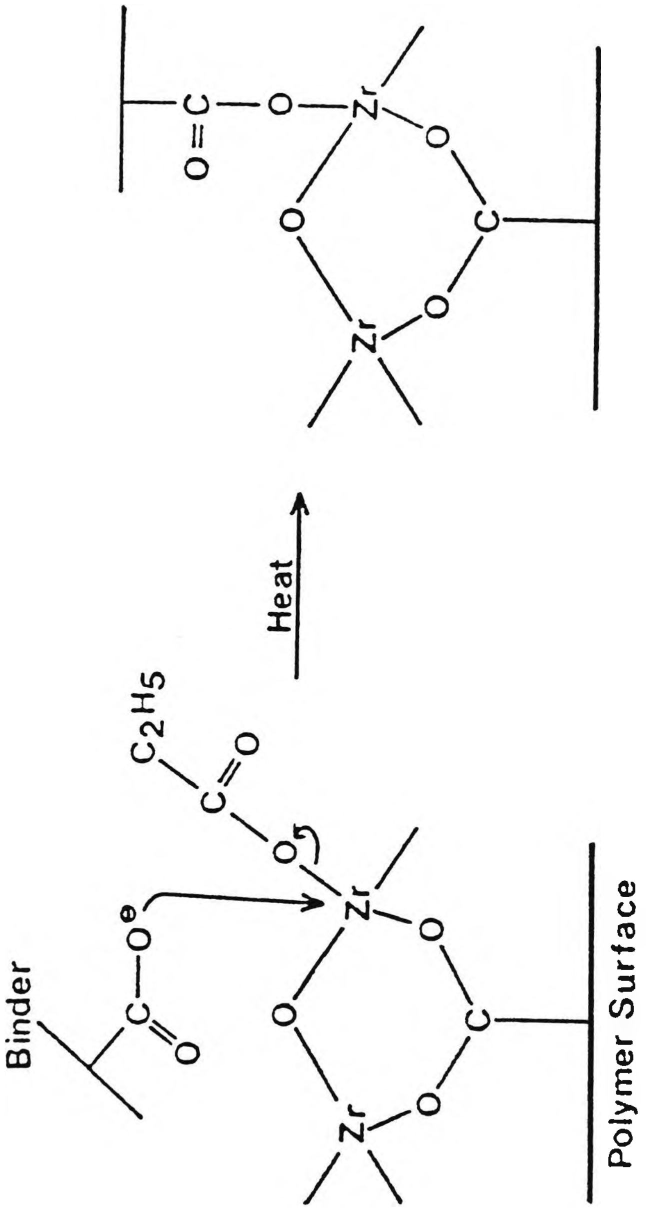

(a) Phosphorus-Containing Compounds.

(b) Chromium-Containing Compounds - primarily for chromium conversion.

(c) Cyclic Alkylene Ureas.

(d) Amines - primarily hydroxybenzyl amines.

(e) Metal Salts of Organic Acids - citrates and benzenesulphonates.

(f) Organic Resins.

3.5 CONCLUSIONS.

This Chapter has attempted to serve as a broad introduction to the complex study of coupling agents. In conclusion it may be said that coupling agents may find a use in any circumstance where good adhesion to the substrate is required. It has been shown to be of particular importance in coating science since this is a prerequisite in most coating applications. Nevertheless, there are many more less obvious potential applications [Walker, 1987]. In a competitive industry, faced with new and difficult substrates and applications, coupling agents will prove to be useful tools in both problem solving and gaining the competitive edge. A recent review has outlined various new areas for consideration of the use of coupling agents [Walker, 1987].

In such an industrially important subject, it is essential that patent literature and information be considered when studying adhesion promoters. A review of the more important patent literature is available [Walker, 1987].

CHAPTER FOUR - THE APPLICATION OF IETS TO THE STUDY OF COUPLING AGENTS

4.1 INTRODUCTION

The application of IETS to adhesion processes generally has been discussed in Section 2.3.1. The applications and modes of action of coupling agents have been reviewed in Chapter 3. In this Chapter the specific application of IETS to the study of coupling agents and other adhesion promoters will be considered.

IETS has primarily been used to consider reactions and interactions on alumina surfaces. This is mostly due to the ease of production of these oxide surfaces (see Section 5.2). Additionally alumina surfaces are the most widely studied substrate for adhesion. IETS has therefore been found useful in the analysis of adhesion promotion systems on alumina substrates (see Section 2.3.1).

As explained earlier, in Section 3.1, silane coupling agents were one of the first adhesion promoters to be proposed. These industrially important coupling agents have been studied by various techniques, as outlined in Section 3.2.2. However, apart from a small number of other types of adhesion promoters, only silane coupling agents have been studied using IETS (see Section 4.3).

The application of most coupling agents affords a surface bond which possesses an increased resistance to environmental effects, such as the hydrolysis of an adhesive bond by water. It is therefore of the utmost importance, when studying the effect of coupling agents on surface reactions, that the role of water and the subsequent hydrolysis of the adhesion promoter be considered. This, in particular, is most likely to affect the performance of the coupling agent and its ability to withstand harsh environmental conditions.

4.2 **IETS STUDIES OF SILANE COUPLING AGENTS.**

The vast majority of the IETS studies of silane coupling agents have been concerned with the surface reactions and interactions of the trialkoxysilanes (primarily trimethoxy- and triethoxysilanes). The adsorption of both monoalkoxy- and trialkoxysilanes have been studied and it has been suggested that monoalkoxysilanes are not adsorbed whereas the trialkoxysilanes are readily adsorbed [Alexander et al., 1985] onto an alumina surface. These silanes were introduced to the surface by spin doping an anhydrous acetone or acetone/water mixed solutions. Section 5.7 outlines the most usual methods of doping the tunnel junction. The reasons proposed for the non-adsorption of monoalkoxysilanes are that either the bonds between the surface-OH groups and the alkoxy group are not so easily produced (siloxane bonds) or that they are not stabilised by further condensation on the surface to form polysiloxanes. Indeed, monoalkoxysilanes were shown to catalyze further oxidation of the alumina surface.

4.2.1 Triethoxysilanes.

The adsorption of triethoxysilane coupling agents has been studied by a number of workers [Henriksen et al., 1988]. This is most probably due to the large industrial interest in the use of triethoxysilanes in the adhesion promotion of epoxide and polyurethane paints (see Section 3.2.3).

The most widely studied triethoxysilane is 3-aminopropyltriethoxysilane (3-APES) [Comyn et al., 1989] [Comyn, 1984] [Brewis et al., 1984] [Werrett et al., 1986] [Furukawa et al., 1983]. It has been suggested that the silane initially adsorbs onto the alumina surface by H-bonding between the terminal amino group ($-NH_2$) and the surface. However it was thought that in an anhydrous doping situation (where little or no hydrolysis is allowed to occur), the primary interaction between the surface and the triethoxysilane was through the ethoxy- groups [Brewis et al., 1984] [Comyn, 1984] [Werrett et al., 1986]. This was proposed as the Si-H stretching mode in the tunnelling spectrum was of considerable intensity and therefore, in compliance with the orientational selection rule, perpendicular to the surface. Hence the major adsorption effect must be through the three ethoxy-groups. It has been suggested that, in this situation, chemical changes in the silane had not occurred. A useful method of highlighting the adsorption mechanism is the use of D_2O as a dopant solvent (either as a part or the whole of the solvent) to help analyse the hydrolysis mechanism of the coupling agent on the surface [Comyn et al., 1989]. This is carried out by examining the extent of isotopic exchange taking place in the adsorption.

In an IETS study, carried out on 3-aminopropyltriethoxysilane (3-APES), the vapour doped silane was exposed to 75% humidity and the effect on the mode of adsorption detected [Furukawa et al., 1983]. It was found that with an anhydrous species the major adsorption or interaction process was the H-bonding of the amino group of the silane to the surface-OH groups. Subsequently, on the exposure of the silane to high humidity, desorption of the majority of the unhydrolyzed silane was observed and the remainder of the silane was hydrolysed on the alumina surface.

Studies of the adsorption of more hydrated solutions of triethoxysilanes have proposed the production of hydrolysed and condensed surface siloxane products and containing the Si-O-Si linkages of polysiloxanes [Henriksen et al., 1988] [Alexander et al., 1985].

4.2.2 Trimethoxysilanes.

The adsorption and reaction of trimethoxysilane coupling agents in comparison to the triethoxysilanes has also been studied using IETS [Comyn et al., 1989] [Comyn, 1984] [Brewis et al., 1984] [Werrett et al, 1986] [Furukawa et al., 1982]. Several differences have been observed in the mode of action of the two different types of trialkoxysilanes. Trimethoxysilanes, such as ethyltrimethoxysilane (ETMS) [Comyn, 1984] [Brewis et al., 1984], have been shown to react with the alumina surface producing a changed chemical species on the surface. This has been compared with the purely H-bonded interactions of the triethoxysilanes. It has been suggested that the trimethoxysilanes condense on the surface, liberating methanol and producing surface-siloxane species. However, at this stage, there has been no evidence, in a less hydrated situation, for the production of polysiloxanes without the presence of a catalyst [Brewis et al., 1984].

The adsorption of 3-glycidopropyltrimethoxysilane [3-GPTMS] has been studied using IETS [Comyn, 1984] (see also [Allen et al., 1981] and [Allen and Stevens, 1982] for i.r. studies). The reaction scheme is shown below. Hydrolysis of the epoxide group was observed, to produce a 1,2,-diol which was thought to dehydrate to produce an enol-keto tautomeric form which in turn accounted for the observation of C=C and C=O vibrational modes in the IET spectrum.

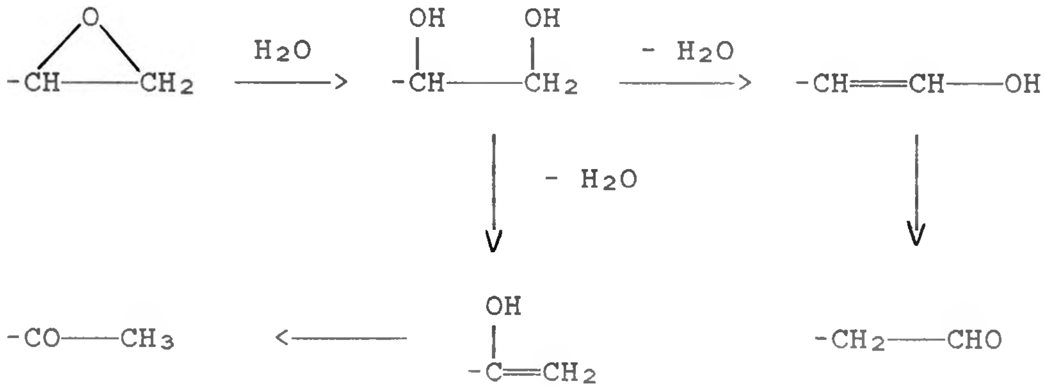

These tunnel junctions were fabricated without the exclusion of water vapour as the reaction mechanism that occurs on the alumina surface is not yet understood and the role of water uncertain.

The surface adsorption of aminophenyltrimethoxysilane (APMS) has been studied using IETS [Comyn et al., 1989] [Furukawa et al., 1982]. The anhydrous silane was vapour doped onto an alumina surface where the initial method of bonding was observed to be H-bonding between the amino group and the surface-OH groups. The exposure of the adsorbed silane to water vapour resulted in marked changes in the IET spectrum produced. Loss of $-CH_3$ deformation and C-H stretching modes suggested a loss of methanol possibly to produce Si-O-Al bonds. A change in the orientational conformation was suggested by the reduction in intensity of $-NH_2$ deformation modes and an increase in the intensity of the C-N stretching mode.

In a comparative study of trialkoxysilanes in a more hydrated situation, the IET spectra of triethoxy- and trimethoxysilanes adsorbed onto alumina were found to be extremely similar. It was therefore assumed that on complete hydrolysis of the silanes, the method of adsorption of the silane after hydrolysis was similar, i.e. the chemisorption of a hydrolysed trialkoxysilane was independent of the alkoxy groups present [Alexander et al., 1985].

IETS has been used to study the reaction of 5-bromo-2-hydroxybenzaldehyde with monomolecular layers of 3-aminopropyltriethoxysilane and 3-(2-aminoethyl)-aminopropyltrimethoxysilane immobilised onto alumina surfaces [Van Velzen, 1984]. It was concluded from the resulting IET spectra that the terminal amino- group of both silanes condensed with the aldehyde group on the aromatic molecule to produce the corresponding 5-bromo-2-hydroxybenzaldimine derivative (see Figure 4.1). The reaction mechanism has been confirmed by results from neutron activation and ESCA studies.

Figure 4.1. Reaction Scheme of Adsorbed Silanes with 5-bromo-2-hydroxybenzaldehyde [Van Velzen, 1984].

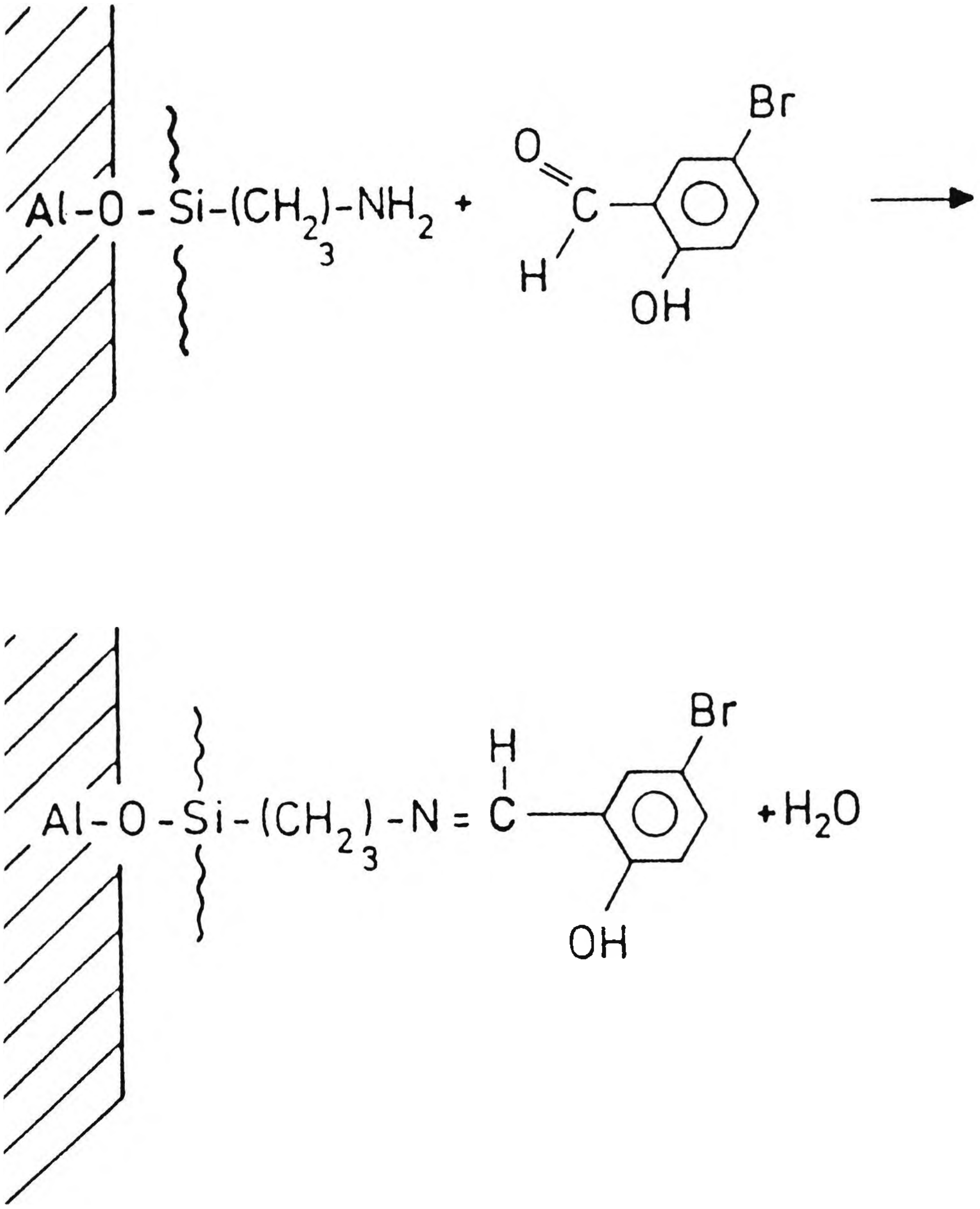

4.3 THE STUDY OF OTHER ADHESION PROMOTERS USING IETS.

Two other small groups of adhesion promoters have been studied using IETS. They are :-

(i) Phosphonic Acids.

(ii) Benzoic acids.

Phosphonic Acids

Phosphonic acids, and several alkylphosphonic acids, are used as surface dehydrating agents prior to bonding. They make the completed bond structure resistant to subsequent water intrusion and are therefore known as hydration inhibitors. Several mechanisms for the surface adsorption have been proposed and IETS has been used to investigate their validity [Henriksen et al., 1988].

The IET spectrum of phosphonic acid adsorbed onto alumina has been produced and it was concluded that phosphonic acid could directly condense onto the surface removing water. The absence of P=O vibration modes suggest that the phosphoryl groups have reacted on adsorption. It has been proposed that the formation of a resonance bond results between the phosphoryl oxygen and an adjacent surface-OH group. The acid therefore becomes an anion which in turn interacts ionically with available aluminium sites on the surface [Henriksen et al., 1988].

Benzoic Acids

The adsorption of 4-hydroxybenzoic and 4-aminobenzoic acids, used occasionally as simple coupling agents, on an alumina surface has been studied using IETS [Chu et al., 1979]. The spectra produced indicated that the bonding between the surface and the acid was through the carboxylate anion, as described in Section 2.1.1, suggesting ionic bonding with the phenyl ring perpendicular to the surface.

4.4 CONCLUSIONS.

As outlined in Chapter 3, the study of coupling agents is highly complex as a wide variety and huge number of coupling agents exist which may react with various surfaces in completely different manners. The application conditions may also determine the extent or indeed the mode of reaction of the adhesion promoter. This chapter has outlined the studies of adhesion promoters carried out using IETS. As yet the vast majority of these studies are concerned with silane coupling agents, with only a very few others considered. Until now only alumina has been considered as the adherand. An intention of this report is to initiate study of the important adhesion promoters; the titanates. As the usefulness of titanates as adhesion promoters is realised so will the use of IETS in their study.

PART II EXPERIMENTAL STUDY OF TITANIUM COUPLING AGENTS

CHAPTER FIVE - EXPERIMENTAL METHODS USED IN THE PRODUCTION OF IET SPECTRA.

5.1 INTRODUCTION.

This chapter is devoted primarily to the experimental techniques used in the fabrication of tunnel junctions, including the different junction doping techniques, and to the construction and modes of operation of the spectrometer, particularly those methods used in this project.

Historically, two types of vacuum preparation systems have been used for junction fabrication. Namely, oil diffusion and turbomolecular pumped vacuum systems. Both systems rely on a rotary pump to evacuate the preparation chamber from atmospheric pressure to less than 10^{-3} torr (τ) at which point the oil diffusion pump or turbo-molecular pump takes over. Both vacuum systems are capable of pumping to a chamber pressure of less than 10^{-7} torr [Lewis, 1985]. It is essential to prevent back streaming pump oil from reaching and contaminating the preparation chamber in the case of the diffusion pump system. This is achieved by using liquid nitrogen and molecular sieve traps at various positions in the vacuum line.

More recently, the turbomolecular pumping system has almost exclusively been used in the preparation of tunnel junctions. This system not only allows a faster rate of pumping than the oil diffusion pump system but also produces a high vacuum with a much reduced possibility of hydrocarbon contamination. This is due to the reduced amount of oil present in the system compared with the diffusion pump system [Lewis, 1985] and to the mode of action of the turbomolecular pump. In this study the turbomolecular pump system was used in the preparation of the tunnel junctions. Figure 5.1 shows a schematic diagram of the turbomolecular pump system and junction preparation chamber. Figure 5.2 is a photograph of the junction preparation chamber.

Figure 5.1. Schematic Diagram of the Turbomolecular Pump System.

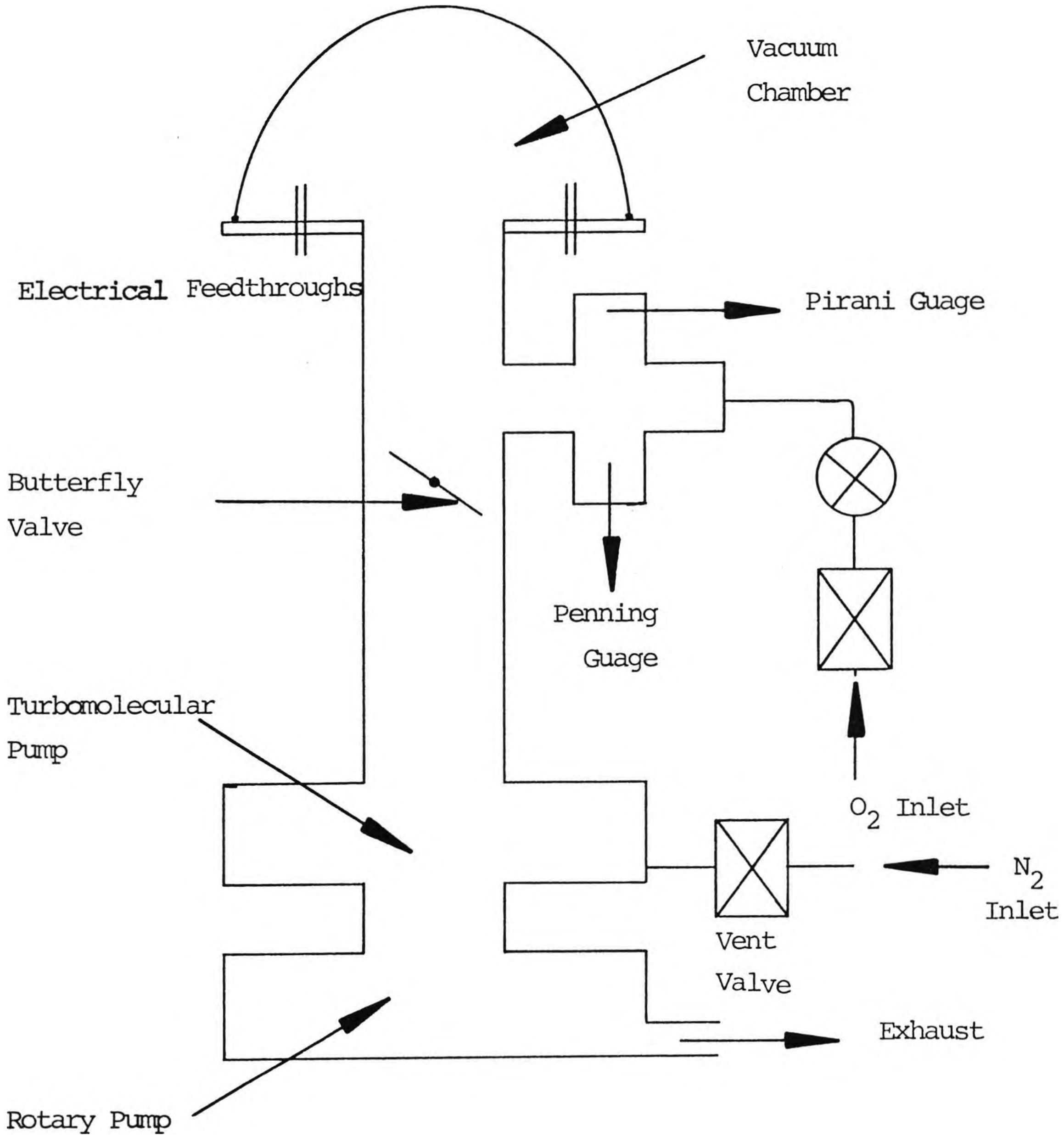

Figure 5.2. Photograph of the Turbomolecular Pump System.

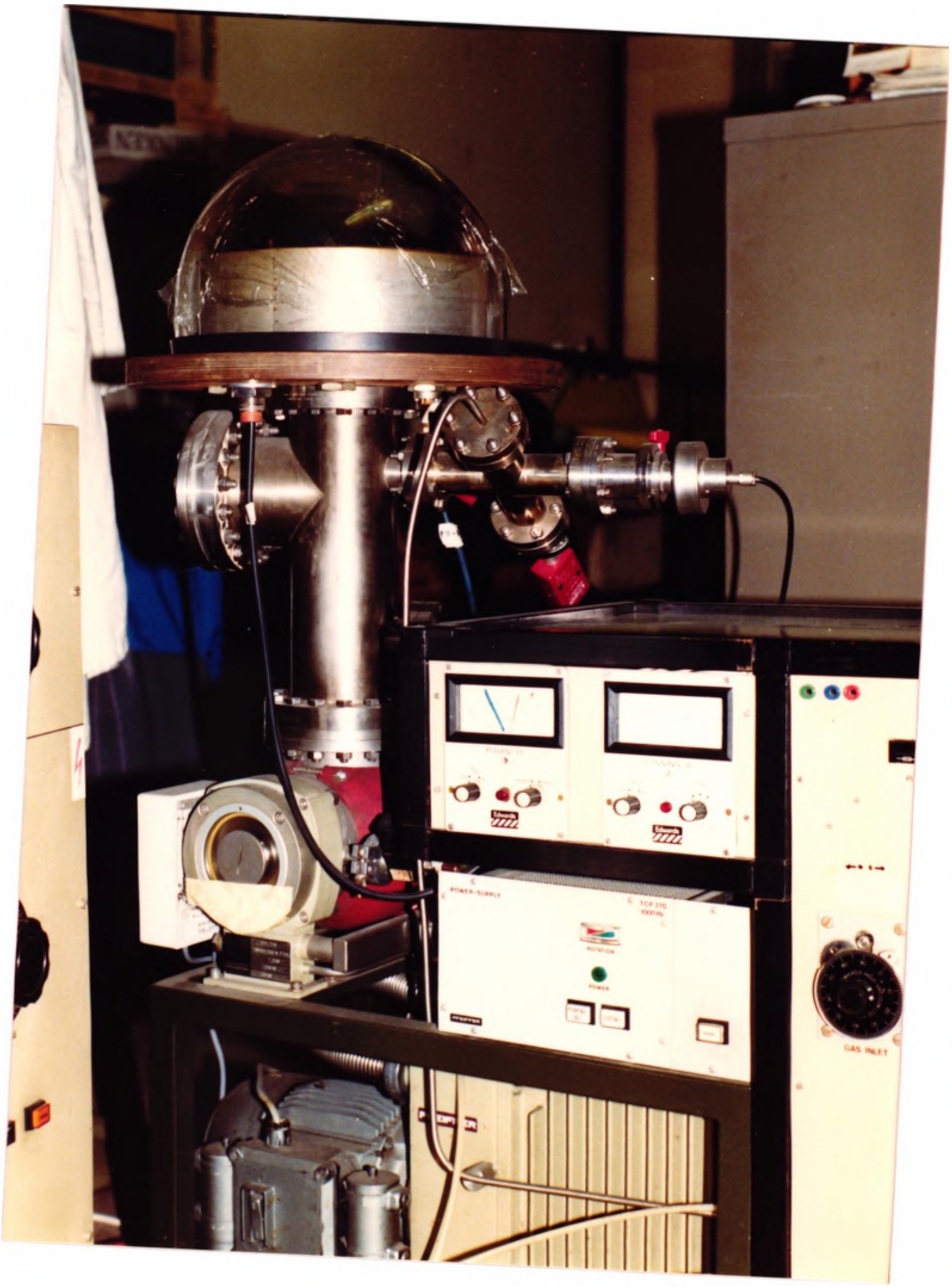

5.2 JUNCTION FABRICATION.

Most tunnelling spectroscopists construct their junctions on a glass microscope slide substrates. This requires lengthy and often unreliable cleaning procedures to remove surface contamination. Junctions can also be fabricated in other ways, such as that originated by Shott which used a printed circuit board as the supporting substrate [Shott and Field, 1979] [Shott and Field, 1980]. The use of a glass fibre printed circuit board as the supporting substrate allows the production of better electrical contacts between the junction electrodes (aluminium and lead) and the liquid helium Dewar probe, as these can be soldered joints. Junctions constructed on a glass supporting substrate (microscope slide) rely on clip connections whose electrical integrity, particularly at cryogenic temperatures, may be doubtful.

During this study it was found that the glass fibre printed circuit board supporting substrates could be reused for the production of tunnelling junctions. The circuit boards were cleaned using an abrasive cloth and water. The wet boards were dried using acetone and left under vacuum for 24 hours.

The junction fabrication process is outlined below.

Figure 5.3. The Tunnel Junction Geometry.

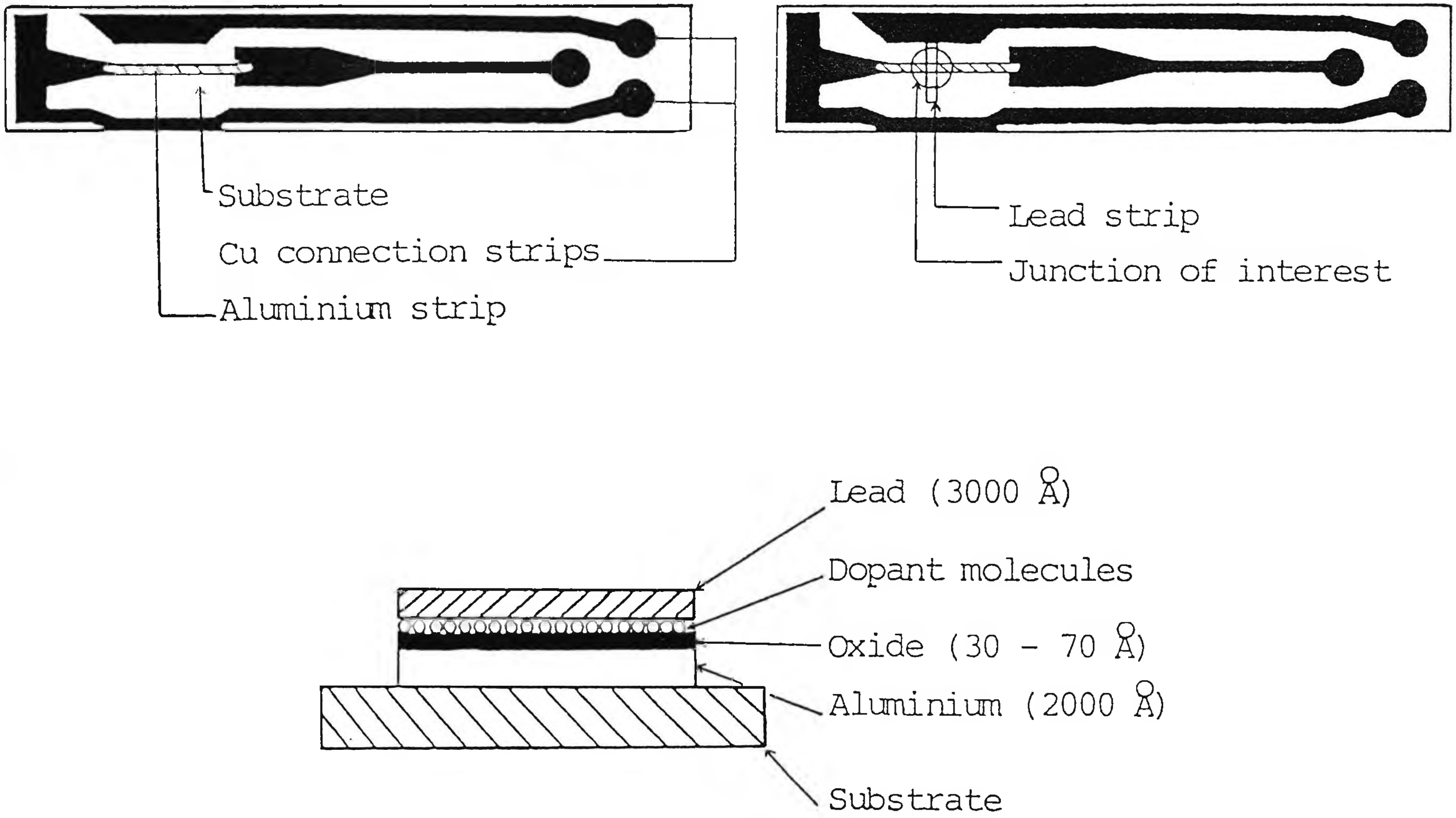

(i) The vacuum chamber is loaded with small pellets of pure aluminium in an electrically heated tungsten basket for the construction of the lower electrode, squares of lead foil on an electrically heated molybdenum boat for the upper electrode and the glass fibre junction supporting substrate. The vacuum chamber is then evacuated to less than 10^{-5} torr ($1\tau \equiv$ 1mm Hg).

(ii) The junction preparation chamber is cleaned from possible organic contamination using an oxygen glow discharge. Commercial grade oxygen is admitted to the chamber at a pressure of 10^{-1} τ and a current of 200 mA at 1 kV applied to the discharge ring for 15 minutes. This cleaning operation removes organic impurities adsorbed onto the inner surface of the vacuum chamber and the glass fibre substrate by oxidation to carbon dioxide and water which are pumped off when the chamber is evacuated again to less than 10^{-5} τ leaving the chamber clean so that uncontaminated junctions can be produced.

(iii) An aluminium strip, approximately 1mm wide and 50mm in length, is then vacuum deposited from the tungsten basket onto the supporting substrate by electrical resistance heating. The evaporation process is collimated onto the substrate by a stainless steel mask. The current supplied to the basket to provide the resistive heating is increased over a period of 3 seconds to about 50 Amps and left at this value for approximately 15 seconds. The current is then switched off and the chamber allowed to evacuate to better than $10^{-5}\tau$.

(iv) Oxidation of the aluminium strip is then carried out using commercial grade (N_2 and H_2O free) oxygen in a glow discharge at a pressure of 3 x $10^{-2}\tau$ and a current of 1 mA at 1 kV. The required oxidation time is varied to give the desired oxide thickness, of about 30-70Å for the tunnelling insulator and an optimum junction resistance after doping. The chamber is then evacuated to better than $10^{-5}\tau$.

The molecule to be studied is introduced to the insulating oxide barrier in a variety of ways (see Section 5.7)

(v) For spin doping, which has been primarily used in this study, the oxidised aluminium electrode on the circuit board, or another supporting substrate, is then removed from the chamber, the chamber being let up to atmospheric pressure using dry nitrogen. Doping is achieved by placing a few drops of the sample in solution or in the liquid state onto the alumina for an empirically determined length of time (normally 1-10 seconds). The excess liquid is spun off on a turntable at 3000 rev/min. The doped substrate is then replaced over the mask for evaporation of the lead electrode and the vacuum chamber is evacuated to better than $10^{-5}\tau$. The exposure of the oxidised aluminium electrode to the atmosphere is kept to a minimum to avoid any atmospheric contamination of the surface.

(vi) Deposition of the top electrode is carried out in a similar fashion to that of the aluminium, but from a molybdenum boat, through a stainless steel collimating mask which produces a strip electrode 1mm wide deposited at right-angles to the lower aluminium electrode. The chamber is then evacuated to better than $10^{-5}\tau$ and the lead electrode allowed to cool for 10 minutes. Removing the junction from the chamber before this cooling period results in an unsatisfactorily high lead strip resistance, apparently due to the pick up of atmospheric impurities by the hot lead [Lewis, 1985].

The junction is then carefully soldered onto the liquid helium Dewar probe. Again, care is taken to minimise the exposure time of the junction to air. The probe is then immersed in the cryogenic Dewar. Connection to the spectrometer, which is housed inside a "Faraday Cage" to minimise external air-born noise, is achieved via a 6 pin DIN-type socket.

The above method outlines the construction of an Al-AlO_x-Pb tunnel junction. Many workers have used other insulators, e.g. MgO, ZnO, AlF_3 [Gauthier et al., 1985] MnF_2, SiO_x and GeO_x [Philips, 1984] as well as other junction electrodes, e.g. Au, In, Cr, using similar methods of construction [Jaklevic and Lambe, 1970] [Klein et al, 1973] [Kirtley, 1980] [Giaever and Zella, 1968] [Al Makashta et al, 1983].

5.3 ELECTRONICS.

As discussed in Section 1.2 the excitation of a vibrational mode of an adsorbed species by an electron tunnelling through an insulator causes a discontinuity in the I-V curve. The derivatives of the I-V curve can be obtained either electronically or by computer [Adler et al., 1971], the second derivative being the most suitable to ascertain the energy of vibrational modes from their position in the spectrum due to the peaks produced. The most common method for the observation of the second derivative is to use voltage modulation techniques. The D.C. voltage across the junction is modulated by superimposing a small A.C. voltage. This gives rise to an alternating signal which, because of the non-linearity, contains harmonics of the fundamental frequency of the modulation. The magnitude of these harmonics is proportional to the derivative of the non-linearity. This approach has become standard in several spectroscopic areas such as NMR and ESR spectroscopy [Poole, 1967] and optical spectroscopy [O'Haver and Green, 1975]. The modulation technique, as applied to IETS, has been widely discussed [Patterson and Shrewchun, 1964] [Thomas and Powell, 1965] [Adler and Jackson, 1966] with Adler and Jackson providing the more comprehensive account. These accounts indicate that, using the schematic circuit diagram shown in Figure 5.4, it is only necessary to measure the amplitudes of the voltages which occur at the fundamental frequency and twice the fundamental frequency. Small voltages such as these, which are of the order of microvolts, can be measured using the lock-in amplifier (a Brookdeal 5206 two phase lock-in amplifier was used in this study), which only selects signals which are in phase with the reference voltage. In this case the fundamental modulation supplied is used as a reference voltage. The electronic apparatus and its operation and the electronic circuitry and the instrumental development have been described in more detail elsewhere [Lewis, 1985]. A block diagram of the spectrometer is supplied in Figure 5.5 and a photograph of the spectrometer is shown in Figure 5.6.

A range of alternative D.C. supplies have been used in recent years with the emphasis on batteries in an attempt to reduce electrical noise levels [Walmsley et al., 1983].

Most workers have used 4 terminal tunnel junction devices [Walmsley et al., 1983] [Edgar and Zyskowski, 1985] in an effort to reduce electrode noise, negate the importance of the intrinsic strip resistances and therefore improve the quality of spectra obtained. The use of these more complex systems is not always necessary and 2 terminal devices may well suffice. As outlined in Section 5.2 and shown in Figure 5.3 the junctions produced in this study were 2 terminal devices.

Figure 5.4. Schematic Circuit for Second Harmonic Detection Measurements.

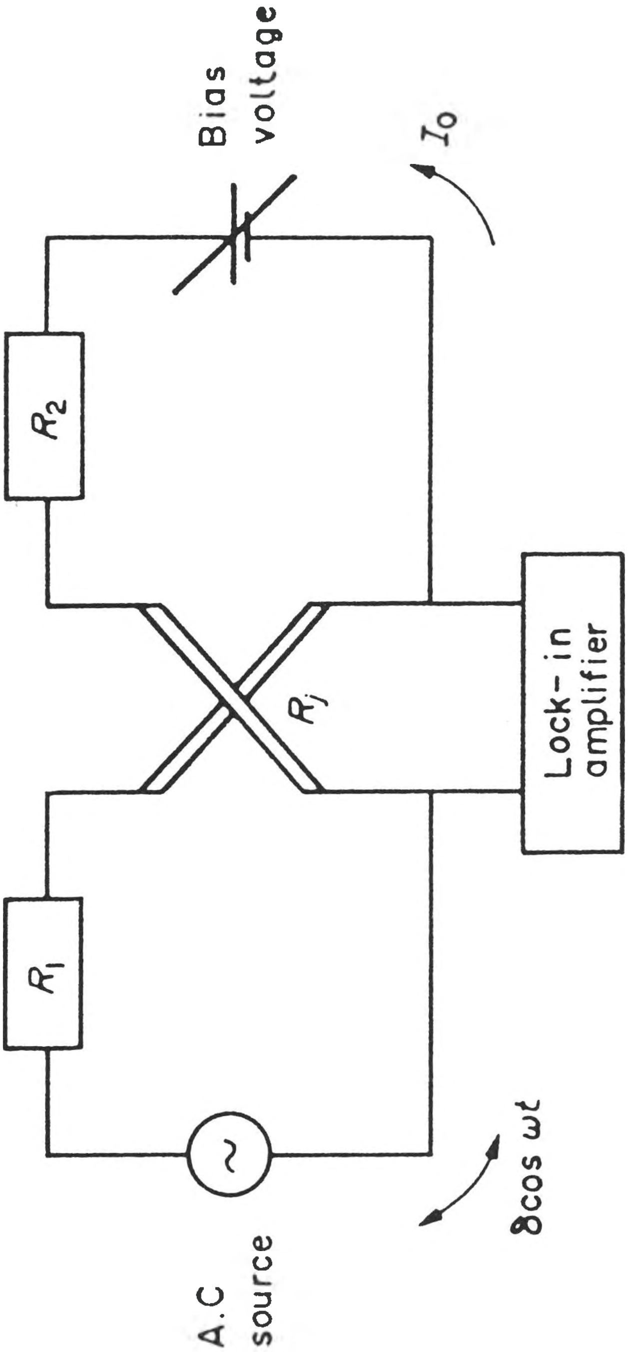

Figure 5.5. Block Diagram of the Spectrometer.

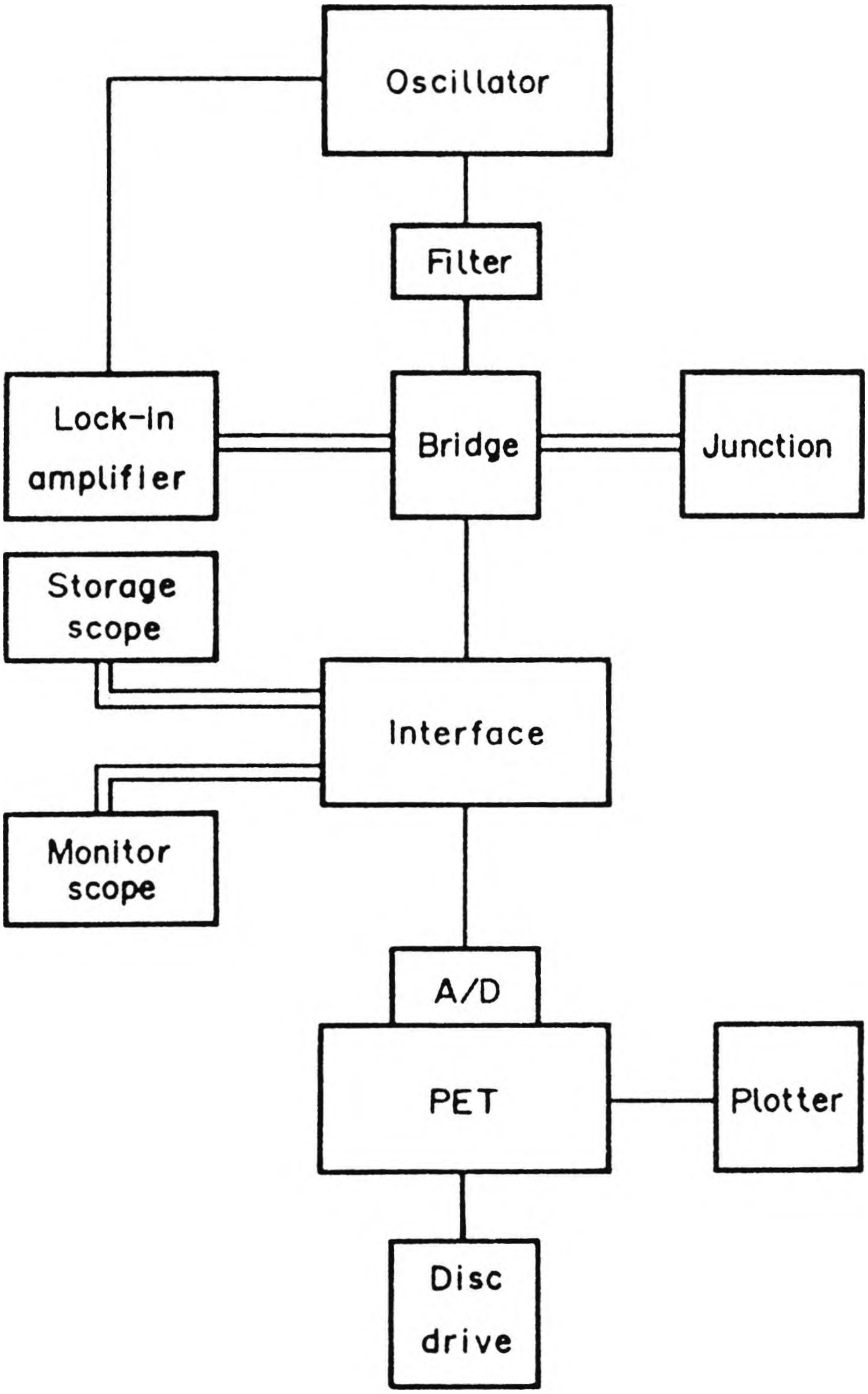

Figure 5.6. The Tunnelling Spectrometer.

5.4 **SIGNAL AVERAGING.**

Several workers have used computer techniques to enhance the signal-to-noise ratios produced from their spectrometers [Ratinen, 1983] [Eib et al., 1984] [Leo, 1982]. The system used in this study employed a Commodore PET as the main microprocessing unit. This allows signal averaging to be carried out. Whilst simple signal averaging is used, good results are produced. The system used in this study involved repeated measurement of each point in turn. These signals are then averaged. A detailed description of the computer hard- and software has been provided previously [Lewis, 1985]. Other workers repeatedly scan the whole spectrum and caution should be exercised here as significant aging of the tunnel junction has been observed on repeated scans.

5.5 **OPTIMIZATION OF THE RUNNING CONDITIONS.**

The junction is incorporated as one arm of a Wheatstone Bridge. The applied A.C. signal provides both a reference voltage for the lock-in amplifier and the required modulation voltage (see Figure 5.5). An X-Y recorder is used to plot the applied sweeping D.C. bias against the second derivative response. A Commodore PET microcomputer is used to drive an A/D interface (PUPI unit) and to store the data on 5.25 inch floppy disk (see

Figure 5.5). The computer program (written in CPM BASIC), which controls the spectrometer in the production and storage of the spectra has been described in detail by Lewis [Lewis, 1985]. The method of spectral production used for this report is essentially the same as employed by Lewis [1985].

The optimization of the spectrometer operating conditions is described below.

5.5.1 The Applied A.C. Modulation Voltage.

Once the junction is connected to the spectrometer the first step is to set the A.C. modulation voltage. As discussed in Section 1.3.1, the peak width is broadened by larger A.C. values. However the larger A.C. values can considerably enhance the sensitivity of the spectrometer due to the more readily detected distortion of the applied A.C. Hence a compromise has to be reached between the two effects caused by the variation in A.C. to obtain a well resolved spectrum. Typically, modulation voltages of between 2 and 10 mV were used in the spectral production in the work cited in this report.

5.5.2 Balancing the Wheatstone Bridge.

Once the A.C. has been set the bridge has to be balanced, the balance point being dependent on the applied A.C. and the resistance of the junction. The bridge is balanced at the highest possible sensitivity that can be achieved with the balance controls. Higher sensitivities give greater resolution, but high background noise levels may necessitate lower sensitivities occasionally being used in practice. In this study this was carried out manually, however novel bridge circuitry has recently been proposed [Edgar, 1987] that affords improvements to the stability and automatic balancing of an "active" bridge circuit for IETS.

5.5.3 The Time Constant.

The time constant controls the response time of the lock-in amplifier to the supplied signal. A long time constant reduces electrical noise levels but can also reduce the required signal. A short time constant, while not affecting the required signal, can allow much more noise into the trace. The loss of signal caused by a long time constant can be overcome by using a long time scan; the time taken for the spectrum to be run. The time constant during the scan was found typically to be 1 second for a 5 minute scan and 3 seconds for a 30 minute scan. Whilst setting the lock-in amplifier to the highest sensitivity possible it was important that the time constant was as small as possible (usually 1 second) to allow balancing to be achieved.

5.5.4 Boosting.

Occasionally junctions are produced which are inherently unstable or of low initial resistance. The performance of such junctions can be remarkably improved by use of a phenomenon called "boosting". This is normally noticed by an immediate change in the junction resistance, usually to a higher value (sometimes to enormous resistances > 100kΩ) when the sweeping D.C. bias is applied to the junction. This results in a change in the size of the modulation voltage (if the resistance of the junction increases then it is usual for the modulation voltage to decrease) and a cleaner signal is seen on the oscilloscope.

To utilise this effect in the production of better resolved spectra, a routine is built into the controlling computer program and the electronics to allow the application of a D.C. voltage of up to 5V [Lewis, 1985] to the junction. Therefore, if an intrinsically unstable junction is produced the spectrometer operator may attempt to boost the junction before any further action.

Two proposed explanations of the effect have previously been outlined [Lewis, 1985].

(i) Two-layer oxides.

(ii) Metallic bridges.

(i) suggests that the oxide can exist as two layers [Dorsey, 1969]. The first is of high dielectric strength and the second of lower dielectric strength. When the two layers exist together the barrier is too thick for all the tunnelling effects to be seen. At larger D.C. biases the second layer breaks down causing a sudden change in resistance. It would be expected that the resistance would be reduced by this effect.

(ii) was proposed by Nayler [1982] who suggests that the presence of very thin, metallic bridges between the electrodes is responsible for the observation of boosting. When a higher D.C. bias is applied the high current density produced "burns out" the filaments giving a sharp change in resistance, to higher resistance. This is consistent with workers who use glass supporting substrates. The deposition of aluminium from the vapour phase is thought to produce spikes which pierce the oxide layer to produce metallic bridges. It was noted by Lewis that if a thicker aluminium electrode is deposited onto the glass fibre substrate a reduction in the number of junctions requiring boosting was observed [Lewis, 1982].

This is suggested as a thicker aluminium electrode (to about 2000Å) would result in a smoother surface.

The effect of the dopant has not been taken into account in the above boosting explanations. It has been noticed by the author that junctions doped from primarily aqueous solutions generally have very low junction resistances in comparison to those junctions doped from more non-polar solutions. This effect could be explained by the more polar dopant acting in effect as an electrolyte between the electrodes and therefore a lower initial resistance is observed. On the application of a large D.C. bias the increased current density could modify the ionic species on the alumina possible. This would result in the immediate change in the resistance of the junction. This effect has yet to be comprehensively analyzed but years of experience suggest that the effect of the dopant molecules on the need for boosting junctions should not be overlooked.

Another, much smaller effect, on the junction resistance could be due to specific reorientation of the dopant molecules on the surface when a large bias is applied. This is most likely to occur with polar or ionic dopant species.

None of the above proposals are completely satisfactory in the explanation of the boosting effect. To fully understand the observation of boosting the meticulous analysis of the junction resistance and the effects on it is necessary.

5.5.5 Conclusions.

No general rules can be laid down to give the optimum spectrometer operating conditions as every junction exhibits its own unique electrical characteristics. Optimization of the instrumental parameters can only be achieved through practice and experience.

5.6 CRYOGENICS.

As discussed in Section 1.3.2, IET spectra peaks are broadened by thermal effects. Liquid helium is therefore required to produce high resolution spectra. There are two methods of retaining the junction at cryogenic temperatures. One is to immerse the junction directly into the liquid helium in a Dewar, as carried out in these studies. This method is quick but does rely on sufficient supplies of liquid helium and work has to be carried out before the liquid helium boils away. However seventeen litres of liquid helium is normally enough to run fifty separate junctions. The second method of achieving cryogenic junction temperatures is to use a cryogenic refrigeration unit. This adds considerably to the cost of setting up an IETS laboratory. Further, depending on the size of the junction substrate, it can take several hours to cool the junction. This process is not very practical as junctions are bound to degrade in electrical characteristics during the cooling period. Provided that the correct safety procedures are carried out, the employment of liquid helium and its associated equipment should not present any experimental difficulty.

The total immersion of the junction substrate in liquid helium is used to attain the cryogenic temperatures (4.2K) required in the experimentation of this report.

5.7 JUNCTION DOPING TECHNIQUES.

Four main experimental techniques may be used to dope the sample of interest onto the insulator contained in the tunnel junction. These are outlined below.

5.7.1 Vapour Doping.

In this method the junction substrate is removed from the vacuum chamber (junction preparation chamber) once the aluminium strip has been deposited and the insulating oxide grown (so the junction is uncompleted). The junction is then placed in a closed vessel above the sample liquid or gas. The exposure time will depend on the nature of the sample and is determined by totally empirical means; polar samples tend to require shorter periods of exposure than nonpolar samples. Finally the newly doped substrate is returned to the vacuum chamber for the deposition of the upper electrode. Alternatively the junction may be doped "in situ" in the vacuum chamber itself by bleeding in the appropriate gases. This technique has been used to remove all possibility of atmospheric contamination [Shklyarevskii et al., 1978].

5.7.2 Spin Doping.

This is similar to external vapour doping in that doping is carried out before junction manufacture is complete. In this instance, neat liquid or a solution is placed directly onto the insulator surface. Once again the exposure time of the insulator to the sample will be determined empirically. Finally the excess liquid is spun off on a turntable at 3000 r.p.m. prior to the vacuum deposition of the upper electrode. This technique has been extensively used in the manufacture of junctions in this study.

5.7.3 Infusion Doping.

In this method of doping the completed, undoped junction is placed over an aqueous solution or suspension of the dopant contained in a desiccator type vessel. The resistance of the junction is monitored and the junction is placed in the cryogenic Dewar once the resistance has reached an appropriate level (normally 50-2000Ω) [Jaklevic and Gaertner, 1978].

5.7.4 Penetration Doping.

This doping technique is similar to infusion doping in that the doping is carried out on the completed junction. Here, neat liquid is placed on the junction top electrode and the junction resistance monitored, as above. Alternatively the completed junction may be exposed to a gas or a vapour contained in a desiccator [Nayler, 1982] [Lewis, 1985].

The construction and application of a novel combination glove-box deposition system has been carried out in order to observe the tunnelling spectra of air-sensitive materials deposited onto the alumina of a tunnel junction [Hipps and Mazur, 1984]. A similar technique has been used to regulate the effect of atmospheric moisture on the air hydrolysis of alkyl titanates (see Section 6.1).

CHAPTER SIX - AN IETS STUDY OF TITANATE COUPLING AGENTS.

Experimental investigations were carried out in order to study the initial adsorption of the titanates onto an alumina surface and the observation of their hydrolysis reactions, both in solution and on the surface. The way in which they may react further with an organic entity on the surface was also studied. All this was done by the technique of IETS and the resulting spectra are presented and their implications discussed.

6.1 THE IETS STUDY OF TITANIUM (IV) PROPOXIDE.

6.1.1 Introduction.

The aim of this study was to investigate the behaviour of titanate coupling agents using IETS by observing the adsorption of an alkyl- (or alkoxy-) titanate on an alumina surface. Titanium (IV) propoxide - $Ti(OCH_2CH_2CH_3)_4$ - was chosen as the particular example for initial study. This choice of dopant material was designed to accomplish two main objectives.

(i) The organic ligands should be simple enough not to over complicate the IET spectrum. By analysis of the spectrum produced it should be possible to determine any changes in the molecular structure of the dopant due to the mode of adsorption onto the alumina surface.

(ii) The dopant should be easily handled, so that on application to the surface of the tunnel junction its initial structure should remain unchanged by the doping procedure. Hence, any changes in the structure noted from the IET spectrum can be attributed totally to the mode of adsorption to the surface.

Although titanium propoxide is not the simplest structured alkyl titanate available, titanium ethoxide and methoxide, as stated earlier in Section 3.3.2, are extremely susceptible to hydrolysis by atmospheric or solution bound water. Although titanium propoxide is also susceptible to hydrolysis it is less so and by taking suitable precautions it should be possible to overcome this difficulty whilst still having a relatively simple molecule.

6.1.2 **Experimental Procedure.**

Titanium (IV) propoxide was applied to the alumina surface in two forms:-

(i) 1% v/v solution in ethanol (absolute alcohol).
(ii) 1% v/v solution in hexane.

These solutions were prepared immediately before spin doping in the following way. The solvents were dried over a particulate zeolytic drying agent (molecular sieve) for at least 24 hours. Together with the titanium propoxide they were transferred to a "dry atmosphere bag". - which was subsequently closed and inflated with dry nitrogen gas which had been dried by passing it through a zeolytic trap. Similar to a "dry-box", the "dry-bag" (an Aldrich "Atmosbag") has two inserted gloves to allow work to be carried out in the bag. The bag was sealed around the stack of the high vacuum equipment, as shown in Figure 6.1.1, to allow the transfer of the junction from the preparation chamber to the spinner during the doping procedure.

The 1% solutions of titanium (IV) propoxide were prepared by diluting 0.05 ml of titanium (IV) propoxide to 5ml with the appropriate solvent under an inert atmosphere of nitrogen. This procedure was carried out to minimise the possibility of atmospheric hydrolysis of the titanium propoxide solutions.

The junctions were fabricated as described in Section 5.2. The freshly made solutions were spin doped onto the alumina surface, again under dry nitrogen. The doped, but uncompleted, junction was replaced in the vacuum preparation chamber and completed by the vacuum deposition of the top lead electrode. The "dry-bag" was deflated and the completed junction was then removed from the preparation chamber and soldered to the Dewar probe after quickly noting the junction and electrode resistances with a low current ohm meter. The probe with the junction was inserted into the liquid helium Dewar as fast as possible to minimise atmospheric exposure. The spectrum was produced as outlined in Section 5.5. The spectral data was stored on $5^1/_4$" floppy disk and an A3 size hard copy of the spectrum was produced by a Graphtec MP1000 plotter.

6.1.3 IET Spectra of Titanium (IV) Propoxide.

(i) 1% v/v Titanium (IV) Propoxide in Dry Ethanol.

In the preparation of the Al-AlO$_x$-Pb tunnel junction doped with a 1% v/v solution of titanium (IV) propoxide in ethanol, a plasma oxidation time of 60 seconds was used to produce the alumina barrier. Although the electrode resistances of the completed junction were found to be negligible the junction resistance was found to be large at 10 kΩ (at 298K). The operating conditions of the spectrometer were as follows.

Sensitivity	0.5	µV
Modulation Voltage	6	mV
Time Constant	1	sec.
Scan Time	15	mins.

Figure 6.1.2 shows the resulting IET spectrum of a junction doped with a 1% titanium propoxide in dry ethanol solution and Table 6.1.1 shows the assignment of the peaks produced in Figure 6.1.2.

Figure 6.1.1. The Dry nitrogen Atmosphere Doping Bag.

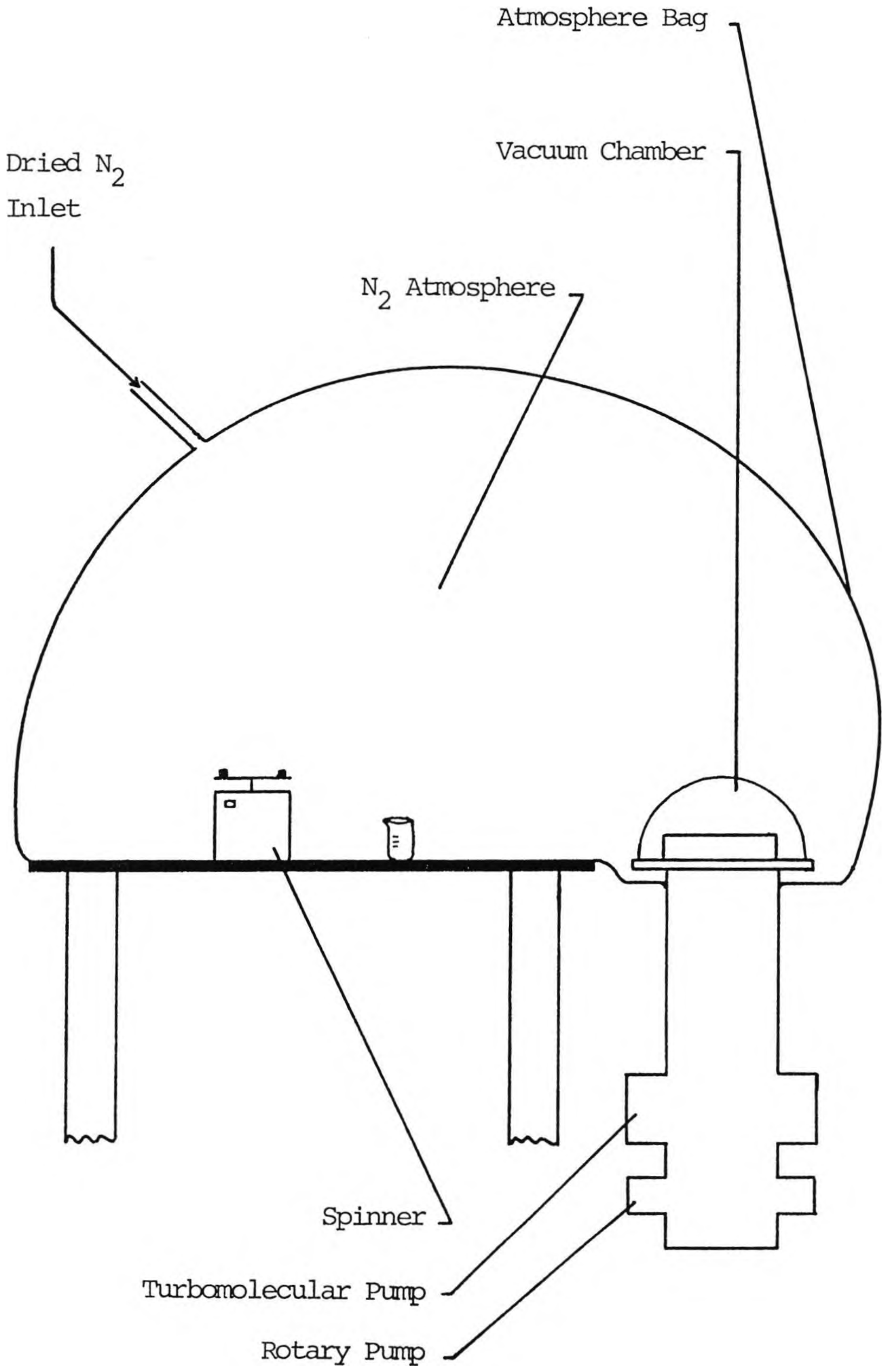

Figure 6.1.2. IET Spectrum of Titanium (IV) Propoxide in Dried Ethanol.

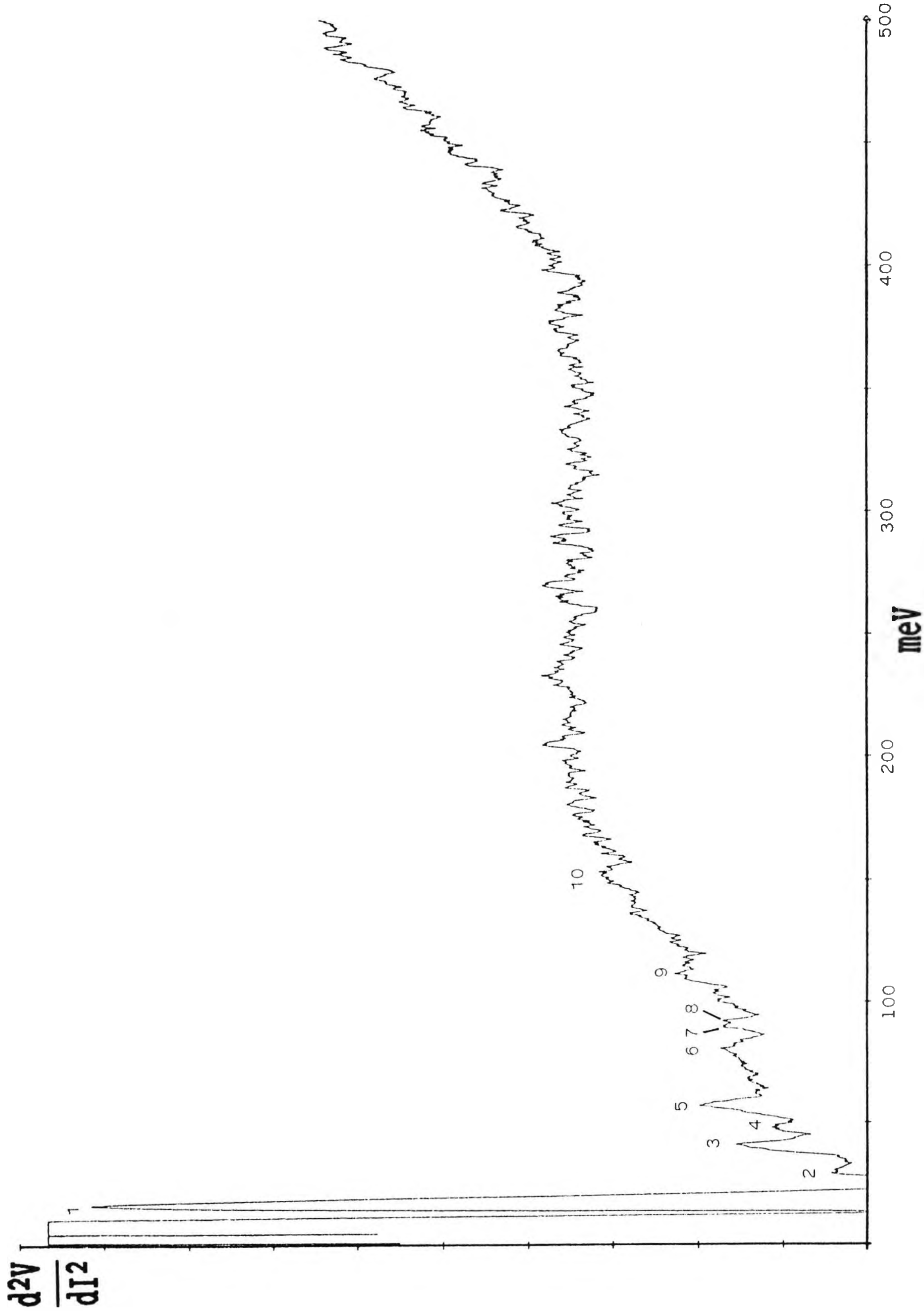

Table 6.1.1. Spectral Assignment of the IET Spectrum of Titanium Propoxide in Dried Ethanol.

Peak No.	Potential (mV)	Wave No. (cm^{-1})	Intens.	Assignment
1	18.6	150	VS	Al Phonon
2	29.6	239	W	Al Phonon
3	41.4	334	M/W	Al Phonon
4	55.7	449	W	Ti-O str.
5	57.9	467	M/W	Ti-O str.
6	81.3	656	W/Br	Ti-O str.
7	90.3	728	W	Ti-O str.
8	92.7	748	W	Ti-O str.
9	111.7	901	W/Br	Ti-O-Ti
10	154.6	1247	W/Br	C-H def.

S=Strong, M=Medium, W=Weak and Br=Broad Intensities.

1meV $\equiv$ 8.065 cm^{-1}

Assignments were made using the following references [Bradley et al., 1978] [Nakamoto, 1986] [Williams and Flemming, 1980].

(ii) 1% v/v Titanium (IV) Propoxide in Dry Hexane.

In the preparation of the Al-AlO$_x$-Pb tunnel junction doped with a 1% v/v solution of titanium (IV) propoxide in zeolytically dried hexane, again, a plasma oxidation time of 60 seconds was used to produce the alumina barrier. The electrode resistances of the completed junction were found to be negligible and the junction resistance was 300Ω (at 298K). The operating conditions of the spectrometer were as follows.

Sensitivity	0.5	μV
Modulation Voltage	6	mV
Time Constant	1	sec.
Scan Time	15	mins.

Figure 6.1.3 shows the resulting IET spectrum of a junction doped with a 1% titanium propoxide in a dry hexane solution and Table 6.1.2 indicates the assignment of the peaks produced in Figure 6.1.3.

Figure 6.1.3. IET Spectrum of Titanium (IV) Propoxide in Dried Hexane.

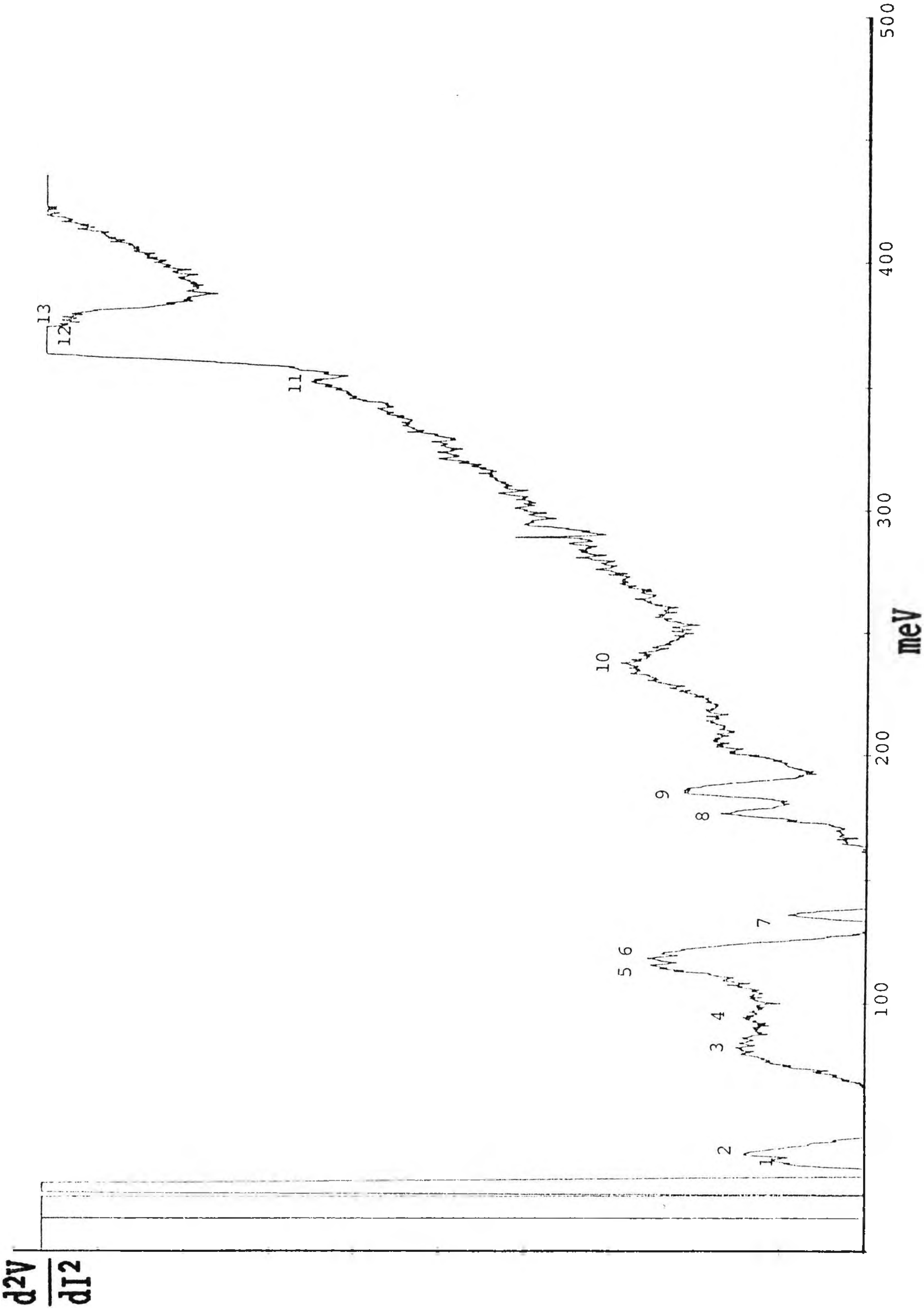

Table 6.1.2. Spectral Assignment of the IET Spectrum of Titanium Propoxide in Dried Hexane.

Peak No.	Energy (meV)	Wave No. (cm^{-1})	Intens.	Assignment
1	36.7	296	S	Al Phonon
2	39.3	317	S	Al Phonon
3	81.7	659	S	Terminal M-O
4	93.9	757	M	Ti-O str.
5	115.0	927	M	Term. C-O
6	117.9	950	S/Br	Al-O str.
7	136.0	1097	M	Term. C-O
8	175.9	1419	M	CH_3 def.
9	184.9	1491	M	CH_3 def.
10	235.0	1895	M/	
11	351.6	2836	W	C-H str.
12	368.1	2969	S	C-H str.
13	380.1	3066	Sh	C-H str.

S=Strong, M=Medium, W=Weak, Br=Broad and Sh=Shoulder Intensities.

$1meV \equiv 8.065\ cm^{-1}$

Assignments were made using the following references [Bradley et al., 1978] [Nakamoto, 1986] [Williams and Flemming, 1980].

6.1.4 Discussion and Interpretation of the IET Spectra of Titanium (IV) Propoxide.

The infrared spectrum of $Ti(OPr)_4$ as a liquid film between sodium chloride plates was produced on a Perkin Elmer 983 spectrophotometer. Table 6.1.3 compares the infrared spectrum of the liquid and the tunnelling spectra of titanium propoxide from the two different solvents.

Bradley et al. [1978] have studied titanium ethoxide in the liquid state by infrared spectroscopy. Their assignments for this spectrum were used to derive the assignments of the infrared spectrum of $Ti(OPr)_4$. Bradley postulated that a trimeric species, shown in Figure 6.1.4, was present in the liquid form of $Ti(OEt)_4$. This was indicated by presence of both terminal and bridging C-O species in the infrared spectrum between 1000 and 1150 cm^{-1}. The peak energies in the infrared spectrum of $Ti(OPr)_4$ correspond very well to those in the infrared spectrum of $Ti(OEt)_4$ with vibrational modes of bridging C-O species at 888 and 1043 cm^{-1}. Therefore it is possible that a similar trimeric species is present in the liquid form of $Ti(OPr)_4$ (as shown in Figure 6.1.4). However, Table 6.1.3 indicates that there are no such bridging C-O modes present in the tunnelling spectra of $Ti(OPr)_4$. This in turn suggests that the trimeric species, possible in the pure liquid state, is lost on the adsorption of the titanium propoxide in solution onto the alumina surface.

Table 6.1.3. Spectral Assignment of the IET Spectra of $Ti(OPr)_4$ in Comparison with the Infrared Spectrum of Liquid Phase $Ti(OPr)_4$.

Peaks in Wave Numbers (cm^{-1})

I.R. of $Ti(OPr)_4$	ETHANOL SPECTRUM	HEXANE SPECTRUM	ASSIGNMENT
577			Bridging Structure
597			
-	666	659	Ti-O str.
	728		
754	748	757	Ti-O str.
786			
863			
888			Bridging C-O str.
907	901	927	Ti-O-Ti / term C-O
970			
994			Ti-O-C str.
1043			Bridging C-O
1076		1097	Terminal C-O
1105			Terminal C-O
1132			Terminal C-O
1248-1360	1247		CH_2 def.
1378		1418	CH_3 def.
1442-1467		1490	C-H def.
2720			C-H str.
2840		2836	C-H str.
2873			C-H str.
2932			C-H str.
2959		2969	C-H str.
-		3066	C-H str.

Assignments were made using the following references [Bradley et al., 1978] [Nakamoto, 1986] [Williams and Flemming, 1980].

Figure 6.1.4. The Trimeric Form of Titanium Ethoxide as Proposed by Bradley et al. [1978] (alkyl (CH_3CH_2-) groups omitted for clarity).

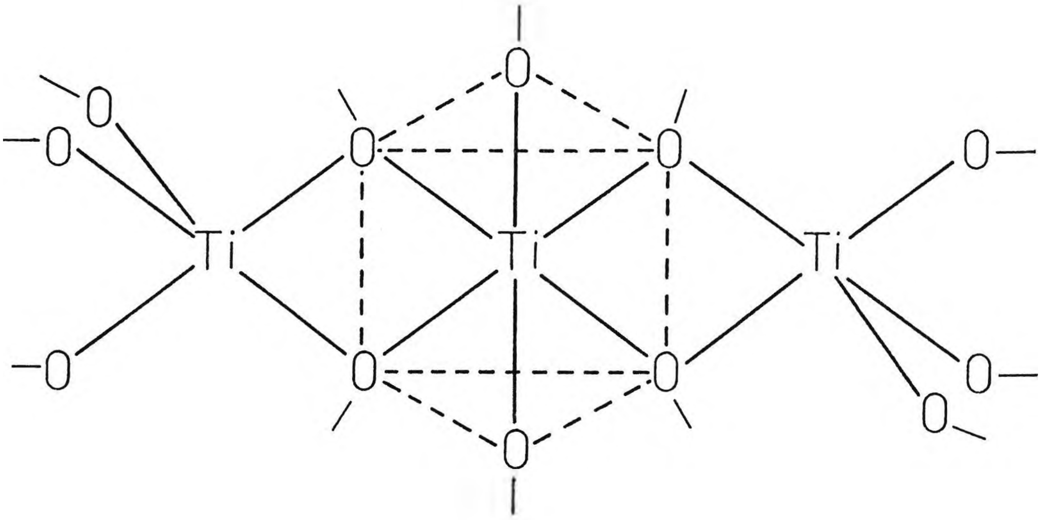

i) **Ethanol Solution**

The IET spectrum produced from the junction that was spin doped with a 1% v/v $Ti(OPr)_4$ in dried ethanol (Figure 6.1.2 and Table 6.1.1) was found to have a very large junction resistance (J_R = 10 kΩ). This factor suppressed the tunnelling signal of the spectrum and therefore only small peaks were seen. The instability (noise) of the spectrum and the high resistance of the junction tend to suggest that hydrolysis, to a certain extent, of the titanium propoxide had already occurred in the dried ethanolic solution, most probably due to residual water in the solution. Atmospheric hydrolysis of the titanate was ruled out by the use of the dried nitrogen atmosphere bag during solution preparation and doping. However, good low energy Ti-O modes definition may be seen. Some C-H deformation modes are seen at 1247 cm^{-1} which tend to indicate that total hydrolysis of the titanate to $Ti(OH)_4$ had not occurred in solution or on the alumina surface. Hydrolysis of the titanate leads to the liberation of propanol which, like ethanol and methanol has been shown not to dope the alumina surface under the conditions used in these experiments. Therefore the observed alkyl-vibration modes in the IET spectrum must be as a result of unhydrolyzed titanate species. The vibrational mode at 901 cm^{-1}, assigned to Ti-O-Ti linkage indicates some formation of polymeric species.

The ethanol solution of titanium propoxide was left in an atmosphere of nitrogen and within 24 hours the solution was seen to go "cloudy" indicating an extensive amount of hydrolysis. This observation also indicates the presence of a significant amount of residual water in the solution.

ii) **Hexane Solution**

The IET spectrum produced from the junction that was spin doped with a 1% v/v $Ti(OPr)_4$ in dried hexane (Figure 6.1.3 and Table 6.1.2) can be seen to be much less noisy than the previous one. With the fact that the junction resistance was much lower than before (300Ω compared with 10 kΩ), it suggests that the extent of hydrolysis of the titanate is much less in the dried hexane solution. A reduction in the number of C-O vibration modes seen in the infrared spectrum of $Ti(OPr)_4$ suggests that the trimeric form is lost on the adsorption onto the alumina surface. Unlike the previous case, no Ti-O-Ti modes can be seen in the hexane solution doped titanate spectrum and so it may be deduced that polymerisation to form Ti-O-Ti linkages has not occurred in the largely anhydrous hexane solution of titanium propoxide.

Both ethanol and hexane were found not to dope the alumina surface in the tunnel junction under the conditions used in the above study (both by the author and previously [Lewis, 1985]). Therefore all the vibrational modes present in the tunnelling spectra of titanium (IV) propoxide can be attributed to the titanate and any species produced on the adsorption of the titanate on the alumina surface.

6.2 AN IETS STUDY OF THREE INDUSTRIALLY IMPORTANT TITANIUM CHELATE COUPLING AGENTS.

Section 3.3.2 has already outlined the importance of titanium chelate complexes as coupling agents for inks, lacquers and paint surface coating systems. Three industrially important titanium chelates have been investigated. Samples of which were generously supplied to us by Dynamit Nobel Chemie (West Germany): titanium acetylacetonate (**TAA**); triethanolamine titanate (**TEAT**) and octylene glycol titanate (**OGT**). The industrial nomenclature for the titanate coupling agents used in this study are not accurate by the IUPAC conventions. The more correct nomenclatures are given below:

TAA - Titanium, bis(2,4,- pentanedionato - O,O') bis(2- propanolato).

TEAT - Titanium, bis[[2,2',2''- nitrilotris-[ethanolato]] (1-) N,O] bis(2-propanolato).

OGT - Titanium, tetrakis(2-ethyl- 1,3-hexanediolato).

The structures of the above titanates are shown in Figure 6.2.1.

Figure 6.2.1. The Three Industrially Important Titanium Chelate Coupling Agents Studied.

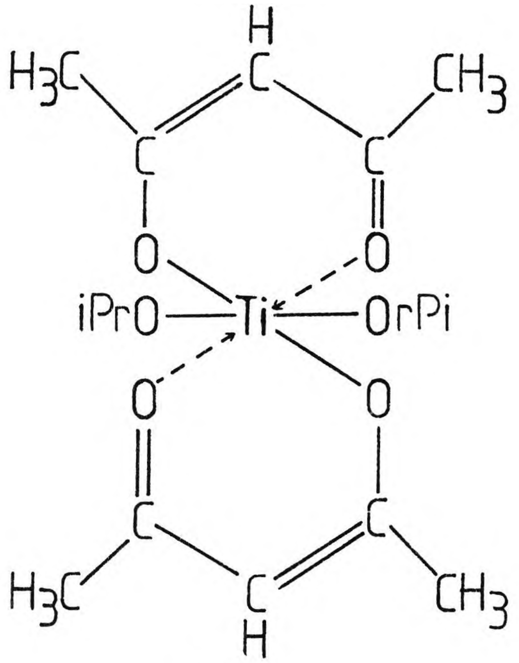

TAA
(Titanium Acetylacetonate)

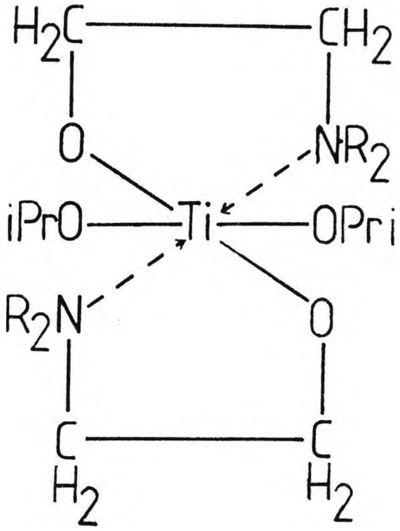

TEAT
(Triethanolamine Titanate)

R = $-CH_2CH_2OH$

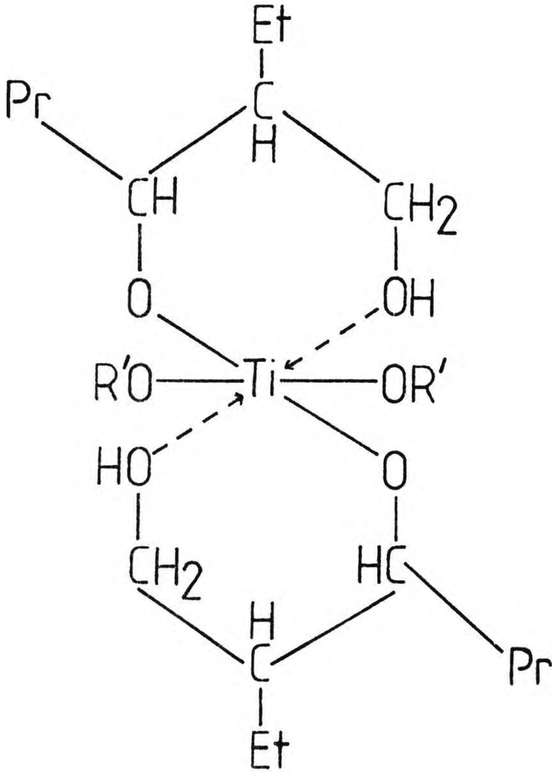

R' =

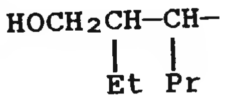

$HOCH_2\underset{Et}{\underset{|}{C}}H-\underset{Pr}{\underset{|}{C}}H-$

OGT
(Octylene Glycol Titanate)

Owing to their special structure these titanium chelates are much more stable to hydrolysis than the corresponding simple alkyl compounds. The alkoxy- groups still present in the chelates are shielded by the chelating groups so that their hydrolytic reactivity is inhibited. Depending on their composition, aqueous solutions of these chelates may exhibit hydrolytic stabilities in solution ranging from a few hours to several weeks.

Titanium chelates are normally applied in industrial applications as water / parent alcohol solution mixes [Anon, 1980]. It is therefore important to note, during this study, the water content of the solutions used. The inclusion of the parent alcohol has been shown to reduce the extent of solution hydrolysis [Anon, 1980]. Industrially, titanium chelates are normally applied in 0.5 - 2% v/v concentration solutions, it was therefore important to mimic this in the course of this study. It was also found that reasonable junction resistances were produced if solutions of this concentration were spin doped onto the alumina surfaces. The specific experimental procedures used in introducing the coupling agents to the alumina surface of the Al-AlO_x-Pb tunnel junctions used in this study are outlined before the presentation of the spectra produced.

6.2.1 Titanium Acetylacetonate Doped Tunnel Junctions.

TAA is a widely used, industrially important, titanium chelate complex. It is first necessary to consider the adsorption of TAA from an anhydrous solution in order to show the mode of titanate adsorption without the presence of hydrolysis reactions in the solution. The dopant solution was again prepared and the junction was doped in the dry-nitrogen atmosphere bag (see Figure 6.1.1) as used in the preparation of the titanium (IV) propoxide solutions in Section 6.1. In this case 0.05ml of TAA was diluted to 10ml with zeolytically dried isopropyl alcohol (IPA). The plasma discharge oxidation of the aluminium strip was carried out for 60 seconds. The junction resistance was found to be 500Ω (at 298K) and the operating conditions of the spectrometer were as follows.

Sensitivity	0.5	μV
Modulation Voltage	6	mV
Time Constant	3	secs.
Scan Time	30	mins.

Figure 6.2.2 shows the resulting IET spectrum produced by doping an Al-AlO$_x$-Pb tunnel junction with a solution of 0.5% v/v TAA in zeolytically dried IPA. Table 6.2.1 shows the spectral assignment of the peaks produced in Figure 6.2.2. The thin-film infrared spectrum of TAA (as

received) between sodium chloride plates was produced on a Perkin Elmer 983 infrared spectrophotometer. Table 6.2.1 also compares the energies of the peaks produced in the IET spectrum (Figure 6.2.2) with those from the infrared spectrum of the liquid TAA.

Figure 6.2.2. IET Spectrum of a Junction Spin Doped with a 0.5% TAA in Dried IPA Solution.

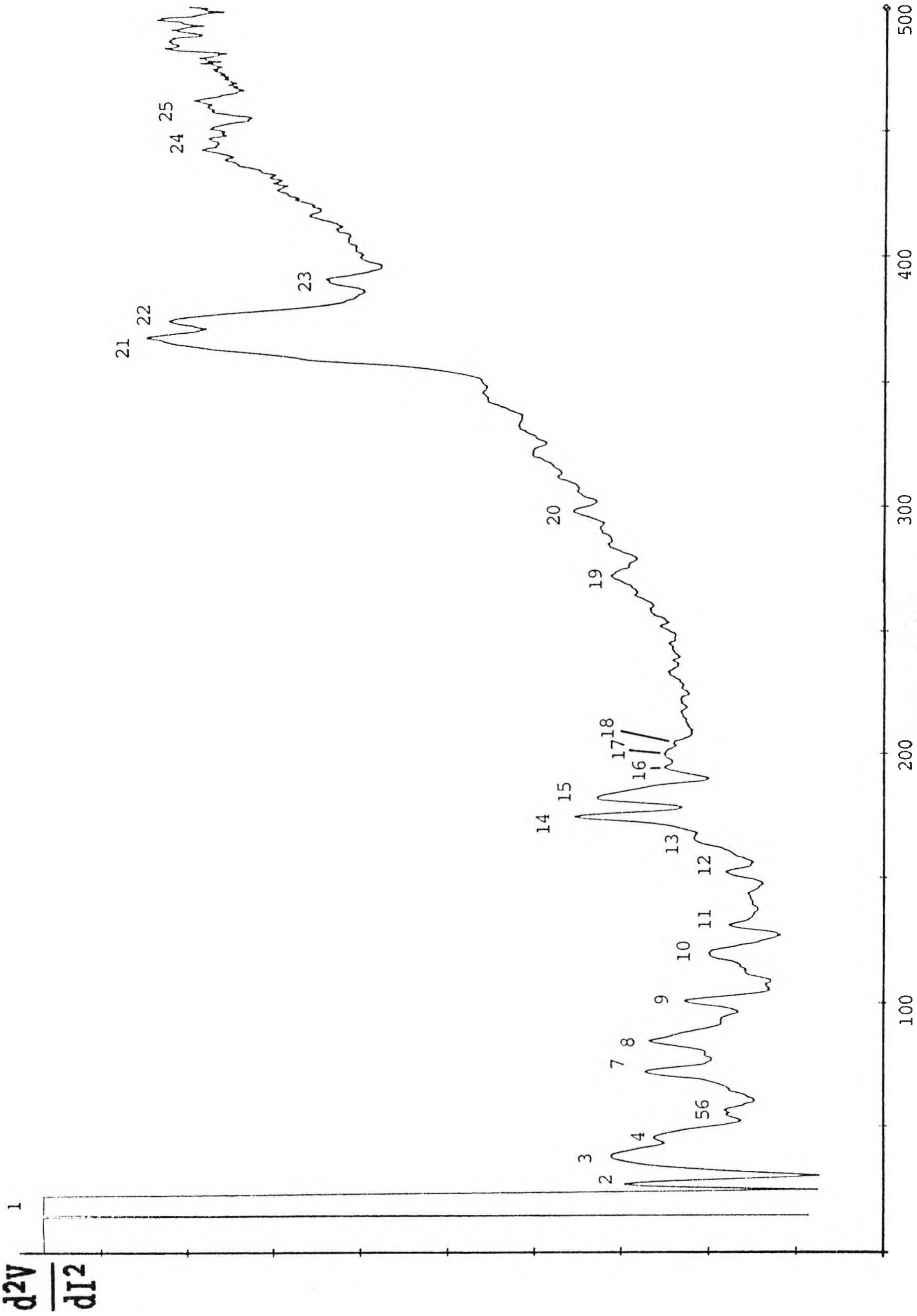

Table 6.2.1. Spectral Assignment of the IET Spectrum of TAA in Dried IPA.

Peak No	Energy (meV)	Wave No. (cm^{-1})	Intens.	IR Spec. (cm^{-1})	ASSIGNMENT
1	17.5	141	VS	-	Al Phonon
2	25.9	209	M	-	Al Phonon
3	37.1	299	M	-	
4	44.1	356	M	353	Ti-O str.
5	53.8	434	W		
6	55.3	446	W	443	Ti-O str.
7	70.7	570	M	547	Ti-O str.
8	83.9	677	M	662	Ti-O str.
9	99.4	803	M	769	O-Ti-O
10	118.2	954	M/W	953	Al-O str.
11	128.8	1039	M/W	1013	C-O str.
12	149.8	1208	M/W	1186	C-O str.
13	162.4	1310	M/W	1327	CH_2 def.
14	171.5	1383	M	1381	-CH_3 def.
15	178.5	1440	M	1428	C-H def.
16-18	190.9-200.9	1541-1620	VW	1523 1583 1610	ring modes C=C and C=O
19	267.3	2156	VW	-	
20	292.6	2360	VW	2311-2334	
21	361.2	2913	M/S	2928	C-H str.
22	366.8	2958	M/S	2969	C-H str.
23	389.2	3139	W	-	
24	429.8 - 440.3	3466-3551	M/W	3363	HO-H str.
25	441.2 - 449.3	3558-3624	M/W	-	O-H str.

S=Strong, M=Medium and W=Weak Intensities.

1meV ≡ 8.065 cm^{-1}

Assignments were made using the following references [Bradley et al., 1978] [Nakamoto, 1986] [Williams and Flemming, 1980].

Having investigated the anhydrous solution doped onto an alumina surface, a junction doped with 0.5% v/v TAA 0.5% v/v H_2O in dried IPA was examined. In effect, the junction was doped with a solution of TAA in wet IPA. The solution was spin doped onto the alumina surface without the use of the dry nitrogen doping chamber illustrated in Figure 6.1.1. The aluminium was plasma oxidised for a period of 60 seconds. The junction resistance was found to be 1000Ω (at 298K) and the electrode resistances were shown to be negligible. The spectrometer operating conditions were as follows.

Sensitivity	0.2 μV
Modulation Voltage	6 mV
Time Constant	10 sec.
Scan Time	60 mins.

Figure 6.2.3 shows the IET spectrum of the Al-AlO_x-Pb tunnel junction spin doped with 0.5% v/v TAA 0.5% v/v H_2O in dried IPA. Table 6.2.2 shows the spectral assignment of the peaks produced in Figure 6.2.3.

Figure 6.2.3. IET Spectrum of a 0.5% v/v TAA and 0.5% v/v H_2O in IPA Spin Doped Junction.

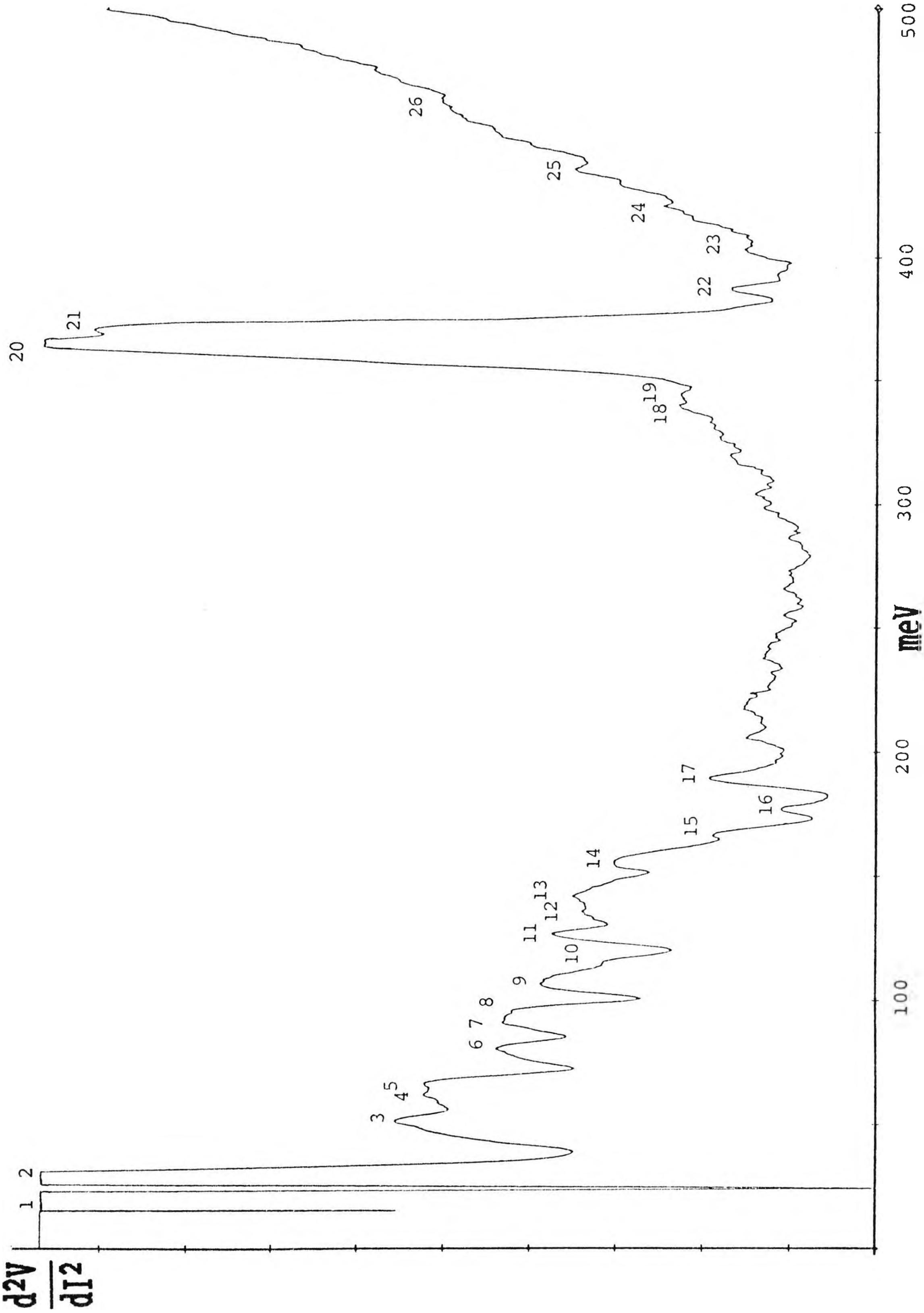

Table 6.2.2. Spectral assignment of Wet Alcohol Solution of TAA.

Peak No.	Energy (meV)	Wave No. (cm^{-1})	Intens.	Assignment
1	17.7	143	S	Al Phonon
2	27.6	223	S	Al Phonon
3	51.1	412	M/S	Ti-O str.
4	61.7	498	M	Ti-O str.
5	66.0	532	M	Ti-O str.
6	80.1	646	M	Ti-O str.
7	90.8	732	M	$>CH_2$ rock
8	95.0	766	M/W	O-Ti-O
9	106.4	858	M/W	CH_3 def.
10	114.9	927	M/W	O-Ti-O
11	126.2	1018	M	Ti=O str.
12	134.8	1087	M/W	Ti=O str.
13	141.8	1144	M/W	C-O str.
14	155.2	1252	M	C-O str.
15	165.9	1338	M/W	C-H def.
16	175.9	1419	M	$-CH_3$ def.
17	188.7	1522	M	
18	337.6	2723	W	C-H str.
19	341.8	2757	W	C-H str.
20	361.7	2917	S	C-H str.
21	366.0	2952	S	C-H str.
22	383.8	3095	M/W	C-H str.
23	399.4	3221	W	
24	417.7	3369	W	HO-H str.
25	432.6	3489	M/W	O-H str.
26	455.3	3672	M	O-H str.

S=Strong, M=Medium and W=Weak Intensities.

1meV ≡ 8.065 cm^{-1}

Assignments were made using the following references [Bradley et al., 1978] [Nakamoto, 1986] [Williams and Flemming, 1980].

The next stage in the study was to investigate the adsorption of a fully hydrolysed titanate system onto the alumina surface. The junction was spin doped with a solution of 0.5% v/v TAA in H_2O (prepared as outlined earlier). Again the inert atmosphere doping chamber was unnecessary as the solution already contained water. The completed junction resistance was found to be very low (15Ω at 298K), the electrode resistances were therefore significantly large (Al_R=5Ω and Pb_R=2Ω at 298K). An explanation for this was proposed in Section 5.5.4; the water still present on the surface could be acting as an electrolyte. The junction was replaced into the vacuum preparation chamber and evacuated to 10^{-6} τ for a further 30 minutes. When removed again the junction resistance was found to be much larger (10 kΩ). The spectra produced were unstable above 300mV. The spectrometer operating conditions were found to be as follows.

Sensitivity	0.5	μV
Modulation Voltage	4	mV
Time Constant	3	sec.
Scan Time	30	mins.

Figure 6.2.4 represents the IET spectrum of the Al-AlO_x-Pb tunnel junction spin doped with 0.5% v/v TAA in H_2O. Table 6.2.3 shows the assignment of the spectrum shown in Figure 6.2.4.

Figure 6.2.4. IET Spectrum of 0.5% v/v TAA in H_2O (After 50 Hours).

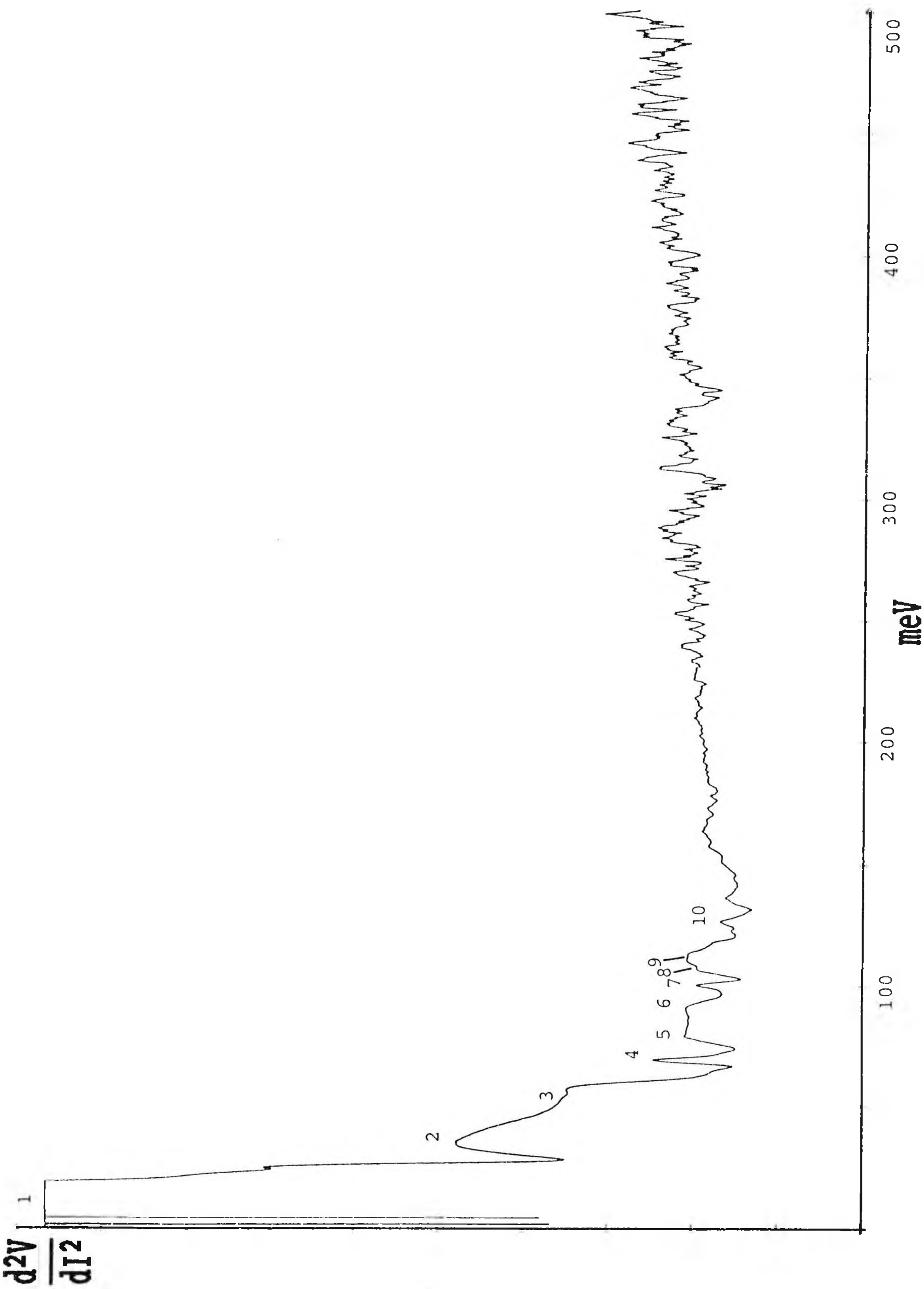

Table 6.2.3. Assignment of the IET Spectrum of TAA in Water (After 50 Hours).

Peak No.	Energy (meV)	Wave No. (cm^{-1})	Intens.	Assignment
1	11.4	92	VS	
2	35.0	282	S	Al Phonon
3	57.2	461	S	Ti-O str.
4	69.3	559	S	Ti-O str.
5	78.6	634	M	Ti-O str.
6	92.1	743	M	O-Ti-O
7	101.3	818	M/W	O-Ti-O
8	108.5	875	M/Sh	
9	112.1	904	M	Ti-O-Ti
10	127.1	1025	W	Possibly TiO-H-OTi

S=Strong, M=Medium, W=Weak and Sh=Shoulder Intensities.

1meV ≡ 8.065 cm^{-1}

Assignments were made using the following references [Bradley et al., 1978] [Nakamoto, 1986] [Williams and Flemming, 1980].

Discussion of the Results from Titanium Acetylacetonate (TAA) Doped Tunnel Junctions

Figure 6.2.2 shows the spectrum of a junction spin doped by an anhydrous solution of 0.5% v/v TAA in IPA. The main peaks of the spectrum may be attributed to C-H and Ti-O vibration modes. The chelate ring modes, normally at 200 meV (1600 cm^{-1}) appeared greatly reduced in intensity indicating, by employing the selection rule, that the rings tend to be parallel to the oxide surface. Otherwise little change and good comparison can be seen between the infrared spectrum of the TAA liquid and the tunnelling spectrum of TAA in an anhydrous IPA solution. The absence of Ti-O-Ti vibrational modes indicates that, at this stage, no cross polymerisation or large amount of hydrolysis of the titanate molecules had occurred. Figure 6.2.5 illustrates the surface orientation of TAA indicated from the spectrum of TAA in the anhydrous doped solution with the chelate rings are parallel to the oxide surface. This shows that no solution hydrolysis had occurred and implies the loss of an isopropyl unit for surface interaction.

Figure 6.2.3 represents the tunnelling spectrum of a solution of 0.5% v/v TAA and 0.5% v/v H_2O in IPA spin doped onto the alumina surface of a tunnel junction. It shows several differences from the previous, anhydrous case. Peaks at 1018 and 1087 cm^{-1} correspond to the symmetric and antisymmetric stretching frequencies, respectively, of a Ti=O bond. The frequencies of the Ti-O stretching modes at 532 and 412 cm^{-1} were found to have been reduced by 30-40 cm^{-1} in comparison to the corresponding modes in the spectrum of the anhydrous TAA solution doped tunnel junction in Figure 6.2.2. The C-H deformation modes were also reduced in intensity. These factors suggest that solution hydrolysis of the TAA molecule had occurred to produce the structure illustrated in Figure 6.2.6. The reduction in the intensity of the C-H deformation modes implies that both isopropyl units of the molecule have been lost in the production of the Ti=O double bond. However the relative low intensity of the chelate ring modes again suggests that the rings tend to be parallel to the oxide surface. A mode of hydrolysis of titanium bisacetylacetonates in moist alcohol has been suggested previously that agrees with the observations made in this study [Puri et al., 1962]. The reaction is:-

$$(iPrO)_2Ti(AcAc)_2 \ + \ H_2O \ \xrightarrow{\text{Alcohol}} \ O{=}Ti(AcAc)_2 \ + \ 2iPr\text{-}OH$$

The absence, at this stage, of Ti-O-Ti modes at 904 cm^{-1} in Figure 6.2.3 implies that although hydrolysis has occurred to a certain extent, there is no evidence for the polymerisation of the hydrolysis products.

Figure 6.2.4 illustrates the IET spectrum of 0.5% v/v TAA in water, in the absence of IPA. This solution was prepared 50 hours prior to doping to allow sufficient time for solution hydrolysis reactions to take place to completion. The spectrum is a result of a high resistance junction and therefore the peaks produced tend to be suppressed in intensity. However, the lack of any fine detail tends to suggest that a number of surface species are present or indeed the possible presence of a polymeric species. The resistance also tends to suggest that more than a monolayer of dopant species are present on the alumina surface. The spectrum shows, by the predominance of Ti-O vibrational modes and the absence of the C-H deformation or stretching modes, that considerable hydrolysis of the TAA had occurred in the aqueous solution and subsequent polymerisation of the hydrolysis products taken place. Figure 6.2.7 illustrates the proposed reaction product. The similar intensity of the Ti-O-Ti vibrational modes at 904 cm^{-1}, compared to that of the O-Ti-O bonds may be explained by the fact that although the Ti-O-Ti bonds would be expected to be predominantly parallel to the surface, the observation from the resistance may be correct, that greater than a monolayer of polymeric species could be present on the surface. The Ti-O-Ti modes therefore appear more intense in the tunnel spectrum than would be expected from the surface structure shown in Figure 6.2.7.

In summary these spectra of titanium acetylacetonate indicate the solution hydrolysis scheme shown in Figure 6.2.8.

Figure 6.2.5. The Surface Orientation of TAA Doped from an Anhydrous IPA Solution.

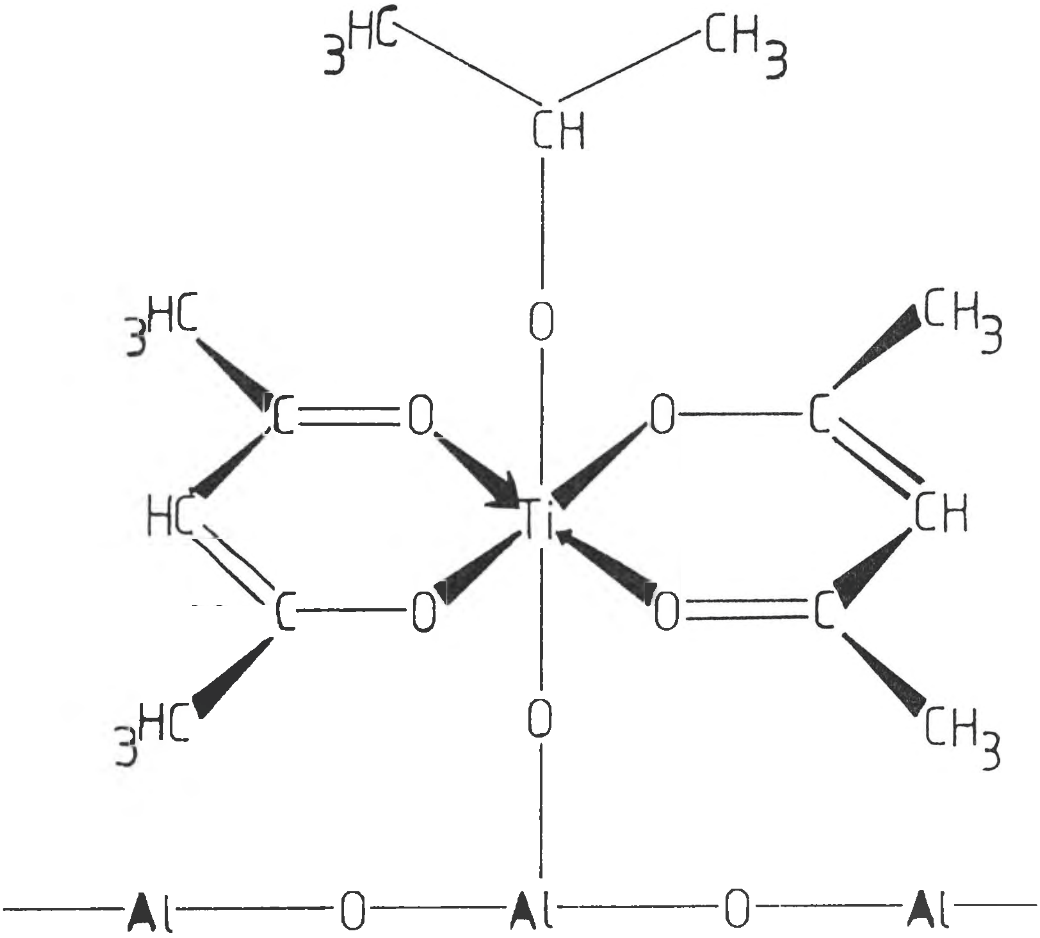

Figure 6.2.6. The Surface Orientation of TAA Doped from a Wet IPA Solution.

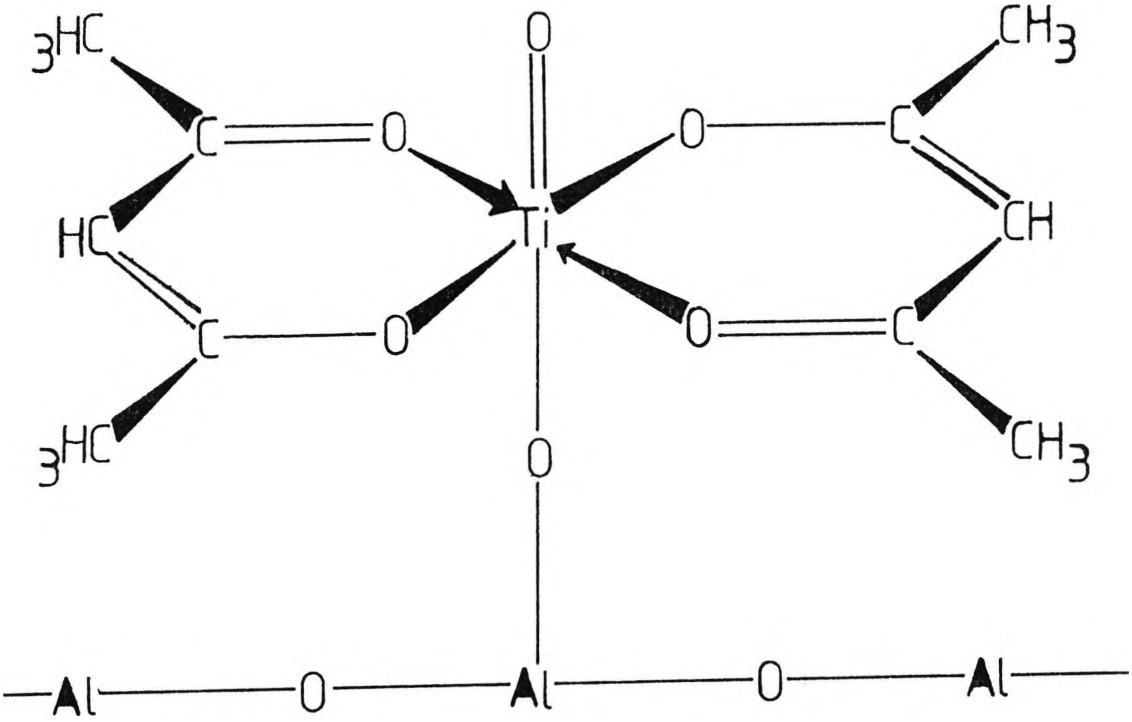

Figure 6.2.7. The Surface Orientation of TAA Doped from an Aqueous Solution.

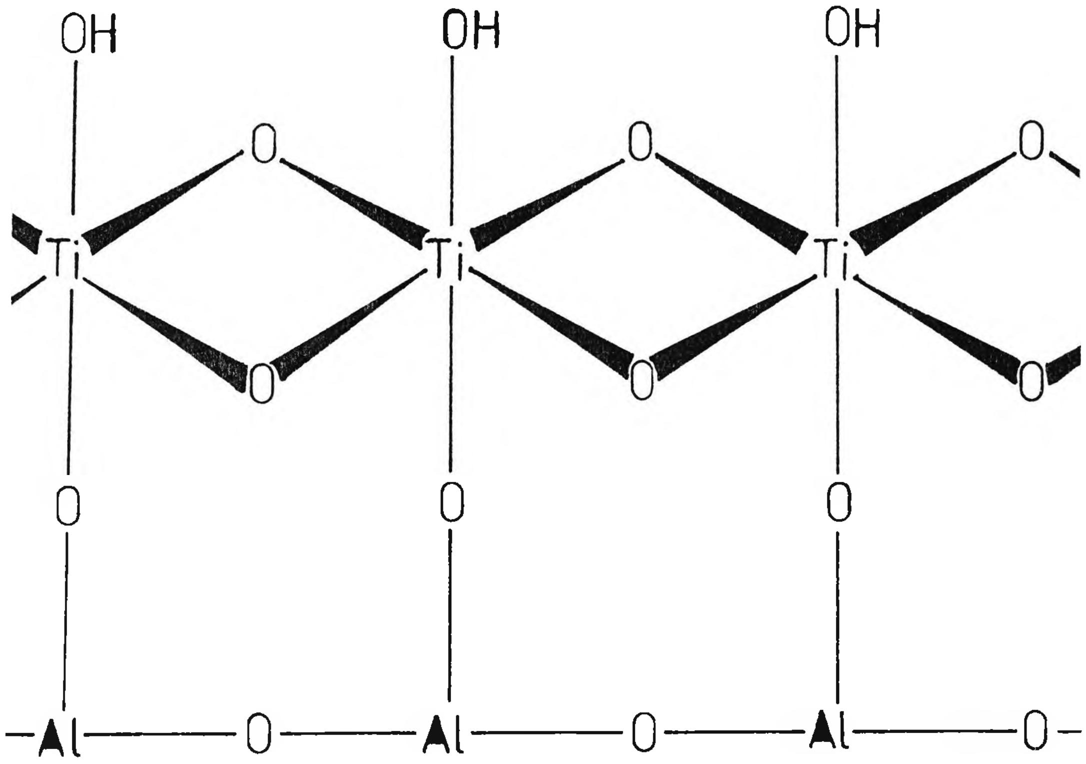

Figure 6.2.8. The Proposed TAA Solution Hydrolysis Scheme.

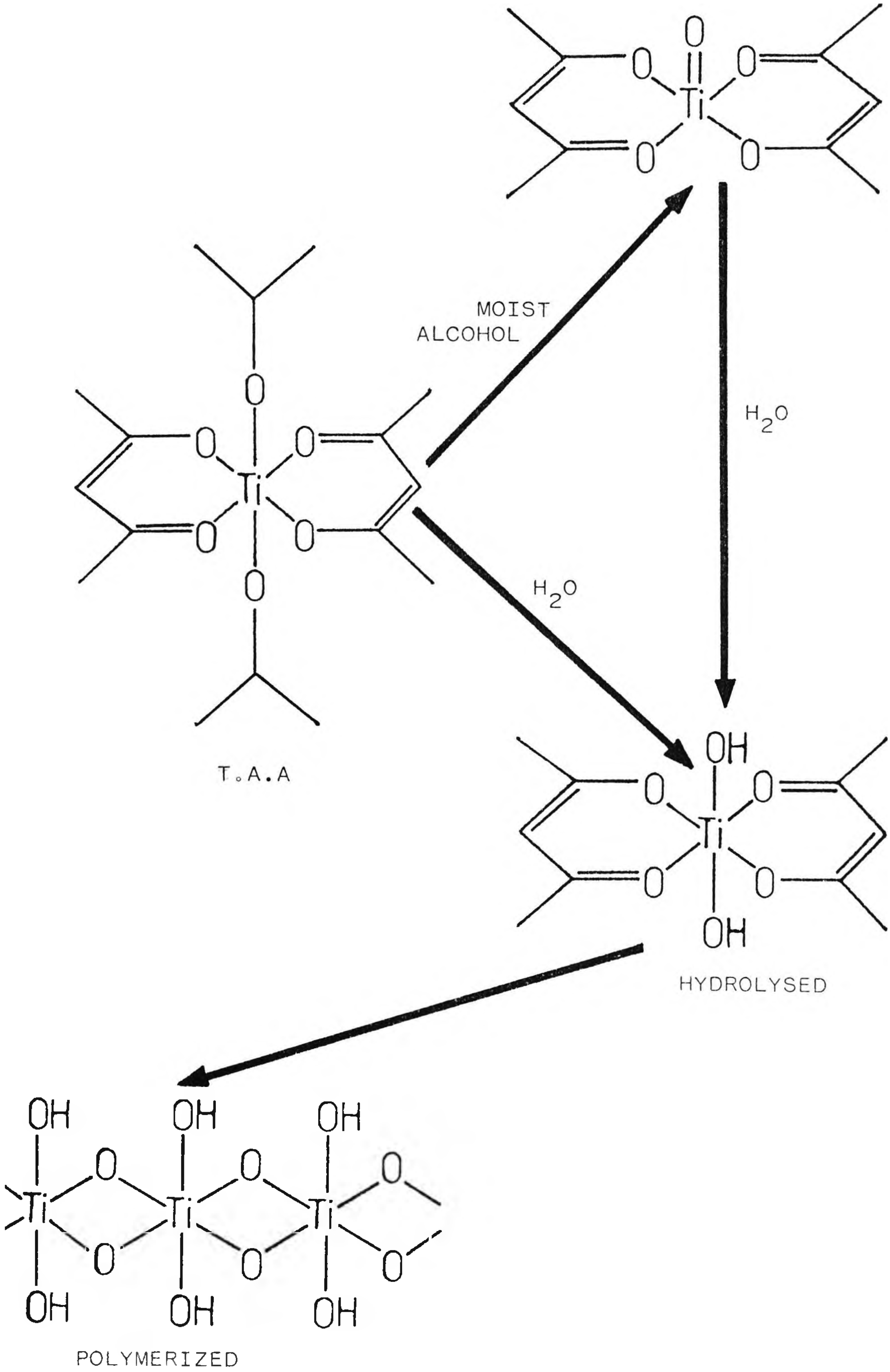

6.2.2 **Triethanolamine Titanate (TEAT) Doped Tunnel Junctions.**

The aim of the initial study of TEAT doped tunnel junctions was to produce the IET spectrum from a solution of 0.5% v/v TEAT in molecular sieve dried IPA. The solution preparation and junction spin doping was again carried out in the nitrogen atmosphere bag, in order to remove the possibility of atmospheric hydrolysis of the titanate in solution, as outlined in Section 6.1.2. The aluminium electrode was again plasma discharge oxidized for a period of 60 seconds during the junction fabrication process. The strip resistances were found to be negligible and the junction resistance was measured to be 2.4 kΩ (at 298K). The spectrometer operating conditions were as follows.

Sensitivity	0.5	µV
Modulation Voltage	6	mV
Time Constant	3	sec.
Scan Time	30	mins.

Figure 6.2.9 shows the resulting IET spectrum of an Al-AlO_x-Pb tunnel junction spin doped with a solution of 0.5% v/v TEAT in molecular sieve dried IPA. Table 6.2.4 shows the spectral assignment of the peaks produced in Figure 6.2.9 and compares the vibration mode energies of the IET spectrum with the infrared spectrum of neat TEAT which was produced on a Perkin Elmer 983 spectrophotometer.

Figure 6.2.9. IET Spectrum of 0.5% v/v TEAT in Dried IPA.

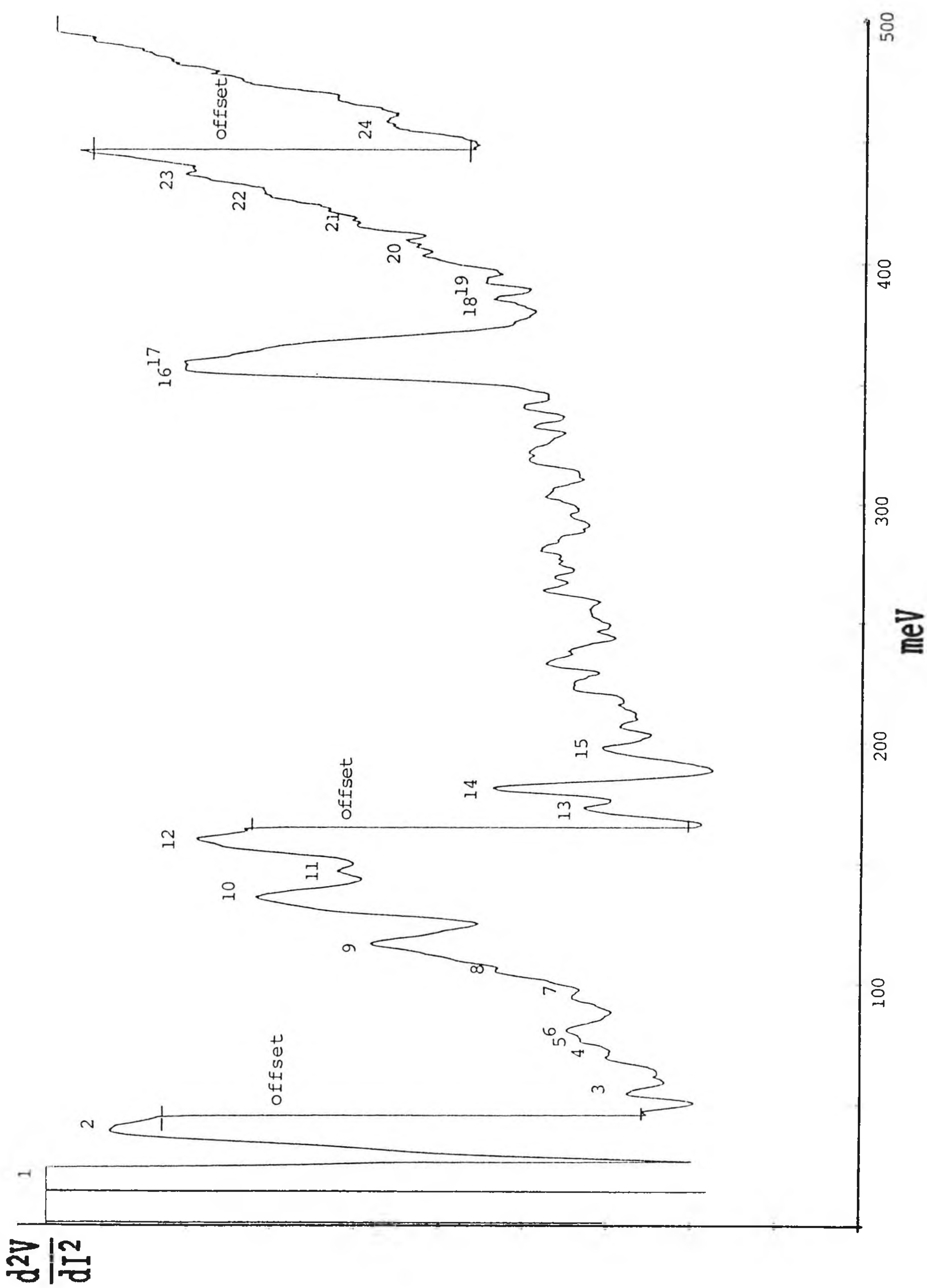

Table 6.2.4. Assignment of the IET Spectrum of TEAT in Dried IPA.

Peak No	Energy (meV)	Wave No. (cm^{-1})	Intens.	IR Spec. (cm^{-1})	ASSIGNMENT
1	17.5	144	VS	-	Al Phonon
2	38.6	311	VS	-	Al Phonon
3	53.6	432	W/M	440	Ti-O
4	69.3	559	W	549	Ti-O
5	76.4	616	Sh	618	Ti-O
6	80.7	651	M/W	661	Ti-O
7	94.3	760	W	769	O-Ti-O
8	105.7	853	W	852	
9	166.4	939	M/S	930	O-Ti-O
				957	Al-O str.
				1040	C-N str.
10	135.7	1094	S	1127	C-O str.
11	146.4	1181	M	1186	C-O str.
12	159.3	1285	S	1277	CH_2 def.
13	173.6	1400	M	1383	CH_3 def.
14	180.7	1457	M	1428	C-H def.
15	197.8	1596	M	1585	NH_2 def.
				1610	
16	356.4	2875	S	2864	C-H str.
17	358.6	2892	S	2927	C-H str.
				2967	C-H str.
18	385.0	3105	W		
19	392.8	3168	W		
20	406.4	3278	M/W		N-H str.
21	415.7	3353	W		N-H str.
22	427.1	3445	W	3413	CO-H str.
23	434.3	3502	W		O-H str.
24	455.7	3675	W		O-H str.

S=Strong, M=Medium, W=Weak and Sh=Shoulder Intensities.

$1 meV \equiv 8.065 cm^{-1}$

Assignments were made using the following references [Bradley et al., 1978] [Nakamoto, 1986] [Williams and Flemming, 1980].

Figure 6.2.10 shows the IET spectrum of a junction spin doped with a wet alcohol solution of TEAT (c.f. TAA study in Section 6.2.1) - 0.5% v/v TEAT and 0.5% v/v H_2O in IPA. No special doping procedures were used in the preparation of this junction. The junction resistance was found to be 550Ω (at 298K) and the aluminium and lead strip resistances to be 9 and 2 ohms respectively. The spectrometer operating conditions were as follows.

Sensitivity	0.2 µV
Modulation Voltage	6 mV
Time Constant	3 sec.
Scan Time	30 mins.

Table 6.2.5 shows the assignment of the peaks present in the spectrum of TEAT in wet IPA shown in Figure 6.2.10.

Figure 6.2.10. <u>IET Spectrum of 0.5% v/v TEAT and 0.5% v/v H_2O in IPA.</u>

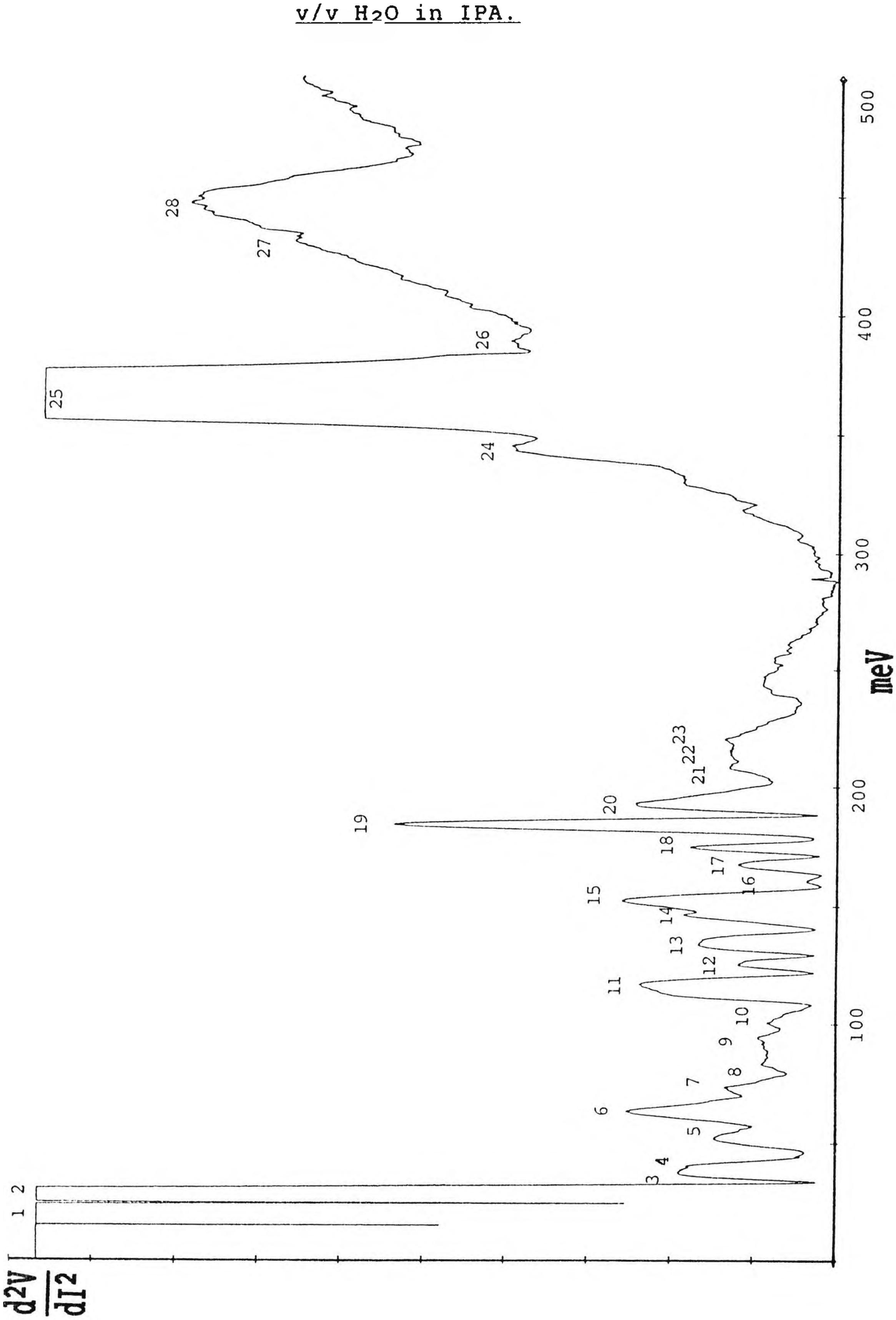

Table 6.2.5. Assignment of the IET Spectrum of TEAT in Wet IPA (Figure 6.2.10).

Peak No.	Energy (meV)	Wave No. (cm^{-1})	Intens.	Assignment
1	17.8	144	VS	Al Phonon
2	26.4	213	VS	Al Phonon
3	37.1	299	M	
4	40	323	M	
5	51.4	415	M/W	Ti-O str.
6	63.6	513	M	Ti-O str.
7	73.6	593	M/W	Ti-O str.
8	84.3	680	W	Ti-O str.
9	91.4	737	W	O-Ti-O
10	101.4	818	W	CH_2 def.
11	116.4	939	M	O-Ti-O
12	125.0	1008	M/W	Ti=O str.
13	134.3	1082	M/W	Ti=O str.
14	146.4	1181	M/W	C-O str.
15	152.8	1233	M	C-O str.
16	160.7	1296	W	C-H def.
17	167.8	1354	M/W	CH_2 def.
18	175.0	1411	M/W	C-H def.
19	184.3	1486	S	C-H def.
20	192.8	1555	M	N-H def.
21	208.6	1682	W	NH_2 def.
22	215.0	1734	W	
23	220.0	1774	W	
24	343.6	2771	W	C-H str.
25	365.0	2944	VVS	C-H str.
26	388.6	3134	W	
27	430.7	3474	M	N-H str. HO-H str.
28	447.1	3606	S	O-H str.

S=Strong, M=Medium and W=Weak Intensities.

1meV ≡ 8.065 cm^{-1}

Assignments were made using the following references [Bradley et al., 1978] [Nakamoto, 1986] [Williams and Flemming, 1980].

Discussion of the Results from the Triethanolamine Titanate Doped Tunnel Junctions.

Figure 6.2.9 shows the IET spectrum of 0.5% v/v TEAT in anhydrous IPA. The comparison between the infrared spectrum of neat TEAT and the IET spectrum in Figure 6.2.9 in Table 6.2.4 indicates good correlation which in turn suggested that no major solution hydrolysis had occurred in the anhydrous IPA solution prior to doping onto the alumina surface. The presence of N-H stretch and $-NH_2$ deformation and stretching modes normally at 1610 and 3300 cm^{-1} respectively suggest that some reaction of the tertiary amine had occurred on the alumina surface. The resulting N-H vibrational modes in the IET spectrum were found to occur at 20-30 cm^{-1} lower energy than would be expected for an unperturbed amine. This is suggested to result from the effect of the Ti-N interaction and possible H-bonding to the alumina surface oxygen atoms. The intensity of the Ti-O vibrational modes suggest a similar surface adsorption of TEAT to that of TAA from the equivalent anhydrous solution in IPA (see Figure 6.2.5). The absence of a C-N stretching mode in Figure 6.2.9 (1040 cm^{-1} in the infrared spectrum of TEAT) implies that the chelate rings again tend to be parallel to the surface. Figure 6.2.11 illustrates the proposed orientation of TEAT from this anhydrous solution on the alumina surface. The ethanol that would be produced from the hydrolysis of the tertiary amine has been shown not to "dope" under the conditions used in the production of this spectrum.

Figure 6.2.10 shows the IET spectrum of 0.5% v/v TEAT and 0.5% v/v H_2O simultaneously in IPA. It indicates that, as in the case of TAA in a moist alcohol solution (Figure 6.2.3), hydrolysis has occurred to produce a species containing a Ti=O bond. This is further substantiated by the reduction of the Ti-O vibrational frequencies by 20-30 cm^{-1} in comparison with the equivalent peaks in the anhydrous solution spectrum (Figure 6.2.9). The growth in the intensity of the O-H stretching modes suggests a not unexpected increase in the hydrolysis of the surface. The N-H and $-NH_2$ modes in the wet solution spectrum are similar in energy but greater in intensity to those of the equivalent peaks in the anhydrous solution spectrum. This suggests that more complete hydrolysis of the amine group has occurred in the wet solution to NH_2 species. This observation implies that the hydrolysis of the amine group occurs as a hydrated surface induced effect. From the evidence above it would be expected that the interaction of TEAT from the moist alcohol solution would be similar to that of TAA in Figure 6.2.6 with the chelate rings parallel to the surface and a Ti=O bond perpendicular to the surface. The absence of Ti-O-Ti vibrational modes around 904 cm^{-1} from Figure 6.2.10 indicates that although hydrolysis of TEAT has occurred, in the moist alcohol solution, there is no evidence for polymerization reactions. However, the similarities of the initial surface interactions of TEAT and TAA and their reactions in moist alcohol solution would suggest that TEAT in aqueous solution would undergo solution hydrolysis and polymerisation as suggested for the case of TAA (see Figure 6.2.8).

Figure 6.2.11. The Proposed Surface Orientation of TEAT Doped from a Dried IPA Solution.

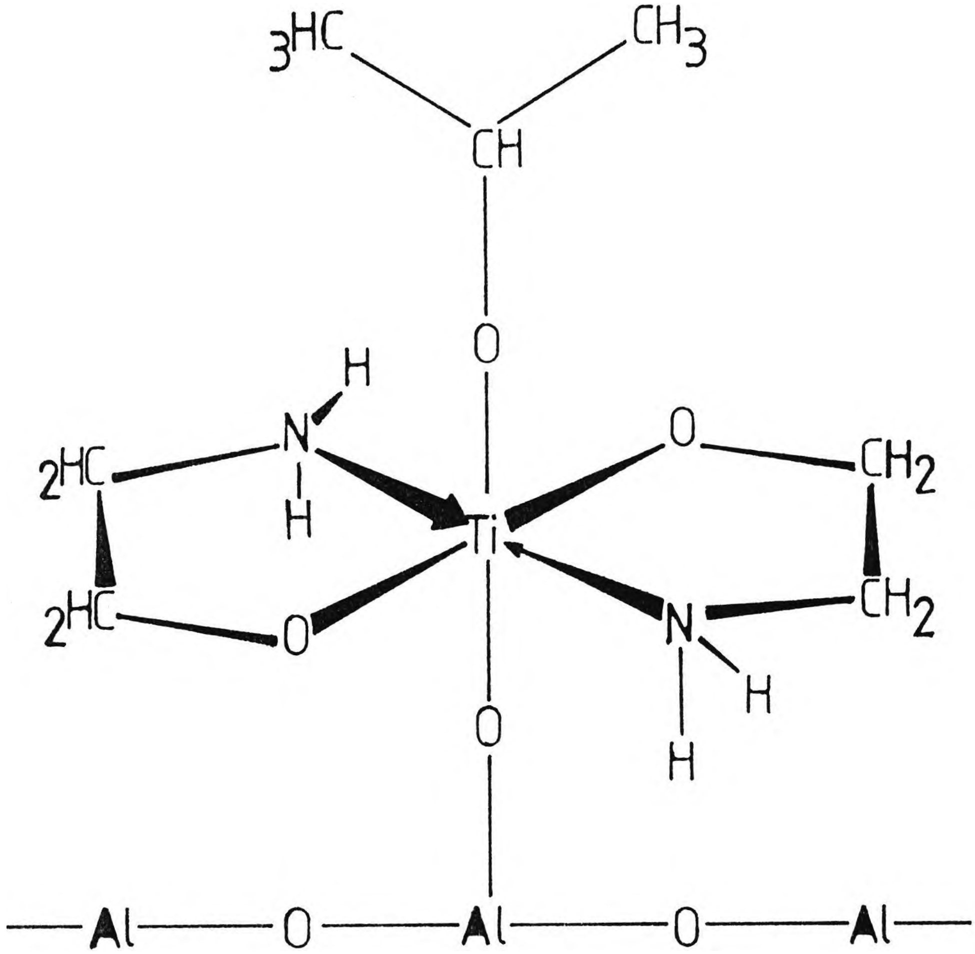

6.2.3 Octylene Glycol Titanate Doped Tunnel Junctions.

The structurally most complex titanate studied is Octylene Glycol Titanate (OGT) - see Figure 6.2.1. In order to compare the initial modes of adsorption onto the alumina of a tunnel junction a solution of 0.5% v/v OGT in zeolytically dried IPA was prepared under nitrogen, in the preparation bag shown in Figure 6.1.1. The solution was spin doped onto a junction whose aluminium strip had been plasma discharge oxidised for a period of 60 seconds. The junction was completed and after being attached to the probe, was inserted into the liquid helium Dewar as quickly as possible. The junction resistance was found to be quite low at 150Ω (at 298K) with the aluminium and lead strip resistances being 8Ω and 2Ω respectively. The spectrometer operating conditions were as follows:-

Sensitivity	0.2 μV
Modulation Voltage	5 mV
Time Constant	3 sec.
Scan Time	30 mins.

Figure 6.2.12 shows the resulting spectrum of 0.5% v/v OGT in dried IPA. Table 6.2.6 shows the assignment of the peaks produced in Figure 6.2.12. They are compared with an infrared spectrum of neat OGT liquid, as received. The infrared spectrum was produced on a Perkin Elmer 983 spectrophotometer.

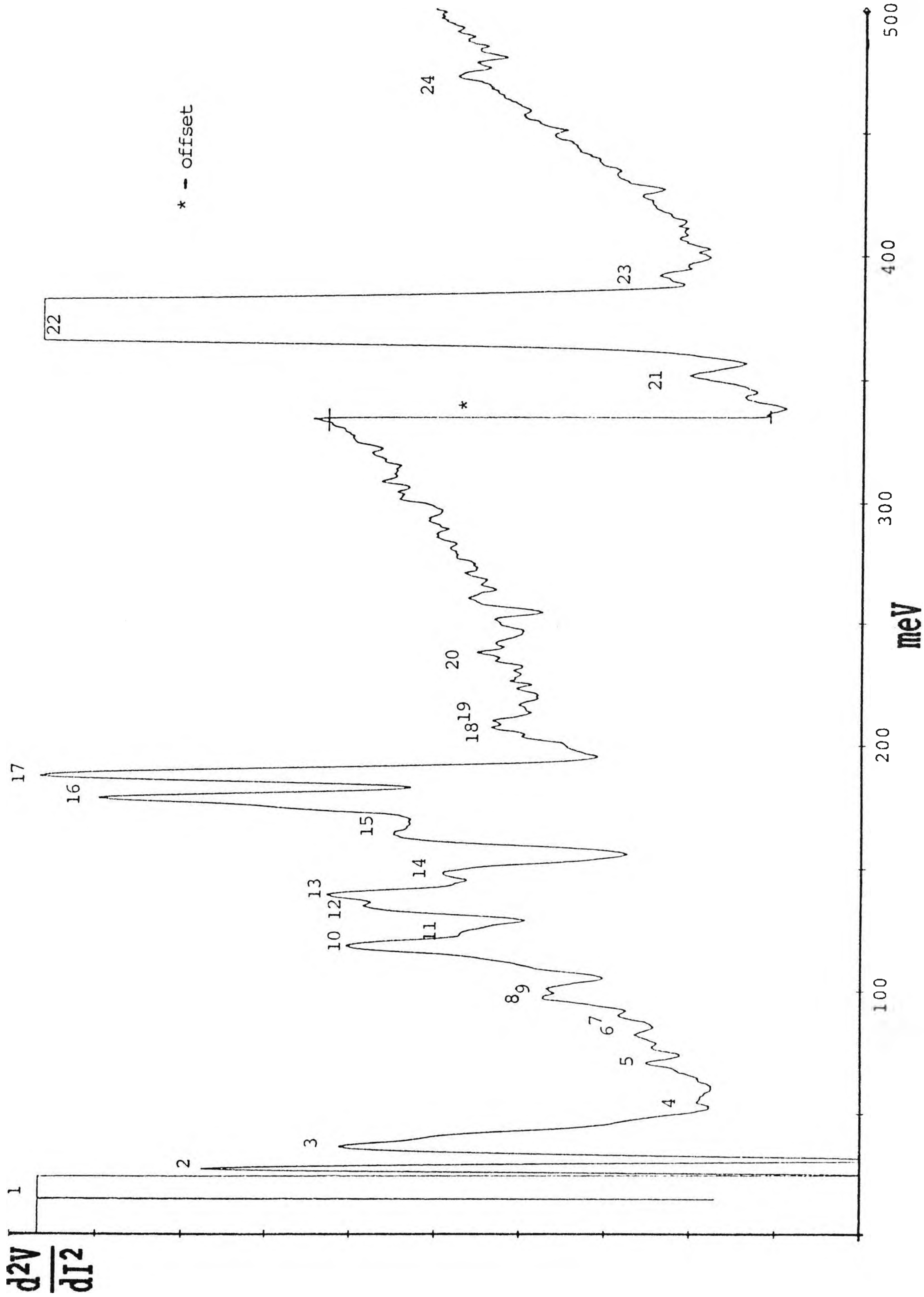

Figure 6.2.12. IET Spectrum of 0.5% v/v OGT in a Dried IPA Solution.

Table 6.2.6. Assignment of the IET Spectrum of OGT in Dried IPA.

Peak No	Energy (meV)	Wave No. (cm^{-1})	Intens.	IR Spec. (cm^{-1})	ASSIGNMENT
1	18.3	148	VS	-	Al Phonon
2	25.9	209	S	-	
3	34.7	280	S		Al Phonon
4	52.4	423	W	450	Ti-O
5	67.5	544	W	550	Ti-O
6	79.0	637	W	640	$C-CH_3$ def.
7	86.4	697	W		Ti-O
8	92.6	747	M/W	750	CH_2 rock
9	96.7	780	M/W	772	O-Ti-O
				831	
	-			864	
10	113.0	911	S	919	O-Ti-O
11	118.5	956	M/W		Al-O str.
				985	
12	128.7	1038	S	1029	C-O str.
13	132.8	1071	S	1070	C-O str.
14	141.6	1142	M	1127	C-O str.
15	156.6	1263	M	1242	C-H def.
16	170.2	1373	S	1379	CH_3 def.
17	179.8	1450	S	1463	C-H def.
18	198.9	1604	W		
19	201.6	1626	W		
20	228.1	1840	W		
21	335.6	2707	M/W	2731	C-H str.
22	356.9	2878	VS/Br	2871	C-H str.
				2931	C-H str.
				2958	C-H str.
23	374.5	3020	W		CO-H chel.
				3336	
24	450.8	3636	W/M		O-H str.

S=Strong, M=Medium, W=Weak and Br=Broad Intensities.

1meV ≡ 8.065 cm^{-1}

Assignments were made using the following references [Bradley et al., 1978] [Nakamoto, 1986] [Williams and Flemming, 1980].

The same junction that was used to produced the spectrum in Figure 6.2.12 was removed from the liquid helium Dewar and placed on the laboratory bench for 10 minutes. The junction resistance was monitored constantly throughout. Condensation of atmospheric water onto the junction was minimised by using a hot air blower, increasing the temperature of the junction rapidly and so reducing condensation. The junction resistance increased on exposure to the air to a steady 450Ω (at 298K) from 140Ω over a period of 10 minutes. The strip resistances remained constant. The junction was replaced into the liquid helium Dewar. The spectrometer operating conditions were as follows.

Sensitivity	0.2	μV
Modulation Voltage	5	mV
Time Constant	10	sec.
Scan Time	60	mins.

Figure 6.2.13 shows the IET spectrum produced. Table 6.2.7 shows the assignment of the peaks produced in the spectrum in Figure 6.2.12, the IET spectrum of OGT in dried IPA exposed to air for 10 minutes.

Figure 6.2.13. IET Spectrum of OGT in Dried IPA Exposed to Air for 10 Minutes.

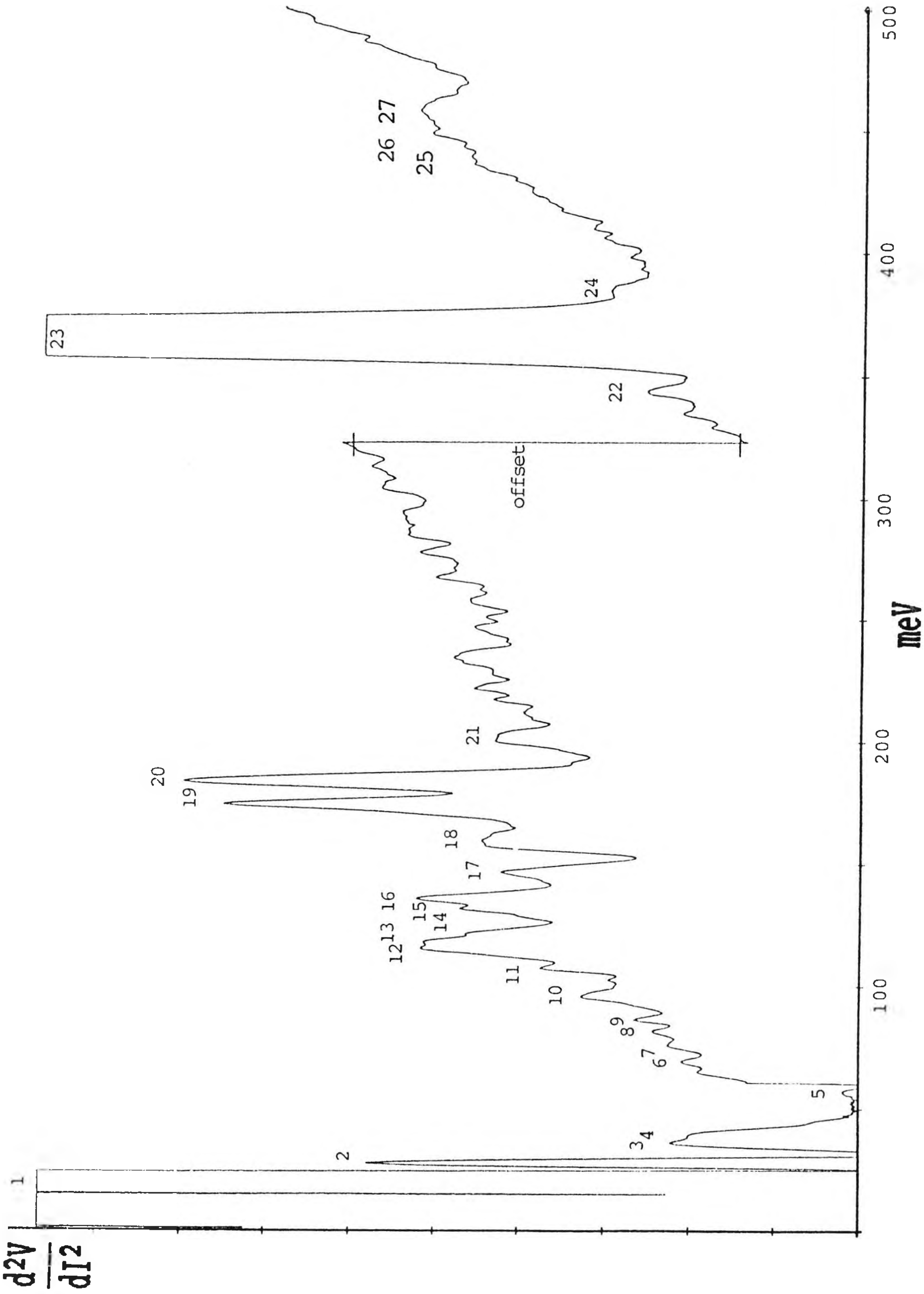

Table 6.2.7. Assignment of the IET Spectrum of OGT in Dried IPA Exposed to Air for 10 Mins.

Peak No.	Energy (meV)	Wave No. (cm^{-1})	Intens.	Assignment
1	18.2	147	VS	Al Phonon
2	26.7	215	S	
3	35.8	289	M	Al Phonon
4	37.9	306	M	
5	56.2	453	W	Ti-O str.
6	68.8	555	W	Ti-O str.
7	75.1	606	W	
8	80.7	651	W	Ti-O str.
9	85.5	690	W	Ti-O str.
10	94.0	758	W	O-Ti-O
11	106.0	855	W	
12	113.6	916	M	
13	115.8	934	M	O-Ti-O
14	119.3	962	M/W	Al-O str.
15	129.1	1041	M/W	C-O str.
16	133.3	1075	M	C-O str.
17	144.6	1166	M/W	O-H def./ C-O str.
18	157.2	1268	M/W	C-H def.
19	171.2	1381	S	CH_3 def.
20	180.4	1455	S	C-H def.
21	199.3	1607	W	
22	337.5	2722	W	C-H str.
23	360.0	2903	VVS	C-H str.
24	378.9	3056	W	C-OH chel.
25	430.9	3475	W	HO-H
26	440.7	3554	W	
27	450.5	3633	W/M	O-H str.

S=Strong, M=Medium and W=Weak Intensities.

1meV $\equiv$ 8.065 cm^{-1}

Assignments were made using the following references [Bradley et al., 1978] [Nakamoto, 1986] [Williams and Flemming, 1980].

The junction that was used to produce the previous two spectra (Figures 6.2.12 and 6.2.13) was removed from the liquid helium Dewar and left in a desiccator of wet air for 15 hours (overnight). The junction was removed from the desiccator and the resistance measured at 8.5 kΩ. The junction strip resistances were shown to have remained constant throughout the study. The junction was then replaced into the liquid helium Dewar and the resulting spectrum is shown in Figure 6.2.14. The spectral assignment is carried out in Table 6.2.8. The spectrometer operating conditions for Figure 6.2.14 were as follows.

Sensitivity	0.5 μV
Modulation Voltage	10 mV
Time Constant	3 secs.
Scan Time	30 mins.

Figure 6.2.14. IET Spectrum of OGT in Dried IPA Exposed to Air for 15 Hours.

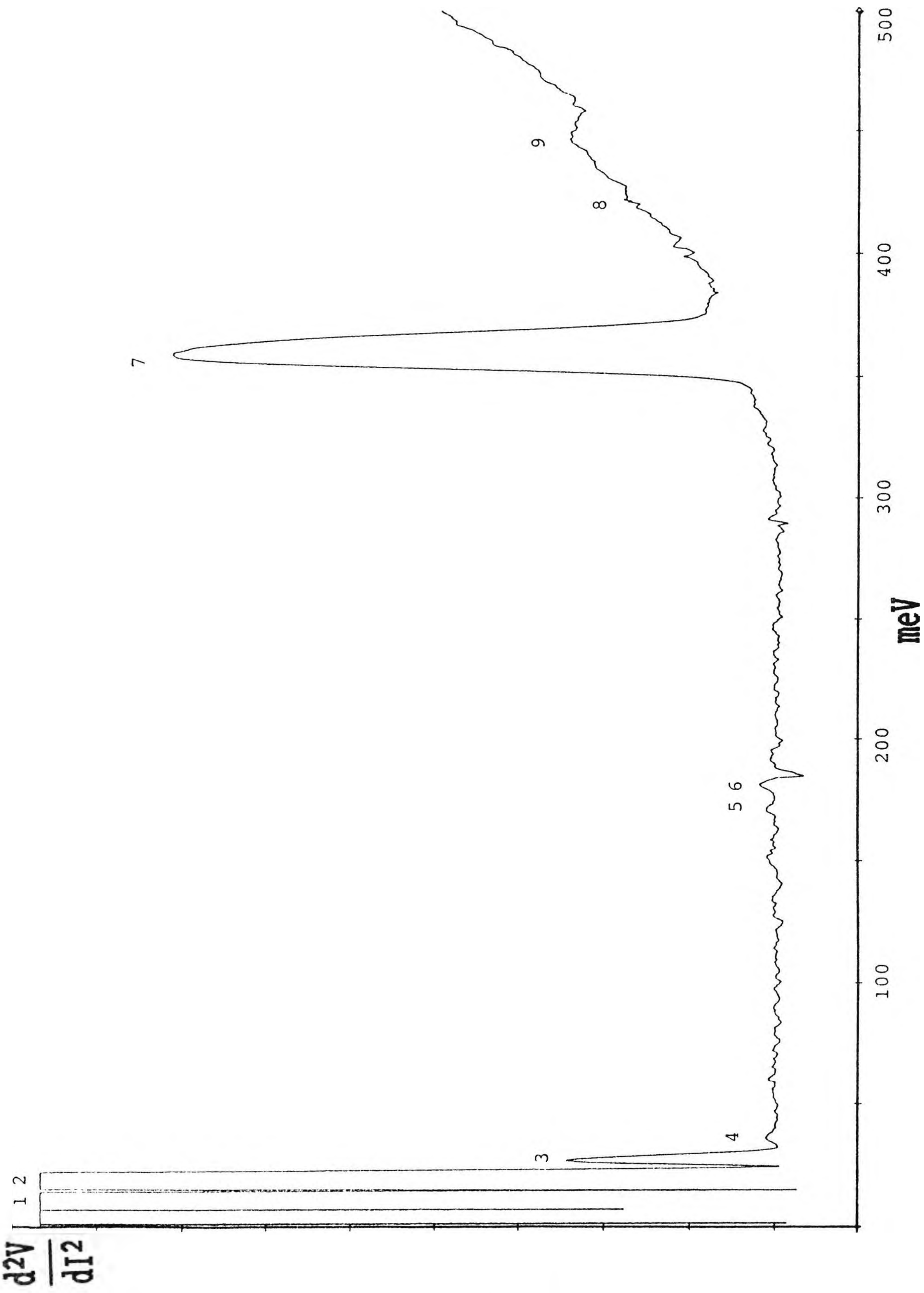

Table 6.2.8. Assignment of the IET Spectrum of OGT in Dried IPA Exposed to Air for 15 Hours.

Peak No.	Energy (meV)	Wave No. (cm^{-1})	Intens.	Assignment
1	10.0	81	VS	
2	17.8	144	VS	Al Phonon
3	27.1	219	M	Al Phonon
4	36.4	294	VW	Al Phonon
5	171.4	1382	VW	CH_3 def.
6	180.0	1452	VW	C-H def.
7	359.3	2898	S	C-H str.
8	422.8	3410	W	HO-H str.
9	447.1	3606	W	O-H str.

S=Strong, M=Medium and W=Weak Intensities.

1meV $\equiv$ 8.065 cm^{-1}

Assignments were made using the following references [Bradley et al., 1978] [Nakamoto, 1986] [Williams and Flemming, 1980].

Discussion of the Results from the Octylene Glycol Titanate Doped Tunnel Junction.

Figure 6.2.12 shows the initial spectra of a junction spin doped with a solution of 0.5% v/v OGT in dried IPA. Figures 6.2.13 and 6.2.14 show the spectra of the same junction, exposed to air for 10 minutes and 15 hours respectively. The aim of this study was to investigate, if possible, the surface hydrolysis of an adsorbed titanate by exposure to atmospheric conditions. One consequence of this exposure is that the thickness of the junction alumina barrier increases which is indicated by an increase in the junction resistance. This effect was seen in this case, the resistance of the junction increased from 140Ω initially to 450Ω after 10 minutes exposure and 8.5 kΩ after a period of 15 hours exposure.

From Figure 6.2.12, the IET spectrum of 0.5% v/v OGT in dried IPA, and Table 6.2.6, the peak assignment and comparison with the infrared of OGT, no distinguishing features could be found to uniquely differentiate the mode of adsorption of OGT onto the alumina surface. However, the energies of the O-Ti-O and Ti-O modes, as well as the absence of Ti-O-Ti vibrational modes, suggests that the surface adsorbed OGT had not undergone any significant hydrolytic reaction either in the solution or on surface adsorption.

From Figure 6.2.13, the IET spectrum from the same junction as before, but exposed to wet air for 10 minutes, the signals and responses seem to be much more unstable than in Figure 6.2.12. A large number of peaks can be seen with energies in between 200 and 350 meV, which are difficult to assign. This instability is probably caused by an amount of surface condensation of atmospheric water during exposure to the air. This is also suggested by the increase in the intensity of the O-H stretching modes at around 3600 cm^{-1} (350 meV) compared with those in the previous anhydrous case. However, again no extensive hydrolysis of the adsorbed surface OGT species can be observed, as only very small differences are seen between Figures 6.2.12 and 6.2.13.

The junction used to produce the spectra was removed from the liquid helium Dewar and placed on a laboratory bench for 15 hours. When replaced in the Dewar the spectrometer produced the IET spectrum shown in Figure 6.2.14. The only spectral features that can be seen are large alumina phonon peaks, minuscule C-H deformation peaks, a huge C-H stretching mode and O-H stretching modes. It should not be forgotten that the junction resistance was large by this stage at 8.5 kΩ (at 298K). Notice also that the modulation voltage required was large (10 mV) to produce any signal from the large resistance junction. The observation of C-H vibrational modes tends to suggest that total hydrolysis to a Ti-O-Ti polymeric species had not occurred in this case (compared to the solution hydrolysis of TAA outlined in Section 6.2.1). All of the Ti-O modes were suppressed to such an extent in

Figure 6.2.14 that they were un-observable. However, this does not mean that all Ti species were desorbed from the alumina surface during atmospheric exposure of the junction, it is just that the high resistance of the junction suppressed the peak intensity. In conclusion, the analysis of atmospheric hydrolysis of surface adsorbed OGT was possible only until the junction conditions made observation of the tunnelling process impossible by increasing the alumina barrier thickness. However it was still impossible to see any large scale surface hydrolysis of the adsorbed OGT.

6.3 AN IETS STUDY OF THE SURFACE INTERACTION OF A TITANIUM CHELATE COUPLING AGENT WITH SECONDARY ORGANIC SPECIES.

Section 6.2 has already outlined the method of surface adsorption and a solution hydrolysis scheme of three important titanium chelate coupling agents. As stated earlier, coupling agents are normally interfaces between primarily inorganic surface substrates and organic coatings or adhesives. It therefore seems sensible to investigate, if possible, the interaction between the adsorbed titanate and secondary organic species. Coating bases are normally polymeric, for example, nitrocellulose is often used in inks and polyurethane and epoxides are normal bases for paints. The decision making process for the choice of dopant species for IET spectra has already been outlined in Section 6.1.1. The production of tunnel junctions doped with polymeric species has been found to be a very difficult process, as junction resistances are normally very large and the spectra very complex. It therefore is suggested that the best way to study the interaction of adsorbed titanates with secondary organic species would most probably be by doping the tunnel junctions with solutions of titanate containing simple organic molecules with different functionality to the titanate (and therefore identifiable) but with similar organic functional groups to coating bases. For this reason chloroform, nitromethane and acetonitrile were investigated, co-doped onto a junction with TAA in solution.

A large number of dopant concentrations and conditions were possible in this study, a huge undertaking, and so only a selection of doping conditions were used. The following systems were investigated.

(i) $CHCl_3$
$CHCl_3$ and TAA
(ii) $MeNO_2$
$MeNO_2$ and TAA
$MeNO_2$, TAA and D_2O
(iii) CH_3CN
CH_3CN and TAA
CH_3CN, TAA and excess H_2O

6.3.1 An IETS Study of TAA and Chloroform.

To investigate the interaction of chloroform ($CHCl_3$) with the alumina surface in the presence of TAA, it was important to consider first the unaffected situation of chloroform adsorbed onto the alumina in the absence of TAA, and so to be able to note any change in the method of surface adsorption. In practice this was found to be more difficult than expected. Production of an electrically stable tunnel junction with a resistance of the correct size to allow electron tunnelling (100 - 5 000Ω) was for some reason very difficult. The aluminium strip had been plasma oxidised for a period of 60 seconds and spin doped under normal conditions with liquid chloroform (99% purity from Aldrich Chemical Co.). On completion of the junction the resistance (J_R) was measured at 1.5 kΩ. The aluminium strip resistance (Al_R) was also discovered to be surprisingly high at 100Ω. The spectrometer operating conditions were as follows.

Sensitivity	0.5 µV
Modulation Voltage	10 mV
Time Constant	3 secs.
Scan Time	60 mins.

Figure 6.3.1 shows the resulting spectrum of the Al-AlO_x-Pb tunnel junction spin doped with chloroform. Table 6.3.1 indicates possible spectral assignment of the peaks produced in the IET spectrum. The spectral assignment was carried out with reference to the following; [Ellialtioglu et al., 1980] - the IETS of CCl_4, [Gabian and McKinney, 1951] - the IR spectrum of $CHCl_3$ and [Zietlow et al., 1950] - the Raman spectrum of $CHCl_3$.

Figure 6.3.1. IET Spectrum of a Junction Spin Doped with Neat Liquid Chloroform.

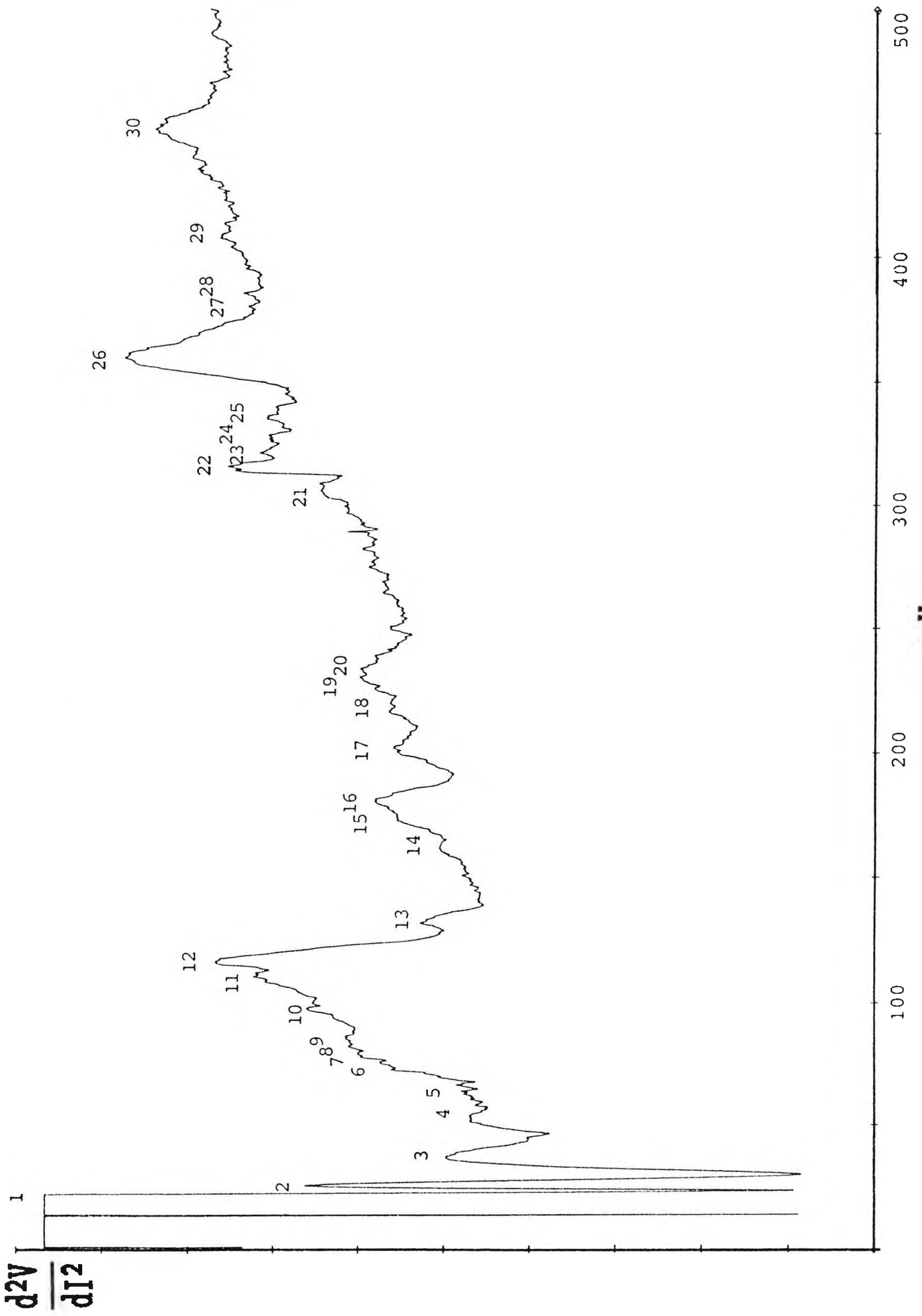

Table 6.3.1. Spectral Assignment of the IET Spectrum of Chloroform.

Peak No.	Energy (meV)	Wave No. (cm^{-1})	Intens.	Assignment
1	17.1	138	VS	Al Phonon
2	25.6	207	S	Al Phonon
3	36.3	293	M	Al Phonon
4	52.7	425	W	Al-Cl str.
5	62.7	505	W	C-Cl str.
6	75.7	609	M/W	Al-Cl str.
7	79.0	638	M/W	Al-Cl str.
8	82.6	666	M/W	C-Cl str.
9	86.9	701	M/W	
10	97.6	787	M	C-Cl str.
11	110.4	890	M/S	C-Cl str.
12	116.8	942	S	Al-O str./ C-Cl str.
13	132.5	1068	M/W	C-O str.
14	161.0	1298	W	C-H def.
15	173.8	1402	M/W	CH_3 def.
16	180.9	1459	M	C-H def.
17	200.8	1620	M/W	
18	217.2	1752	M/W	
19	230.8	1861	M/W	
20	233.6	1884	M/W	
21	306.3	2470	W	
22	316.2	2550	M	
23	321.2	2591	M/W	
24	327.6	2642	M/W	
25	336.2	2711	M/W	
26	360.4	2907	S	C-H str.
27	380.3	3067	W	C-H str.
28	386.0	3113	W	
29	408.8	3297	W	O-H H-Bonding
30	453.0	3653	M	O-H str.

S=Strong, M=Medium and W=Weak Intensities.

1meV ≡ 8.065 cm^{-1}

As with the previous chloroform doped junction it was found to be very difficult to produce a suitable spectrum of chloroform with TAA. The alumina surface was prepared by plasma discharge in oxygen for 60 seconds. The solution of 0.5% v/v TAA in chloroform was prepared and spin doped onto the junction as outlined in Section 6.1.2. The junction resistance was measured at 3 kΩ (at 298K) with the aluminium strip resistance still significant at 80Ω (at 298K). The spectrometer operating conditions were as follows.

Sensitivity	0.5	µV
Modulation Voltage	7	mV
Time Constant	3	secs.
Scan Time	30	mins.

Figure 6.3.2 shows the resulting IET spectrum of TAA in chloroform. Table 6.3.2 details the spectral data and indicates possible spectral assignments of the peaks produced in Figure 6.3.2. Again the spectral assignment was carried out with reference to the following; [Ellialtioglu et al., 1980] - the IETS of CCl_4, [Gabian and McKinney, 1951] - IR spectrum of $CHCl_3$ and [Zietlow et al., 1950] - the Raman spectrum of $CHCl_3$, as well as to previous TAA spectra in Section 6.2.1 especially Figure 6.2.2.

Figure 6.3.2. IET Spectrum of 0.5% v/v TAA in Chloroform.

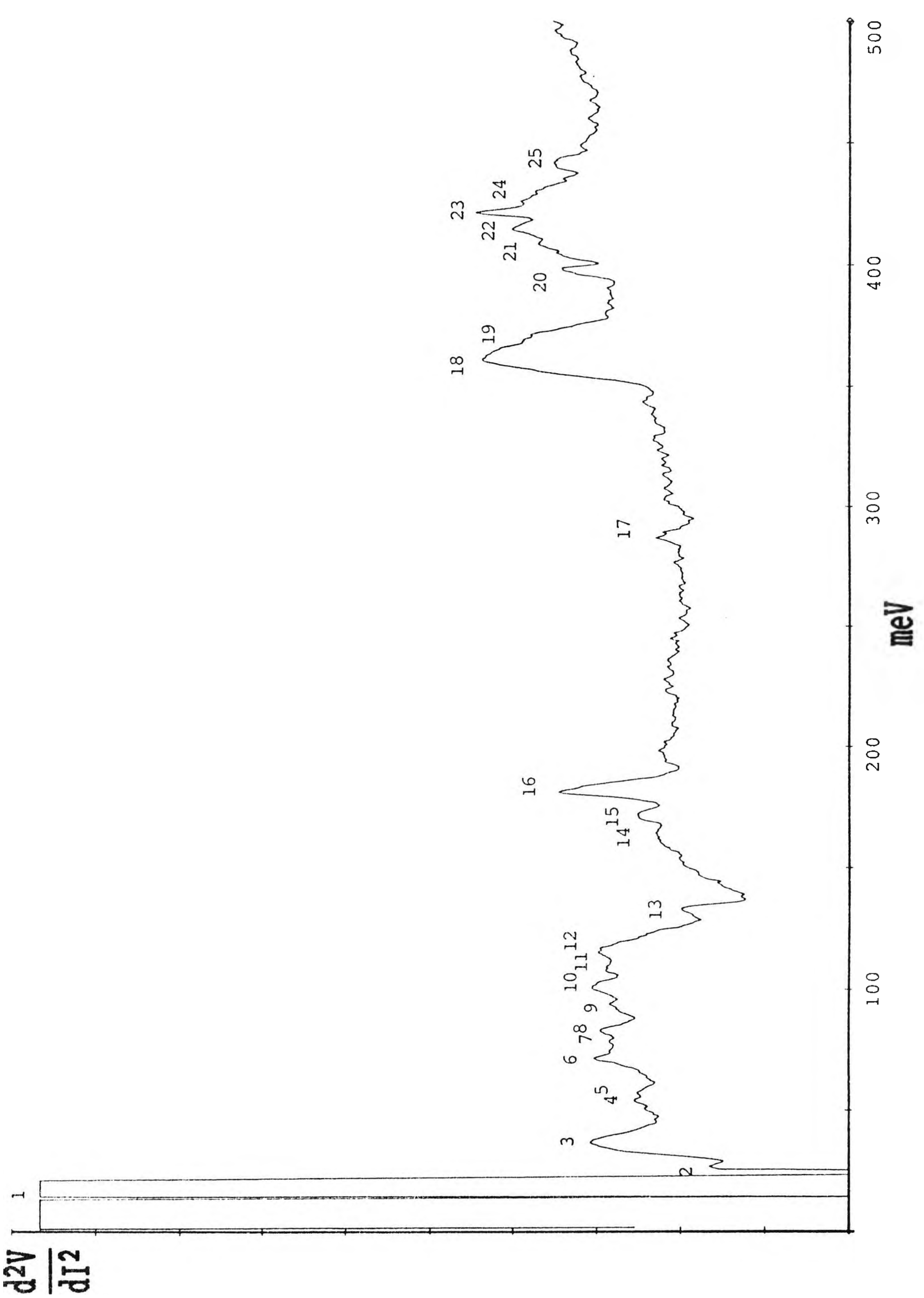

Table 6.3.2. Spectral Assignment of the IET Spectrum of TAA in Chloroform.

Peak No.	Energy (meV)	Wave No. (cm^{-1})	Intens.	Assignment
1	17.8	144	VS	Al Phonon
2	27.1	218	W	Al Phonon
3	37.0	299	M	Al Phonon
4	54.1	437	W	Al-Cl str.
5	57.0	459	W	Ti-O str.
6	71.9	580	M/W	Ti-O str.
7	78.3	632	W	Al-Cl str.
8	83.3	672	W	C-Cl str.
9	94.0	758	W	O-Ti-O
10	99.7	804	M/W	C-Cl str.
11	108.3	873	W	C-Cl str.
12	115.4	930	M/W	Al-O str./ C-Cl str.
13	132.5	1068	W	C-O str.
14	162.5	1309	VW	C-H def.
15	172.4	1390	W	CH_3 def.
16	180.9	1459	M	C-H def.
17	287.0	2315	W	
18	360.4	2906	M	C-H str.
19	368.9	2975	M/W	C-H str.
20	397.4	3205	M/W	]
21	408.1	3291	M/W	]
22	414.5	3343	M/W	] O-H H-
23	420.9	3395	M	] bonding
24	425.9	3435	W	]
25	441.6	3561	W	AlO-H str.

S=Strong, M=Medium and W=Weak Intensities.

1meV ≡ 8.065 cm^{-1}

Discussion of the Results from the Chloroform Doped Tunnel Junctions.

Figure 6.3.1 shows the IET spectrum of spectroscopic grade chloroform. The junction strip resistance, at 100Ω, tends to suggest that either chloroform does not dope the alumina surface of the junction or that the surface is being attacked by the dopant to produce an electrically unstable spectrum. A large modulation voltage (10 mV) was required to produce any spectral detail from the junction. The presence of Al-Cl stretching modes in the IET spectrum also suggest some surface corrosion. All these observations illustrate the difficulties encountered in trying to produce a tunnel junction doped with chloroform (N.B. Walmsley and Tomlin [1985] do not show a spectrum of chloroform). The peak energies and assignments shown in Table 6.3.1 concur with the observations for those of spin doped carbon tetrachloride [Ellialtioglu et al., 1980]. This tends to suggest that doping chloroform onto a tunnel junction alumina surface produces a similar type of corrosive effect as doping carbon tetrachloride suggested by Ellialtioglu et al.. Thus results in a complex and unstable junction spectrum as shown in Figure 6.3.1 containing such species as $AlCl$, $AlCl_2$, $AlCl_3$, $\cdot CCl_3$, C_2Cl_6 etc. As in the carbon tetrachloride case, it is impossible to say with complete certainty what type of corrosive mechanism of chloroform on alumina takes place. However it can be suggested, by the observation of a high aluminium strip resistance before spectral production, that the corrosive effect was not as a result of an electrochemical process started by application of the tunnelling D.C. potential.

One observation in Figure 6.3.1 that cannot be assigned by either the IET spectra of CCl_4 or the IR or Raman spectra is the significant peak at 2550 cm^{-1}. The most probable assignments are either: (i) an inherent junction instability or (ii) junction contamination.

A significant O-H stretching mode can be seen in Figure 6.3.1 which indicates the presence of some hydrolysis of the alumina surface. This is most probably due to atmospheric water contamination of the surface during spin doping. This may be explained as follows: Ellialtioglu et al. [1980] showed large C-H stretching modes in the IET spectrum of spin doped CCl_4. These were not explained sufficiently. The C-H modes in Table 1 of their paper (at 2900 cm^{-1}) cannot be seen in the "background spectrum" of Figure 3 of that paper. Therefore - Where do the C-H modes come from? It is suggested by the authors to be due to junction contamination. However the explanation may be that the following radical reaction occurs due to the presence of atmospheric water and active aluminium surface sites,

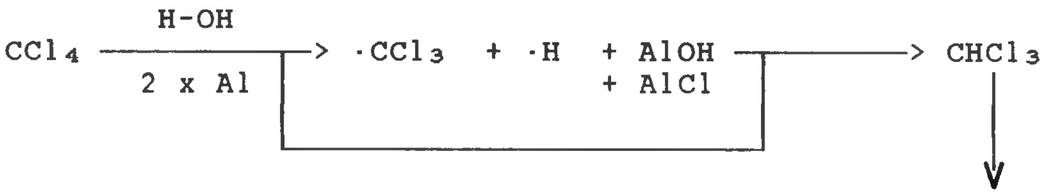

$$CCl_4 \xrightarrow[2 \times Al]{H-OH} \cdot CCl_3 + \cdot H \begin{array}{l} + AlOH \\ + AlCl \end{array} \longrightarrow CHCl_3 \downarrow$$

and in a similar way for chloroform.

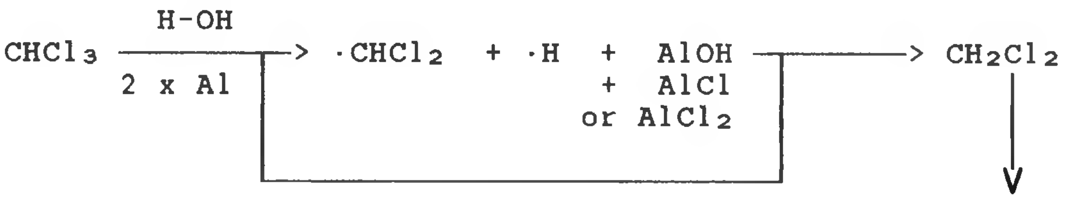

$$CHCl_3 \xrightarrow[2 \times Al]{H-OH} \cdot CHCl_2 + \cdot H + \begin{matrix} AlOH \\ + \ AlCl \\ \text{or } AlCl_2 \end{matrix} \longrightarrow CH_2Cl_2 \downarrow$$

and so on, giving rise to a number of different surface species.

Figure 6.3.2 shows the IET spectrum of a tunnel junction doped with a 0.5% v/v TAA in chloroform solution. The spectral assignment of the spectrum, carried out in Table 6.3.2, suggests several important features.

(i) Peaks with very similar energies to those in the spectrum of the chloroform doped junction are produced, therefore indicating a similar corrosion of the alumina surface, as outlined above.

(ii) Ti-O and Ti-O-Ti Stretching modes similar in energy to those observed in the spectrum of TAA in anhydrous IPA (shown in Figure 6.2.2 and Table 6.2.1) are present. This with the noted absence of the chelate ring modes at 1600 cm^{-1} and the absence of any Ti=O or Ti-O-Ti modes, as reported in certain cases in Section 6.2.1, suggests that the TAA is again adsorbed in the manner shown in Figure 6.2.5, with no evidence of hydrolysis or surface polymerization.

(iii) The large number of peaks reported in the spectrum of purely chloroform (Figure 6.3.1), at about 2550 cm^{-1}, are absent in the spectrum of TAA in chloroform. This observation seems to indicate that these peaks were produced by an inherent junction instability of the chloroform doped junction.

(iv) A large number of peaks in Figure 6.3.2, from 3200 - 3440 cm^{-1}, indicate a variety of H-O hydrogen bonding situations compared with either the anhydrous TAA (Figure 6.2.2) or solely chloroform (Figure 6.3.1) doped junctions. This suggests that the chloroform corrosion reactions may produce Al-OH surface species (as proposed before) which are able to hydrogen bond to, say, the methyl group on the chelate ligands of the TAA, or to other corrosion products.

In conclusion, it should be noted that from the spectral data produced from the IET spectra of chloroform doped junctions that there is no evidence for any adaptation of the surface adsorption or reaction of chloroform in the presence of TAA in the solutions considered in this study. This is most probably due to the inability of the titanate to adapt or prime the alumina surface without considerable hydrolysis and polymerization. For this to occur a constituent of water has been shown to be required (see Section 6.2.1).

However, it has been possible to analyze the surface corrosion of alumina by chloroform.

6.3.2 **An IETS Study of TAA and Nitromethane.**

Nitrocellulose is a widely used base for aqueous inks. It therefore seems important that the interaction of a nitro-functional organic molecule, such as nitromethane, with a primed and unprimed alumina surface should be investigated in this study.

The nitromethane (99% purity from Aldrich Chemical Co.) was already dried over a zeolytic molecular sieve for 24 hours prior to doping onto the junction using the nitrogen atmosphere bag, as shown in Figure 6.1.1. Again the plasma oxidation time of 60 seconds was used to prepare the alumina surface. The junction resistance was measured at 270Ω (at 298K) with the aluminium and lead strip resistances at 15Ω and 5Ω respectively. The spectrometer operating conditions were as follows.

Sensitivity	0.2	μV
Modulation Voltage	5	mV
Time Constant	3	secs.
Scan Time	30	mins.

Figure 6.3.3 shows the IET spectrum of nitromethane spin doped on an alumina surface of a tunnel junction. Table 6.3.3 details the spectral data and indicates possible spectral assignments of the peaks produced in Figure 6.3.3, the IET spectrum of nitromethane. The spectral assignment was carried out with reference to the following; [Williams and Flemming, 1980] [Smith et al., 1950] [Monjushiro et al., 1985] [Ratinen and Kiviharju, 1989a].

Figure 6.3.3. IET Spectrum of Nitromethane.

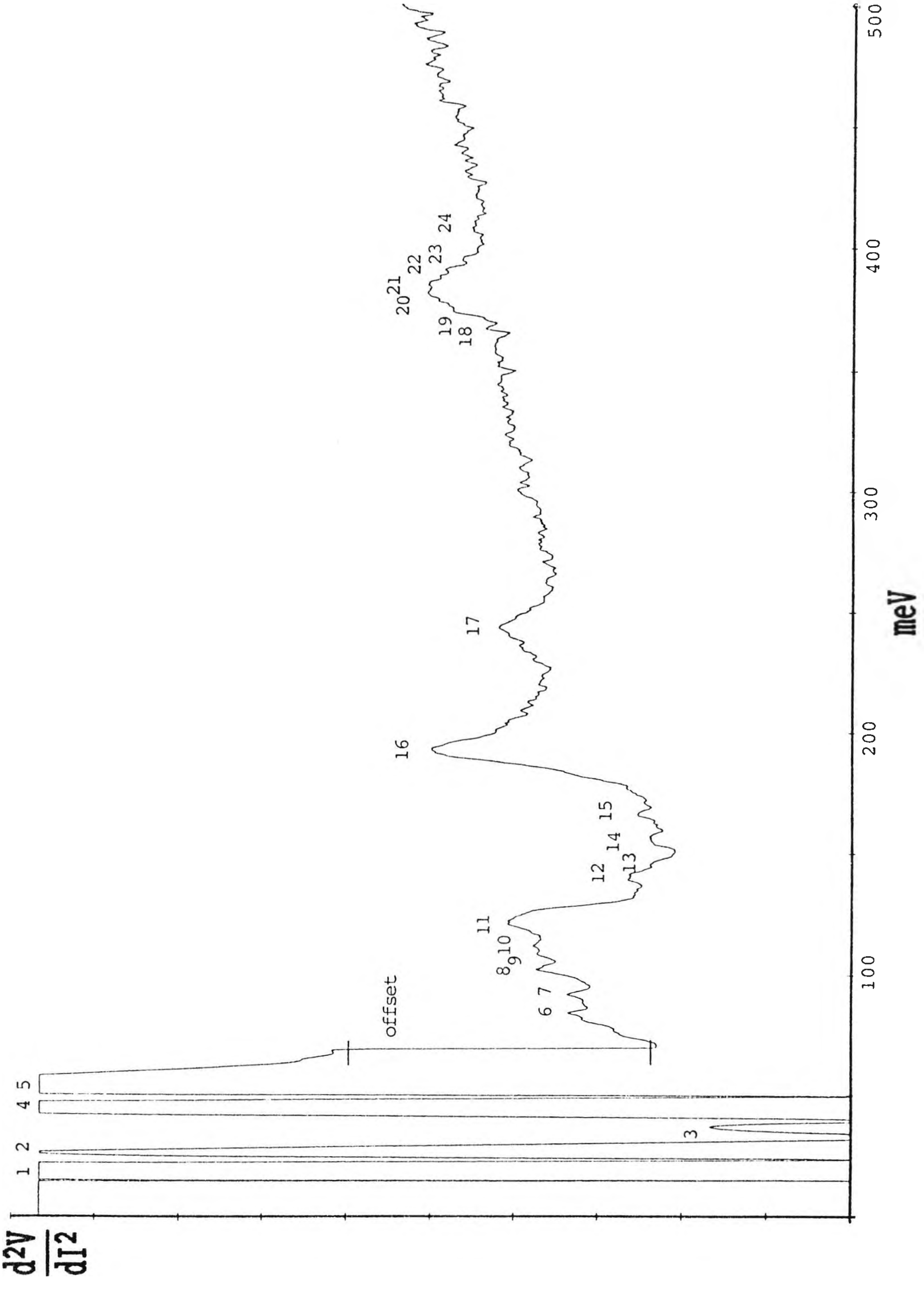

Table 6.3.3. Assignment of the Peaks Produced in the IET Spectrum of Nitromethane.

Peak No.	Energy (meV)	Wave No. (cm^{-1})	Intens.	Assignment
1	17.8	144	VS	Al Phonon
2	25.4	205	S	Al Phonon
3	35.7	288	M	Al Phonon
4	43.9	354	VS	
5	53.4	431	VS	
6	81.0	653	M/W	NO_2 rock
7	88.5	714	M/W	Al-O-Al
8	98.7	796	M	
9	104.9	846	M/W	CH_3 wag
10	108.4	874	M/W	
11	116.6	940	M	Al-O str.
12	134.4	1084	W	C-N str.
13	139.9	1128	W	
14	149.4	1205	W	C-H def.
15	159.1	1283	W	C-H def.
16	185.1	1493	M/S	CN=O str./ C-H def.
17	234.6	1892	M	
18	352.5	2843	W	C-H str.
19	359.3	2898	M/W	C-H str.
20	366.3	2954	M	C-H str.
21	370.4	2987	M	C-H str.
22	375.8	3031	M/W	C-H str.
23	380.7	3070	W	C-H str.
24	392.3	3164	W	

S=Strong, M=Medium and W=Weak Intensities.

1meV ≡ 8.065 cm^{-1}

The aim in this study was to see if any changes occurred in the surface adsorption or reaction of the anhydrous nitromethane in the presence of TAA and D_2O. D_2O was incorporated into the solution as well as H_2O to further assist the identification of any hydrolysis products and adsorption mechanism. The alumina surface of the junction was again prepared by plasma discharge for 60 seconds in oxygen. The solution of 0.5% v/v TAA 1% v/v D_2O and 0.5% v/v $MeNO_2$ in IPA was spin doped under normal conditions. The junction resistance was measured at 350Ω (at 298K) and the aluminium and lead strip resistances were found to be 30Ω and 5Ω respectively. The spectrometer operating conditions were as follows.

Sensitivity	0.2	µV
Modulation Voltage	6	mV
Time Constant	3	secs.
Scan Time	30	mins.

Figure 6.3.4 shows the resulting IET spectrum. Table 6.3.4 details the peak energies and indicates possible spectral assignments of the peaks produced in Figure 6.3.4, the IET spectrum of 0.5% v/v TAA, 0.5% v/v nitromethane and 1% v/v D_2O in IPA. The spectral assignment was again carried out with reference to the following; [Williams and Flemming, 1980] [Smith et al., 1950] [Monjushiro et al., 1985] [Ratinen and Kiviharju, 1989a] and IET spectra of TAA detailed in Section 6.2.1.

Figure 6.3.4. <u>IET Spectrum of 0.5% v/v TAA 0.5% v/v $MeNO_2$ and 1% v/v D_2O in IPA.</u>

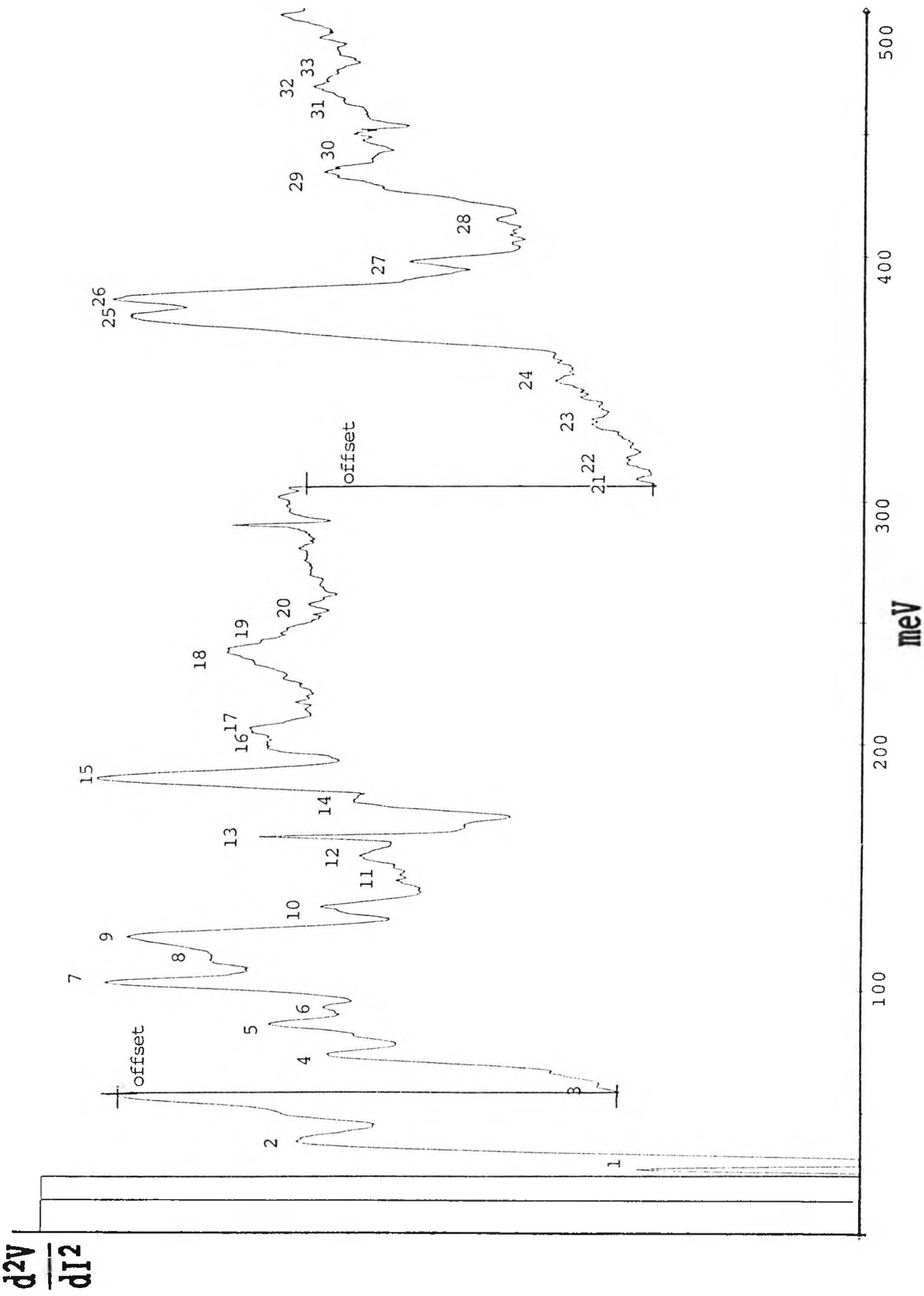

Table 6.3.4. Assignment of the Peaks Produced in the IET Spectrum of TAA, $MeNO_2$ and D_2O in IPA.

Peak No.	Energy (meV)	Wave No. (cm^{-1})	Intens.	Assignment
1	25.3	204	M	Al Phonon
2	36.3	293	M	Al Phonon
3	57.5	464	W	Ti-O str.
4	70.1	569	M/W	Ti-O str.
5	82.2	663	M	Ti-O str.
6	89.0	718	M/W	Al-O-Al
7	98.7	796	S	O-Ti-O
8	107.6	868	M	O-D def.
9	116.6	940	S	O-Ti-O or Al-O str.
10	128.1	1033	M/W	C-N str. or NH_2 twist
11	138.4	1116	W	C-O str.
12	148.0	1194	W	C-O str.
13	155.6	1255	M/W	C-O str.
14	170.0	1371	M/W	C-H def.
15	178.8	1442	S	CH_3 def.
16	191.2	1542	M/W	N-H def.
17	197.4	1592	M/W	N-H def.
18	228.9	1846	M	
19	235.7	1901	W	
20	246.7	1990	W	
21	296.7	2393	W	ND_2 str.
22	302.9	2443	W	NDH str.
23	317.9	2564	W	ND_2 str.
24	335.8	2708	W	O-D str.
25	359.7	2901	S	C-H str.
26	367.3	2962	S	C-H str.
27	381.6	3078	M	C-H str.
28	398.8	3216	W	O--H H-bonding
29	415.9	3353	M	N-H str.
30	429.0	3460	M/W	N-H str.
31	444.0	3581	M/W	O-H str.
32	450.2	3631	M	O-H str.
33	456.4	3681	M/W	O-H str.

S=Strong, M=Medium and W=Weak Intensities.

1meV ≡ 8.065 cm^{-1}

Discussion of the Results from the Nitromethane Doped Tunnel Junctions.

Figure 6.3.3 shows the IET spectrum of spin doped nitromethane. Several important features should be noticed, as follows.

(i) Figure 6.3.3 shows two highly intensive peaks at low energies (354 and 431 cm^{-1}) which are difficult to assign using the references quoted (infrared and Raman spectra of liquid and vapour $MeNO_2$). These peaks' appearance seems to be out of character with the rest of the spectrum which tends to show low intensity peaks. This observation tends to suggest that these peaks are caused by an inherent instability in the tunnel junction.

(ii) Assignment of spectral peaks in the mid-region of Figure 6.3.3 shows marked differences from classical infrared and Raman spectra of nitromethane [Smith et al., 1950]. A large signal at 1493 cm^{-1} in Figure 6.3.3 can only be assigned to the presence of a nitroso-type compound on the surface (C-N=O) [Williams and Flemming, 1980]. There is no sign in the IET spectrum of anhydrous nitromethane of peaks at 1530 and 1320-1350 cm^{-1} which would be attributed to normal C-NO_2 stretching modes. This observation concurs with the findings of other IETS studies into nitro- organic molecules adsorbed onto alumina [Ratinen and Kiviharlu, 1989a and 1989b] [Monjushiro, 1985].

(iii) The C-H stretching modes in Figure 6.3.3 are small in intensity and broad in energy. This observation tends to suggest that a large number of different surface orientations and environments of the -CH_3 group maybe caused by surface hydrogen bonding.

In conclusion, it must be noted from Figure 6.3.3 that the IET spectrum of nitromethane produced in this study does not agree with infrared and Raman data on nitromethane. This suggests that some sort of surface reaction may be taking place possibly via the formation of a nitrosomethane type compound ($H_3C-N=O$). This idea concurs with studies by Monjushiro et al. [1985] that suggest that the surface reduction of nitrobenzene compounds on a hydrated alumina surface occurs in a similar manner. [Ratinen and Kiviharju, 1989a].

Figure 6.3.4 shows the IET spectrum of the complex solution of 0.5% v/v TAA. 0.5% v/v nitromethane and 1% v/v D_2O in IPA. Several spectral features should be noted. They are as follows.

(i) The intense low energy bands at 354 and 431 cm^{-1} in Figure 6.3.3 are absent from Figure 6.3.4. This observation implies and confirms that these peaks in Figure 6.3.3 were caused by an inherent junction instability.

(ii) Figure 6.3.4 indicates a TAA adsorption in a similar manner as normally occurring in anhydrous doping conditions, see Section 6.2.1. This is due to the absence of peaks assignable to Ti=O stretching modes and the observation of normal energy Ti-O and O-Ti-O vibrational modes. It may be that the water of hydrolysis, primarily D_2O, does not in this case hydrolyse the TAA to any extent. This may be due to the presence of a competing reaction in solution or on the surface or to the reduced hydrolytic activity of D_2O.

(iii) The peak at 1080 cm^{-1} in Figure 6.3.3 is seen at 1033 cm^{-1} in Figure 6.3.4. This may be assigned as a "normal" C-N stretching mode. The shift in energy from 1080 cm^{-1} may have been caused by reduction of the N group from say N=O to NH_2.

(iv) New tunnelling peaks are observed in Figure 6.3.4 at 1542 and 1592 cm^{-1}. These peaks are assigned to NH deformation modes, possibly slightly reduced in energy due to H-bonding with hydrated surface species.

(v) Weak bands from 2400 - 2700 cm^{-1} finger-print very well with ND_2, NHD and OD stretching modes also observed by Monjushiro et al. [1985].

(vi) New and intense N-H stretching modes in Figure 6.3.4 are seen at 3354 and 3460 cm^{-1} that again suggest reduction of the nitro group in nitromethane.

(vii) O-H stretching modes in Figure 6.3.4, are not unexpectedly, shown to become more intense than in the spectrum of anhydrous doped nitromethane (Figure 6.3.3).

So in conclusion from Figure 6.3.4, the IET spectrum of TAA, nitromethane, and deuterium oxide in IPA, several suggestions can be proposed. Firstly, there is a large amount of evidence to suggest increased reduction of the $-NO_2$ group to an amine type group in the presence of a more hydrated alumina surface. Also $-ND_2$ and -NHD are thought to be produced in the presence of D_2O. Secondly, the evidence suggests that the TAA is adsorbed onto the surface as shown in Figure 6.2.5 - the anhydrous doping conditions - in the presence of 1% v/v D_2O. No evidence has been put forward, in this case, of polymerization or hydration of the titanate. Lastly, no evidence can be seen for any interaction of the reduced nitromethane surface species with the adsorbed TAA. Only on extensive hydrolysis and polymerization of the titanate would a significant change in the surface adsorption of nitromethane be expected to occur.

From both the spectra of junctions doped with nitromethane, a possible reaction sequence may be proposed, as below. However, further work using IETS and other techniques, such as XPS by Monjushiro et al. [1985], may elucidate the specific surface reactions present in the doping of nitromethane onto alumina.

$$\mathbf{Me\text{-}NO_2} \xrightarrow{\text{Al surf.}} \mathbf{Me\text{-}N{=}O} \text{----Al} \xrightarrow{H_2O/D_2O} \mathbf{Me\text{-}NH_2} \text{----HO-Al}$$

Ratinen and Kiviharju [1989a] have studied the IET spectra of nitrobenzoic acids. In the spectra of nitrobenzene and 3-nitrobenzoic acid broad signals, assigned to N-H stretching modes were observed, which in turn concurs with the work carried out by Monjushiro et al. [1985]. It has also been suggested that a similar reaction takes place on the adsorption of nitro-naphthalenes onto an alumina surface [Ratinen and Kiviharju, 1989b].

6.3.3 An IETS Study of TAA and Acetonitrile.

As with the previous section on nitromethane doped IETS junctions, the first aim of this study was to investigate the initial mode of adsorption of acetonitrile alone on the alumina surface within a Al-AlO_x-Pb tunnel junction. The acetonitrile was dried over a molecular sieve for 24 hours prior to doping. Doping itself was carried out in the nitrogen bag, illustrated in Figure 6.1.1. The alumina surface was prepared by plasma discharge oxidation under normal conditions for 60 seconds. The junction was completed and the junction resistance measured at 3.5 kΩ (at 298K). The resistances of the electrode strips were found to be negligible. The spectrometer operating conditions were as follows.

Sensitivity	0.5	μV
Modulation Voltage	8	mV
Time Constant	3	secs.
Scan Time	30	mins.

Figure 6.3.5 shows the resulting IET spectrum of spin doped acetonitrile. Table 6.3.5 details the spectral data and indicates possible spectral assignments of the peaks produced in Figure 6.3.5. The spectral assignment was carried out with reference to the following; [Williams and Fleming, 1980] [Venkateswarlu, 1951] [Jaklevic and Gaertner, 1978].

Figure 6.3.5. <u>IET Spectrum of Acetonitrile.</u>

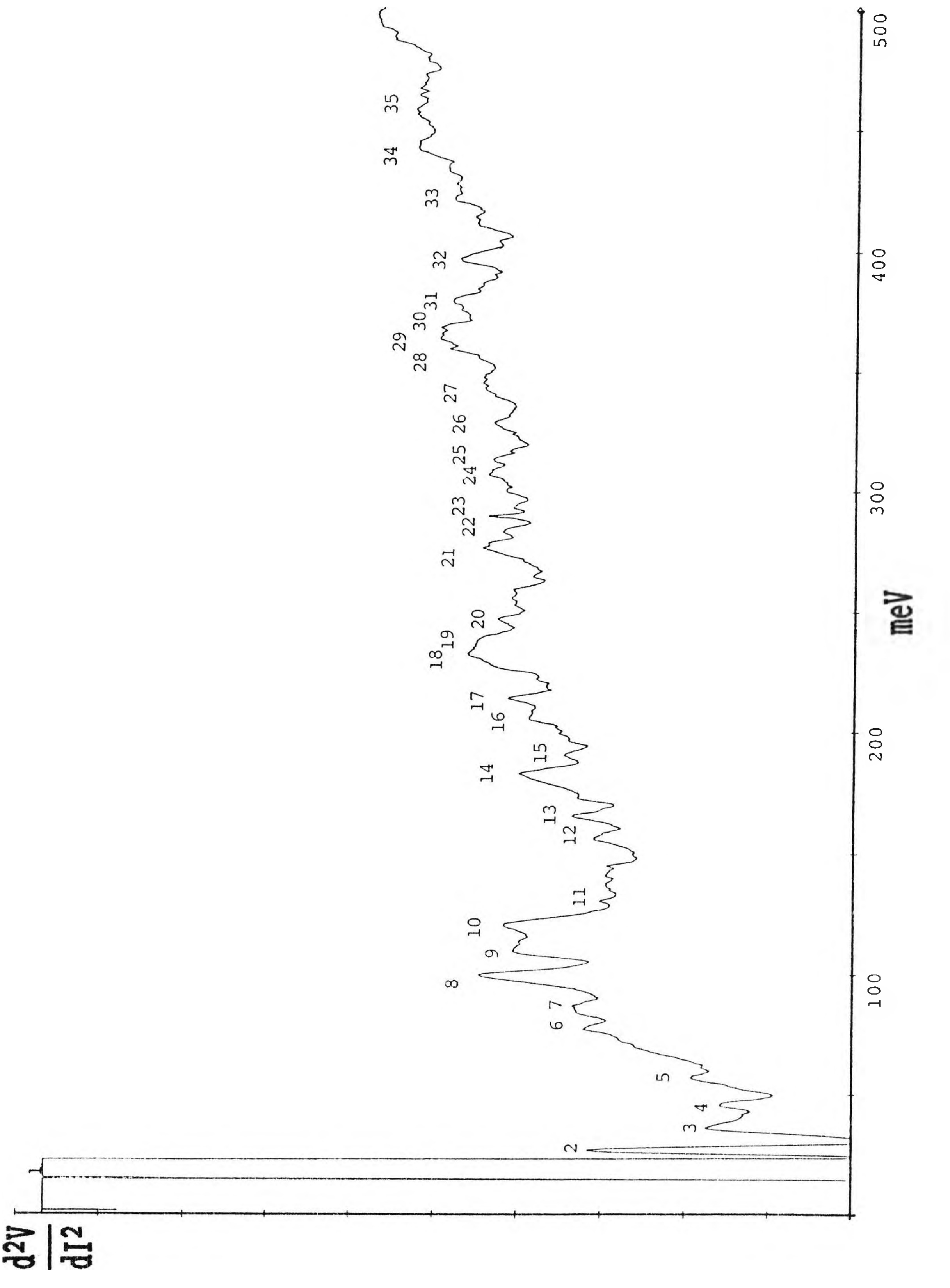

Table 6.3.5. Assignment of the Peaks Produced in the IET Spectrum of Acetonitrile.

Peak No.	Energy (meV)	Wave No. (cm^{-1})	Intens.	Assignment
1	17.8	144	VS	Al Phonon
2	27.1	219	M	Al Phonon
3	35.7	288	M/W	Al Phonon
4	45.7	369	M/W	$C\equiv N$ bend
5	57.1	461	W	Al-N
6	77.1	622	M/W	
7	85.7	691	M/W	
8	99.3	801	M	C-H def.
9	110.0	887	M	C-C str.
10	120.7	973	M	Al-O str.
11	130.7	1054	W	CH_3 rock
12	156.4	1261	M/W	C-H def.
13	165.7	1336	M/W	CH_3 def.
14	182.8	1475	M	C-H def.
15	190.7	1538	W	
16	205.7	1659	M/W	
17	213.6	1722	M/W	
18	232.1	1872	M	weak $C\equiv N$
19	238.6	1924	M/Sh	weak $C\equiv N$
20	247.1	1993	M/W	
21	277.1	2235	M/W	$C\equiv H$ str.
22	283.6	2287	W	$C\equiv N$ str.
23	290.0	2339	M/W	
24	307.1	2477	W	
25	312.8	2523	W	
26	328.6	2650	W	
27	344.3	2777	W	
28	359.3	2897	M/W	C-H str.
29	362.8	2926	M/W	C-H str.
30	368.6	2973	M/W	C-H str.
31	379.3	3059	W	C-H str.
32	396.4	3197	M/W	H-bonding
33	421.4	3399	W	H-bonding
34	442.8	3572	M/W	O-H str.
35	457.8	3697	M/W	O-H str.

S=Strong, M=Medium Sh=Shoulder and W=Weak Intensities.

$1 meV \equiv 8.065 cm^{-1}$

To investigate the interaction of acetonitrile and TAA in an anhydrous situation, a solution of 0.5% v/v TAA and 0.5% v/v acetonitrile in dried IPA was prepared under nitrogen (as outlined in Section 6.1.2). The aluminium strip of the junction was plasma discharge oxidised for a period of 60 seconds. Spin doping of the junction was again carried out in the dry-bag. The resistance of the completed junction was measured at 550Ω (at 298K). The junction electrode strip resistances were once more found to be of negligible value. The spectrometer operating conditions were as follows.

Sensitivity	0.5 μV
Modulation Voltage	6 mV
Time Constant	3 secs.
Scan Time	30 mins.

Figure 6.3.6 shows the resulting IET spectrum of a junction spin doped with a solution of 0.5% v/v TAA and 0.5% v/v acetonitrile in dried IPA. Table 6.3.6 details the spectral data and indicates possible spectral assignments of the peaks produced in Figure 6.3.6. The spectral assignment was carried out with reference to the following; [Williams and Fleming, 1980] [Venkateswarlu, 1951] [Jaklevic and Gaertner, 1978] and earlier IET spectra of TAA from Section 6.2.1.

Figure 6.3.6. IET Spectrum of 0.5% v/v TAA and 0.5% v/v Acetonitrile in Dried IPA.

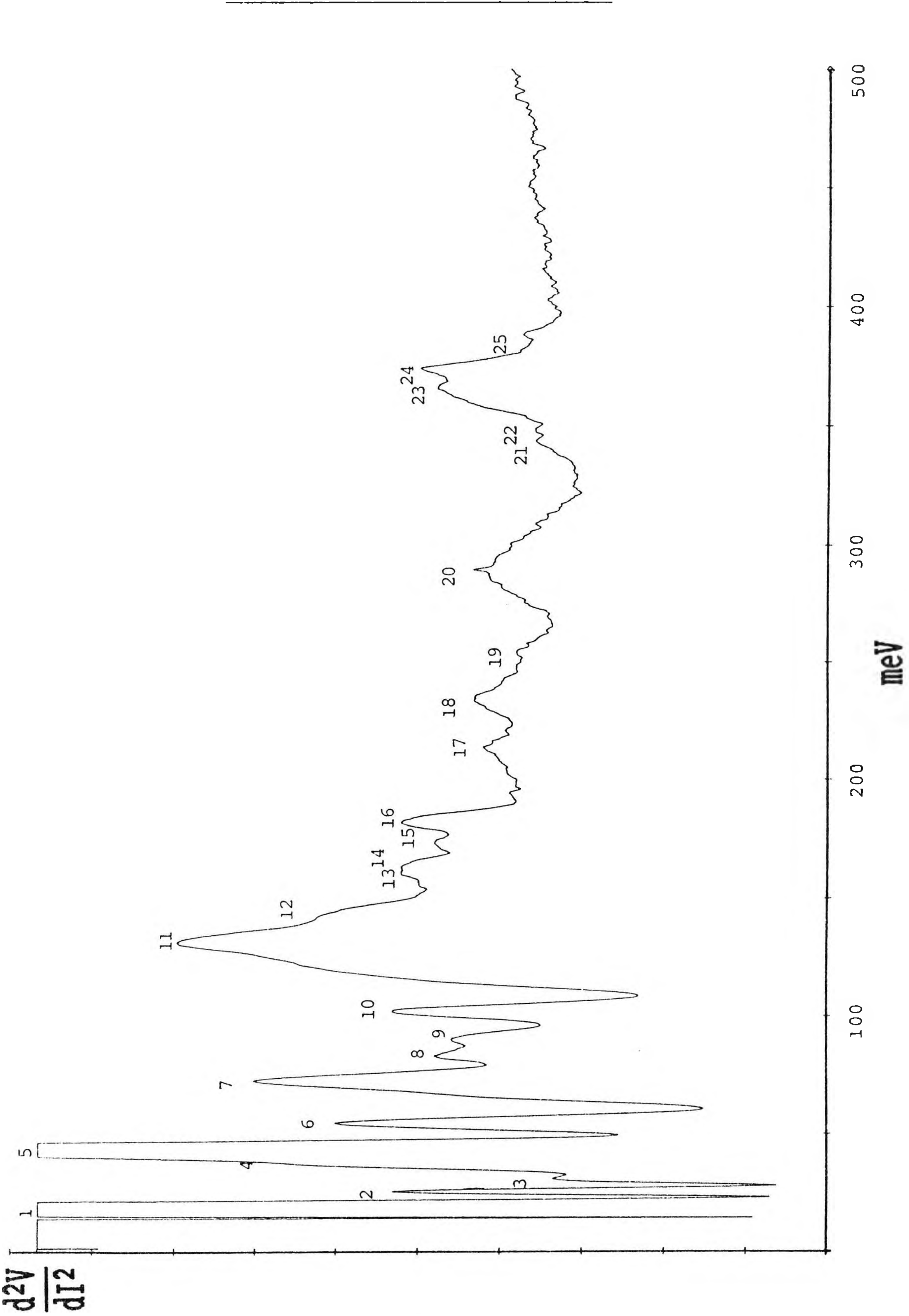

Table 6.3.6. Assignment of the Peaks Produced in the IET Spectrum of TAA and Acetonitrile in Dried IPA.

Peak No.	Energy (meV)	Wave No. (cm^{-1})	Intens.	Assignment
1	17.1	138	VS	Al Phonon
2	25.7	207	M	Al Phonon
3	30.7	247	W	
4	37.1	299	S/Sh	Al Phonon
5	42.1	340	VS	
6	54.3	438	M	Ti-O str./ C≡N def.
7	71.4	576	S	Ti-O
8	82.8	668	M/W	Ti-O
9	90.0	726	M/W	O-Ti-O
10	101.4	818	M	C-H def.
11	130.7	1054	S/Br	C-C str./ CH_3 rock
12	142.1	1146	M/Sh	C-O str.
13	160.0	1290	W	C-H def.
14	163.6	1319	W	C-H def.
15	172.8	1394	W	CH_3 def.
16	181.4	1463	M/W	C-H def.
17	213.6	1722	M/W	
18	234.3	1889	M/Br	weak C≡N
19	254.3	2051	W/Sh	
20	290.0	2339	Br/M	C≡N str.
21	344.3	2776	M/W	weak C-H
22	346.4	2794	W	weak C-H
23	365.7	2949	M	C-H str
24	373.6	3013	M	C-H str.
25	387.8	3128	W	C-H str

S=Strong, M=Medium, Br=Broad, Sh=Shoulder and W=Weak Intensities.

1meV ≡ 8.065 cm^{-1}

The next aim of this study was to investigate the effect of total hydrolysis of the TAA on the adsorption of acetonitrile on the primed alumina surface. A solution of 0.5% v/v TAA and 0.5% v/v acetonitrile in water was prepared under normal conditions and left to stand on the bench for 95 hours, with occasional shaking. The solution was spin doped onto the alumina surface under normal conditions. The junction resistance was found to be 3.7 kΩ (at 298K). The spectrometer operating conditions were as follows.

Sensitivity	0.5	µV
Modulation Voltage	10	mV
Time Constant	3	secs.
Scan Time	30	mins.

Figure 6.3.7 shows the resulting IET spectrum of 0.5% v/v TAA and 0.5% v/v acetonitrile in water. Table 6.3.7 details the spectral data and indicates possible spectral assignments of the peaks produced in Figure 6.3.7. The spectral assignment was carried out with reference to the following; [Williams and Fleming, 1980] [Venkateswarlu, 1951] [Jaklevic and Gaertner, 1978] and earlier IET spectra of TAA from Section 6.2.1.

Figure 6.3.7. IET Spectrum of 0.5% v/v TAA and 0.5% v.v Acetonitrile in Water (After 95 Hours).

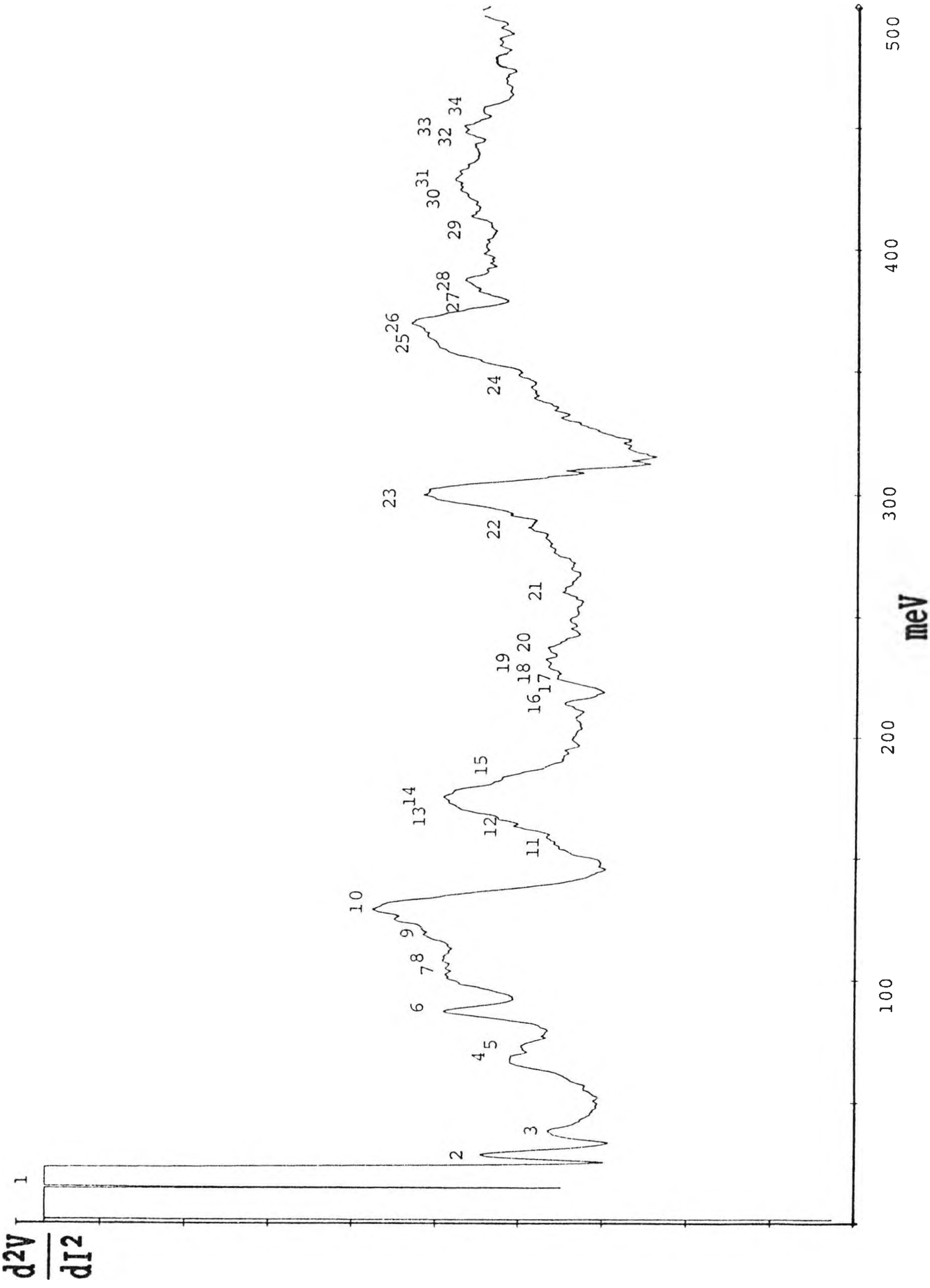

Table 6.3.7. Assignment of the IET Spectrum of TAA and Acetonitrile in Water (After 95 Hours).

Peak No.	Energy (meV)	Wave No. (cm^{-1})	Intens.	Assignment
1	19.2	155	VS	Al Phonon
2	28.5	230	M	Al Phonon
3	37.7	304	M/W	Al Phonon
4	66.9	540	M	Ti-O
5	72.6	586	M/W	Ti-O
6	86.9	701	M	C-H def.
7	102.6	827	M/W	O-Ti-O
8	109.0	879	M	Ti-O-Ti
9	119.0	959	M	Al-O str./ Ti-O-Ti
10	128.9	1040	W	CH_3 rock
11	158.8	1281	W/Sh	C-H def.
12	163.1	1315	M/Sh	CH_3 def.
13	170.9	1379	M/Br	C-H def.
14	175.2	1413	M/Br	C-H def.
15	183.0	1476	W/Sh	C-H def.
16	213.7	1723	W	
17	224.3	1809	W	
18	229.3	1850	W	weak C≡N
19	232.2	1873	W	weak C≡N
20	237.2	1913	W	weak C≡N
21	250.0	2097	W	
22	292.0	2355	W/Sh	C≡N str.
23	299.8	2418	M	C≡N str.
24	348.3	2809	W	C-H str.
25	361.8	2918	M/Br	C-H str.
26	370.4	2987	M	C-H str.
27	383.2	3090	M/W	C-H str.
28	387.5	3124	M/W	H-bonding
29	414.5	3343	W	] H-bonded
30	424.5	3424	W	] O-H str.
31	428.8	3458	W	]
32	448.0	3613	W	O-H str.
33	450.8	3636	W	O-H str.
34	457.3	3687	W	O-H str.

S=Strong, Br=Broad M=Medium, Sh=Shoulder and W=Weak Intensities.

1meV ≡ 8.065 cm^{-1}

Discussion of the Results from the Acetonitrile Doped Tunnel Junctions.

Figure 6.3.5 shows the IET spectrum of spin doped anhydrous acetonitrile. Table 6.3.5 indicates several features of Figure 6.3.5 that should be noted. They are as follows.

(i) The large junction resistance (3.5 kΩ) makes the production of large signals impossible even with an A.C modulation voltage of 10mV.

(ii) The spectrum of acetonitrile contains a large number of peaks. Good correlation between some of the IETS peaks and the infrared and Raman spectra is seen. However, some signals from the IET spectrum are not easily assignable using the infrared and Raman spectra of acetonitrile.

(iii) Two peaks are seen in the mid-region of Figure 6.3.5 that may be attributed to the C≡N stretching mode. The first, a large broad band between 1872 and 1924 cm^{-1}, shows that the C≡N bond energy had been reduced significantly. This is most probably caused by the mode of surface adsorption of the acetonitrile. The other band shows the C≡N stretching mode at a more usual energy. The energy of this band concurs with the

C≡N stretching energy in the IET spectrum of infusion doped acetonitrile produced by Jaklevic and Gaertner [1978]. This in turn, suggests a different mode of surface adsorption of the C≡N bond is present in Figure 6.3.5.

(iv) Figure 6.3.5 shows relatively weak and broad C-H stretching modes that suggests, as above, that the acetonitrile may be adsorbed in more than one way.

These observations, taken as a whole, suggest two types of surface adsorbed species of acetonitrile on alumina in anhydrous conditions.

(a) A normal C≡N energy but H- atoms in different environments suggests H-bonding of the methyl group and therefore indicates adsorption perpendicular to the surface.

(b) A reduced energy C≡N bond suggests a π-interaction of the C≡N bond with an electron deficient Al surface site.

IETS studies by Jaklevic and Gaertner [1978] do not show a reduced energy C≡N stretching mode in their study of acetonitrile. This is almost certainly due to the different doping procedures employed in their study. They use infusion doping techniques which totally hydrate the alumina surface during the doping of acetonitrile.

Figure 6.3.8 illustrates the proposed surface adsorption modes of acetonitrile in anhydrous conditions. It is important to note that classically, due to the orientational selection rule (see Section 1.3.5), vibration modes of bonds parallel to the alumina surface would normally not be observed in the IET spectrum. However, with a multiple (triple) bond this is not always the case. The observation of the parallel bond is thought to be due to the increased electron density of the triple bond that allows interaction with the tunnelling electron [Lewis, 1985].

Figure 6.3.6 shows the IET spectrum of 0.5% v/v TAA and 0.5% v/v acetonitrile in dried IPA (as before primarily anhydrous conditions). This was investigated in order to observe any interaction between TAA and acetonitrile in anhydrous conditions on the alumina surface. Several spectral features are seen in Table 6.3.6, the spectral assignment of Figure 6.3.6. They are as follows.

(i) Ti-O and O-Ti-O vibrational modes show energies very similar to those in the anhydrous IPA study in Section 6.2.1. Therefore the TAA can be said to have been adsorbed onto the alumina surface as shown in Figure 6.2.5.

Figure 6.3.8. Proposed Mode of Adsorption of Acetonitrile on an Unprimed and Anhydrous Alumina Surface.

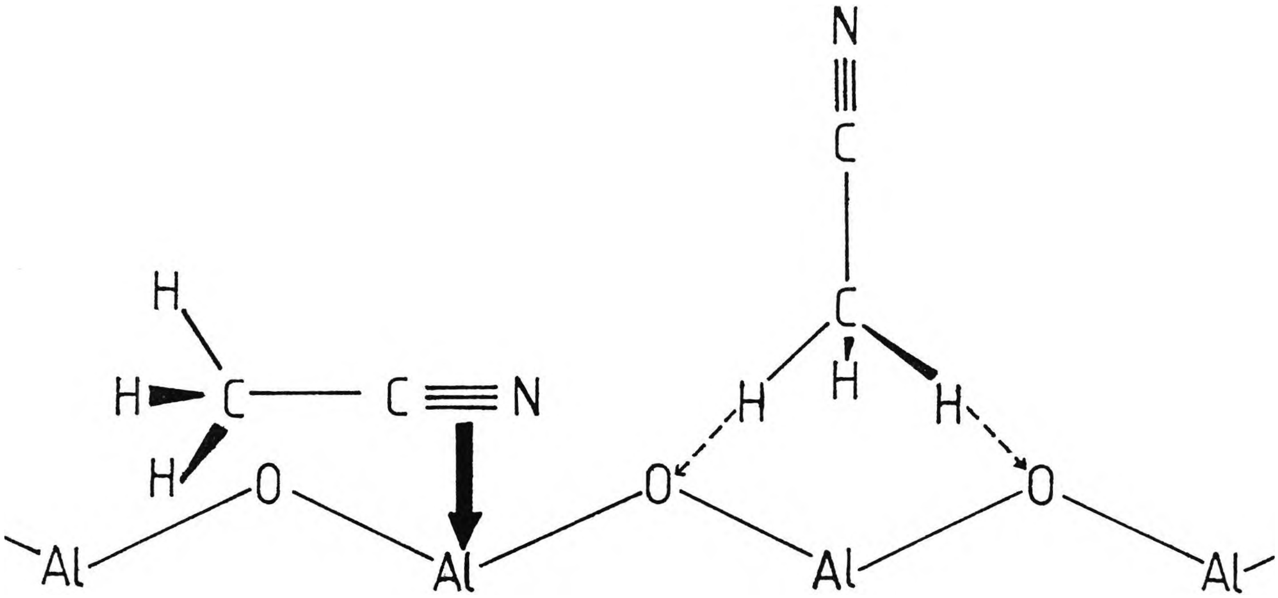

(ii) A more intense $-CH_3$ deformation mode in Figure 6.3.6 than in Figure 6.3.5 suggests that the π-complex like adsorption mode outlined above, may not be as often present in this case. An increase in unperturbed CH_3 modes would indicate more of the perpendicularly adsorbed acetonitrile.

(iii) Again both types of C≡N stretching modes are present in Figure 6.3.6. The unperturbed signal, at higher energy, is much better defined in this case. This suggests that the TAA adsorption (or maybe an increase in water present) may reduce the number of π-complex adsorption sites on the surface, and therefore increasing the number of perpendicularly adsorbed acetonitrile molecules.

(iv) Again broad C-H stretching mode signals suggest some sort of H-bonding adsorption mode.

So, in conclusion, from Figure 6.3.6, both types of acetonitrile adsorption (as shown in Figure 6.3.8) are observed with a possible increase in the number of perpendicularly adsorbed molecules due to the normal adsorption of TAA (shown in Figure 6.2.5) which may use most of the aluminium surface sites.

Figure 6.3.7 shows the IET spectrum of a tunnel junction doped with a solution of 0.5% v/v TAA and 0.5% v/v acetonitrile in water. The solution was allowed to stand for 95 hours prior to doping. Having studied the adsorption of acetonitrile and TAA separately and together it was important to observe any change in the adsorption of acetonitrile, if any, caused by the hydrolysis of the TAA, the priming of the surface. Several spectral features were noted from Table 6.3.7. They are as follows.

(i) Similar Ti-O, O-Ti-O and Ti-O-Ti modes to those in Figure 6.2.4 (the study of totally hydrolysed TAA alone) are seen in Figure 6.3.7. This tends to indicate total hydrolysis of the TAA to the adsorbed polymeric form shown in Figure 6.2.7. This is supported by the fact that no C-O stretching modes are seen in Figure 6.3.7 therefore indicating the loss of all the organic ligands from the titanium centres, through hydrolysis.

(ii) Figure 6.3.7 shows broad and complex C-H deformation and stretching modes which suggest H-bonding of the acetonitrile's methyl group on adsorption onto the surface.

(iii) The C≡N stretching mode with the normal energy is much more intense than the corresponding peak of the reduced energy C≡N stretching mode. This indicates that in the hydrated and primed surface situation the H-bonded adsorption mode is predominant.

(iv) A variety of O-H stretching modes from 3100cm^{-1} upwards suggest a complex H-bonding situation onto the surface or the primer.

These observations concur with the IETS study of acetonitrile by Jaklevic and Gaertner [1978], in which only the normal C≡N stretching mode was observed when acetonitrile was infusion doped onto the alumina surface. During infusion doping the surface is totally hydrated and the possibility of aluminium centres which allow surface π-complexing, as seen in the anhydrous surface doped acetonitrile cases in this study (and illustrated in Figure 6.3.8), is greatly reduced.

In conclusion, the overwhelming evidence from Figure 6.3.7 suggests that in the presence of a primed and hydrated surface the π-complex adsorption mode does not occur. The evidence suggests that only a H-bonding mode of adsorption of acetonitrile to the hydrated or primed surface may be seen, as shown in Figure 6.3.9.

In the study of acetonitrile it has been possible using IETS to analyse the effect of a surface primer or coupling agent not only with the inorganic substrate but also with the surface adsorption of a secondary organic species.

Figure 6.3.9. Proposed Mode of Adsorption of Acetonitrile on a Titanate Primed Alumina Surface.

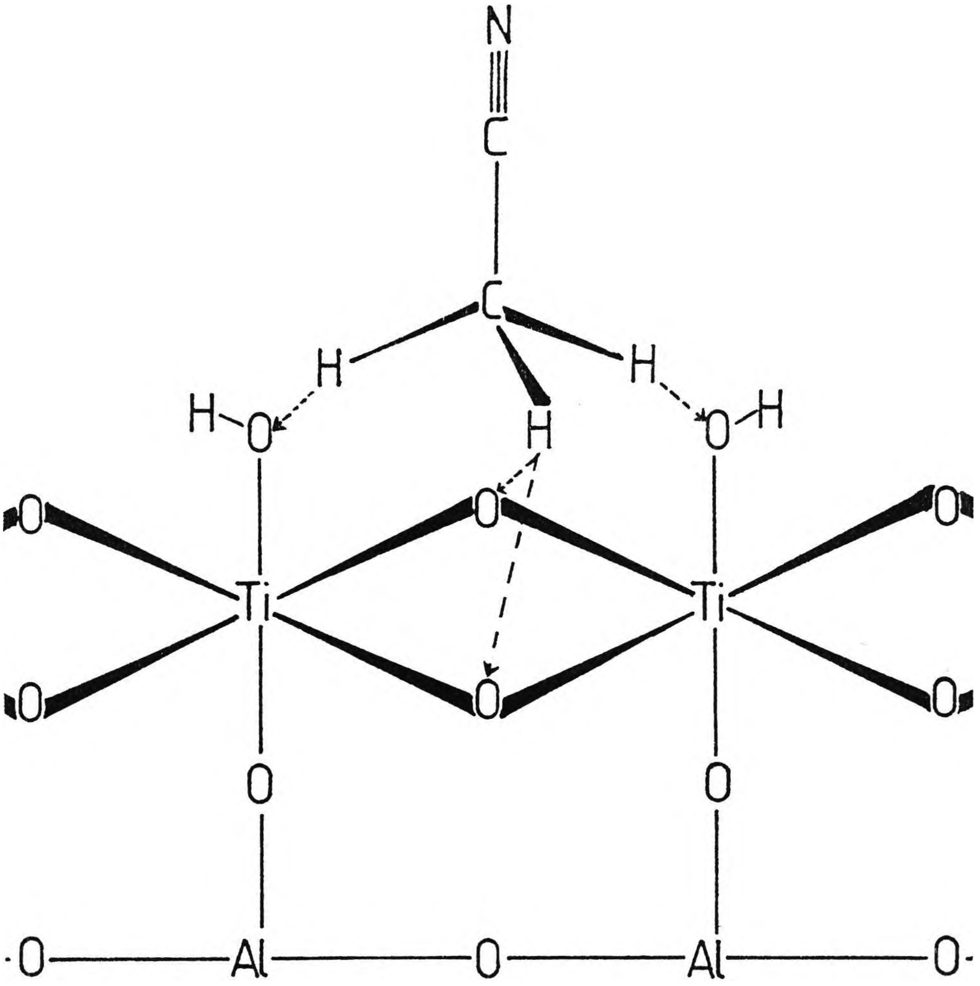

6.4 CONCLUSIONS

During this IETS study of titanate coupling agents it has been possible to analyse the methods of surface adsorption of alkoxy-titanate and titanium chelate complexes onto alumina surfaces (Sections 6.1 and 6.2) and to propose solution hydrolysis schemes for titanium acetylacetonate and triethanolamine titanate (Section 6.2). It has also been possible to study the surface hydrolysis of octylene glycol titanate (Section 6.2.3). As well as drawing conclusions on the method of interaction of titanates with alumina surfaces, it has also been possible to study the effect or non-effect of a titanate coupling agent, in this case TAA, on the surface adsorption processes of several simple organic molecules (Section 6.3). This has provided information on the probable interaction of titanium based primers with polymeric coating bases. Unfortunately the field of study is huge as the number of titanate primers for specific applications is enormous (detailed in Chapter 3). However, it has been possible in this study to produce an insight into the method of adhesion promotion of titanate coupling agents using IETS.

IETS has also shown, in Section 6.3, how it is extremely useful in the observation of other surface effects than adhesion such as the corrosion of alumina by chloroform, in Section 6.3.1, and the surface reduction of nitromethane on alumina, in Section 6.3.2.

CHAPTER SEVEN - CONCLUSIONS AND FUTURE WORK

7.1 CONCLUSIONS

The results and conclusions contained in this thesis indicate the effectiveness of IETS for the investigation of an area of research which is both industrially important and academically significant.

In the study of organotitanium coupling agents, in Chapter 6, the initial mode of surface adsorption of three titanate primers TAA, TEAT and OGT has been established and the solution hydrolysis scheme of such species elucidated. The interaction between the titanate, in its various hydrolysed forms, and the alumina surface has been studied and both the bonding and surface orientation of the molecules has been established. Also the interaction between the adsorbed titanate and other organic species on the surface, which might represent model adhesives, has been explored. Thus a complete picture of the surface reactions involved in the behaviour of some organotitanium coupling agents has been established.

Some interesting peripheral studies from the main investigation have been carried out. Both the surface corrosive effect of chloroform and the surface induced reduction of nitromethane on the anhydrous alumina surface of the Al-AlO_x-Pb tunnel junction have been investigated.

Other surface induced reactions concerning the possible contamination of the alumina substrate by atmospheric species has been considered in Appendix A. Such reactions have implications in the subsequent mode of bonding of primers and adhesives to oxide surfaces and will influence the integrity of the metal-adhesive joint.

New experimental techniques including the reuse of glass fibre junction substrates, and the use of an inert-atmosphere doping chamber, for the preparation of atmospherically sensitive junction dopants, have been developed and used in the present work.

These studies have demonstrated unequivocally the extreme value of IETS in investigating the behaviour and reactions associated with very thin films of material on the surface of metallic oxides. Particularly, they have provided fresh information about titanium-based films of adhesive coupling agents or primers.

7.2 FUTURE WORK

In considering work which might extend the results presented in this report, major areas of study should be examined:

(i) Further study of titanate and other adhesive coupling agents by IETS.
(ii) Development of the spectrometer and its associated equipment used in this study.
(iii) The future of IETS as a spectroscopic technique.

(i) Titanate Coupling Agents

The first investigation by IETS into the mode of action of organotitanium coupling agents has been presented here. It has been shown that titanates, as well as silanes, can be studied effectively using IETS.

IETS studies using isotopically labeled dopant molecules (^{18}O and ^{2}D for H_2O or organic species) would undoubtedly help to confirm the surface reactions and solution hydrolysis schemes proposed earlier. Work carried out into the surface adsorption and reaction of chloroform and nitromethane reported here would also benefit from isotopic substitution studies.

It is not inconceivable that work using IETS could optimize the solution and surface preparation of coupling agents and their application. This would be valuable to industry and could result in more reliable adhesion promotion as tested by more conventional analytical tools of adhesion scientists. Obviously, other specific adhesion promotion problems over a broad field with alumina surfaces or aluminium substrates would benefit from IETS study.

The work presented shows that an analysis of the interactions between primed substrates and coatings is possible using IETS. It therefore follows that a variety of adhesive, lacquer, ink and paint bases could be investigated. The adhesion of such bases could be studied on a variety of primed substrates such as iron and silicon oxides and organic surfaces by investigating different insulators within the tunnel junction.

(ii) The Spectrometer

Several changes to the spectrometer used in this study should be considered.

(a) It would be extremely useful to be able to measure the junction resistance at 4.2K and throughout the spectral production. This would facilitate the analysis of the junction electrical characteristics and possibly shed light on the problem of boosting.

(b) Other spectral flexibility such as the production of offset scanning (i.e. from 250 mV to 750 mV), spectral expansion and reverse scanning, could all prove important and useful. Reverse bias IETS has been used by some workers (e.g. Ratinen [1983]).

(c) The possibility of using 4-terminal IET junctions remains. This would overcome the problems associated with low resistance junctions with significant electrode resistances. Such a system warrants consideration but would also require considerable change in the hardware configuration of the spectrometer.

Since the construction of the spectrometer used in this and other studies [Lewis, 1985], in its present form, it has been controlled by a PET microcomputer. This is now outdated and the advance in computer technology makes it imperative that if any considerable amount of future work is to be carried out on the existing system a new computer system should be incorporated. An IBM (or compatible) machine with a new A/D conversion processor could give the operator many advantages over those at present available, i.e.:

- Faster data manipulation and operation.
- Enormous data storage capacity (at least 4000x more than at present).
- Spectral flexibility built into the new software.
- Automatic peak energy measurement and graphical display ability.

It is not inconceivable to imagine the computer aided spectral interpretation with the aid of an on-line database linkage to the spectrometer similar to that incorporated into current infrared spectrometers.

The investments in time, expertise and equipment outlined above are imperative to ensure the continued use of the spectrometer at the forefront of IETS studies.

(iii) The Future of IETS

For IETS to have the same acceptability as other more conventional surface spectroscopic techniques, it must be shown to improve in three areas. Namely,

(a) Theoretical quantification of the tunnelling electron interaction with the molecular bonds within the tunnel junction, and work on the spectral intensity of IET spectra must be verified so as to make quantitative work possible. Such studies using radio-labeled benzoic acid suggest that this is possible [Langan and Hansma, 1975].

(b) The understanding of tunnel junction electrical characteristics and the reproducibility of tunnel junctions must be improved. At present, a mystique has developed over the need for junction boosting. This in turn has fueled a mistrust of the spectra produced from tunnel junctions with peculiar electrical characteristics.

(c) To enable the technique of IETS to expand, greater emphasis must be placed on the use of surface substrates other than alumina in tunnel junctions. Although alumina is a most important insulator used in the study of surface reactions and species, industrial applications require the use of other oxides, especially those of iron and silicon, sulphides and organic insulators.

(a) and (b) must primarily be the responsibility of physicists involved in the development of IETS. It is suggested that only when these problems are totally understood can the chemists involved with IETS exploit this most important surface spectroscopic technique to its maximum potential. To enable this to happen it is important that the standardization of experimental techniques and the reporting of the results take place to allow the direct comparison of spectra from different workers. This will facilitate a greater dialogue between the different groups of workers in IETS. Without such a dialogue a remarkable spectroscopic technique could be overlooked when it promises to aid the investigation of many important areas of study.

A most interesting concept could be the marriage of the tunnelling spectrometer with a tunnelling microscope. This would provide a stereo view of the molecule-surface orientation (using the microscope) with an assessment of the strength of the molecule-surface interaction using the spectrometer. The data obtained from such an instrument, i.e. steric surface conformation and bond strengths, would enable information to be accumulated regarding vibrational spectral intensities relative to bond-surface orientation. This, in turn, would facilitate a quantification of the orientational Selection Rule.

REFERENCES

ADANE A., FOUCONNET A., KLEIN J., LÉGER A., BELIN M. and DEFOURNEAU D.; 1975. Solid State Commun. **16**, 1071.

ADLER J.G. and JACKSON J.E.; 1966. Rev. Sci. Inst. **37**, 1049.

ADLER J.G.; 1969. Solid State Commun. **7**, 1635.

ADLER J.G., CHEN T.T. and STRAUSS J.; 1971. Rev. Sci. Inst. **42**, 362.

ALLEN K.W. and STEVENS M.G.; 1982. J. Adhesion **14**, 137.

ALLEN K.W., HANSRANI A.K. and WAKE W.C.; 1981. J. Adhesion **12**, 199.

ALEXANDER J.D., GENT A.N. and HENRIKSEN P.N.; 1985. J. Chem. Phys. **83**, 5981.

AL MAKASHTA F., DARANZO C.U. and SHEPPARD N.; 1983. J. Chem. Soc. Chem. Commun. 1259.

ANON; 1962. Deutsche Farben - Zeitschrift, No. 4, 157.

ANON; 1980. Dynamit Nobel Chemicals, Report no. ZP 344/9.80/2000.

ANON; 1985. Ken-React Reference manual, KR-1084L, Kenrich Petrochemical Inc., Bayonne, NJ.

ARCHER W.L. and HARTER M.K.; 1978. Corrosion (Houston) **34**, 159.

BASCOM W.D.; 1972. Macromol. **5**, 792.

BOERIO F.J. and WILLIAMS J.W.; 1981. <u>Applications of Surface Science</u>, Vol. 8, North Holland Pub. Comp., Amsterdam, p. 19.

BOGATINA N.I., YANSON, I.K., VERKIN B.I. and BATRAK, A.G.; 1974. Sov. Phys. J.E.P.T. **38**, 1162.

BRADLEY D.C., MEHROSTRAAND R.C. and GAUR D.P.; 1978. <u>Metal Alkoxides</u>, Academic Press.

BREWIS D.M., COMYN J., OXLEY D.P., PRITCHARD R.G., REYNOLDS S., WERRETT C.R. and KINLOCH A.J.; 1984. Surf. Interf. Anal. **6**, 40.

BROWN N.M.D., TURNER R.J., AFFROSSMAN S., DUNKIN I.R., PETHRICK R.A. and SHIELDS C.J.; 1985. Spectrochim. Acta **40B**, 847.

BROWN N.M.D., MEENAN B.J., AFFROSSMAN S., PETHRICK R.A. and THOMSON B.; 1987. Surf Interf. Anal. **10**, 184.

BROWN N.M.D.; 1988. Spectroscopy Of Surfaces, Edited by R.J.H. Clark and R.E.Hester, Wiley. Advances in Spectroscopy, **16**, 215.

BURZYNSKI R., HUANG X. and PRASAD P.; 1987. Polym. Prep. **28**, 213.

CALVERT P.D., LALANANDHAM R.R. and WALTON D.R.M.; 1983. Adhesion: Aspects of Polymer Coating (Edited by K.L. Mittal), Plenum Press, 457.

CASSIDY P.E. and YAGER W.J.; 1971. J. Macromol. Sci. Revs. Polym. Technol. **D1**, 1.

CASSIDY P.E. and YAGER W.J.; 1972. J. Polym. Technol. **1**, 1.

CHU H.T., EIB N.K., GENT A.N. and HENDRIKSEN, P.N.; 1979. Probing Polymer Structures, Chapter 7, 174th meeting of the A.C.S., Edited by J.L.Koenig, 87.

CLARK J.M. and COLEMAN R.V.; 1976. Proc. Nat. Acad. Sci. USA **73**, 1598.

CLARK J.M. and COLEMAN R.V.; 1980. J. Chem. Phys. **73**, 2156.

CLEVELAND SOCIETY FOR COATINGS TECHNOLOGY; 1979. J. Coat. Technol. **51**, 38.

COMYN J., HORLEY C.C., OXLEY D.P., PRITCHARD R.G. and TEGG J.L.; 1981. J. Adhes. **12**, 171.

COMYN J.; 1984. Adhesion 9, Elsevier Applied Science Pub., Edited by K.W.Allen, 147.

COMYN J., HORLEY C.C., MALLIK R.R., PRITCHARD R.G.; 1986. Int. J. Adh. Adh. **6**, 73.

COMYN J., OXLEY D.P., PRITCHARD R.G., WERRETT C.R. and KINLOCH A.J.; 1989. J. Adhes. **28**, 171.

CUNNINGHAM S.L. and WEINBERG W.H.; 1979. Appl. Surf. Sci. **2**, 640.

DeCHEVEIGNE S., LÉGER A. and KLEIN J.; 1975. Proc. 14th Int. Conf. Low Temp. Phys., Finland.

DeCHEVEIGNE S., LÉGER A., KLEIN J., BELIN M. and DEFOURNEAU D.; 1977. Phys. Rev. B 15, 750.

DeCHEVEIGNE S., GAUTHIER S., GUINET C., LEBRUN M.-M., KLEIN J. and BELIN M.; 1985. J. Chem. Soc. Farad. Trans. 2, 81.

DeTHOMAS F.A.; 1987. Ph.D. Thesis, University of Delaware, USA. Diss. Abstr. Int. B **47**, 3734.

DORSEY G.A.; 1969. J. Electrochem. Soc. 113, 169.

EDGAR A. and ZYSKOWSKI A.; 1985. J. Phys. E: Sci Instrum. 18, 863.

EDGAR A.; 1987. J. Phys. E: Sci. Instrum. **20**, 340.

EIB N.K., FUNIKAWA T. and MITTAL K.L.; 1984. Rev. Sci. Inst. 55, 1161.

ELLIALTIOGLU R.M., WHITE H.W., GODWIN L.M. and WOLFRAM T.; 1980. J. Chem. Phys. **72**, 5291.

ELLIALTIOGLU R.W., WHITE H.W., GODWIN L.M. and WOLFRAM T.; 1981. J. Chem. Phys. **75**, 2432.

ELLIALTIOGLU R.W.; 1984. Ph.D. Thesis. University of Missouri, U.S.A.

ERICKSON P.W. and PLUEDDEMANN E.P.; 1974. Composite Materials, Vol. 6.(Edited by E.P. Plueddemann) Academic Press, New York.

EVANS H.E. and WEINBERG W.H.; 1980. J. Amer. Chem. Soc. **102**, 2554.

FALCONER D.J., MacDONALD N. and WALKER P.; 1964. Chem. Ind., 1230.

FAVIS B.D., BLANCHARD L.P., LEONARD J. and PRUD'HOMME R.E.; 1984. Polymer Composites, 5, 11.

FIELD B.O., LEWIS D.M. and HART R.; 1985. Spectrochim. Acta **41A**, 1069.

FIELD B.O. and SPENCER J.E.D.; 1989. Spectrochim. Acta 45A, 445.

FURUKAWA T., EIB N.K., MITTAL K.L. and ANDERSON H.R.Jnr.; 1982. Surf. Interf. Anal. 4, 240.

FURUKAWA T., EIB N.K., MITTAL K.L. and ANDERSON H.R.Jnr.; 1983. J. Colloid Interf. Sci. **96**, 322.

GAUTHIER S., DeCHEVEIGNE S., SALACE G., KLEIN J. and BELIN M.; 1985. Surf. Sci. 155, 31.

GETTINGS M. and KINLOCH A.J.; 1977. J. Mater. Sci. **12**, 251.

GIAEVER I., HART N. and MERGERLE K.; 1962. Phys. Rev. **126**, 941.

GIAEVER I. and ZELLA H.R.; 1968. Phys. Rev. Lett. **21**, 1385.

GIAEVER I.; 1974. Science **183**, 4131.

GIBIAN T.G. and McKINNEY D.S.; 1951. Amer. Soc. **73**, 1431.

HALL J.T. and HANSMA P.K.; 1978. Surf.Sci. **71**, 1.

HANSMA P.K. and COLEMAN R.V.; 1974. Science **184**, 1369.

HANSMA P.K., KASKA W.C. and LAINE R.M.; 1976. J. Amer. Chem. Soc. **98**, 6064.

HANSMA P.K. (Editor); 1982. Tunneling Spectroscopy, Plenum Press, 287.

HENRIKSEN P.N., GENT A.N., RAMSIER R.D. and ALEXANDER J.D.; 1988. Surf. Interf. Anal. **11**, 283.

HIGO H., MIZUTARU S. and KAMATA S.; 1985. Bull. Chem. Soc. Jpn. **58**, 2960.

HILLIARD L.J. and GOLD H.S.; 1985. Appl.Spectros. **39**, 124.

HIPPS K.W. and MAZUR U.; 1980. J. Phys. Chem. **84**, 3162.

HIPPS K.W. and MAZUR U.; 1981. Inorg.Chem. **20**, 1391.

HIPPS K.W. and MAZUR U.; 1984. Rev. Sci. Instrum. **55**, 1120.

JAKLEVIC R.C. and LAMBE J.; 1966. Phys. Rev. Lett. **17**, 1139.

JAKLEVIC R.C. and LAMBE J.; 1970. Phys.Rev. B **2**, 808.

JAKLEVIC R.C. and GAERTNER M.R.; 1978. Appl. Surf. Sci. **1**, 479.

JAKLEVIC R.C., ELIE L. and YAO H.C.; 1986. Surf. Sci. **171**, 279.

JENNINGS R.J. and MERRILL J.R.; 1972. J. Phys. Chem. Solids **33**, 1262.

KAUL M. and KAMFRATH G.; 1986. Thin Solid Films **137**, 293.

KIRTLEY J.R.; 1980. Vibrational Spectroscopy for Adsorbed Species (Edited by A. Bell et al), A.C.S. Symposium no. 137.

KLEIN J., LÉGER A., BELIN M., DEFOURNEAU D.and SANGSTER M.J.L.; 1973. Phys. Rev. B **7**, 2336.

KROEKER R.M., KASKA W.C. and HANSMA P.K.; 1980. J. Catal. **61**, 87.

LAMBE J. and JAKLEVIC R.C.; 1968. Phys. Rev. **165**, 821.

LANGAN J.D. and HANSMA P.K.; 1975. Surf. Sci. **52**, 211.

LÉGER A.; 1971. Ph.D. Thesis, Université de Paris, PARIS.

LÉGER A., KLEIN J., BELIN M. and DEFOURNEAU D.; 1972. Solid State Commun. **11**, 1331.

LEO V.; 1982. Rev. Sci. Inst. **53**, 997.

LEWIS D.M.; 1982. B.Sc. Project Report. The City University, LONDON.

LEWIS D.M.; 1985. Ph.D. Thesis, The City University, LONDON.

LEWIS D.M. and FIELD B.O.; 1985. Spectrochim. Acta **41A**, 477.

LEWIS D.M., SPENCER J.E.D. and FIELD B.O.; 1988. Spectrochim. Acta **44A**, 247.

LUTH H., ROLL U. and EWERT S.; 1978. Phys. Rev. B **18**, 4241.

MAGNO R. and ADLER J.G.; 1985. Prog. Surf. Sci. **18**, 278.

MALLIK R.R., PRITCHARD R.G. HORLEY C.C. and COMYN J.; 1985. Polymer **26**, 556.

MOLES P.J.; 1983. Polymers Paint Colour Journal, June 15.

MOLES P.J.; 1985. Polymers Paint Colour Journal, **175**, 447.

MONJUSHIRO H., MURATA K. and IKEDA S.; 1985. Bull. Chem. Soc. Jpn. **58**, 957.

MONTE S.J. and SUGERMAN G.;1982. Advances in Organic Coating and Technology Series (Proc. 6th Int. Conf. Coat. Sci. Technol.) Vol. 4, 267.

MONTE S.J. and SUGERMAN G.; 1983a. Polyurethane; New Pathways and Progress in Maket Technology (Proc. 6th Int. Tech. Mark. Comf., 131.

MONTE S.J. and SUGERMAN G.; 1983b. Elastomerics, July, 30.

MONTE S.J. and SUGERMAN G.; 1983c. Adhesion: Aspects of Polymer Coating (Edited by K.L. Mittal), Plenum Press, 421.

MONTE S.J. and SUGERMAN G.; 1984. Polym. Eng. Sci. **24**, 1369.

NAKAMOTO K.; 1986. Infrared and Raman Spectra of Inorganic and Coordination Compounds, 4th Edition, Wiley-Interscience.

NAYLER R.; 1982. Ph.D. Thesis, The City University, LONDON.

O'HAVER T.C. and GREEN G.L.; 1975. Am. Lab. **7**, 15.

PATTERSON W.R. and SHREWCHUN J.; 1964. Rev. Sci. Inst. **35**, 1704.

PHILLIPS W.A.; 1984. Physica **127B**, 112.

PLUEDDEMANN E.P.; 1981. Electrochem. Soc. Symposium on Coatings, 14 May, Minneapolis, USA.

PLUEDDEMANN E.P.; 1982. Silane Coupling Agents, Plenum Press, New York, p. 16.

POOLE C.P.; 1967. Electron Spin Resonance, Interscience N.Y., pp. 387, 775.

PURI D.M., PANDEY K.C. and MEHROTRA R.C.; 1962. J. Less Common Metals **4**, 393.

RATINEN H.; 1983. Rev. Sci. Inst. **54**, 697.

RATINEN H. and KIVIHARJU M.; 1989a. Spectrochim. Acta **45A**, 729.

RATINEN H. and KIVIHARJU M.; 1989b. Spectrochim. Acta **45A**, 163.

REYNOLDS S., OXLEY D.P. and PRITCHARD R.G.; 1982. Spectrochim. Acta **38A**, 103.

REYNOLDS S., PEASGOOD A., OXLEY D.P., PRITCHARD R.G., WALMSLEY D.G., TOMLIN J.L. and TURNER R.J.; 1987. J. Phys. C: Solid State Phys. **20**, 4297.

ROSEN M.R.; 1978. J. Coat. Technol. **50**, 70.

SCALAPINO D.J. and MARCUS S.M.; 1967. Phys. Rev. Lett. **18**, 459.

SCHRÖDINGER E.; 1926. Ann. Phys. **79**, 631.

SHOTT P.N. and FIELD B.O.; 1979. Spectrochim. Acta **35A**, 301.

SHOTT P.N. and FIELD B.O.; 1980. Spectrochim. Acta **36A**, 549.

SIMONSEN M.G. and COLEMAN R.V.; 1973a. Phys. Rev. B **8**, 5875.

SIMONSEN M.G. and COLEMAN R.V.; 1973b. Nature **244**, 218.

SIMONSEN M.G., COLEMAN, R.V. and HANSMA, P.K.; 1974. J. Chem. Phys. **61**, 3789.

SMITH D.C., PAN C.-Y. and NIELSEN J.R.; 1950. J. Chem. Phys. **18**, 706.

STERN M. and UHLIG H.H.; 1953. J. Electrochem. Soc., **100**, 543.

SUNG C.S.P., LEE S.H. and SUNG N.H.; 1980. Adhesion and Adsorption of Polymers (Edited by L.H. Lee), Plenum Press, New York, p.757.

SUNG N.H., NI S. and SUNG C.S.P.; 1980. Org. Coat. Plast. Chem. **42**, 379

SUNG N.H., KAUL A., NI S., SUNG C.S.P. and CHIN I.J.; 1981. 36th Annual Conference, Reinforced Plastics and Composites Institute. Feb. 16th, Session 2-B, 1.

SUNG N.H., KAUL A., NI S., SUNG C.S.P. and CHIN I.J.; 1983. Adhesion: Aspects of Polymer Coating (Edited by K.L. Mittal), Plenum Press, 379.

TEMPLETON M.K.; 1984. Ph.D. Thesis. Dis. Abstr. Int. B **45**, 1808.

THOMAS D.E. and POWELL J.M.; 1965. Rev. Sci. Inst. **36**, 1301.

VAN VELZEN N.T.; 1984. Surf. Sci. **146**, 319.

VENKATESWARLU P.; 1951. J. Chem. Phys. **19**, 293.

WALKER K.R; July 1986. Surf. Coat. Austrail., 14.

WALKER P.; 1987. Surface Coatings - 1 (Edited by A.D. Wilson et al.) Elsevier, 189.

WALMSLEY D.G., McNORRIS I.W.N. and TURNER W.E.; 1983. J. Phys. E. Sci. Instr. **16**, 1052.

WERRETT C.R., COMYN J., OXLEY D.P., PRITCHARD R.G., REYNOLDS S. and KINLOCH A.J.; 1986. Silanes, Surfaces and Interfaces (Edited by D.E. Leyden), Chem. Mod. Surf., 1, Gordon and Breach, 305.

WHITE H.W., GODWIN L.M. and WOLFRAM T.; 1978. J. Adhes. 9, 237.

WHITE H.W., GODWIN L.M. and WOLFRAM T.; 1981. J. Adhes. **13**, 177.

WILLIAMS S.D.; 1984. Diss. Abstr. Int. B **44**, 3424.

WILLIAMS D.H. and FLEMING I.; 1980. Spectroscopic Methods in Organic Chemistry, 3rd. Edition, McGraw Hill.

WOLFRAM T. (Editor); 1978. Inelastic Electron Tunnelling Specroscopy, Springer-Verlag (New York), 34.

WOODRUFF D.P. and DELCHAR T.A.; 1986. Modern Techniques of Surface Science., (Edited by R.W. Cahn, E.A. Davis and I.M. Ward) Cambridge University Press.

ZIETLOW J.P., CLEVELAND F.F. and MEISTER A.G.; 1950. J. Chem. Phys. **18**, 1076.

APPENDIX A - AN IETS STUDY OF POTENTIAL SURFACE CONTAMINANTS AND THE ORIGIN OF LIFE.

A.1 INTRODUCTION.

The results considered in the main body of this work concern the molecular bonding of coupling agents and other species to a super-clean alumina surface. In industrial situations this is an ideal unlikely to be achieved. It is therefore important to consider the possible modification of these surface interactions by atmospheric contaminants. We have considered a series of such contaminants which incidentally has provided the first experimental support for the mineralogical theory of the origin of life.

The origin of life has been a central intellectual problem for Man since records began. The traditional religious teachings have from time to time been challenged, but have throughout tended to dominate this field of thought. Genesis informs us that God said "Let the earth bring forth the living creature after His kind. And it was so". Most religions have a variant on this creationalist theme which in turn gives rise to the theory of Spontaneous Generation. This is defined by John Farley [1977] "as the belief that some living entities may arise suddenly from matter independently of any parents". This theory is well established in classical writings, but in the 17th century an Italian physician - Francesco Redi [Farley, 1977] - was amongst the first to provide cause for doubt by demonstrating that meat, not exposed to the air, did not develop maggots. In 1862, Louis Pasteur won a prize from the French Academy of Sciences for developing this idea and for demonstrating that the supposed cases of spontaneous generation were due to contamination of broths by microorganisms in the air. However, the theory of spontaneous generation is not totally dead even today. Nobel prizewinner George Wald [1979] has written "we are here as a result, I believe, of spontaneous generation". Hoyle and Wickramasinghe [1978] have calculated the chance of obtaining an enzyme spontaneously as "only" 1 in 10^{20}.

In the 1920s Oparin and Haldane independently developed similar schemes for the origin of life as follows [Oparin, 1964]:-

(i) The earth, when life began, had an oxygen-free, reducing atmosphere containing methane, ammonia, hydrogen and water.

(ii) This atmosphere, exposed to a variety of energy sources such as lightening, solar radiation or volcanic heat, produced organic molecules.

(iii) These organic molecules gradually accumulated in the primitive oceans to produce a hot, dilute "soup".

(iv) By further transformation, life developed in this soup.

Miller and Urey in 1952 performed a classical experiment [Miller, 1953] [Miller and Orgel, 1974] to test the validity of the Oparin-Haldane hypothesis. This exposed various mixtures of methane, ammonia, hydrogen and water to a spark discharge and showed that carboxylic and amino acids were present amongst the reaction products (see Figure A.1.1). This experiment has had a dominating effect on contemporary thought regarding the origin of life, particularly amongst organic chemists who predominate in this field. This is now somewhat surprising since the Miller - Urey hypothesis has many drawbacks as a valid model for the origin of life. Namely,

(i) Geochemists are now confident that a reducing atmosphere on the primitive earth would be destroyed by solar radiation within a thousand years - too quickly for life to have originated in this way. Current composition estimates of the prebiotic atmosphere are that NH_3, H_2O and CO_2 were the principal constituents. It is not possible to produce amino acids from these constituents by the Miller - Urey experimental method without at least 1% hydrogen present.

(ii) The major reaction products from the original Miller - Urey experiment are 4% formic acid, 2.1% glycine and only minute traces of other amino acids.

(iii) The Miller - Urey experiment has no stereospecific selectivity.

(iv) The problem of molecular condensation reactions of small molecules in a dilute aqueous medium has not been adequately considered [Cairns-Smith, 1982].

A variant on the spontaneous generation theory is the "Extra-Terrestrial Origin of Life" theory. The principal exponents of this view are Sir Fred. Hoyle and Wickramasinghe [1978]. Carbonaceous chondritic meteorites have been found to contain small amounts of amino acids and carboxylic acids among polymeric tars in the interstices of these meteorites. The origin of these organic molecules is highly controversial at present. Hoyle and Wickramasinghe have also suggested that epidemics on earth are due to new viral strains invading our environment contained in meteorites or on interstellar dust particles.

Carl Sagan, in his television series "Cosmos", equated the origin of life with the formation of the first self-copying molecule. The most important self-copying biological molecule known today is the DNA molecule carrier of the genetic code. It is highly unlikely that a molecule as structurally complex as DNA was the original self-replicating molecule so this progenitor must be found elsewhere.

J.D. Bernal [1951] proposed that the origin of molecular asymmetry in important biological molecules was due to their original synthesis on a mineral surface which acts as a template. Graham Cairns-Smith [1982] has developed this concept in some detail and proposes that the original self-replicating system was the growth of naturally occurring minerals. The stimulus for the present work was to provide experimental evaluation of the Bernal - Cairns-Smith hypothesis. The modern mineralogical origin of life may form a fitting link to the earliest of concepts described in Genesis 2: 6-7...

> "But there went up a mist from the earth and watered the whole face of the ground. And the Lord God formed Man of the dust of the ground and breathed into his nostrils the breath of life, and Man became a living soul."

In this chapter we describe reactions taking place on an alumina surface incorporated into an Al-AlO_x-Pb tunnel junction. This alumina surface represents a chemically clean equivalent to the naturally occurring mineral proposed by Bernal and Cairns-Smith.

Figure A.1.1. The Apparatus Designed by S. Miller for the "Spark Chamber" Experiments.

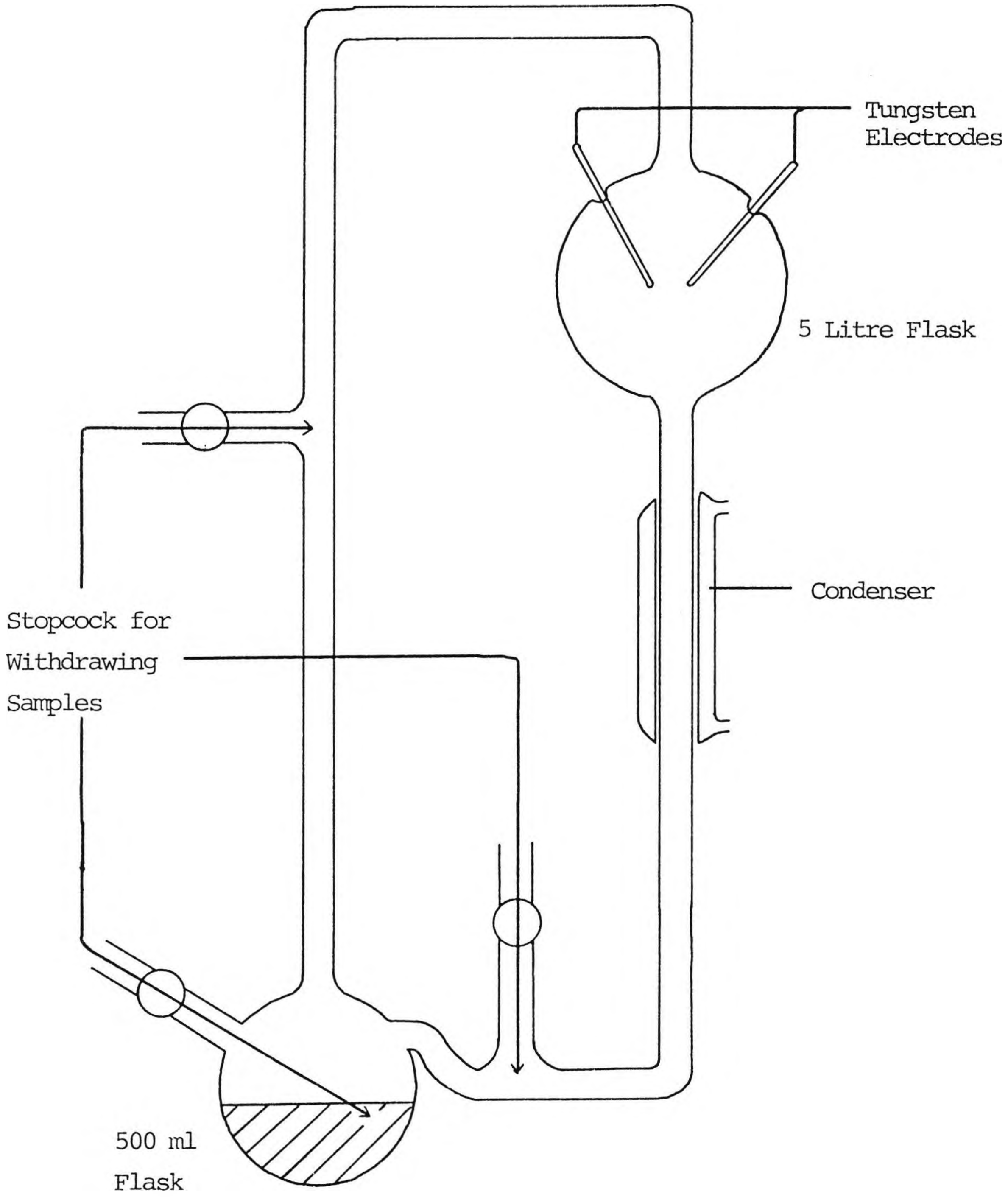

A.2 AMINO ACID PRODUCTION FROM PREBIOTIC GASES.

A.2.1 Aqueous Ammonia Doped Tunnel Junctions.

Ammonia vapour was incorporated into an Al-AlO_x-Pb junction by exposing the alumina surface of an uncompleted junction to a stream of wet ammonia gas under atmospheric conditions for 15 seconds at 298K. The junction was then completed by the deposition of the upper lead electrode. The junction resistance was found to be very large at 10 kΩ. The electrode strip resistances were of negligible value. The spectrometer operating conditions were as follows:

Sensitivity	0.1	µV
Modulation Voltage	10	mV
Time Constant	3	secs.
Scan Time	30	mins.

Table A.2.1 indicates the assignment of the peaks produced in the spectrum of NH_3, CO_2 and H_2O, Figure A.2.1.

Figure A.2.1. IET Spectrum of Vapour Doped Wet Ammonia Gas.

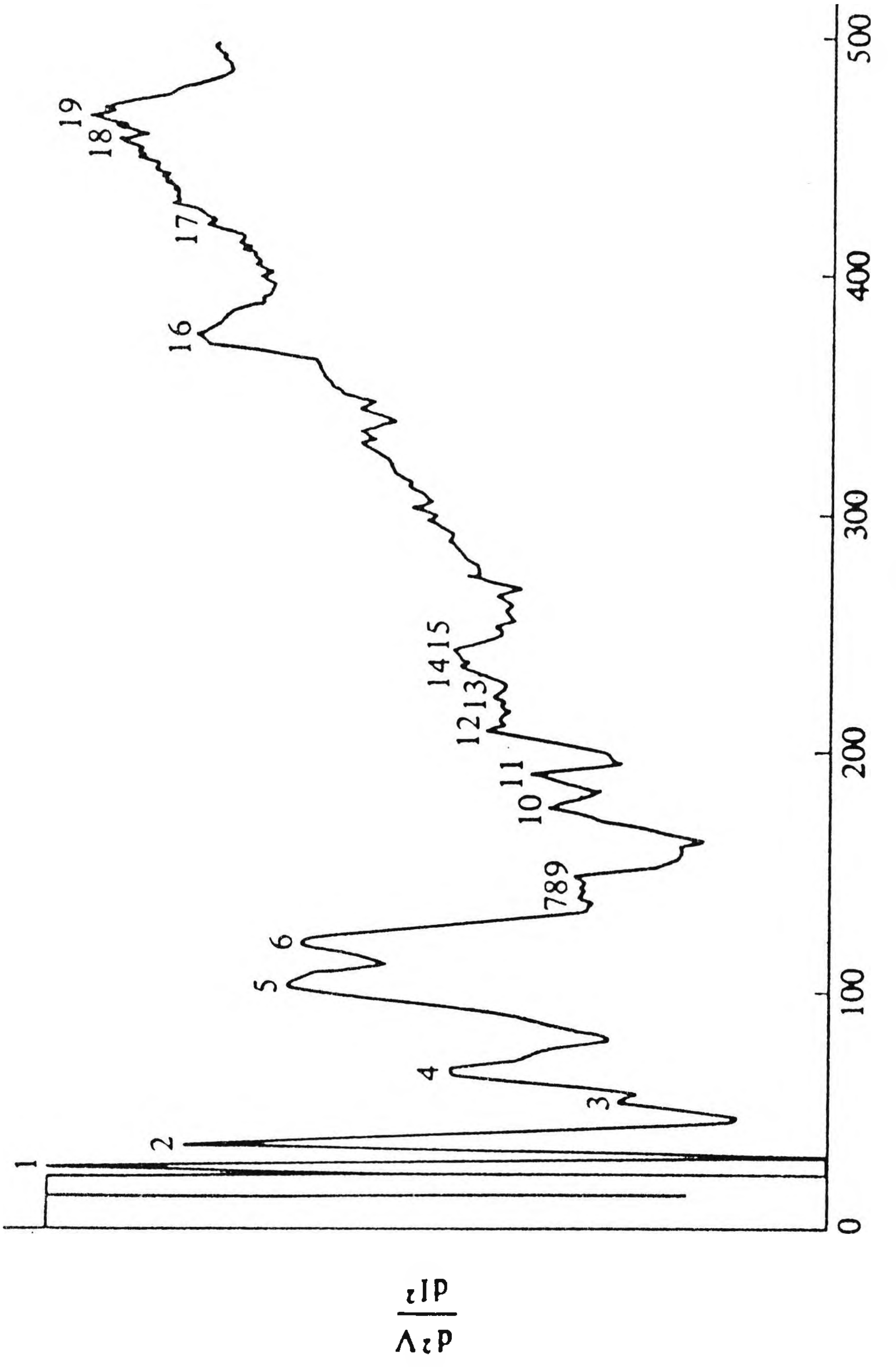

Table A.2.1 Spectral Assignment of the Vapour Doped Wet Ammonia Gas.

Peak No.	Energy (meV)	Wave No. (cm^{-1})	Intens.	Assignment
1	27.8	224	S	AlO_x Phonon
2	36.3	293	S	AlO_x Phonon
3	54.3	438	W	CO_2^- rock
4	66.5	536	M	NH_3^+ tort.
5	102.0	823	S	C-C str.
6	120.6	973	S	C-N str./ Al-O str.
7	139.4	1124	W	NH_3^+ rock
8	143.0	1153	W	NH_3^+ def.
9	147.9	1193	W	C-O str.
10	177.1	1428	M/W	C-H def./ CO_2^- str
11	190.7	1538	M/W	CO_2^- str./ CH_2 scissor
12	209.3	1688	W	N-H def.
13	223.6	1803	W	
14	235.7	1901	M/W	
15	242.9	1959	M/W	
16	375.0	3024	M	C-H str.
17	421.5	3399	W	N-H str.
18	461.4	3721	W	O-H str.
19	469.3	3785	W	O-H str.

S=Strong, M=Medium and W=Weak Intensities.

$1meV \equiv 8.065\ cm^{-1}$

In order to assess the importance of atmospheric CO_2 in the formation of amino acid like species on the alumina surface from aqueous ammonia, a completed Al-AlO_x-Pb tunnelling junction was penetration doped with a suspension of CaO in aqueous ammonia by introducing a drop of this suspension onto the top of the lead electrode. Monitoring the resistance of the junction allowed termination of the doping at a suitable value. The calcium oxide is expected to prevent atmospheric CO_2 from reaching the alumina surface by preferentially reacting to produce insoluble calcium carbonate. Both before and after this doping procedure the exposure of the completed junction to atmospheric CO_2 was minimised. Again the junction resistance was found to be very large at 10 kΩ. The spectrometer operating conditions were as follows.

Sensitivity	0.1	µV
Modulation Voltage	10	mV
Time Constant	3	secs.
Scan Time	30	mins.

Figure A.2.2 shows the spectrum produced. Table A.2.2 indicates the spectral assignment of the IET spectrum of aqueous ammonia over CaO (Figure A.2.2).

Figure A.2.2. IET Spectrum of Penetration Doped Aqueous Ammonia over CaO.

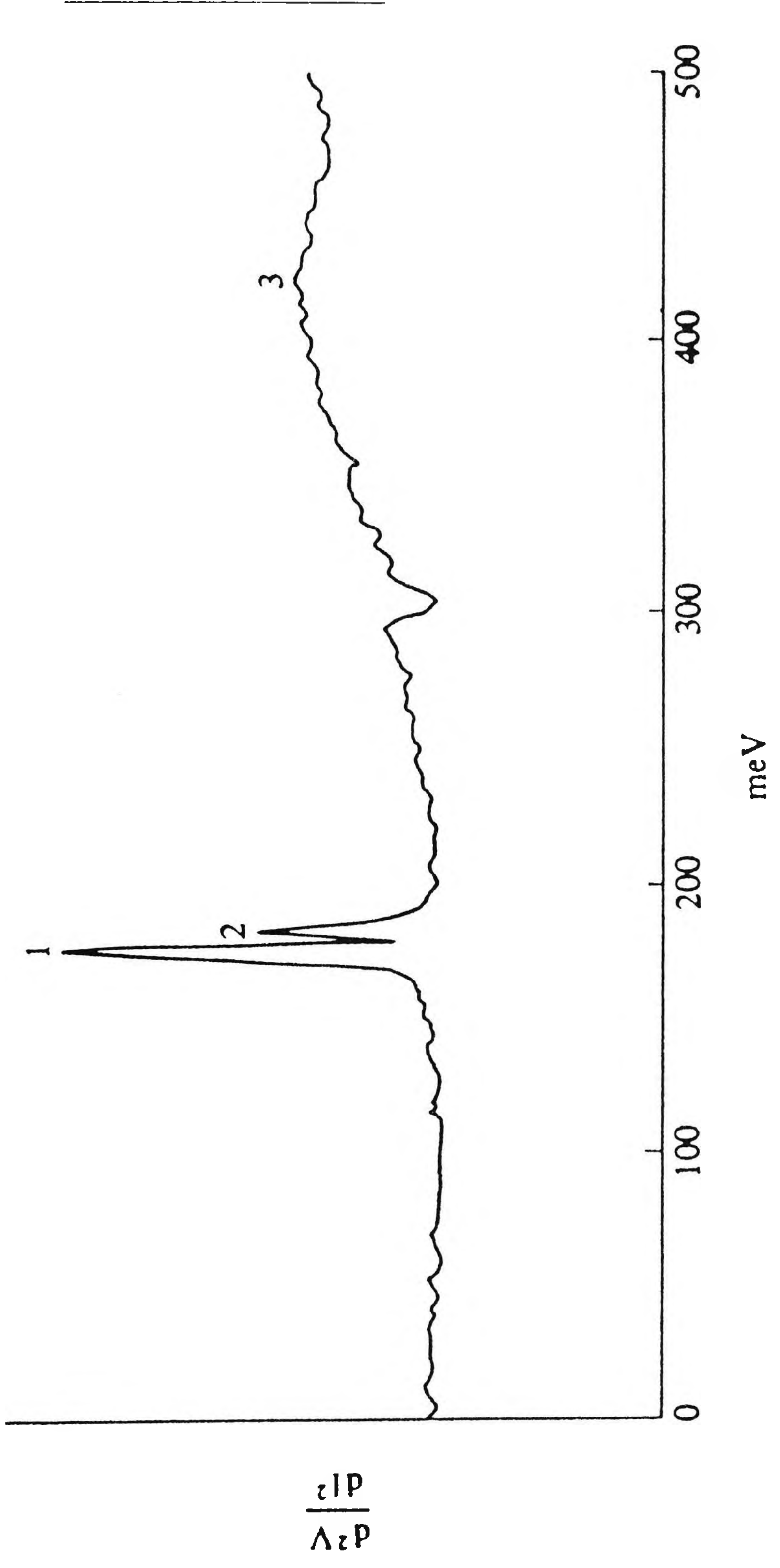

Table A.2.2. Spectral Assignment of Penetration Doped Aqueous Ammonia over CaO.

Peak No.	Energy (meV)	Wave No. (cm^{-1})	Intens.	Assignment
1	175.9	1419	S	
2	183.9	1483	M	NH_4^+ def.
3	396.8	3200	W/Br	O-H str.

S=Strong, M=Medium, Br=Broad and W=Weak Intensities.

1meV ≡ 8.065 cm^{-1}

A.2.2 A Glycine Doped Tunnel Junction.

An Al-AlO$_x$-Pb junction spin doped with a saturated solution of glycine in methanol. The solution was allowed to stand for 20 seconds on the alumina surface (contact time 20 secs.) at 298K before being spun off and the lead electrode deposited. It was confirmed that methanol alone did not dope the alumina surface under these conditions. The junction resistance was found to be 130Ω. The spectrometer operating conditions were as follows.

Sensitivity	0.2	μV
Modulation Voltage	6	mV
Time Constant	3	secs.
Scan Time	30	mins.

Figure A.2.3 shows the IET spectrum of the junction spin doped with a saturated solution of glycine in methanol. Table A.2.3 shows the peak assignment of the IET spectrum in Figure A.2.3.

Figure A.2.3. IET Spectrum of a Saturated Solution of Glycine in Methanol.

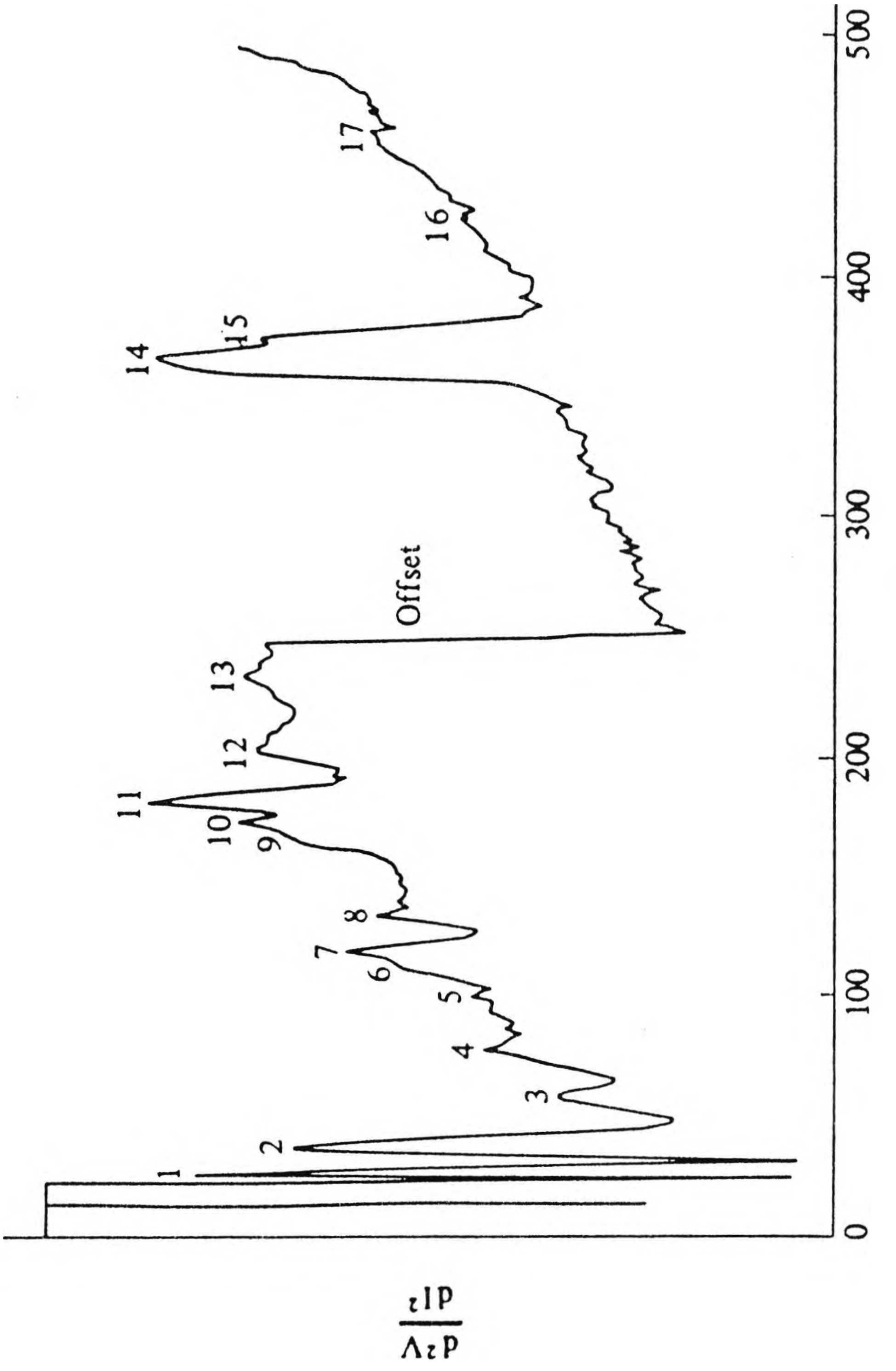

Table A.2.3. Spectral Assignment of Saturated Solution of Glycine in Methanol.

Peak No.	Energy (meV)	Wave No. (cm^{-1})	Intens.	Assignment
1	26.3	212	S	AlO_x Phonon
2	39.1	315	S	AlO_x Phonon/ -CCN bend
3	58.9	475	M/W	CO_2^- rock
4	78.1	630	M	CO_2^- def.
5	102.3	825	W	C-C str.
6	115.8	934	M/W	C-C str.
7	120.8	974	M	C-N a. str./ Al-O str.
8	136.4	1100	M/W	NH_3^+ rock
9	169.0	1363	W/Sh	CO_2^- str./ C-H def.
10	176.8	1426	M/W	C-H def./ CO_2^- str
11	184.6	1489	M	CO_2^- str./ CH_2 def.
12	206.0	1661	M/W	NH_3^+ def.
13	237.2	1913	M/W	
14	367.9	2967	S	C-H str.
15	376.4	3036	M	C-H str.
16	425.4	3431	W	N-H str.
17	448.1	3614	W	O-H str.

S=Strong, M=Medium, W=Weak and Sh=Shoulder Intensities.

$1meV \equiv 8.065\ cm^{-1}$

A.2.3 Discussion of Results from Amino Acid Doped Tunnel Junctions.

Figure A.2.1 shows the tunnelling spectrum of vapour doped ammonia in laboratory air. This spectrum has also been compared to the infrared study of glycine by Suzuki et al. [1963]. The comparison indicates that the ammonia is adsorbed on the alumina surface as a glycine like molecule. All the important vibrational modes present in the infrared spectrum of glycine are seen in the tunnelling spectrum of this ammonia doped junction. Various modes attributed to $-COO^-$ and $-NH_3^+$ ions in the infrared study are present in the tunnelling spectrum. Both the COO^- asymmetric and symmetric modes at 1538 cm^{-1} and 1428 cm^{-1} respectively are consistent with the infrared study as are the NH_3^+ deformation mode at 1688 cm^{-1} and the NH_3^+ rocking mode 1124 cm^{-1}.

A C-N asymmetric stretching mode is identified in the infrared spectrum of glycine at 1034 cm^{-1}, this is also present in the tunnelling spectrum at 973 cm^{-1}. The reduction in the strength of this bond is due to the interaction of the NH_3^+ ion with the alumina surface thus producing a deformation from the normal glycine structure. The CH_2 rocking mode and C-C stretching mode give rise to peaks in the region 880-930 cm^{-1} in the infrared study, but this region is difficult to assign in the tunnelling spectrum due to a contribution from aluminium oxide vibrational modes. At the lower energy end of the spectrum

COO^- deformation modes can be observed consistent with those in the infrared study.

In Table A.2.4 the assignments of the tunnelling spectrum of atmospherically doped ammonia is compared with that of glycine; the similarity between the two can easily be seen. Comparison of the energies of the vibrational modes of the two molecules on the alumina surface show close agreement. This coupled with the infrared study strongly suggests that the ammonia is adsorbed on the alumina surface as a "glycine-like" molecule. As a glycine like molecule has been identified on the alumina surface from an atmospherically doped junction, it would seem likely that atmospheric carbon dioxide plays a similar role in the formation of this "glycine like" species as it does in that of formic acid from water [Field et al., 1985]. The only peaks present in the spectrum of wet ammonia in the absence of atmospheric carbon dioxide are a broad peak at 3200 cm^{-1}, AlO-H stretching modes, and a NH_4^+ deformation peak at 1483 cm^{-1}. This may be compared with a tunnelling spectrum of ammonia doped "in situ" in the junction preparation chamber in the absence of CO_2 and H_2O [Shklyarevskii et al., 1978] (see Figure A.2.4) where only the expected N-H vibrational modes are observed. In our study, no peaks due to "glycine" are observed since the carbon dioxide reacts with the calcium hydroxide to give calcium carbonate in preference to reaction with the ammonia on the surface to give glycine. The N-H stretching modes prominent in the anhydrous ammonia spectra are greatly reduced in the aqueous system where they appear as NH_4^+ and are deformed due to surface interaction with the tunnelling barrier. Presumably no calcium carbonate modes are observed in the spectrum because the high vapour pressure of the ammonia enables it to preferentially occupy all the active sites on the alumina.

The spectra produced from the wet ammonia and from the glycine doped tunnel junctions support the assertion that a glycine-like molecule is indeed produced by a reaction involving atmospheric carbon dioxide and aqueous ammonia vapour on the alumina surface.

The tunnelling spectrum of spin doped glycine in methanol is shown in Figure A.2.3. The spectrum has been compared with results of an infrared study of glycine by Suzuki et al. [1963] and the IET spectra of Simonsen et al. [1974] and Magno and Adler [1985].

Amino acids in solution exist almost entirely as dipolar ions. Various modes can be assigned to the $-COO^-$ (carboxylate ion) and the $-NH_3^+$ ion in the infrared analysis. These modes can be seen in the tunnelling spectrum, a COO^- stretching mode and a NH_3^+ deformation mode occur near 1600 cm^{-1}.

Table A.2.4. A Comparison of the IET Spectra of Glycine in Methanol (Figure A.2.3) and the $NH_3/CO_2/H_2O$ Doped Tunnel Junction (Figure A.2.1).

Spectral Wavenumbers cm^{-1}

Glycine Soln.	$NH_3/CO_2/H_2O$	Possible Assignments
212	224	Transverse AlO_x Phonon
315	294	Longitudinal AlO_x Phonon
	438	CO_2^- rock
475		CO_2^- rock
	536	C-O wag
630		NH_2 torsion
825	823	C-C stretch
934		
974	973	C-N str. / Al-O stretch
1100	1123	C-O stretch
	1153	NH_3^+ deformation
1362		CO_2^- symmetrical stretch
1426	1428	CO_2^- asym. str. / C-H def.
1489		NH_3^+ deformation
	1538	$>CH_2$ deformation
1661		
1913	1901	
	1959	
2967		C-H unperturbed stretch
3036	3025	C-H stretch
3431	3399	N-H stretch
3614	3721	O-H stretch

1 meV ≡ 8.065 cm^{-1}

Figure A.2.4. IET Spectrum of an AlO_x-Pb Tunnel Junction Doped "in situ" with Ammonia Vapour [Shklyarevskii et al., 1978].

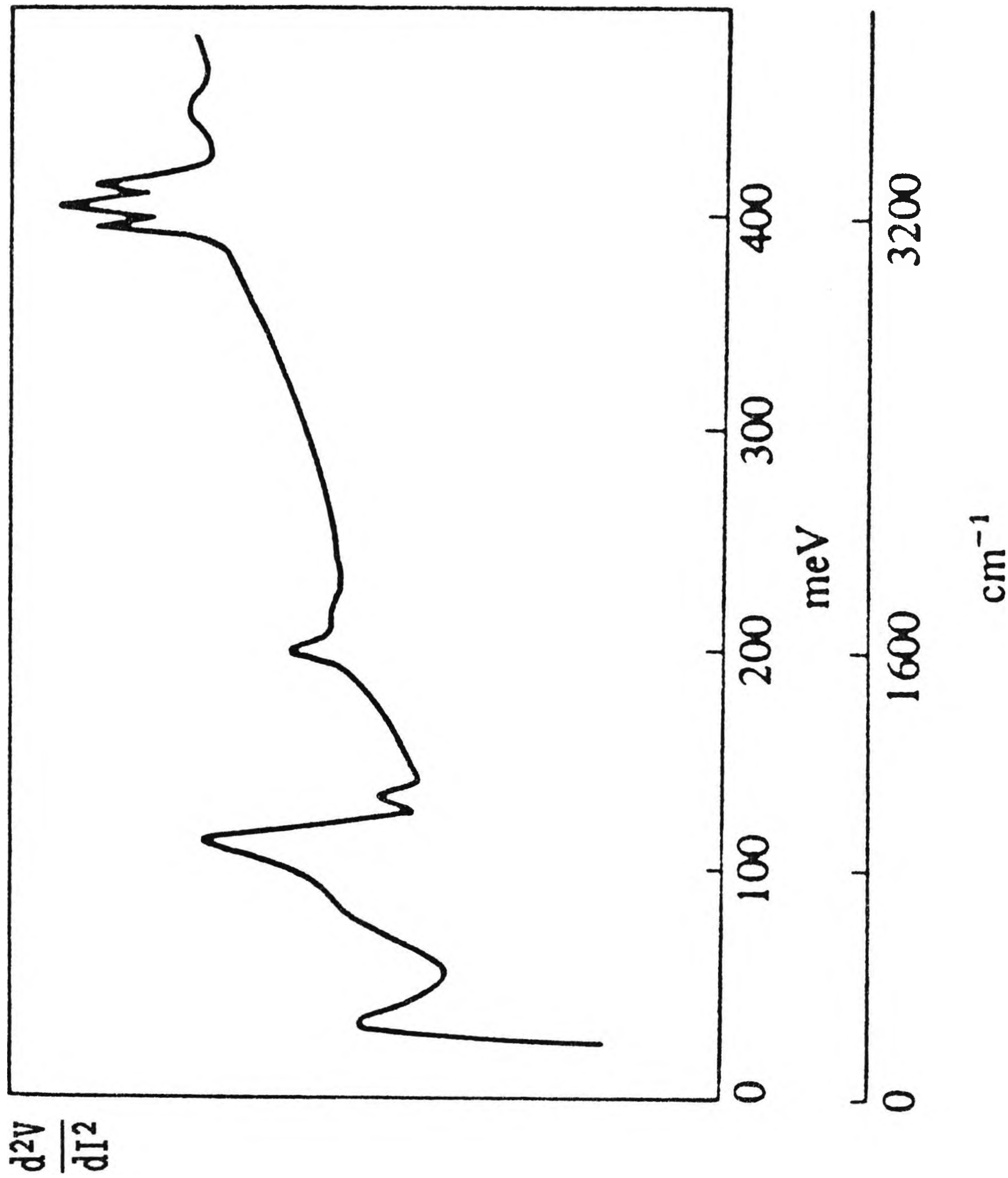

The region from 1300-1500 cm^{-1} is dominated by CH_2 bending modes, although a NH_3^+ deformation could contribute in this region. However this must be weak for glycine since deuteration of the NH_3^+ group by Suzuki et al. shows no shift of the infrared modes in this region. Other modes present in the tunnelling spectrum are a COO^- symmetric stretch at 1363 cm^{-1} and a NH_3^+ rocking mode at 1100 cm^{-1}, both of these modes correspond to peaks in the infrared spectrum.

The probable orientation of the glycine molecule on the alumina surface is shown in Figure A.2.5. The molecule is considered to be adsorbed on the surface through both the carboxylate ion and the NH_3^+ ion.

Figure A.2.5. The Proposed Surface Orientation of Glycine.

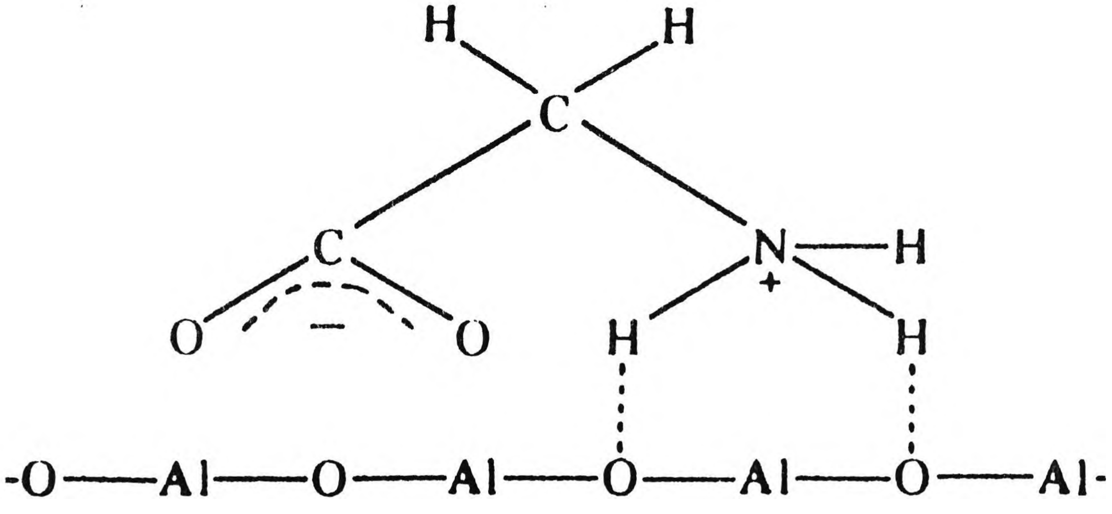

A.3 SUGAR PRODUCTION FROM SIMPLE MOLECULES.

The production of sugars from formaldehyde in the presence of alkaline catalyst (the formose reaction) is well known. Gabel and Ponnamperuma [1967] have shown that alumina can be used to catalyse this reaction.

A.3.1 Aqueous Formaldehyde Doped Tunnel Junctions.

An Al-AlO$_x$-Pb tunnel junction was infusion doped by exposing the completed junction, in a sealed glass vessel, to aqueous formaldehyde vapour. The resistance of the junction was monitored and doping terminated at a suitable value. The junction resistance was 250Ω when removed from the doping chamber. The spectrometer operating conditions were as follows.

Sensitivity	0.2	µV
Modulation Voltage	4	mV
Time Constant	1	secs.
Scan Time	15	mins.

Figure A.3.1 shows the resulting IET spectrum of infusion doped formaldehyde. Table A.3.1 indicates the assignment of the peaks produced in Figure A.3.1.

Figure A.3.1. IET Spectrum of Infusion Doped Formaldehyde.

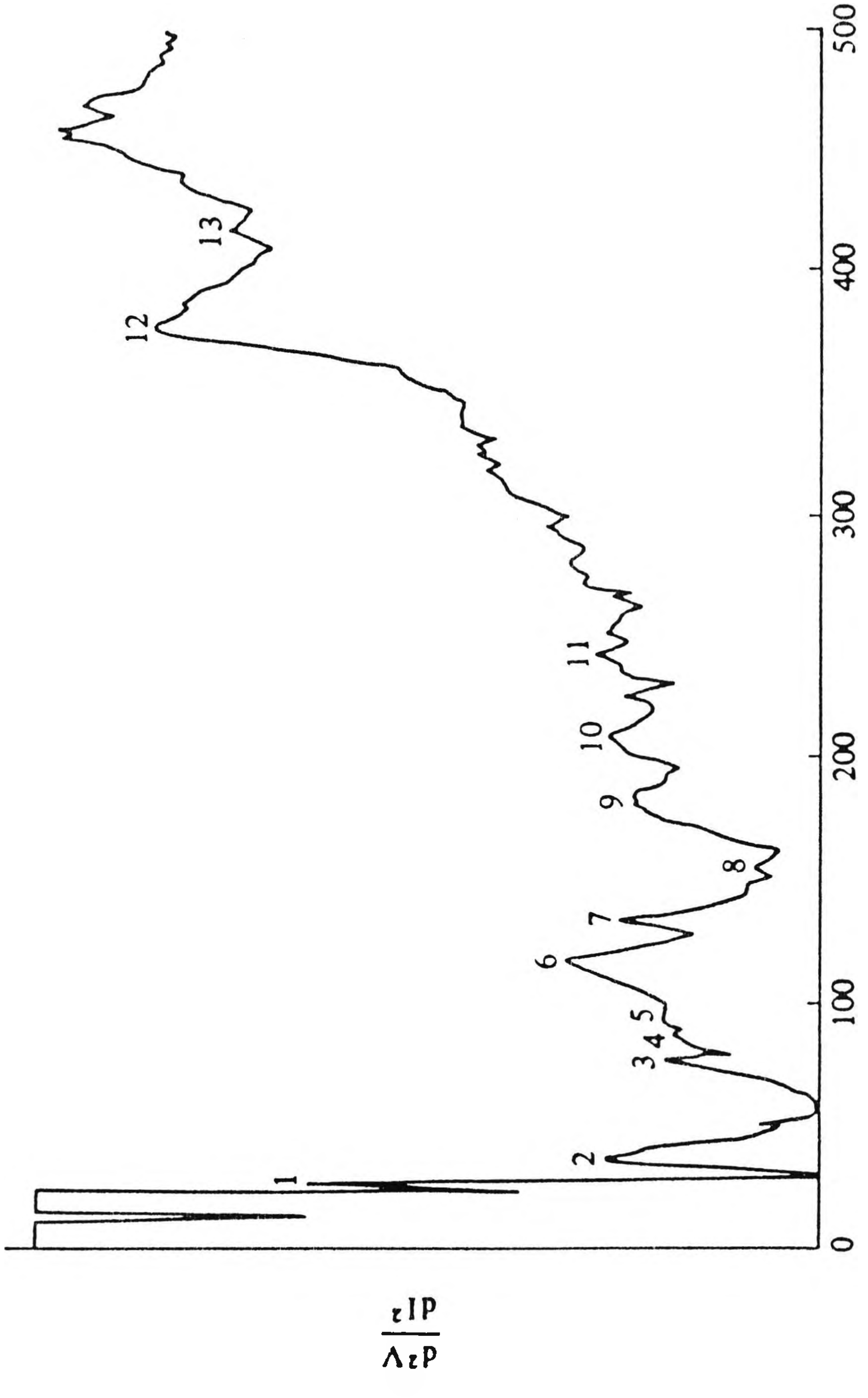

Table A.3.1. Spectral Assignment of Infusion Doped Aqueous Formaldehyde.

Peak No.	Energy (meV)	Wave No. (cm^{-1})	Intens.	Assignment
1	26.5	214	S	AlO_x Phonon
2	39.2	316	M	AlO_x Phonon
3	79.7	643	M/W	C-O-H twist
4	89.0	718	W	CH_2 rock
5	93.5	756	W	
6	119.7	965	M	Al-O str.
7	137.1	1106	M/W	C-O str./ C-O def.
8	159.6	1287	W	
9	186.9	1507	M/W	CH_2 def.
10	212.8	1716	M/W	
11	240.7	1941	M/W	
12	377.6	3045	M	C-H str.
13	411.5	3319	W	

S=Strong, M=Medium and W=Weak Intensities.

1meV ≡ 8.065 cm^{-1}

After recording the spectrum shown in Figure A.3.1 the junction was removed from the liquid helium Dewar and immediately exposed to wet ammonia vapour for 20 seconds at 298K before returning it to the liquid helium Dewar. This was carried out in order to investigate any potential reaction between the surface adsorbed species with ammonia. Figure A.3.2 shows the IET spectrum of the junction used to produce Figure A.3.1 after exposure to ammonia vapour. The junction resistance did not change from the value for the initial infusion doped junction (J_R = 250Ω). The spectrometer operating conditions were as follows.

Sensitivity	0.5	µV
Modulation Voltage	4	mV
Time Constant	1	secs.
Scan Time	15	mins.

The IET spectrum of infusion doped formaldehyde exposed to ammonia vapour (Figure A.3.2) is assigned in Table A.3.2.

Figure A.3.2. IET Spectrum of Infusion Doped Formaldehyde Exposed to Aqueous Ammonia Vapour.

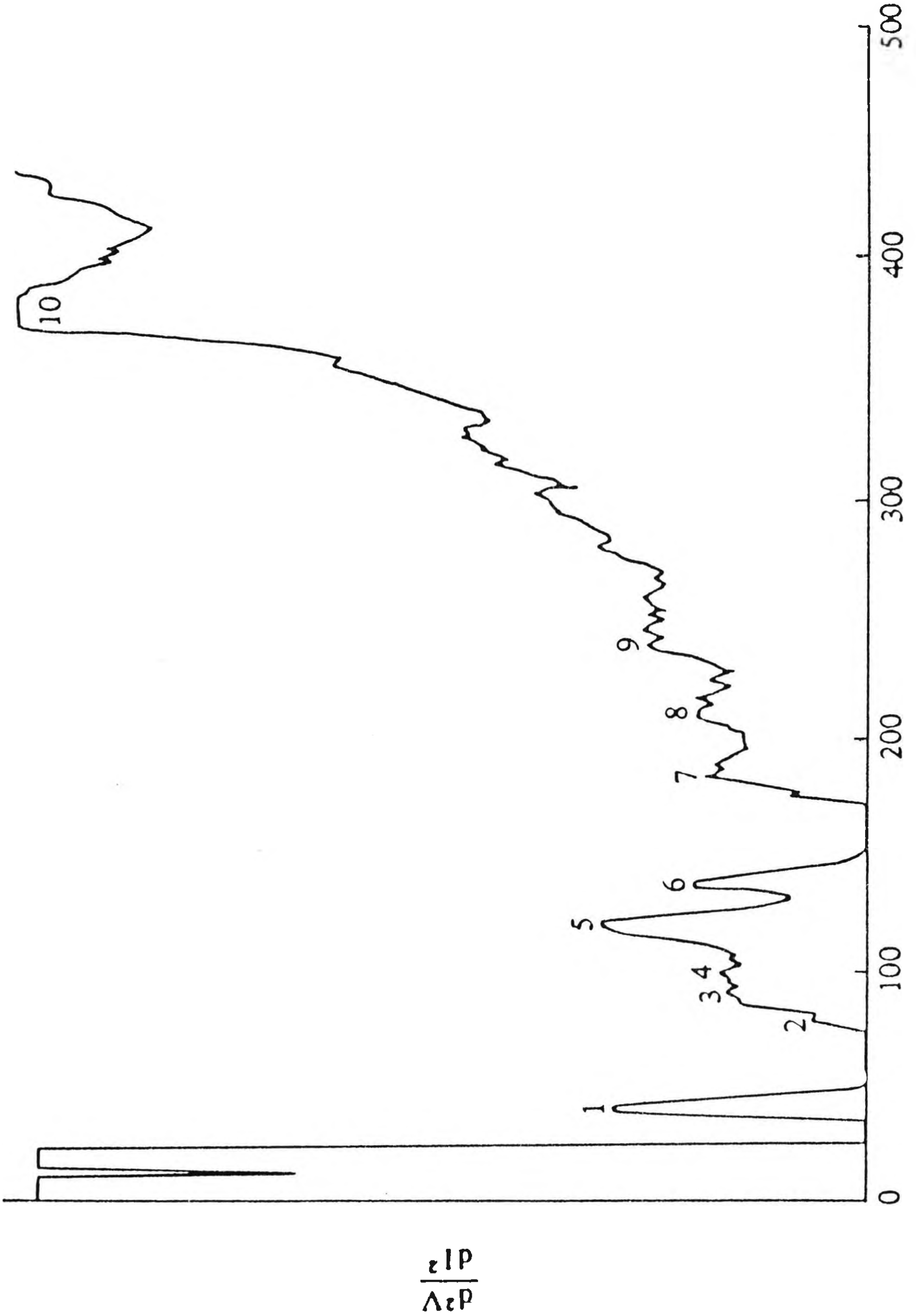

Table A.3.2. Assignment of IET Spectrum of Infusion Doped Aqueous Formaldehyde and Exposed to Aqueous Ammonia Vapour.

Peak No.	Energy (meV)	Wave No. (cm^{-1})	Intens.	Assignment
1	41.9	338	M	AlO_x Phonon
2	77.9	627	W	C-O-H twist
3	90.4	729	W	CH_2 rock
4	99.7	804	W	
5	122.4	987	M	Al-O str.
6	138.3	1115	M/W	C-O str./ C-O def.
7	184.7	1490	M/W	C-H def.
8	214.0	1726	M/W	
9	238.8	1926	M/W	
10	378.9	3056	M	C-H str.

M=Medium and W=Weak Intensities.

1meV ≡ 8.065 cm^{-1}

A.3.2 Carbon Monoxide Doped Tunnel Junctions.

Carbon dioxide and water have previously been introduced onto the alumina surface of a tunnel junction and reactions noted [Field et al., 1985]. On this occasion a completed Al-AlO_x-Pb tunnel junction was infusion doped with wet carbon monoxide gas in a sealed vessel at atmospheric pressure and room temperature for 15 hours. The junction resistance was low at 45Ω. The spectrometer operating conditions were as follows:

Sensitivity	0.2	µV
Modulation Voltage	6	mV
Time Constant	3	secs.
Scan Time	30	mins.

Figure A.3.3 shows the resulting IET spectrum produced by infusion doped with wet CO gas and the spectral assignment is indicated in Table A.3.3.

Figure A.3.3. IET Spectrum of Infusion Doped Carbon Monoxide Gas.

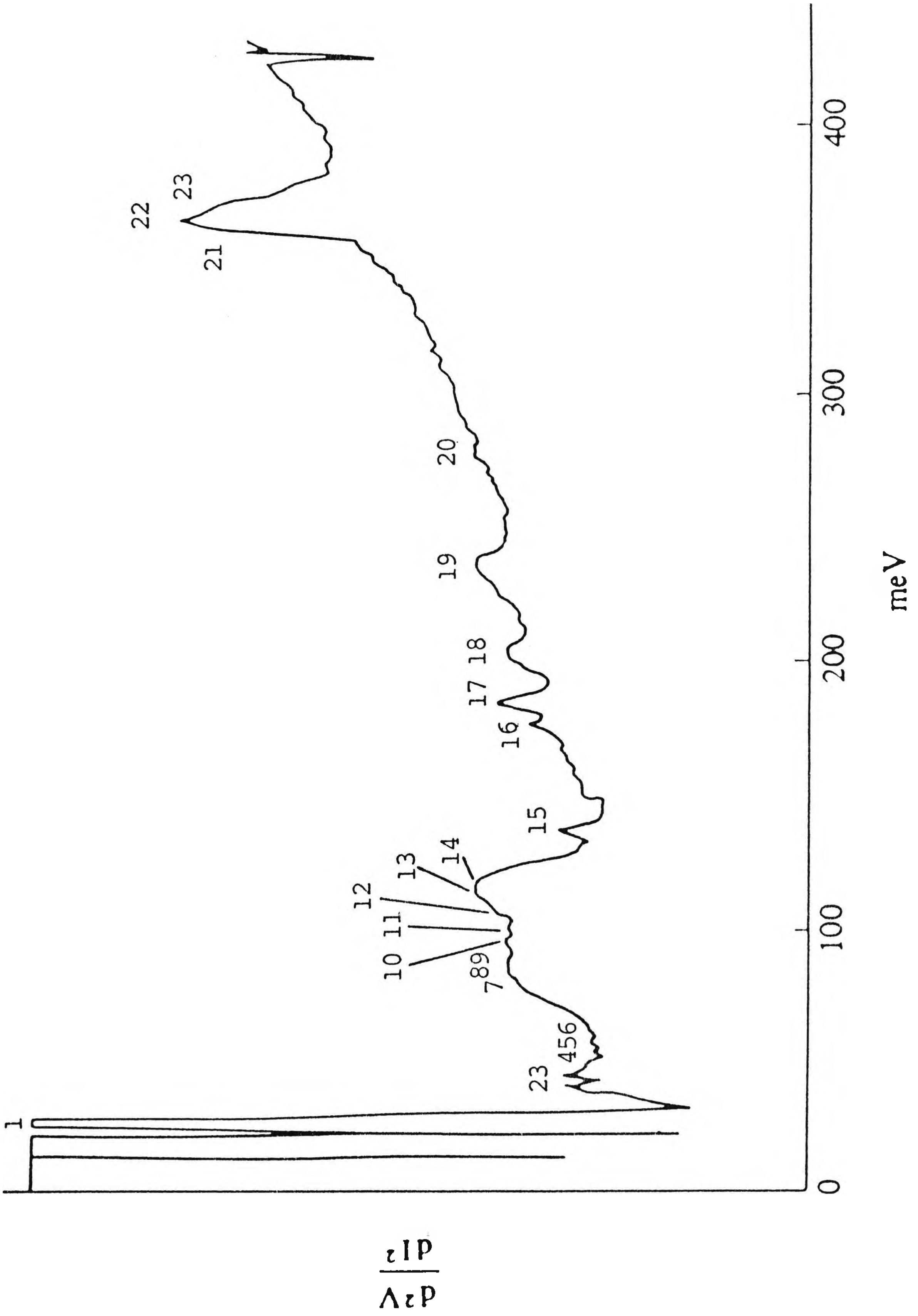

Table A.3.3. Spectral Assignment of Infusion Doped CO Gas.

Peak No.	Energy (meV)	Wave No. (cm^{-1})	Intens.	Assignment
1	26.3	212	VS	Al Phonon
2	41.2	332	S	Al Phonon
3	44.1	356	M	Al-C≡O
4	48.2	389	W	Al-C≡O
5	53.1	428	W	Al-C≡O
6	58.5	472	W	
7	77.7	627	W	ring modes
8	81.5	657	W	ring modes
9	88.0	710	W	C-H def.
10	94.1	759	W	as Fig.A.3.1
11	98.7	796	W	C-C str.
12	103.5	835	W	C-C str.
13	111.5	899	W	C-C str.
14	116.7	941	M/Br	Al-O str.
15	133.8	1079	M	C-O str.
16	173.7	1401	M/W	C-H def.
17	178.3	1458	M	C-H def.
18	201.0	1621	M/Br	C≡O (2 Coord.)
19	235.0	1895	M/Br	C≡O (4 Coord.)
20	265.8	2174	W	C≡O linear
21	357.5	2883	M/Sh	C-H str.
22	361.8	2918	S	C-H str.
23	366.6	2957	M/Sh	C-H str.

S=Strong, M=Medium, W=Weak, Br=Broad and Sh=Shoulder Intensities.

1meV ≡ 8.065 cm^{-1}

A.3.3 D (-) Fructose Doped Tunnel Junctions.

To aid the assignment of the aqueous formaldehyde surface species as a carbohydrate, the tunnelling spectrum of D(-) fructose in ethanol was investigated. A saturated solution was spin doped onto the alumina surface which was then incorporated into an Al-AlO$_x$-Pb junction. The junction resistance was again found to be quite low at 40Ω. The spectrometer operating conditions were as follows.

Sensitivity	0.2	μV
Modulation Voltage	6	mV
Time Constant	3	secs.
Scan Time	30	mins.

Figure A.3.4 illustrates the resulting IET spectrum and Table A.3.4 indicates the assignment of the peaks produced in Figure A.3.4. It has been confirmed by the author and by previous studies [Lewis, 1985] that ethanol alone did not dope under the conditions used in the above experiment.

Figure A.3.4. IET Spectrum of a Saturated Solution of D(-) Fructose in Ethanol.

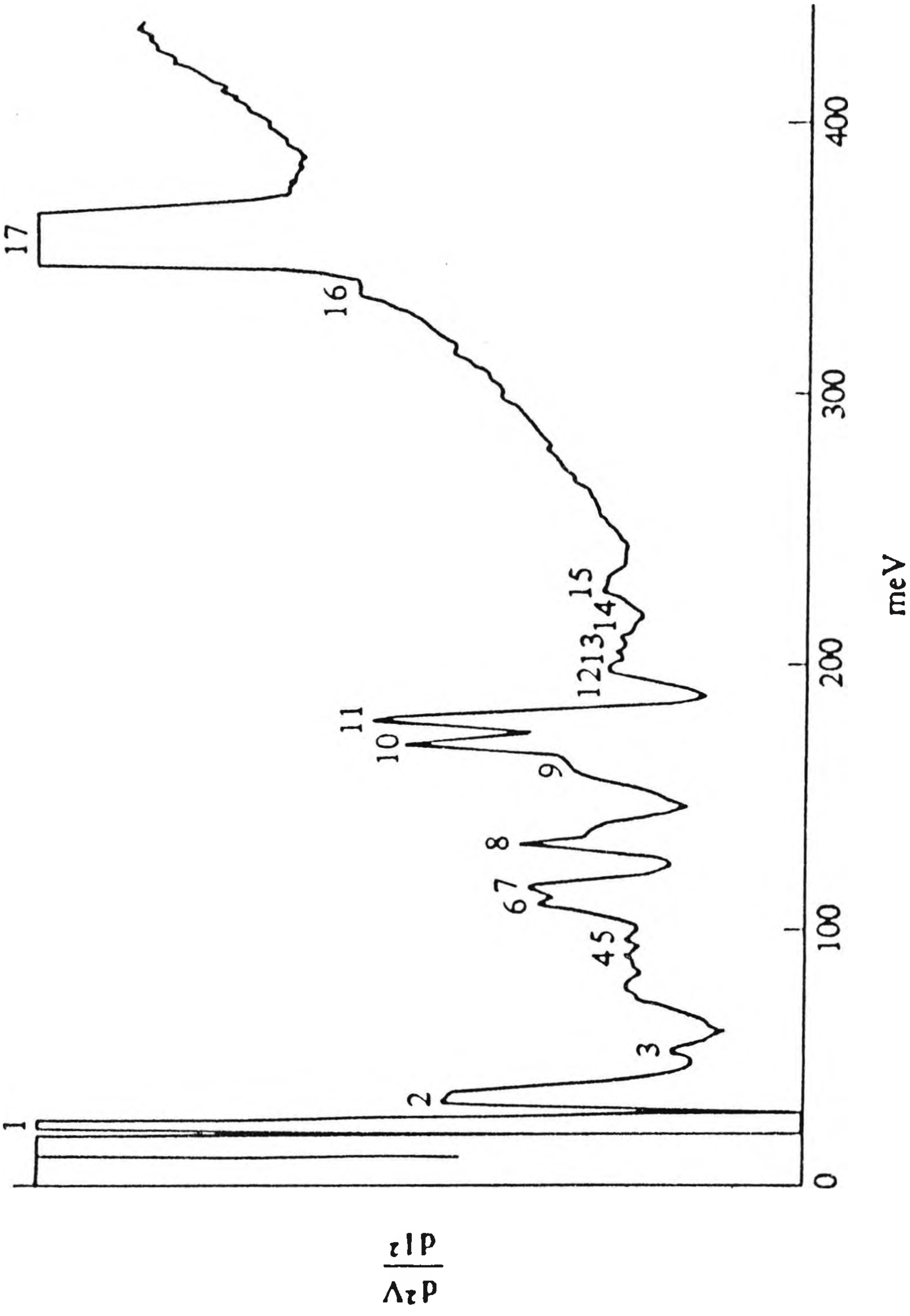

Table A.3.4. Assignment of IET Spectrum of D(-) Fructose in Ethanol.

Peak No.	Energy (meV)	Wave No. (cm^{-1})	Intens.	Assignment
1	23.4	189	S	AlO_x Phonon
2	34.7	280	M	AlO_x Phonon
3	52.5	423	W	Ring Modes
4	88.5	714	M/W	CH_2 rock
5	95.6	771	M/W	
6	107.6	868	M	C-H def. (sugar)
7	113.8	918	M	C-OH str.
8	131.1	1057	M	C-O str.
9	160.1	1291	W/Sh	C-OH def./ O-H def.
10	169.7	1369	M	CH_2 def. (sugar)
11	178.4	1439	M	CH_2 def.
12	198.1	1598	W	C-O str.
13	204.5	1649	W	C=O str.
14	210.2	1695	W	C=O str.
15	227.2	1832	W	
16	337.4	2721	W	C-H str.
17	358.9	2895	S	C-H str.

S=Strong, M=Medium, W=Weak and Sh=Shoulder Intensities.

1meV ≡ 8.065 cm^{-1}

A.3.4 Fructose and Glycine Co-doped on a Tunnel Junction.

An Al-AlO$_x$-Pb tunnel junction was spin doped with a saturated solution mixture of glycine and D(-) fructose in ethanol. The aim of this study was to investigate whether any surface induced reaction took place on the alumina of the tunnel junction. The junction resistance was measured at 150Ω. The spectrometer operating conditions were as follows.

Sensitivity	0.5	µV
Modulation Voltage	6	mV
Time Constant	1	sec.
Scan Time	5	mins.

Figure A.3.4 illustrates the resulting spectrum and Table A.3.5 indicates the proposed spectral assignment of Figure A.3.5.

Figure A.3.5. IET Spectrum of a Saturated Solution of Glycine and D(-) Fructose in Ethanol.

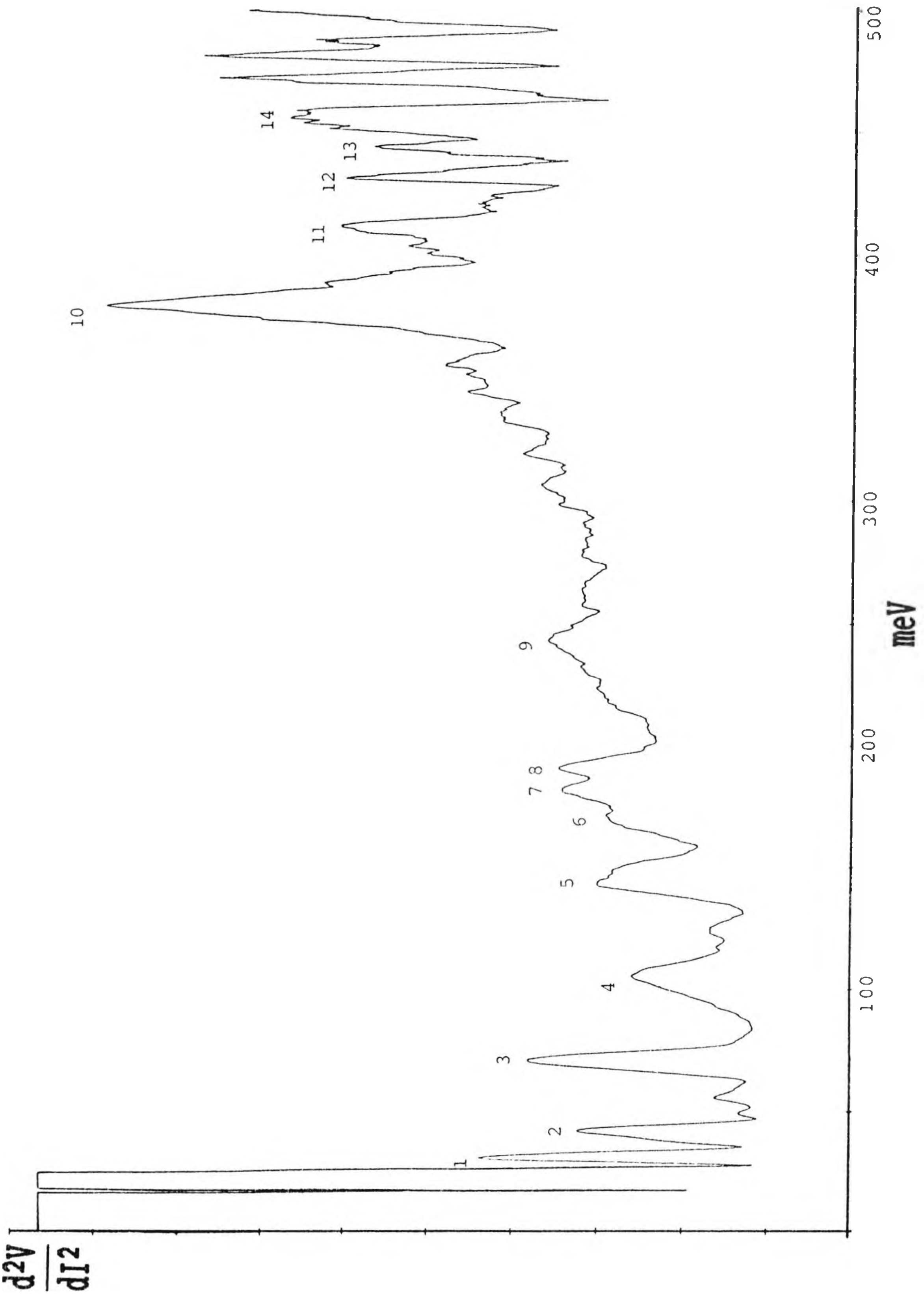

Table A.3.5. Assignment of the IET Spectrum of a Saturated Solution of Glycine and D(-) Fructose in Ethanol.

Peak No.	Energy (meV)	Wave No. (cm^{-1})	Intens.	Assignment
1	31.4	253	M	Al Phonon
2	41.4	334	M	Al Phonon
3	71.4	576	M	CO_2 wag
4	107.1	864	M/Br	C-C str.
5	144.3	1164	M/Br	NH_2 twist and C-O str.
6	172.9	1394	M/W	C-H def.
7	182.4	1471	M	C-H def.
8	191.4	1544	M	
9	242.8	1958	W/Br	
10	380.0	3064	S	C-H str.
11	411.4	3318	M	N-H str.
12	430.0	3468	M	O-H str.
13	444.3	3583	M	O-H str.
14	452.8	3652	M	O-H str.

S=Strong, M=Medium, W=Weak and Br=Broad Intensities.

1meV ≡ 8.065 cm^{-1}

A.3.5 Discussion of Results from the IET Spectra of Sugar Producing Molecules.

Figure A.3.1 shows the tunnelling spectrum produced from aqueous formaldehyde. The junction was infusion doped from the vapour phase; this is the first time so far as can be discovered that a tunnelling junction has been successfully infusion doped with formaldehyde.

The main peaks in Figure A.3.1 may be assigned as follows:

The peaks at 643 and 1106 cm^{-1} can be assigned to vibrations, which are typical of sugars. The peak at 643 cm^{-1} is assigned to a C-O-H twist and that at 1106 cm^{-1} to a C-O stretch. Both of these vibrations indicate that the formaldehyde has polymerized on the surface to form a carbohydrate. The peak at 1507 cm^{-1} is assigned to a CH_2 deformation and the peak at 3045 cm^{-1} to a C-H stretch.
This spectrum is consistent with the formaldehyde having polymerised on the alumina surface, which catalyses the formose reaction, as found by Gabel and Ponnamperuma [1967].

Similarities may be seen between the infusion doped spectrum of formaldehyde (Figure A.3.1) and that of wet carbon monoxide (Figure A.3.3). Particular emphasis is made of the conjunction of the sugar ring modes, at 627-657 cm^{-1} in CO/H_2O (in Figure A.3.3); at 643 cm^{-1} in $HCHO/H_2O$ (Figure A.3.1) and at 714 cm^{-1} in D(-) fructose, and of the sugar C-O stretching modes appearing at 1079

cm^{-1} in CO/H_2O; 1106 cm^{-1} in $HCHO/H_2O$ and 1057 cm^{-1} in D (-) fructose. However there are also significant differences which would be expected from the range of condensation products which may be present if a formose reaction had indeed taken place between the formaldehyde dopant or the wet CO gas and the alumina surface.

A well known reaction of formaldehyde is with ammonia to form hexamethylenetetramine.

$$6HCHO + 4NH_3 \Longrightarrow (CH_2)_6N_4 + 6H_2O$$

Consequently if free formaldehyde molecules were present on the alumina surface, they would react with ammonia to form hexamethylenetetramine. Thus in order to confirm that no free formaldehyde molecules were present, the junction was removed from the liquid helium vessel and exposed to aqueous ammonia vapour for 20 seconds. The resulting spectrum is shown in Figure A.3.2. This spectrum is almost identical to that of aqueous formaldehyde. Thus it can be assumed that the ammonia has not reacted with the species present on the alumina. It can therefore be concluded that the formaldehyde has reacted on the alumina surface. Since Gabel and Ponnamperuma [1967] have shown that the formose reaction is catalyzed by alumina, it seems probable that such a reaction has taken place on the alumina within the junction to produce a mixture of sugars.

The assignment of the peaks produced from the IET spectrum of glycine and D(-) fructose in ethanol (Figure

A.3.5) is shown in Table A.3.5. It tends to suggest that the peaks produced form a mixture of the IET spectra glycine and D(-) fructose shown in Figure A.2.3 and Figure A.3.4 respectively. No spectral signals can be observed to indicate any surface induced linkage of the two solute molecules on the alumina surface.

A.4 CONCLUSIONS AND FUTURE WORK

A.4.1 Conclusions.

The normal atmospheric constituents, water and carbon dioxide, have been shown to produce formic acid on the alumina surface in tunnel junctions [Field et al., 1985]. However, there is no evidence to suggest the presence of formic acid on the surface of the tunnel junctions doped with solutions of organotitanates outlined in Chapter 6. This is most probably due to the short exposure times of the alumina surface to the atmosphere prior to the doping of the organotitanate solutions. The work presented here has shown that atmospheric pollutants, such as ammonia and carbon monoxide, also react on the alumina surface. These pollutants may be expected in an industrial environment and may interfere with subsequent adhesive bonding of the alumina surface.

It has been shown that aqueous ammonia vapour reacts on an aluminium oxide surface within an Al-AlO$_x$-Pb tunnel junction with atmospheric carbon dioxide. The IET spectrum shows similarities with a genuine glycine spectrum. Inhibition of access of atmospheric carbon dioxide by the presence of calcium oxide prevents surface reaction to allow "glycine" formation and the spectrum in this case consists of simple N-H deformation bands.

This observation is of considerable interest in connection with theories concerning the origin of life on Earth. Present speculation holds that the primitive Earth atmosphere was mainly carbon dioxide and that the oceans contained concentrations of dissolved ammonia. Bernal [1951] has suggested that biological molecular asymmetry had its origin in the use of naturally occurring crystals such as L- or D- quartz as a template for their formation. More recently Cairns-Smith [1975] has proposed that the replication of surface defects in clay minerals had a critical role in the formation of biologically important molecules. The present results support this assertion as the alumina substrate in the tunnel junction would inevitably simulate the defect solid state. Now that it has been demonstrated that an alumina surface has a potential for the formation of amino acid type species from water, ammonia and carbon dioxide, all of which were present in the primitive environment, the credibility of Bernal's and Cairns-Smith's hypotheses is increased; particularly with regard to the possible production of chirally stereospecific molecules on the synthetic surface. Also the low energy requirements for this process as opposed to the high energetic conditions of Miller's experiments [Miller, 1953] may make surface synthesis a more favoured route for the formation of biologically important molecules. It is possible to speculate that sugars and amino acids may be synthesized side by side on the same mineral substrate. This may explain how the various sub-units of larger molecules, such as proteins, came together in their preferred manner. The IET spectrum of a mixture of glycine and D(-) fructose tends to suggest that no surface reaction occurs from the adsorption of these two pre-formed species on the alumina substrate of a tunnel junction. However, this need not suggest that the coupling of surface formed amino acids and sugars, as produced in this study from simple prebiotic precursors, may not take place.

In this concept the prebiotic soup is replaced by the structurally more sensitive epitaxially oriented adsorbate. The mineral substrate, acting as a catalytically active surface, not only for the synthesis of amino acids and sugars themselves but also orienting these molecules on the mineral surface to enable them to produce their most biologically useful condensation products. It could be that in this way a cleaved mineral surface, in a vain attempt to replicate its own surface forces, produced the first self-replicating organic molecule.

Further support for the proposed prerequisite of an inorganic substrate to act as a synthetic template for biologically important chemicals comes from the observation that the tunnelling spectrum of aqueous formaldehyde vapour may be interpreted as indicating that the formaldehyde molecule has polymerized on the alumina surface, possibly into a sugar-like compound.

Hence it has been shown that two of the essential requirements for living processes, i.e. amino acids and sugars may be synthesized readily from components available in the primitive Earth atmosphere.

These observations coupled with the potential of an inorganic substrate imposing a structural orienting influence on the product(s) will enhance the credibility of Bernal's original concept of biogenesis.

A.4.2 Future Work.

The results presented here indicate the surface production of amino acids and sugars from simple gases or vapour molecules. Verification of the reaction mechanisms could be carried out by the isotopic substitution (^{18}O or ^{2}D) of the reactant molecules. Analysis of the resultant spectrum could allow the complete role of the alumina surface to be elucidated. After confirming the basic synthesis of small biologically important molecules it should be possible, although the spectra would be complex, to look for the production of more complex, biologically important molecules. The observation of a -CO-NH- linkage would indicate the production of a peptide bond. As stated previously, the alumina used in these studies cannot totally mimic the prebiotic situation. It is therefore important that other surface substrates, such as silica, which are also important in the mineralogical theory of the origin of life, should also be considered using IETS. Gunter Wächtershäuser [1988] has suggested that iron pyrites (FeS) could be a site for the autotrophic origin of life. IETS studies on FeS would prove very interesting.

The consideration of other biologically important ingredients in the production of life, such as phosphates and metallic ions could be studied by their incorporation into a tunnel junction. It is possible to imagine amino acids and sugars doped onto a phosphate barrier, possibly to produce nucleotides.

With regard to the surface contamination consequences of the above work in the context of adhesive bonding, it is important to repeat the work carried out in Chapter 6 but with prior exposure of the alumina surface to these atmospheric contaminants for various periods of time. In this way the influence of the contaminants on the adhesive process may be determined.

APPENDIX REFERENCES

BERNAL J.D.; 1951. The Physical Basis of Life. Routledge and Keegan.

CAIRNS-SMITH A.G; 1975, Proc. Roy. Soc. Lond. B., 189, 249.

CAIRNS-SMITH A.G.; 1982. Genetic Takeover and the Mineral Origin of Life. Cambridge University Press.

FARLEY J.; 1977. The Spontaneous Generation Controversy from Descartes to Oparin. John Hopkins Univ. Press.

FIELD B.O., LEWIS D.M. and HART R.; 1985. Spectrochim. Acta **41A**, 1069.

FIELD B.O. and SPENCER J.E.D.; 1989. Spectrochim. Acta **45A**, 445.

GABEL N.W. and PONNAMPERUMA C.; 1967. Nature **216**, 453.

HOYLE F., OLAVESEN A.H. and WICKRAMASINGHE N.C.; 1978. Nature **271**, 229.

LEWIS D.M.; 1985. Ph.D. Thesis, The City University, LONDON.

MAGNO R. and ADLER J.G.; 1985. Prog. Surf. Sci. 18, 278.

MILLER S.L.; 1953. Science **117**, 528.

MILLER S.L. and ORGEL L.E.; 1974. The Origins of Life on Earth. Prentice-Hall.

OPARIN A.I.; 1964. Life, its Nature, Origin and Development. Academic Press (N.Y.).

SIMONSEN M.G., COLEMAN, R.V. and HANSMA, P.K.; 1974. J. Chem. Phys. **61**, 3789.

SHKLYAREVSKII O.I., LYSYKH A.A. and YANSON I.K.; 1978. Soviet J. Low Temp. Phys. **4**,717.

SUZUKI S., SHIMANOUCHI T. and TSUBOI M.; 1963. Spectrochim. Acta **19A**, 1195.

WACHTERSHAUSER G.; 1988. System. Appl. Microbiol. **10**, 207.

WALD G.; 1979. Life, Origin and Evolution. W.H. Freeman (S.F.).